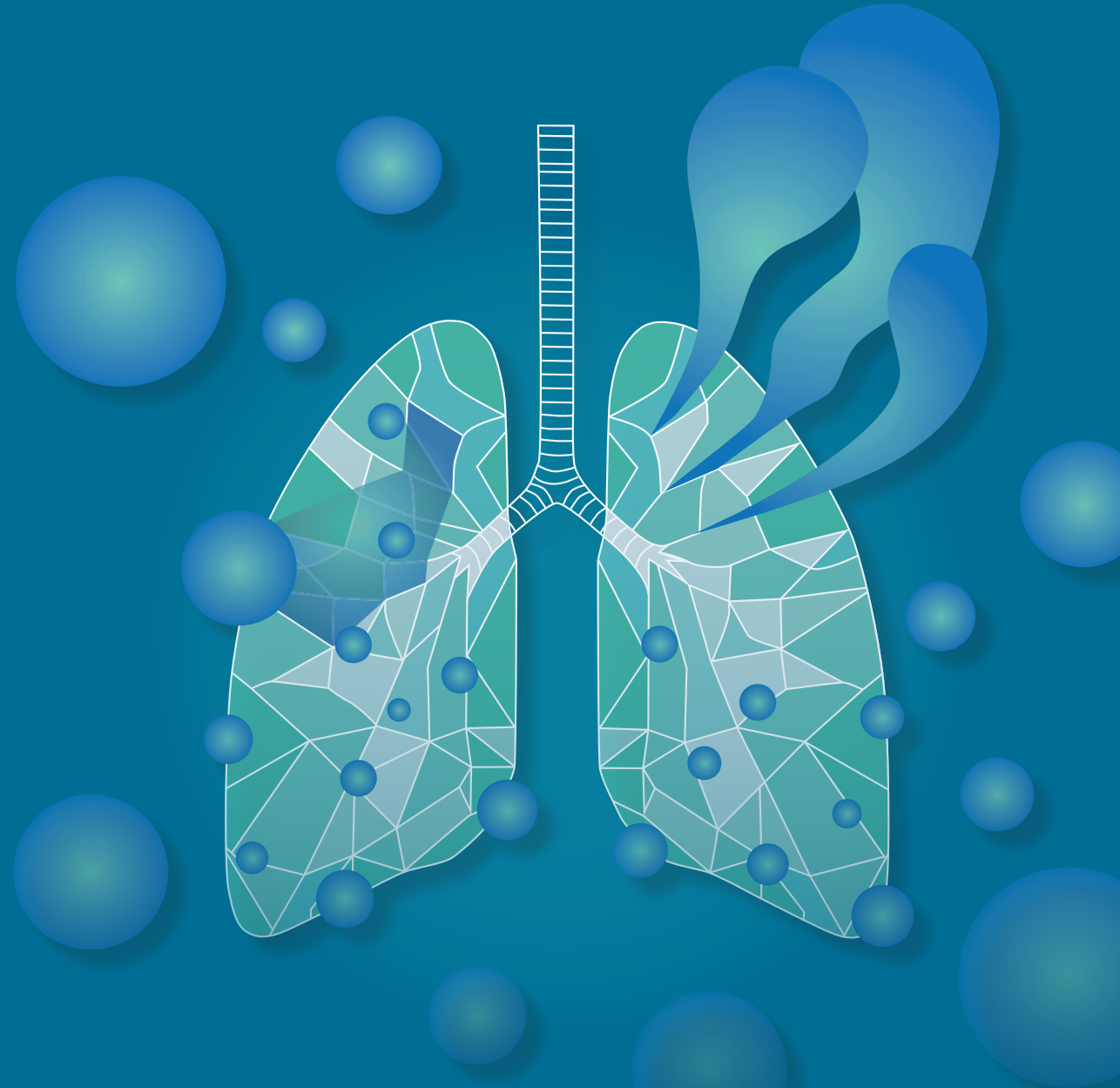
Exploring a novel lung sealant based on functionalized polyoxazolines



Bob P. Hermans

RADBOUD UNIVERSITY PRESS

Radboud Dissertation Series

Exploring a novel lung sealant based on functionalized polyoxazolines

Bob Petrus Hermans

Author: Bob Petrus Hermans

Title: Exploring a novel lung sealant based on functionalized polyoxazolines

Radboud Dissertations Series

ISSN: 2950-2772 (Online); 2950-2780 (Print)

Published by RADBOUD UNIVERSITY PRESS Postbus 9100, 6500 HA Nijmegen, The Netherlands www.radbouduniversitypress.nl

Design: Proefschrift AIO | Annelies Lips Cover: Proefschrift AIO | Guntra Laivacuma

Printing: DPN Rikken/Pumbo

ISBN: 9789493296626

DOI: 10.54195/9789493296626

Free download at: www.boekenbestellen.nl/radboud-university-press/dissertations

© 2024 Bob Petrus Hermans

RADBOUD UNIVERSITY PRESS

This is an Open Access book published under the terms of Creative Commons Attribution-Noncommercial-NoDerivatives International license (CC BY-NC-ND 4.0). This license allows reusers to copy and distribute the material in any medium or format in unadapted form only, for noncommercial purposes only, and only so long as attribution is given to the creator, see http://creativecommons.org/licenses/by-nc-nd/4.0/.

Exploring a novel lung sealant based on functionalized polyoxazolines

Proefschrift ter verkrijging van de graad van doctor
aan de Radboud Universiteit Nijmegen
op gezag van de rector magnificus prof. dr. J.M. Sanders,
volgens besluit van het college voor promoties
in het openbaar te verdedigen op

dinsdag 17 december 2024 om 16.30 uur precies

door

Bob Petrus Hermans

geboren op 18 augustus 1998 te Veldhoven

Promotoren:

Prof. dr. A.F.T.M. Verhagen

Prof. dr. H. van Goor

Prof. dr. H.F.M. van der Heijden

Copromotor:

Dr. R.P.G. ten Broek

Manuscriptcommissie:

Prof. dr. O.C. Boerman

Prof. dr. M. van den Heuvel

Prof. dr. J. Braun (Universiteit Leiden)

Table of contents

Chapter 1	General introduction and outline of thesis	7
Chapter 2	Characterization of pulmonary air leak measurements using a mechanical ventilator in a bench setup	33
Chapter 3	Evaluating and developing sealants for the prevention of pulmonary air leakage: a systematic review of animal models	61
Chapter 4	Sealing effectiveness of a novel NHS-POx based patch: experiments in a dynamic <i>ex-vivo</i> porcine lung	87
Chapter 5	Intrinsic pulmonary sealing, its mechanisms and impact on validity and translational value of lung sealant studies: a pooled analysis of animal studies	111
Chapter 6	Proof-of-principle of a lung sealant based on functionalized polyoxazolines: experiments in an ovine acute aerostasis model	141
Chapter 7	Biocompatibility of a novel lung sealant based on functionalized polyoxazolines in an ovine model of parenchymal lung injury	159
Chapter 8	General discussion	211
Chapter 9	Summary Dutch summary(Nederlandse samenvatting)	234 237
Attachments		
Research data management		242
Portfolio		243
Dankwoord		244
Curricilum vitae		249
Publication list		250



Chapter 1

General introduction and outline of thesis

After lung resection a modest degree of pulmonary air leakage (PAL) is a common phenomenon, which decreases within a few days. However, at least one in ten patients suffer from prolonged air leakage (pPAL), lasting more than five days after the operation. It is the most prevalent complication following lung resection, with a detrimental impact on post-operative recovery. PAL increases the occurrence of other post-operative complications, prolongs duration of chest tube drainage, and extends hospital stay. PAL additionally raises hospital costs (**Figure 1**). Present treatment strategies encompass surgical techniques including reinforcement of staple lines, utilization of surgical sealants and optimized post-operative drainage protocols, but the incidence of PAL remains high. PAL remains high.

In the area of lung sealants, there is a distinct unmet clinical need for a better biomaterial. (5) Such a biomaterial should possess adequate adhesion to achieve an airtight seal, display elasticity to endure repetitive deformation, demonstrate proper biocompatibility and biodegradability characteristics, be user-friendly and produced at a relatively low cost. (2, 9)

This thesis comprises preclinical research into the pathophysiological mechanisms of pPAL and its treatment, by validating models of PAL and testing a novel adhesive patch for hermetically sealing injuries to the lung.

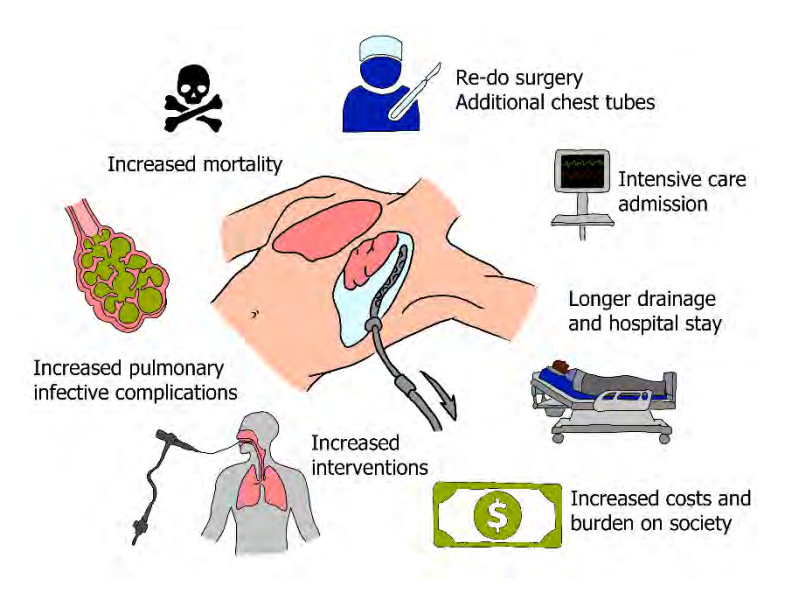


Figure 1: The associated problems of prolonged pulmonary air leakage. Drawing by Bob Hermans.

Burden of pulmonary air leakage

Lung resections are routinely performed to treat lung cancer or, under some circumstances, infectious diseases and lung emphysema (lung volume reduction surgery). PAL is common after resection and is monitored over chest tubes postoperatively. These cannot be removed in the presence of PAL, risking the development of a potentially life-threatening (tension)pneumothorax. Depending on the surgical approach, technique used and the innate healing capabilities of the patient, PAL may stop spontaneously or persist for a longer duration. When PAL persists for longer than five days, the air leak is considered to be prolonged (pPAL). (6) Incidences have been reported between 5.6% and 30%. (7) For the Netherlands the incidence varies between 2.6% and 19%. (8) It is estimated worldwide that more than 50.000 patients are at risk for developing pPAL on a yearly basis (assuming 2.26 million new cases of lung cancer, 25% undergo surgery and 10% develop pPAL). (8,10-13)

In pPAL, there is a fistula between (non-sterile) airways and pleural cavity, increasing post-operative infective complications (empyema: 8.2% vs 0% in one study) and doubling the risk of mortality. (4, 14, 15) Furthermore, pPAL leads to increased readmissions and reinterventions (e.g. additional chest tubes, bronchoscopy, re-operations or life support). (3, 16) Prolonged chest drainage in pPAL can increase postoperative pain and lengthen the duration of hospital stay (4-7.9 days longer). (5, 17, 18) As a result of these problems, there is an increased financial burden, and 90-day postoperative costs are estimated to be 40% higher. (5, 14, 17)

Chronic obstructive pulmonary disease (COPD) and pulmonary emphysema are considered important risk factors for pPAL. (7, 19, 20) As an illustration, in patients undergoing lung volume reduction surgery for pulmonary emphysema, 90% of patients developed pPAL, which lasted on average seven days. (22) Due to the mutual association of both lung cancer (as primary indication for lung resection) and COPD (as risk factor for pPAL) with air pollution and cigarette smoking, pPAL is prospected to remain a daily concern for the thoracic surgical practice. (21)

Pathophysiology of air leaks

PAL is classified as an alveolo-pleural fistula when the leak is distal to the segmental bronchus in the parenchyma, and a broncho-pleural fistula if it involves larger bronchi. (**Figure 2 and 3A**). (23) The driving forces of PAL

are analogous to respiration, so for large broncho-pleural fistulas, there is higher airflow due to lower resistance (normal pulmonary biomechanics described in frame on Page 13-14). Broncho-pleural fistulas are rare after lobectomy (incidence 0.5%), but require urgent interventions and carry a high mortality. (24) Alveolar PAL on the other hand is generally treated by careful monitoring and chest drainage. (6, 25) Because both require different surgical management, this thesis only focusses on alveolar PAL. The incidence of alveolar PAL is correlated with multiple factors.

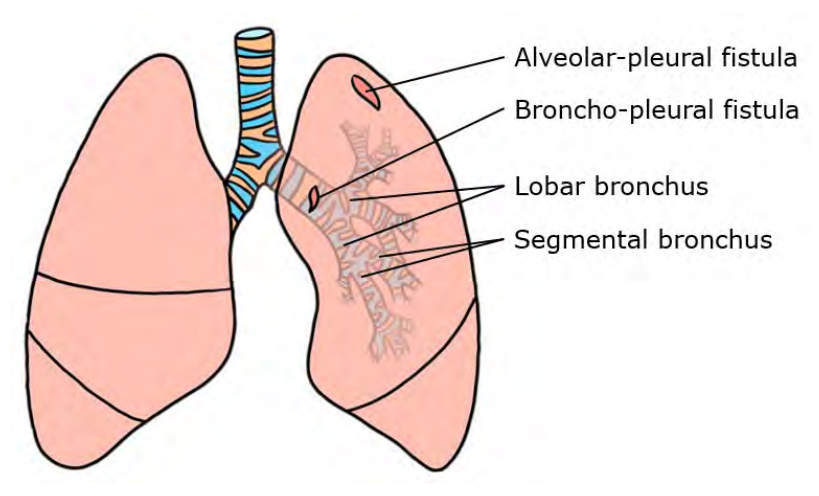


Figure 2: Schematic drawing illustrating the difference between an alveolar-pleural fistula (distal to segmental bronchus) and broncho-pleural fistula (proximal to segmental bronchus). Drawing by Bob Hermans.

Firstly, COPD is strongly associated with pPAL. (7) Predominant emphysema (Figure 3B/C) in COPD may be more predictive of pPAL, supported by studies using radiological emphysema grading. (19, 20, 26) However, the obstructive component may also be involved in the pathophysiology. Eberlein suggested that increased resistance in normal airways might cause preferential airflow through collateral pathways, which may connect the entire lung without fissures, and increase airflow towards the leakage site. (27)

The driving pressure of PAL (**Figure 4**) is affected by the clinical circumstances. For instance, positive pressure is required during mechanical ventilation to overcome chest wall inertia, which has been associated with longer PAL duration. (28-30) Similarly, a stronger vacuum applied to the chest tube increases the driving pressure, which may explain why water seal is preferred over active suction for shortening PAL duration.(31)

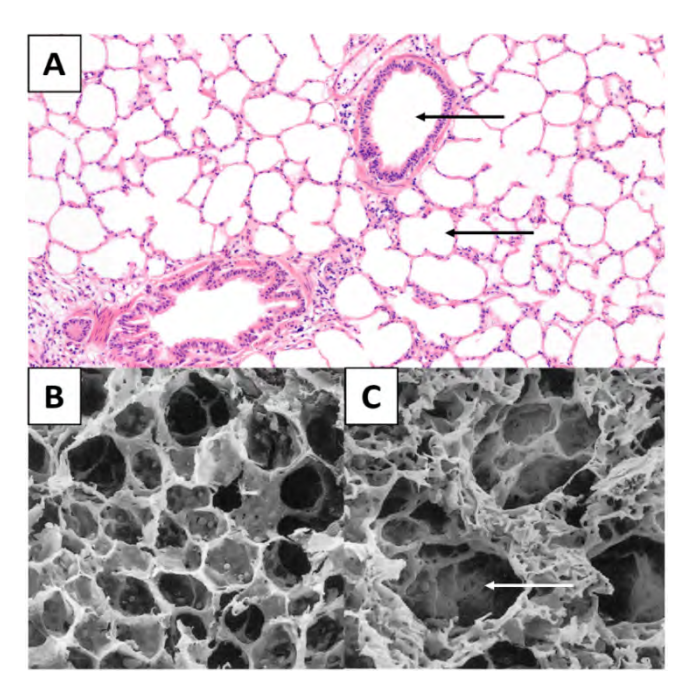


Figure 3: A) Histological sections through the lung parenchyma of a healthy sheep. Leakage from parenchymal lacerations can occur from both alveoli (bottom arrow) and small bronchioles (top arrow) (20x magnification, HE-stain). B) Electron microscope image of healthy lung alveoli. C) Electron microscopy image from emphysematous lungs. "Reprinted from CHEST, Volume 117, Issue 5, Steven D. Shapiro, Animal Models for COPD, Pages 223S-227S, 2000, with permission from Elsevier.

After lung resection, pleural apposition is important to seal the leaking orifice. (32) This is more challenging in specific cases, such as bi- or upper lobectomies, which have been associated with pPAL. (7, 26) In cranial lesions, the gravity gradient increases ΔP_{lesion} due to more negative intra-pleural pressure (P_{ID}), which may explain increased PAL in upper lobectomy. (26, 32, 33) Lung overdistention, which is larger for extended lobectomies, may also increase air leaks. (34) Surgical techniques can be applied to restore pleural apposition, including mobilization of the pleural ligament and pleural tenting. (6, 32)

Finally, healing mechanisms play a role in the duration of PAL. Healing occurs through fibrosis in the lung alveoli when the basement membranes are injured, and the mesothelial cell layer of the pleura can regenerate within seven to ten days. (35, 36) Factors inhibiting wound healing such as steroid use, cigarette smoking or a low body-mass index have been associated with pPAL. (7)

In summary, patient and procedure characteristics play an important role in the development of pPAL. This is relevant when designing preclinical disease models to test novel treatments.

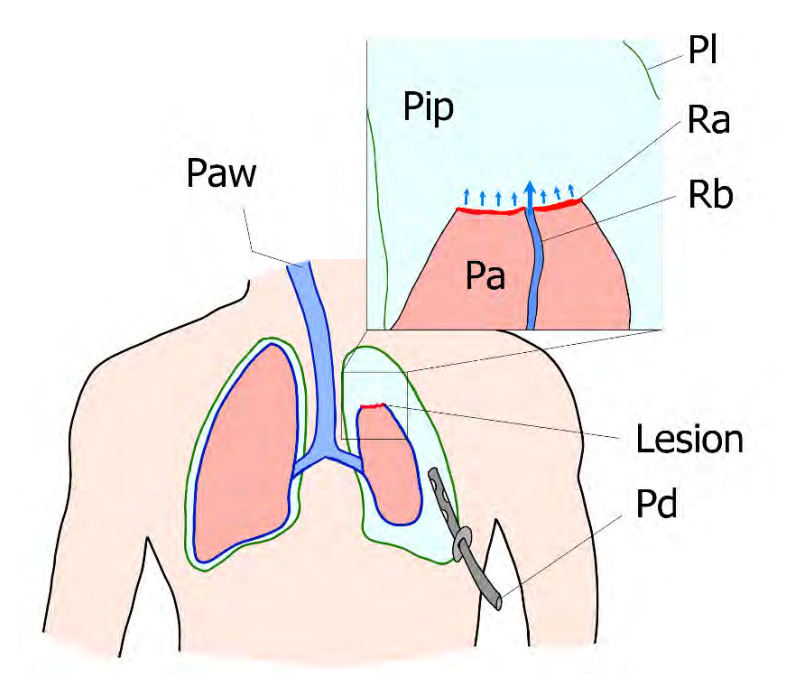


Figure 4: PAL is determined by the pressure difference (Δ Plesion) between the interpleural space (Pip) and the alveoli (Pa) or the bronchi (Paw). The lacerated structure determines the resistance for the air leak, estimated higher for alveolar leaks (Ra) compared to more central bronchiole leak (Rb). Drawing by Bob Hermans.

Theoretical framework: relevant pulmonary biomechanics

Pulmonary physiology results from the local mechanics of alveoli (ø75-300µm). (37) These are coated with a liquid lining causing inward surface-tension forces (T), but specialized amphiphilic molecules (surfactant) reduce the surface tension. The equilibrium pressure (P) required to open the alveolus is thereby reduced, given by the Laplace equation $(p = \frac{2T}{T})$ (Figure 5) (37). Airways and alveoli are embedded in the parenchyma and r therefore mechanically interrelated, causing airway opening during inspiration (more negative P_{ID}) and compression during expiration or coughing. (32, 34, 37-39) (Figure 6).

Airflow (Q) is driven by a pressure gradient (ΔP) that results from variation in P_{IP} during volume changes in the thorax (assuming lamellar flow: $Q = \frac{\Delta P}{R_{AW}}$) (37). The resistance $(R_{\Delta W})$ is mainly dependent on the airway radius (r) and can be estimated using Poiseuille's equation (assuming lamellar flow: $R_{AW} = \frac{8\mu l}{m_{e} A}$) (37)

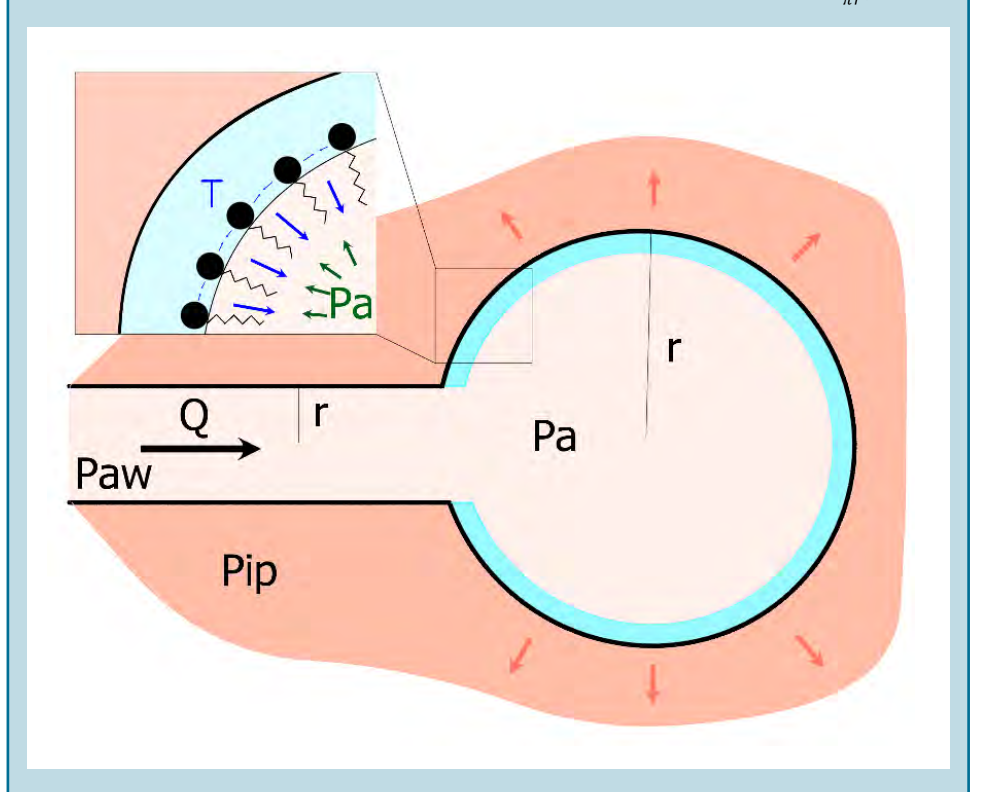


Figure 5: Surface tension forces (T) collapse the alveolus, which are lowered by the interaction between surfactant and water molecules. The alveolar pressure (Pa) required to prevent this from occurring is given by the Laplace equation. Mechanical interplay between units is illustrated by red arrow. r = radius, Q = airflow, Paw = airway pressure. Drawing by Bob Hermans.

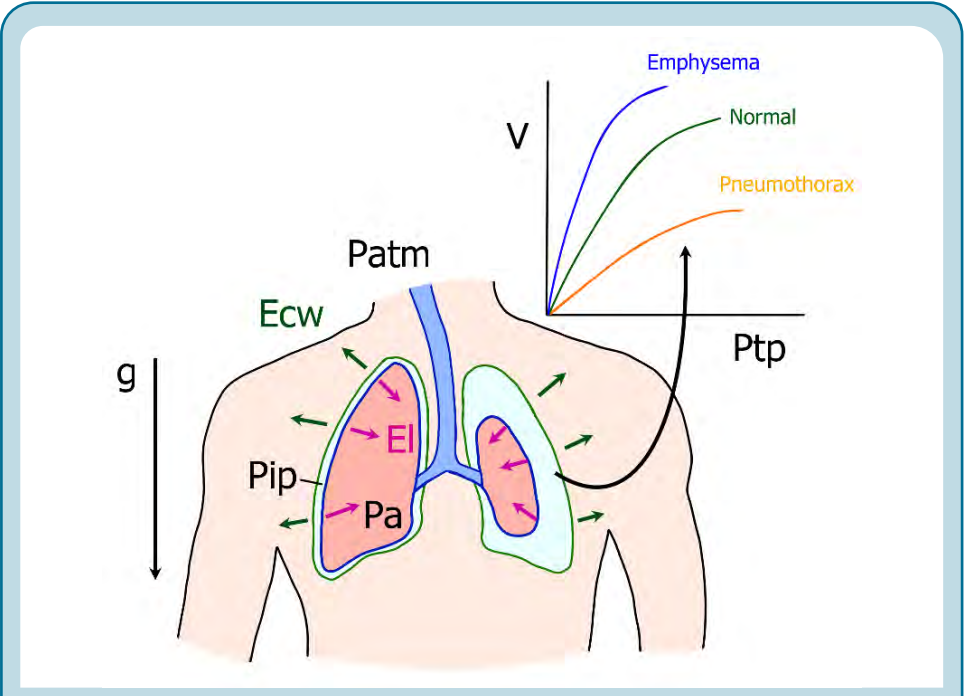


Figure 6: Outward elastic recoil of the chest wall (Ecw) and inward elastic recoil of the lung (El) result in an equilibrium negative pressure in the interpleural space (Pip) with respect to the atmospheric pressure (Patm) under physiological circumstances. Pip is more negative apically in an upright position, due to the gravity gradient (g). When air enters the interpleural space, the equilibrium is disrupted and the lung collapses. As shown in the top-right graph, the compliance of the lung is reduced in this case (orange line), and higher transpulmonary pressure (Ptp = Pa - Pip) is required for a similar change in volume. Pa = alveolar pressure. *Drawing by Bob Hermans*.

Intraoperative management of air leaks

Identification and classification

Valid methods for identification and grading of intra-operative air leaks (IAL) are essential to standardize research and treatment. Conventionally, the thoracic cavity is filled with saline solution to perform a leak test, similar to checking a leaking bike tire. Grading the severity of IAL with this approach may be challenging and prone to interobserver variability (e.g. Macchiarini bubble scale, **Table 1**). (40-42) A more standardizable approach is the mechanical ventilator test. (43) IAL size (in mL/min) is calculated as the difference between the inspiratory and expiratory tidal volumes. Literature suggests that the derived IAL size is predictive of pPAL, but the validity of these measurements in terms of accuracy and repeatability is not described (Table 1). (43-45)

Table 1: Air leak grading and classification

Visual bubble scale by Macchiarini (41)

Grade 0: no leak

Grade 1: countable bubbles Grade 2: stream of bubbles Grade 3: coalesced bubbles

Mechanical ventilator test by Zaraca (43)

Mild: <100 mL/min Moderate: 100-400 mL/min Severe: >400 mL/min

Surgical management and lung sealing devices

In patients with normal healing and no other comorbidities, standard techniques using surgical staples or sutures are generally sufficient for attaining aerostasis. (7, 26) Surgical staplers can be used to divide lung tissue and operate by deploying two rows of staples and cutting in between these rows. Certain injuries to the lung, such as stab or crush lesions, may be better treated by conventional suturing.

However, in some circumstances, additional intervention is needed, for which a multitude of lung sealing devices (SDs) have been developed. For example, in cases of poor tissue quality (due to smoking, emphysema, steroid use), sutures or staplers can cause tears and leave residual holes for air leaks (Figure 7). Surgical division of pleural adhesions can result in superficial pleural defects which are difficult to treat using conventional techniques. (7) Similarly difficult to suture lesions can develop when dissecting in the pulmonary hilum or segment borders during anatomical resections (Figure 7), or when performing pleural decortications. (7, 46)

Tears in the lung parenchyma can be prevented using buttressing materials as an SD, distributing the force on the suture or staple over a larger surface area (Figure 7). Several materials are described, including poly(tetrafluoroethylene) (PTFE), bovine pericardium, collagen patches, poly(glycolic acid) (PGA) and autologous pericardium/pleura. (26) Staplers with pre-loaded buttressing material exist to increase ease of use. (47)



Figure 7: Left: in poor quality lungs, sutures or staplers may tear through the tissue, leaving behind air leaks. Staple line buttresses or suture pledgets may be used to prevent this. Right: parenchymal damage due to dissection of the lung hilum or segmental borders may be difficult to suture or staple, requiring different methods of tissue repair. Drawing by Bob Hermans.

Tissue adhesives are another form of SD that can be applied as a patch, glue or spray and generally have an active component (e.g. in-situ polymerizing gels). Mechanisms are illustrated in **Figure 8**. They were grouped by Bouten et. al. according to their chemical structure into synthetic polymeric (e.g. Coseal®, Glubran®), polysaccharide-based (e.g. chitosan) and protein-based/ biomimetic (e.g. Progel®, TachoSil®). (48, 49) Devices commonly used include fibrin/thrombin coated collagen patches (TachoSil®), fibrin/thrombin glues (Tisseel®, Tissuecol®), a functionalized poly(ethylene glycol) coated collagen patch (Hemopatch®) and a human serum albumin/poly(ethylene glycol) based spray (Progel®) (common use is partially based on unpublished survey data in the Netherlands). (50)

Finally, localized energy delivery devices can be used for achieving aerostasis, including conventional coagulation⁽⁵¹⁾, high-frequency focused ultrasound⁽⁵²⁾ or laser tissue welding. (53). For instance, specialized clamps can be used during dissection, simultaneously cutting and sealing the lung (e.g. Harmonic Ace™).

Figure 8: Forces of lung sealants can be divided into adhesive and cohesive forces. The cohesive matrix must withstand lung expansion and prevent penetration of air. The adhesion to the tissue needs to be strong enough for rapid application and prevent debonding. Mechanisms responsible may depend on the sealant used, and can include mechanical interlocking, entanglement of molecular chains and intermolecular forces (covalent bonds, dipole-dipole interactions, hydrogen bonding) as well as electrostatic forces. (9,54) Drawing by Bob Hermans.

Current evidence and unmet clinical need

SD availability is abundant, but evidence in literature remains controversial. (2, 26) A systematic review by Belda-Sanchis et. al. described a significant reduction in length of hospital stay for sealant use in only 3/16 included trials. (58) A metaanalysis by Malapert et. al. showed that sealants and buttresses could reduce the occurrence of pPAL after surgery, but advise cautious interpretation due to publication bias. (55) More recently, McGuire et. al. performed a meta-analysis investigating polymeric sealants, showing a small but significant reduction in one day length of stay, but with inter-trial heterogeneity. (56) Multiple different sealants are pooled in these analyses, and considering differences in efficacy, more comparative data is required. (56-58) Another meta-analysis investigated only one sealant that is frequently used in clinical practice (TachoSil®), describing an average reduction of almost two days length of stay. (50, 59) These results are promising, but considering the average increase of four to eight days in length of stay for pPAL, improvements are still to be made. (5, 17)

Patient selection is important to prevent overtreatment, side effects and reduce costs. If patients at risk for pPAL are not properly identified, large sample sizes are needed to show treatment effects. (26) Because lung sealants and buttressing materials are expensive, evidence-based use in the right patient is essential to maintain affordable health care systems (e.g. TachoSil® and Progel® cost around €400,- per usage). (60, 61) Prior studies describe risk factor models based on patient, radiological and intraoperative factors (19, 20, 62-64), which may be useful in this regard.

In summary, no perfect lung sealant is available for use in current clinical practice. The findings for TachoSil® are promising, but this patch has a long application time (3-5 minutes) and requires human plasma for production. (65) Furthermore, different application methods might be beneficial for different circumstances (e.g. spray, patch, viscous glue), requiring additional product development. (50) The unmet need for lung sealants has been described by Brunelli et. al. as:

"There is therefore an unmet need to produce a specialty specific, single-component and more effective surgical sealant capable of sealing air leaks in wet and dynamic biological environments while maintaining adequate mechanical and adhesive properties without inhibiting tissue repair."(2)

Novel lung sealants

Requirements for novel lung sealants

Precise requirements should be formulated to fulfill the unmet clinical need for lung sealants. (66) Proper biodegradability (after healing is completed), optimal biocompatibility (no adverse inflammatory response or reactions due to antigenicity, systemically non-toxic) and no infection potentiation are minimal requirements from a safety perspective. (67-69) Advantageously, the device would accelerate wound healing and exhibit bactericidal properties. (49, 70) Biomechanically, it should be impenetrable to air, strongly adhesive and have elastic properties similar to the lung (described to be around 5-30kPa). (9, 71) It should allow for complete lung inflation without causing impairment of respiratory function. (72, 73) Also, it should resist the respiratory cyclic deformation in the wet pleural environment, without failing before healing is achieved. (2, 9) These mechanical perguisites might be expressed as respiratory

pressures to be resisted, which can be up to 35-40cmH20 during mechanical ventilation recruitment maneuvers or up to 71cmH20 during coughing in postthoracotomy patients. (71, 74, 75) Most anesthesiologists attempt to limit the peak ventilation pressures <30cmH20 during thoracic surgery. (76)

For usability during surgery, it needs to be available with minimal preparation time and intuitive to apply. (1, 2) As procedures are increasingly performed thoracoscopically, every patch should be pliable enough for this purpose and spray systems should come with lengthened application tips. (2) From societies perspective, it needs to be safe, effective, environmentally sustainable and cost-effective. (55, 58) From an ethics perspective, synthetic materials are preferable over animal materials, also eliminating zoonotic disease transmission and reducing antigenicity. (65, 77)

Specific considerations relating to possible sites of application should be taken into account. Lung injury will generally occur through the following mechanisms during elective surgery (7, 46):

- i. Dissection of pleural adhesions or pleural decortications, leading to superficial visceral pleural injuries;
- Dissection of the lobar or segmental plane (Figure 7), leading to ii. superficial parenchymal injuries;
- Completion of fissures using staplers; iii.
- latrogenic injury of surgical instruments (clamp crush injuries, heat iv. injuries, sharp injuries).

Defect types (i) and (ii) are difficult to suture due to their location or superficial nature, and could be treated using patch or gel based sealants. Defect type (iii) can be treated using staple line reinforcement, and spray sealants may be preferred over patches due to mechanical interlocking mechanisms (Figure 8). (48, 50) For a patch to be applied to a staple line, it should be pliable enough to fold around the acute angle. Lastly, the remaining injuries (iv) might best treated using a combination of techniques (e.g. suturing and patch/ spray reinforcement).

Novel polyoxazoline based tissue adhesives

Poly(2-oxazoline)s are promising materials for tissue adhesive purposes that may be tuned to specific needs. Previous authors have described synthesis of copolymers with different compositions of 2-n-propyl-2-oxazoline (nPropOx)

and 2-methoxycarbonylethyl-2-oxazoline (MestOx). (78) The hydrolysable methyl- ester of MestOx can be used for functionalization, and by varying the MestOx/nPropOx ratios, the degree of functionality can be adjusted. (78)

For bio-adhesive purposes, different functional side chains exist. (79) N-hydroxysuccimide (NHS) esters are capable of rapidly forming covalent bonds with primary amines and thiols, which are abundantly present in tissues (**Figure 9**). (9, 79) This functional group is already used in commercially available products such as a collagen patch coated with NHS functionalized poly(ethylene-glycol) (Hemopatch®).(80) Boerman et. al. extensively described functionalization of polyoxazolines with NHS esters (NHS-POx), as well other modifications including addition of hydroxyl groups to improve hydrophilicity, amine groups to improve crosslinking or hydrolytically cleavable groups to tune biodegradation properties (Figure 9). (81, 82) This technology has been developed by GATT-Technologies B.V. (Nijmegen, the Netherlands).

$$\begin{array}{c} & & & & \\ & & &$$

Figure 9: Top reaction: bioconjugation reactions of NHS-esters with tissue amines and thiols. Upon formation of the amide or thioester bond, an NHS leaving group is formed. The amide or thioester bonds are degraded in-vivo by hydrolysis (based on Nam et. al. (9)). Bottom reaction: 2-ethyl-2oxazoline (EtOx monomer) and 2-methoxycarbonylethyl-2 oxaczoline (MetOx monomer) are polymerized through cationic ring opening polymerization (CROP). The MestOx side chains can be functionalized after polymerization. (i) shows functionalization of a carboxylic acid group with NHS esters and (ii) shows the presence of a hydrolyzable ester moiety to introduce biodegradability, (iii) shows the addition of a hydroxyl group (structure formulas based on Boerman et. al.(81))

The hemostatic capabilities of NHS-POx were investigated by Roozen et. al. in a model of experimental liver resection. For prototype selection, various carrier materials were coated with a combination of amine- functionalized and NHS-functionalized (nucleophilically- activated) polyoxazolines (electrophilically activated). Superior hemostatic efficacy of gelatin patches coated with these polymers was observed compared to a commercially available hemostatic agent (TachoSil®).(82)

The mode of action is based on the following mechanisms: 1) rapid adhesion to tissue proteins by covalent bonding with NHS esters, 2) blood uptake by hydrophilic patch causing tamponade 3) crosslinking within the adhesive matrix between NHS esters and amines in polyoxazoline, gelatin and blood contents, 4) blood coagulation within the gelatin matrix and 5) water uptake forming a sealing hydrogel (Figure 10). (81, 82) Based on promising pre-clinical results, the NHS-POx patch has been investigated in clinical trials of liver resections (ClinicalTrials.gov: NCT04819945 and NCT05385952). Approval for the European market has been obtained in 2023 (marketed as ETHIZIATM, Ethicon Inc., United States). (83)

Hemostasis vs Aerostasis Water uptake Blood protein Gelatin Trombocyte Crosslink Red blood cel Fibrin Polyoxazoline Blood uptake Primed surface Bleeding surface Air leak

Figure 10: Mechanisms of action of the novel polyoxazoline impregnated gelatin patch. Amide and thioester bonds form on both the tissue-adhesive interface (with tissue proteins) and within the cohesive matrix (between gelatin, polyoxazolines and absorbed blood contents). Blood uptake enhances the hemostatic efficacy due to coagulation mechanisms. Water uptake ensures the formation of a sealing hydrogel. Drawing by Bob Hermans.

It is hypothesized that this NHS-POx patch can also be used as a strong aerostatic sealant. For this purpose, some modifications are considered to the mode of application:

- Priming of the lung with a higher pH fluid compared to saline (0.9% NaCl, pH ~5.5), which is generally used for hemostatic application.
- Application with gauzes soaked in the same priming solution.
- Longer compression time to allow for more complete crosslinking and water absorption, leading to a stronger sealing hydrogel.
- Application of a thicker layer of the material, ensuring a stronger cohesive matrix.

Using a solution with a higher pH (e.g. phosphate buffered saline, pH ~7.4 or buffered NaHCO3-, pH ~8.3-8.5) ensures that the degree of protonation in amines (NH₂:NH₃⁺) turns more favorable towards the more nucleophilic NH₂. This increases the rate of covalent bond formation with the electrophilic NHS esters, resulting in a faster and stronger adhesion. (79) Such priming method is also described in instructions for use of Hemopatch® (based on NHS-PEG esters). (84) The aspect of the surgically applicable patch is shown in **Figure 11**.



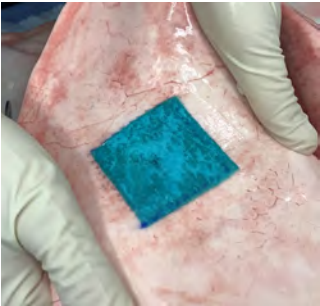


Figure 11: Left: Aspect of dry-stored gelatin patch impregnated with functionalized poly (2-oxazoline)s before application (GATT-Technologies B.V., Nijmegen, The Netherlands). Right: Aspect of formed hydrogel on an ex-vivo lung surface after application.

Preclinical research

Before new technologies can be used on patients, extensive preclinical research is required, to demonstrate safety and efficacy (Figure 12). Generally, novel technologies are first tested and optimized in in-vitro and bench-testing setups, followed by higher fidelity ex-vivo models and lastly in-vivo models. When the standards of relevant legislation are met and ethical approval is obtained, the first in-human clinical trial can be executed. Finally, market approval needs to be obtained from the governing authorities (e.g. Conformité Européenne [CE] in Europe and Food and Drug Administration [FDA] in U.S.A). (66)

In-vitro platforms

In-vitro research is furthest away from clinical practice, but has the advantage of being relatively low-cost and quickly applicable, allowing for many different product iterations. Examples include standardized material property testing (e.g. American Society for Testing and Materials [ATSM] standards) and cell cultures to investigate toxicity, bacteriostatic or bactericidal properties. (71)

Ex-vivo platforms

For lung sealant investigations, ex-vivo models generally consist of mechanically ventilated animal lungs (e.g. from slaughterhouse) which are lacerated and subsequently sealed. (49, 57, 85, 86) Pressure is increased until leakage occurs, which is noted as the bursting pressure. These models allow for comparative testing of previously optimized products to available competitors in more realistic environments, including surgical application to organs, volumetric strain exposure and physiological conditions (e.g. temperature and pH).

More advanced models can be designed, such as ex-vivo porcine lung perfusion models or perfusion of human donor lungs rejected for transplantation. (87-89) Future ex-vivo models may consist of a combination of organosynthetic respirator models to simulate negative ventilation mechanisms, and exvivo lung perfusion models to simulate physiological homeostasis, further diminishing the need for *in-vivo* experiments. (90)

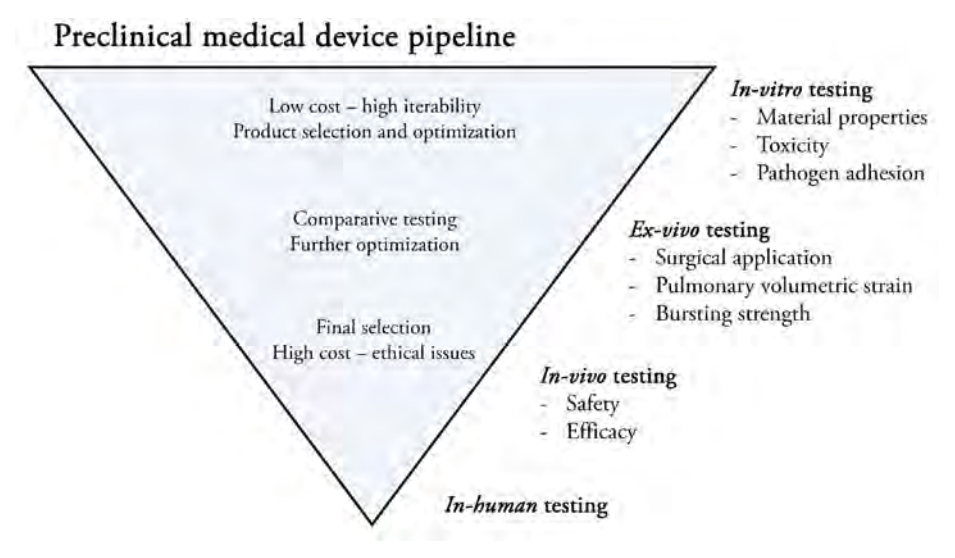


Figure 12: Overview of preclinical testing phases of medical devices

In-vivo models

Experimentation with live animals is subject to strict legislation and ethical assessment. Animal experiments should only be performed when there is no other alternative, according to principles of the three R's (Replacement, Reduction and Refinement). (91) In the final phases of product testing before use in humans, the use of animals is mandatory, to allow for a final judgement of efficacy and safety in a living organism. As of now, the complete integration of relevant physiological mechanisms (negative pressure ventilation, pleural mechanics, coagulation, immune system) in an ex-vivo platform is not feasible. necessitating these experiments. Specifically for lung sealant research, no standardized in-vivo model is described in literature.

Outline of this thesis

In summary, pPAL remains a primary concern in lung surgery with insufficient solutions, causing morbidity, mortality and high costs. In this thesis, the novel lung sealant based on NHS-POx impregnated gelatin patches will be investigated in preclinical studies aimed at high translational value. Validity will be supported by integrating model verification studies, but the main goal will be to investigate the aerostatic efficacy and safety profile for surgically treating and preventing the clinical problem of pPAL.

Valid measurement methods of IAL are necessary to standardize the investigations, but the characteristics of current techniques are unknown. To this end, a validation study is performed and results are described in **Chapter 2**. Using a bench testing setup, various IAL measurement techniques on the mechanical ventilator are compared, to assess repeatability and accuracy for use in further studies.

Since a standardized in-vivo model of PAL is lacking, a systematic review of previous animal experiments is performed to identify the best animal model (Chapter 3). This systematic review will investigate internal validity of previous models, and attempt to derive which model offers the highest translational value for clinical practice based on various factors such as disease model, surgical approach and outcome measures. Based hereon, recommendations for design of future models are described, which will be used in subsequent chapters.

The NHS-POx patch is investigated as a lung sealant in an ex-vivo porcine lung model (Chapter 4). Standardized superficial lesions are used to test the pressure resistance and PAL reduction of the novel patch in comparison to different commercially available SDs. The results of this study provide a rationale for further in-vivo experimentation.

In order to verify the validity of the in-vivo model to be used for efficacy and safety testing of the NHS-POx patch, the baseline PAL capacity of various lesions are investigated and described in **Chapter 5**. The lesion that results in a valid model of PAL will be used for testing the aerostatic efficacy of the NHS-POx patch. The intrinsic sealing mechanisms of lesions in healthy animal models are also investigated.

The aerostatic efficacy of the NHS-POx patch described in **Chapter 4** will be validated in more clinically realistic scenario's. This is investigated in a large animal model of surgical application, and described in **Chapter 6**. The lung sealing integrity will be monitored several hours after application under both mechanical ventilation and physiological breathing mechanics to simulate the direct postoperative period, using untreated lesions as control.

In Chapter 7, the biocompatibility and biodegradability of the NHS-POx patch will be investigated in a long term animal model of intrathoracic application. In comparison to control groups, the histological response and mechanisms will be studied at various time points after application.

In **Chapter 8**, the implications of the findings are discussed, as well as directions for future research and development.

References

- Cardillo G, Nosotti M, Scarci M, Torre M, Alloisio M, Benvenuti MR, et al. Air leak and intraoperative bleeding in thoracic surgery: a Delphi consensus among the members of Italian society of thoracic surgery. J Thorac Dis. 2022;14(10):3842-53.
- Brunelli A, Bölükbas S, Falcoz PE, Hansen H, Jimenez MF, Lardinois D, et al. Exploring consensus for the optimal sealant use to prevent air leak following lung surgery: a modified Delphi survey from The European Society of Thoracic Surgeons. Eur J Cardiothorac Surg. 2020.
- Attaar A, Luketich JD, Schuchert MJ, Winger DG, Sarkaria IS, Nason KS. Prolonged Air Leak After Pulmonary Resection Increases Risk of Noncardiac Complications, Readmission, and Delayed Hospital Discharge: A Propensity Score-adjusted Analysis. Ann Surg. 2021:273(1):163-72.
- Brunelli A, Xiume F, Al Refai M, Salati M, Marasco R, Sabbatini A. Air leaks after lobectomy increase the risk of empyema but not of cardiopulmonary complications: a case-matched analysis. Chest. 2006;130(4):1150-6.
- Brunelli A, Chapman K, Pompili C, Chaudhuri N, Kefaloyannis E, Milton R, et al. Ninetyday hospital costs associated with prolonged air leak following lung resection. Interact Cardiovasc Thorac Surg. 2020;31(4):507-12.
- Singhal S, Ferraris VA, Bridges CR, Clough ER, Mitchell JD, Fernando HC, Shrager JB. Management of alveolar air leaks after pulmonary resection. Ann Thorac Surg. 2010;89(4):1327-35.
- Attaar A, Tam V, Nason KS. Risk Factors for Prolonged Air Leak After Pulmonary Resection: A Systematic Review and Meta-analysis. Ann Surg. 2020;271(5):834-44.
- Hoeijmakers F, Hartemink KJ, Verhagen AF, Steup WH, Marra E, Röell WFB, et al. Variation in incidence, prevention and treatment of persistent air leak after lung cancer surgery. Eur J Cardiothorac Surg. 2021.
- Nam S, Mooney D. Polymeric Tissue Adhesives. Chem Rev. 2021;121(18):11336-84.
- 10. Sung H, Ferlay J, Siegel RL, Laversanne M, Soerjomataram I, Jemal A, Bray F. Global Cancer Statistics 2020: GLOBOCAN Estimates of Incidence and Mortality Worldwide for 36 Cancers in 185 Countries. CA Cancer J Clin. 2021;71(3):209-49.
- 11. Niet kleincellig longcarcinoom Landelijke richtlijn, Versie: 2.3 2015 [Available from: https:// www.oncoline.nl/index.php?pagina=/richtlijn/item/pagina.php&id=39344&richtlijn id=991.
- 12. Jakobsen E, Olsen KE, Bliddal M, Hornbak M, Persson GF, Green A. Forecasting lung cancer incidence, mortality, and prevalence to year 2030. BMC Cancer. 2021;21(1):985.
- 13. Didkowska J, Wojciechowska U, Mańczuk M, Łobaszewski J. Lung cancer epidemiology: contemporary and future challenges worldwide. Ann Transl Med. 2016;4(8):150.
- 14. Yoo A, Ghosh SK, Danker W, Kassis E, Kalsekar I. Burden of air leak complications in thoracic surgery estimated using a national hospital billing database. Clinicoecon Outcomes Res. 2017;9:373-83.
- 15. Okereke I, Murthy SC, Alster JM, Blackstone EH, Rice TW. Characterization and importance of air leak after lobectomy. Ann Thorac Surg. 2005;79(4):1167-73.
- 16. Liang S, Ivanovic J, Gilbert S, Maziak DE, Shamji FM, Sundaresan RS, Seely AJE. Quantifying the incidence and impact of postoperative prolonged alveolar air leak after pulmonary resection. J Thorac Cardiovasc Surg. 2013;145(4):948-54.

- 17. Varela G, Jimenez MF, Novoa N, Aranda JL. Estimating hospital costs attributable to prolonged air leak in pulmonary lobectomy. Eur J Cardiothorac Surg. 2005;27(2):329-33.
- 18. Miyazaki T, Sakai T, Yamasaki N, Tsuchiya T, Matsumoto K, Tagawa T, et al. Chest tube insertion is one important factor leading to intercostal nerve impairment in thoracic surgery. Gen Thorac Cardiovasc Surg. 2014;62(1):58-63.
- 19. Moon DH, Park CH, Kang DY, Lee HS, Lee S. Significance of the lobe-specific emphysema index to predict prolonged air leak after anatomical segmentectomy. PLoS One. 2019;14(11):e0224519.
- 20. Murakami J, Ueda K, Tanaka T, Kobayashi T, Hamano K. Grading of Emphysema Is Indispensable for Predicting Prolonged Air Leak After Lung Lobectomy. Ann Thorac Surg. 2018;105(4):1031-7.
- 21. Global burden of 87 risk factors in 204 countries and territories, 1990-2019: a systematic analysis for the Global Burden of Disease Study 2019. Lancet. 2020;396(10258):1223-49.
- 22. DeCamp MM, Blackstone EH, Naunheim KS, Krasna MJ, Wood DE, Meli YM, McKenna RJ, Jr. Patient and surgical factors influencing air leak after lung volume reduction surgery: lessons learned from the National Emphysema Treatment Trial. Ann Thorac Surg. 2006;82(1):197-206; discussion -7.
- 23. Elsayed H, McShane J, Shackcloth M. Air leaks following pulmonary resection for lung cancer: is it a patient or surgeon related problem? Ann R Coll Surg Engl. 2012;94(6):422-7.
- 24. Cerfolio RJ. The incidence, etiology, and prevention of postresectional bronchopleural fistula. Semin Thorac Cardiovasc Surg. 2001;13(1):3-7.
- 25. Sakata KK, Reisenauer JS, Kern RM, Mullon JJ. Persistent air leak review. Respir Med. 2018;137:213-8.
- 26. Singhal S, Shrager JB. Should buttresses and sealants be used to manage pulmonary parenchymal air leaks? J Thorac Cardiovasc Surg. 2010;140(6):1220-5.
- 27. Eberlein M, Parekh KR, Keech J, Redwan B, Bolukbas S. Prolonged Air Leak After Lung Resection and Emphysema. Ann Thorac Surg. 2017;104(2):723-4.
- 28. Nicotera SP, Decamp MM. Special situations: air leak after lung volume reduction surgery and in ventilated patients. Thorac Surg Clin. 2010;20(3):427-34.
- 29. Cho MH, Malhotra A, Donahue DM, Wain JC, Harris RS, Karmpaliotis D, Patel SR. Mechanical ventilation and air leaks after lung biopsy for acute respiratory distress syndrome. Ann Thorac Surg. 2006;82(1):261-6.
- 30. Akoumianaki E, Maggiore SM, Valenza F, Bellani G, Jubran A, Loring SH, et al. The application of esophageal pressure measurement in patients with respiratory failure. Am J Respir Crit Care Med. 2014;189(5):520-31.
- 31. Cerfolio RJ, Bass C, Katholi CR. Prospective randomized trial compares suction versus water seal for air leaks. Ann Thorac Surg. 2001;71(5):1613-7.
- 32. Mentzer SJ, Tsuda A, Loring SH. Pleural mechanics and the pathophysiology of air leaks. J Thorac Cardiovasc Surg. 2018;155(5):2182-9.
- 33. Glazier JB, Hughes JM, Maloney JE, West JB. Vertical gradient of alveolar size in lungs of dogs frozen intact. J Appl Physiol. 1967;23(5):694-705.
- 34. Pompili C, Miserocchi G. Air leak after lung resection: pathophysiology and patients' implications. J Thorac Dis. 2016;8(Suppl 1):S46-54.
- 35. Mutsaers SE, Prêle CM, Lansley SM, Herrick SE. The origin of regenerating mesothelium: a historical perspective. Int J Artif Organs. 2007;30(6):484-94.

- 36. Raphael Rubin DSS. Rubin's Pathology: Clinicopathologic Foundations of Medicine. Rubin's Pathology: Clinicopathologic Foundations of Medicine. Sixth edition ed: Wolters Kluwer; 2012.
- 37. Walter F. Boron ELB. Medical Physiology Medical Physiology 3rd edition ed: Elsevier 2017.
- 38. Ma H, Fujioka H, Halpern D, Gaver DP, 3rd. Surfactant-Mediated Airway and Acinar Interactions in a Multi-Scale Model of a Healthy Lung. Front Physiol. 2020;11:941.
- 39. McCool FD. Global physiology and pathophysiology of cough: ACCP evidence-based clinical practice guidelines. Chest. 2006;129(1 Suppl):48s-53s.
- 40. Chang PC, Chen KH, Jhou HJ, Lee CH, Chou SH, Chen PH, Chang TW. Promising Effects of Digital Chest Tube Drainage System for Pulmonary Resection: A Systematic Review and Network Meta-Analysis. J Pers Med. 2022;12(4).
- 41. Macchiarini P, Wain J, Almy S, Dartevelle P. Experimental and clinical evaluation of a new synthetic, absorbable sealant to reduce air leaks in thoracic operations. J Thorac Cardiovasc Surg. 1999;117(4):751-8.
- 42. Anegg U, Lindenmann J, Matzi V, Smolle J, Maier A, Smolle-Jüttner F. Efficiency of fleecebound sealing (TachoSil) of air leaks in lung surgery: a prospective randomised trial. Eur J Cardiothorac Surg. 2007;31(2):198-202.
- 43. Zaraca F, Brunelli A, Pipitone MD, Abdellateef A, Abu Akar F, Augustin F, et al. A Delphi Consensus report from the "Prolonged Air Leak: A Survey" study group on prevention and management of postoperative air leaks after minimally invasive anatomical resections. Eur J Cardiothorac Surg. 2022.
- 44. Kim WH, Lee HC, Ryu HG, Yoon HK, Jung CW. Intraoperative ventilatory leak predicts prolonged air leak after lung resection: A retrospective observational study. PLoS One. 2017;12(11):e0187598.
- 45. Brunelli A, Salati M, Pompili C, Gentili P, Sabbatini A. Intraoperative air leak measured after lobectomy is associated with postoperative duration of air leak. Eur J Cardiothorac Surg. 2017;52(5):963-8.
- 46. Zhang R, Bures M, Höffler K, Jonigk D, Haverich A, Krueger M. In vitro comparison of two widely used surgical sealants for treating alveolar air leak. Thorac Cardiovasc Surg. 2014;62(8):705-9.
- 47. Shigeeda W, Deguchi H, Tomoyasu M, Kaneko Y, Kanno H, Tanita T, Saito H. The utility of the Stapler with PGA sheet for pulmonary wedge resection: a propensity score-matched analysis. J Thorac Dis. 2019;11(4):1546-53.
- 48. Bouten PJM, Zonjee M, Bender J, Yauw STK, van Goor H, van Hest JCM, Hoogenboom R. The chemistry of tissue adhesive materials. Progress in Polymer Science. 2014;39(7):1375-405.
- 49. Ono K, Ishihara M, Ozeki Y, Dequchi H, Sato M, Saito Y, et al. Experimental evaluation of photocrosslinkable chitosan as a biologic adhesive with surgical applications. Surgery. 2001;130(5):844-50.
- 50. Rocco G, Rendina EA, Venuta F, Mueller MR, Halezeroglu S, Dienemann H, et al. The use of sealants in modern thoracic surgery: a survey. Interact Cardiovasc Thorac Surg. 2009;9(1):1-3.
- 51. Rena O, Papalia E, Mineo TC, Massera F, Pirondini E, Turello D, Casadio C. Air-leak management after upper lobectomy in patients with fused fissure and chronic obstructive pulmonary disease: a pilot trial comparing sealant and standard treatment. Interact Cardiovasc Thorac Surg. 2009;9(6):973-7.

- 52. Shigemura N, Akashi A, Nakagiri T, Ohta M, Matsuda H. A new tissue-sealing technique using the Ligasure system for nonanatomical pulmonary resection: preliminary results of sutureless and stapleless thoracoscopic surgery. Ann Thorac Surg. 2004;77(4):1415-8; discussion 9.
- 53. Schiavon M, Marulli G, Zuin A, Lunardi F, Villoresi P, Bonora S, et al. Experimental evaluation of a new system for laser tissue welding applied on damaged lungs. Interact Cardiovasc Thorac Surg. 2013;16(5):577-82.
- 54. Pandey N, Soto-Garcia LF, Liao J, Philippe Z, Nguyen KT, Hong Y. Mussel-inspired bioadhesives in healthcare: design parameters, current trends, and future perspectives. Biomater Sci. 2020;8(5):1240-55.
- 55. Malapert G, Hanna HA, Pages PB, Bernard A. Surgical sealant for the prevention of prolonged air leak after lung resection: meta-analysis. Ann Thorac Surg. 2010;90(6):1779-85.
- 56. McGuire AL, Yee J. Clinical outcomes of polymeric sealant use in pulmonary resection: a systematic review and meta-analysis of randomized controlled trials. J Thorac Dis. 2018;10(Suppl 32):S3728-s39.
- 57. Pedersen TB, Honge JL, Pilegaard HK, Hasenkam JM. Comparative study of lung sealants in a porcine ex vivo model. Ann Thorac Surg. 2012;94(1):234-40.
- 58. Belda-Sanchis J, Serra-Mitjans M, Iglesias Sentis M, Rami R. Surgical sealant for preventing air leaks after pulmonary resections in patients with lung cancer. Cochrane Database Syst Rev. 2010(1):Cd003051.
- 59. Zhou J, Lyu M, Pang L, Gao Y, Ning K, Wang Z, Liu L. Efficiency and safety of TachoSil® in the treatment of postoperative air leakage following pulmonary surgery: a meta-analysis of randomized controlled trials. Jpn J Clin Oncol. 2019;49(9):862-9.
- 60. Zaraca F, Vaccarili M, Zaccagna G, Maniscalco P, Dolci G, Feil B, et al. Cost-effectiveness analysis of sealant impact in management of moderate intraoperative alveolar air leaks during video-assisted thoracoscopic surgery lobectomy: a multicentre randomised controlled trial. J Thorac Dis. 2017;9(12):5230-8.
- 61. Nederland Z. TACHOSIL WEEFSELLIJM MATRIX 9,5X4,8CM [Available from: https://www. medicijnkosten.nl/medicijn?artikel=TACHOSIL+WEEFSELLIJM+MATRIX+9%2C5X4%2C8 CM&id=bdf60190266605019055d1a26e5115c7.
- 62. Zaraca F, Pipitone M, Feil B, Perkmann R, Bertolaccini L, Curcio C, Crisci R. Predicting a Prolonged Air Leak After Video-Assisted Thoracic Surgery, Is It Really Possible? Semin Thorac Cardiovasc Surg. 2021;33(2):581-92.
- 63. Zaraca F, Vaccarili M, Zaccagna G, Maniscalco P, Dolci G, Feil B, et al. Can a standardised Ventilation Mechanical Test for quantitative intraoperative air leak grading reduce the length of hospital stay after video-assisted thoracoscopic surgery lobectomy? J Vis Surg. 2017;3:179.
- 64. Pompili C, Falcoz PE, Salati M, Szanto Z, Brunelli A. A risk score to predict the incidence of prolonged air leak after video-assisted thoracoscopic lobectomy: An analysis from the European Society of Thoracic Surgeons database. J Thorac Cardiovasc Surg. 2017;153(4):957-65.
- 65. Horowitz B, Busch M. Estimating the pathogen safety of manufactured human plasma products: application to fibrin sealants and to thrombin. Transfusion. 2008;48(8):1739-53.
- 66. Mels F, van Dort D. V+ model-a Medical Perspective for Device Development. Research in Medical & Engineering Sciences. 2020;8(5).
- 67. Araki M, Tao H, Nakajima N, Sugai H, Sato T, Hyon SH, et al. Development of new biodegradable hydrogel glue for preventing alveolar air leakage. J Thorac Cardiovasc Surg. 2007;134(5):1241-8.

- 68. Balakrishnan B, Payanam U, Laurent A, Wassef M, Jayakrishnan A. Efficacy evaluation of anin situforming tissue adhesive hydrogel as sealant for lung and vascular injury. Biomed Mater. 2021;16(4).
- 69. Joglekar MM, Slebos DJ, Leijten J, Burgess JK, Pouwels SD. Crosslink bio-adhesives for bronchoscopic lung volume reduction: current status and future direction. Eur Respir Rev. 2021;30(162).
- 70. Assmann A, Vegh A, Ghasemi-Rad M, Bagherifard S, Cheng G, Sani ES, et al. A highly adhesive and naturally derived sealant. Biomaterials. 2017;140:115-27.
- 71. Annabi N, Zhang YN, Assmann A, Sani ES, Cheng G, Lassaletta AD, et al. Engineering a highly elastic human protein-based sealant for surgical applications. Sci Transl Med. 2017;9(410).
- 72. Yamaoka M, Maki N, Wijesinghe A, Sato S, Yanagihara T, Kobayashi N, et al. Novel Alaska Pollock Gelatin Sealant Shows High Adhesive Quality and Conformability. Ann Thorac Surg. 2019;107(6):1656-62.
- 73. Petter-Puchner AH, Simunek M, Redl H, Puchner KU, Van Griensven M. A comparison of a cyanoacrylate glue (Glubran) vs. fibrin sealant (Tisseel) in experimental models of partial pulmonary resection and lung incision in rabbits. J Invest Surg. 2010;23(1):40-7.
- 74. Byrd RB, Burns JR. Cough dynamics in the post-thoracotomy state. Chest. 1975;67(6):654-7.
- 75. Marini JJ. Recruitment by sustained inflation: time for a change. Intensive Care Med. 2011;37(10):1572-4.
- 76. Kuo CY, Liu YT, Chen TS, Lam CF, Wu MC. A nationwide survey of intraoperative management for one-lung ventilation in Taiwan: time to accountable for diversity in protective lung ventilation. BMC Anesthesiol. 2020;20(1):236.
- 77. White RZ, Kerr L, White TJ, Sampson MJ. Review of topical gelatin-based haemostatic agents; an insidious culprit of intraoperative anaphylaxis? ANZ J Surg. 2021;91(10):2002-7.
- 78. Boerman MA, Van der Laan HL, Bender JCME, Hoogenboom R, Jansen JA, Leeuwenburgh SC, Van Hest JCM. Synthesis of pH- and thermoresponsive poly(2-n-propyl-2oxazoline) based copolymers. Journal of Polymer Science Part A: Polymer Chemistry. 2016;54(11):1573-82.
- 79. Hermanson GT. Chapter 3 The Reactions of Bioconjugation. In: Hermanson GT, editor. Bioconjugate Techniques (Third Edition). Boston: Academic Press; 2013. p. 229-58.
- 80. Lewis KM, Kuntze CE, Gulle H. Control of bleeding in surgical procedures: critical appraisal of HEMOPATCH (Sealing Hemostat). Medical devices (Auckland, NZ). 2015;9:1-10.
- 81. Boerman MA, Roozen E, Sánchez-Fernández MJ, Keereweer AR, Félix Lanao RP, Bender J, et al. Next Generation Hemostatic Materials Based on NHS-Ester Functionalized Poly(2oxazoline)s. Biomacromolecules. 2017;18(8):2529-38.
- Roozen EA, Warlé MC, Lomme R, Félix Lanao RP, van Goor H. New polyoxazoline loaded patches for hemostasis in experimental liver resection. J Biomed Mater Res B Appl Biomater. 2021.
- 83. Ethicon Introduces ETHIZIATM Hemostatic Sealing Patch, Clinically Proven to Stop Disruptive Bleeding [Available from https://www.jnj.com/ethicon-introduces-ethiziatmhemostatic-sealing-patch-clinically-proven-to-stop-disruptive-bleeding]. 2023.
- 84. Schebesch KM, Hrbac T, Jančálek R, Krska L, Marquez-Rivas J, Solar P. Real-World Data on the Usage of Hemopatch® as a Hemostat and Dural Sealant in Cranial and Spinal Neurosurgery. Cureus. 2023;15(1):e34387.

- 85. Bures M, Höffler HK, Friedel G, Kyriss T, Boedeker E, Länger F, et al. Albumin-glutaraldehyde qlue for repair of superficial lung defect: an in vitro experiment. J Cardiothorac Surg. 2016;11(1):63.
- 86. Itano H. The optimal technique for combined application of fibrin sealant and bioabsorbable felt against alveolar air leakage. Eur J Cardiothorac Surg. 2008;33(3):457-60.
- 87. Klassen C, Eckert CE, Wong J, Guyette JP, Harris JL, Thompson S, et al. Ex Vivo Modeling of Perioperative Air Leaks in Porcine Lungs. IEEE Trans Biomed Eng. 2018;65(12):2827-36.
- 88. Cárdenes N, Sembrat J, Noda K, Lovelace T, Álvarez D, Bittar HET, et al. Human ex vivo lung perfusion: a novel model to study human lung diseases. Sci Rep. 2021;11(1):490.
- 89. Weathington NM, Álvarez D, Sembrat J, Radder J, Cárdenes N, Noda K, et al. Ex vivo lung perfusion as a human platform for preclinical small molecule testing. JCI Insight. 2018;3(19).
- 90. Horvath MA, Hu L, Mueller T, Hochstein J, Rosalia L, Hibbert KA, et al. An organosynthetic soft robotic respiratory simulator. APL Bioeng. 2020;4(2):026108.
- 91. Hubrecht RC, Carter E. The 3Rs and Humane Experimental Technique: Implementing Change. Animals (Basel). 2019;9(10).



Chapter 2

Characterization of pulmonary air leak measurements using a mechanical ventilator in a bench setup

Bob P Hermans¹, Jeroen LM van Doorn², Lisanne H Roesthuis³, Jan Hofland⁴ Wilson WL Li¹, Daniël IM van Dort¹, Erik HFM. van der Heijden⁵, Harry van Goor⁶ and Ad FTM Verhagen¹

Radboud university medical center, Radboud Institute for Health Sciences, Nijmegen, The Netherlands.

¹Department of Cardio-thoracic surgery

³Department of Intensive Care

⁴Department of Anesthesiology

⁵Department of Pulmonology

⁶Department of General surgery

Radboud university medical center, Donders institute for Brain, Cognition and Behavior, Nijmegen, The Netherlands.

²Department of Neurology

Reprinted by permission of Informa UK Limited, trading as Taylor & Taylor & Francis Group, http://www.tandfonline.com from "Hermans BP, van Doorn JLM, Roesthuis LH, Hofland J, Li WWL, van Dort DIM, van der Heijden EHFM, van Goor H, Verhagen AFTM. Characterisation of pulmonary air leak measurements using a mechanical ventilator in a bench setup. J Med Eng Technol. 2024 Jul 25:1-11. doi: 10.1080/03091902.2024.2381540. © CC BY-NC-ND 4.0 [2024]." The version in this thesis differs slightly from the published version, after processing following peer review comments.

ABSTRACT

Prolonged air leakage (AL) following pulmonary resections leads to prolonged hospital stay and post-operative complications. Intra- and postoperative quantification of AL might be useful for improving treatment decisions, but these measurements have not been characterized. AL calculations based on inspiratory and expiratory tidal volumes were investigated in an Intensive Care Unit mechanical ventilator circuit (Servo-I). AL was also measured by a digital chest drainage system. This study shows that AL measurements increase in accuracy when corrected for baseline deviations (R: 0.904 > 0.997, p<0.001). Corrected measurements were most accurate when AL was >500 mL/min, with an estimated mean systemic bias of 7.4% (95%-limits of agreement [LoA]: 1.1%-13.7%) at 500 mL/min air leak. Breath-by-breath analysis showed most accurate results at AL >20 mL/breath (R: 0.989-0.991, p<0.001) at tidal volumes between 350-600 mL. The digital drain had a mean systemic bias of -11.1% (95%-LoA: -18.9% to -3.3%). This study indicates that the Servo-I can be used for air leak quantification in clinically relevant ranges (>500 mL/min), but is unsuited for small leak detection due to a detection threshold. Researchers and clinicians should be aware of varying accuracy and interoperability characteristics between AL measurement devices.

Introduction

The use of pulmonary air leak (AL) measurements is increasingly being reported to predict the occurrence of prolonged pulmonary air leakage (pPAL) following lung resections. (1-3) pPAL, defined as AL lasting longer than five days, affects 5.6-30% of patients. (4) This increases the risk for postoperative pulmonary and pleural complications such as empyema, mortality, length of chest drainage, hospital stay, hospital costs, readmissions and reinterventions. (5-9) Intraoperative AL measurements can be performed. deriving AL volumes from inspiratory (TVi) and expiratory (TVe) tidal volumes on a mechanical ventilator. (2, 3) Postoperatively, measurements can be derived from a digital chest drainage system. (10)

Objective digitalized measurements of AL may standardize clinical decisionmaking and reduce practice variation. (11-13) It offers a more reliable method of grading the severity of AL compared to conventional methods, such as the Macchiarini visual bubble scale used during water submersion tests, or the Cerfolio scale in the chest drain collection system. (12, 14, 15) Few clinical studies have been performed using intraoperative AL measurements, but all seem to indicate the potential for identifying patients at risk for pPAL. (2, 3)

A risk prediction model based on calculating intraoperative AL percentage of TVi, showed that AL >9.5% is predictive of pPAL. (2) Similarly, AL >500mL/min was demonstrated to be predictive of pPAL. (3) Another study showed that usage of a lung sealant based on ventilator measurements can be cost-effective. (11) Conversely, in preclinical animal studies testing lung sealing interventions, AL measurements are infrequently used. However, these may be useful for improving the quality and translational value, by ensuring clinically relevant AL and a reliable AL-reduction measurement from baseline values. (16, 17)

Despite preclinical and clinical relevance of AL measurements, the accuracy, reliability and interoperability of these measurements are not well known. Some studies reported modelling of AL during non-invasive ventilation (i.e. mask), but such leaks have different mechanics and lack a closed circuit. (18, 19) To illustrate a possible problem with AL measurements using a mechanical ventilator, consider that flow is generally measured using two separate channels for TVi and TVe. In such a setup, both measurement errors can add up when measuring AL as the difference between these volumes, and result in inaccuracies. Moreover, the measurement characteristics are selected to measure flows in the range of tidal volumes, and are not necessarily suited to detect small volumes associated with AL. Even in the context of measuring tidal volumes, a previous bench study has shown a large volume error between nine different ICU ventilators, possibly compromising interoperability of AL measurements.(20)

The aim of this study is to determine the most accurate AL measurement methodology, when using a ventilator. Furthermore, the accuracy of a digital chest drain system is tested.

Materials and methods

Experiments comparing a standardized and volumetrically calibrated AL measurement (Omron, model D6F-02A1-110, Omron Electronics, 0-2000mL/min, accuracy $\pm 3\%$ and reliability $\pm 0.3\%$) to four other AL measurement methodologies were performed in a mechanical ventilator (SERVO-I®, Getinge, Gotenburg, Sweden) bench setup. These methods were (1) mechanical ventilator monitor values, average AL over one (MV1) or (2) five breathing cycles (MV5)(2,3) and (3) continuous flow signal analysis over a proximal flow sensor (PROX, model SFM3300-D, Sensirion, ±250 slm, accuracy ±3%) or 4) the mechanical ventilator flow signal output (SERV). AL was calculated as an average flow in mL/min or in mL/breath in a breath-by-breath analysis. In addition, flow measurements provided by a digital drainage system (Thopaz®, Medela, Baar, Switzerland) are compared to the standardized AL measurement.

Measurement setup

In order to simulate AL, a bench setup with a mechanical ventilator circuit using a test lung which mimics physiological lung compliance (Delta Medic B.V., IJsselstein, the Netherlands) was used. An AL simulation side port was added, and all air flowing over this side port was measured directly using the Omron sensor, serving as the standard method to which the other AL quantification methods were compared. To adjust the AL magnitude, either mechanical ventilator settings determining the driving pressure (ΔP) or the configuration of the tubes determining the resistance (R) were adjusted. The same principle was used for the digital drain system validation setup. The experimental setups are shown in Figure 1 and all settings and configurations used for the measurements are shown in **Table 1**. In the configurations, AL was ensured to be below 2000mL/ min, to stay within the critical measurement limits of the Omron flow sensor.

Measurement protocol

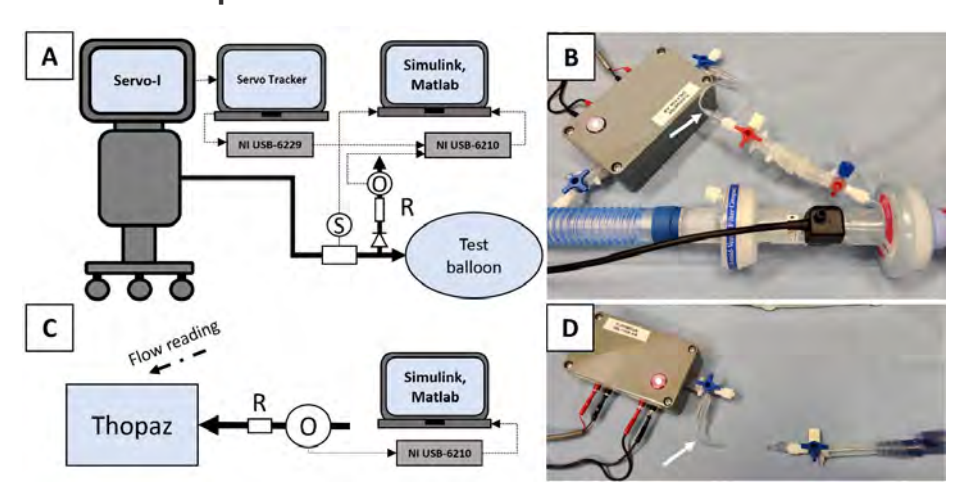


Figure 1: Experimental setup. A) Schematic of mechanical ventilation circuit (S = proximal flow sensor [PROX], O = standardized air leak detection flow sensor [Omron], R = resistance) and B) Photograph of the relevant connections. The standard resistance trough the AL side port is formed by four three-way luer locks and a one-way valve. The thin piece of tubing (white arrow) is swapped out to configure the resistance (Table 1). C) Schematic and D) photograph of the Thopaz® setup. The standard resistance consists of three three-way luer locks and the thin piece of tubing (white arrow) is swapped out to configure the resistance (Table 1).

Firstly, to explore measurement characteristics, various settings were tested for each measurement method, calculating AL in mL/min for 10 measurements per settings and 60 seconds per measurement unless otherwise stated. During each measurement cycle, the baseline was first determined with the AL side port closed, followed by AL simulation. Secondly, AL was recorded in mL/breath comparing the mechanical ventilator monitor readings to the Omron measurement for 30 breaths per setting. Finally, aerostatic efficacy outcomes were measured. AL-reduction was measured on the mechanical ventilator by measuring baseline, AL and reduced AL (extra resistance component).

For the digital drain system measurements, three separate calibrated drainage devices were evaluated at 9 measurements each (Supplement 2A). At each setting, the system was first allowed to stabilize, after which the flow was observed from the monitor, and the Omron sensor was used to measure for 30 seconds. Before every experiment, airtightness was ensured by applying soap solution on all made connections, with system pressures exceeding those of the intended protocol settings. The protocol settings are listed in **Table 1**.

Table 1: Measurement configurations

	Pressure settings (ΔP)	Resistance components (R) ¹				
Air leak measurements using mechanical ventilator						
Small leak (SL)	RR 12/min, I:E 1:2, FiO ₂ 21%, PEEP 5 cmH20 Variable: PC 10/20/30 cmH20	Luer-lock tube (10 cm, 0.9 mm∅)				
Big leak (BL)	RR 12/min, I:E 1:1, FiO_2 21%, PEEP 4cmH2O, Variable: PC 8/12/16 cmH2O	No extra components				
VC/no PEEP	RR 12/min, FiO ₂ 21%, PEEP 0 cmH20 Variable: I:E 1:2/VC 700 mL, I:E 1:1/VC 850 mL	No extra components				
30s vs 90s	RR 12/min, I:E 1:2, FiO_2 21%, PEEP 5 cmH20, PC 20 cmH20	Luer-lock tube (10 cm, 0.9 mm∅)				
Mechanical ventilator breath-by-breath analysis						
Breath-by- breath	RR 12/min, I:E 1:1, FiO ₂ 21%, PEEP 5 cmH20, Tpause 10% Variable: tidal volume 300/350/400/450/500/550/600 mL	Small leak: luer-lock tube (10 cm, 0.9 mmø) Medium leak: luer-lock tube (30 cm, 1.8 mmø) Big leak: No extra components				
Aerostatic efficacy outcomes						
AL-reduction	RR 12/min, I:E 1:1, FiO ₂ 21%, PEEP 4 cmH2O, PC 12 cmH2O	100% leak: no extra components 50% leak: 2x luer-lock tube (30cm, 1.8mmø)				
Thopaz validatio	n setup					
High resistance	-1, -5, -10, -15 and -20 cmH2O	Luer-lock tube (10 cm, 0.9 mmø)				
Low resistance	-3, -5, -10 and -15 cmH2O	One extra 3-way luer lock				

¹Standard resistive components are shown in figure 1.

RR = respiratory rate; I:E = inspiratory:expiratory ratio; PEEP = positive end expiratory pressure; PC = pressure control setting above PEEP; VC = volume control

Data-acquisition

For the Omron measurement, sensor output is recorded into Simulink, Matlab (version R2020/2021a). Tidal volumes displayed on the mechanical ventilator monitor were manually noted for the MV1 and MV5 measurements. To ensure repeatable measurements, the mechanical ventilator internal calibration was executed before every series of measurements, and compensation for compressible volume was always turned on. During breath-by-breath acquisition from the mechanical ventilator monitor, a custom optical character recognition (OCR) algorithm was developed using Matlab (Figure 2, Supplement 2A). The PROX and SERV measurement output is acquired using dedicated software (ControlCenter and ServoTracker respectively), and the SERV output is additionally recorded into the Simulink model. For digital drain system measurements, the flow values are noted from the monitor once a stable value is reached (displayed in 10mL steps at 0-1000mL/min and 100mL steps at >1000mL/min). Data-acquisition details and calibrations are described in Supplement 2A.

Data processing

Data processing was performed using Matlab (version R2021a). AL (mL/min) was calculated from the mechanical ventilator monitor as:

$$AL = \frac{\sum_{k=1}^{n} (TVi_k - TVe_k)}{n} \times f \tag{1}$$

where k denotes the breath index, n the number of breaths used for the average and f the respiratory frequency in breaths/min. MV1 and MV5 were calculated for n=1 and n=5, respectively. (3) AL (in mL/min) was derived from the Omron, PROX and SERV flow signals (\dot{V}) using the following calculation:

$$AL = \frac{\int_a^b \dot{v} \, dt}{\Delta t} \tag{2}$$

The integral was calculated using the "cumulative numeric trapezoid integral" function in Matlab, and the measurement interval (a, b) was manually selected, from which Δt was derived (**Figure 2**). In the breath-by-breath analysis protocol, a peak detection algorithm using Matlab was used to identify individual breaths for AL calculation. The PROX sensor measured flow in standard litres per minute (\dot{V}_{std}) , which was corrected to give a volumetric flow measure at ambient temperature (\dot{V}_{vol}) for comparison to the other measures, using the following formula:

$$\dot{V}_{vol} = \dot{V}_{std} \times \frac{T}{273.15} \tag{3}$$

where T is the mean temperature acquired by the flow sensor over the measurement period in Kelvin. The pressure changes during mechanical ventilation around atmospheric pressure were excluded from this calculation, as they were calculated to be negligible in the combined gas law. AL values were also corrected for baseline measurements as $AL_c = AL_{leak} - AL_{Baseline}$. AL percentage per breath of TVi was calculated as(2):

$$AL\%_k = \frac{TVi_k - TVe_k}{TVi_k} \times 100 \tag{4}$$

Statistical analysis

Statistical analysis was performed using IBM SPSS Statistics for Windows, Version 26.0 (Armonk, New York; IBM Corp). Measurement accuracy was assessed by comparing differences to the control measurement (Omron). Correlations were computed using Pearson's R and statistically compared using a web-based tool of the cocor R package. (21,22) Measurement precision was assessed by computing a mean centred coefficient of variation. Statistical comparisons for AL accuracy and precision were performed using an ANOVA and Tukey's post-hoc test. For AL-reduction, variances were compared using Levene's test and differences versus Omron with a one-sample t-test, and both adjusted for multiple testing using a Bonferroni-Holm method. (23) Tests are performed two-tailed with α =0.05. In the breath-by-breath analysis, linear regression fits were calculated using Matlab (version R2021a, Supplement 2B). Bland-Altman plots were generated using Graphpad Prism 9. In case of an inhomogeneous scatter, the limits of agreement were estimated based on a variable variance function developed in Matlab for this purpose (Supplement 2B).

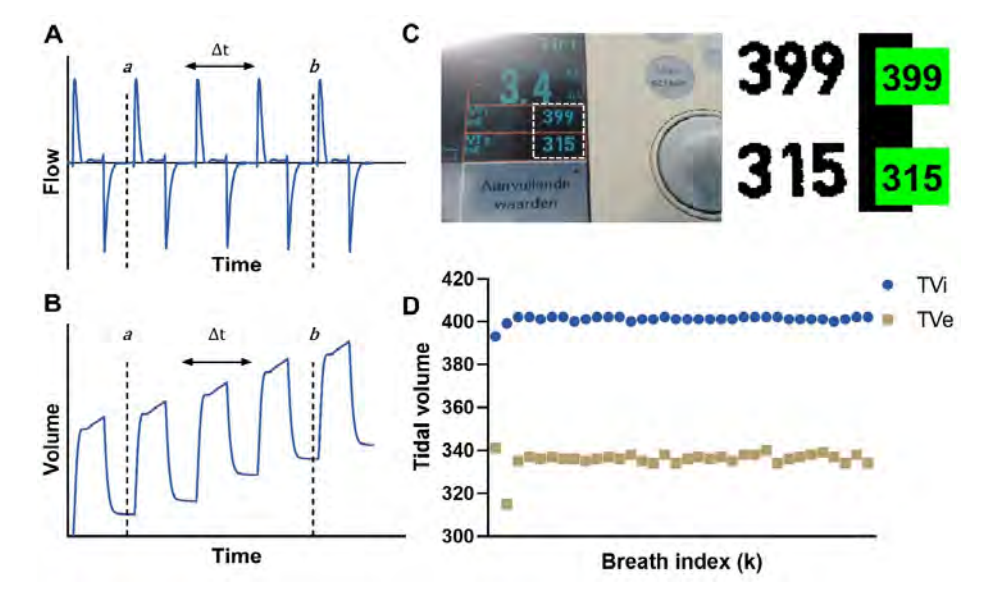


Figure 2: A/B) Representative example of the air leak calculations from a flow signal (A) using a cumulative integral (B). In selecting the measurement period, care is taken that both the start and end indices are either at a local maxima or local minima. C) Screenshot from the control algorithm of the custom built OCR application, allowing for breath by breath analysis. Values in green boxes are calculated by the algorithm and checked for correctness by the experiment executor, and stored per breath to allow continuous monitoring (D).

Results

Air leak measurements using mechanical ventilator

AL was produced in the range of 168-941 mL/min as measured by Omron, with a low coefficient of variation (CV) (mean: 0.011, 95%-CI: 0.002-0.021). The accuracy of the mechanical ventilator methods varied based on the measurement protocol used (Figure 3). Correction for baseline measurements resulted in a significantly improved correlation between Omron and MV1 (R: 0.901 > 0.974, p<0.001), MV5 (R: 0.904 > 0.997, p<0.001), PROX (R: 0.876)> 0.951,p<0.001), but not for SERV (R: 0.823 > 0.849, p=0.39). Correction for baseline also significantly increased precision in PROXc (p=0.023) and SERVc (p=0.025), but not MV1c (p=0.608) and MV5c (p=0.487). The correlation between Omron and MV5c (R: 0.997) was significantly stronger compared to MV1c (R: 0.974, p<0.001), PROXc (R: 0.951, p<0.001) and SERVc (R: 0.849, p<0.001).

MV5c showed the highest precision (CV mean: 0.076, 95%-CI: 0.039-0.113), which was significantly better compared to PROXc (CV mean 0.279, 95%-CI 0.152-0.406, p=0.042) and SERVc (CV mean: 0.431, 95%-CI: 0.244-0.618, p<0.001), but not compared to MV1c (CV mean: 0.108, 95%-CI 0.054-0.161, p=0.97). MV1c was also more precise compared to SERVc (p<0.001), but not PROXc (p=0.108). Bland-Altman plots of MV1c and MV5c (corrected for baseline deviations) revealed an inhomogeneous scatter with a funnel shape, with wider LoA at lower averages (Figure 3B/D). At 500mL/min average AL, the estimated mean bias compared to Omron was 7.4% (estimated 95% LoA 1.1%-13.7%) for MV5c.

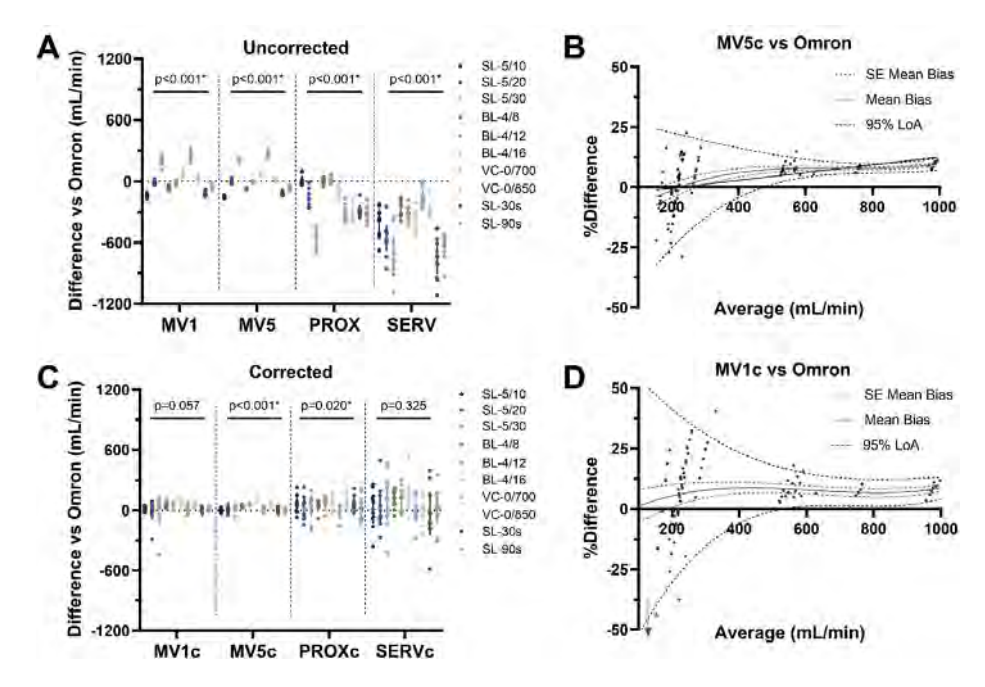


Figure 3: A/C) Difference of mechanical ventilator methods versus Omron, uncorrected **(A)** and corrected **(C)** for baseline deviations. **B/D)** Bland-Altman plots of MV1c and MV5c versus Omron, which are both corrected for baseline deviations.

MV = mechanical ventilator, PROX = proximal flow sensor, SERV = SERVO-I[®] mechanical ventilator flow signal analysis, c = corrected for baseline deviations.

Mechanical ventilator breath-by-breath analysis

Breath-by-breath analysis of mechanical ventilator readings using OCR, showed a strong and statistically significant correlation with Omron over all settings (R: 0.985, p<0.001). Upon subgroup-analysis, correlations (Pearson's R) were found significantly stronger for medium (R: 0.991, p<0.001) and large leak (R: 0.989, p<0.001) settings, corresponding to >20mL AL/per breath, compared to small leak settings (R: 0.733). Measurement of AL between \sim 5% and \sim 15% of the TVi were found to be accurate within \sim 1% of the tidal volume between 350-600mL TVi (**Figure 4**).

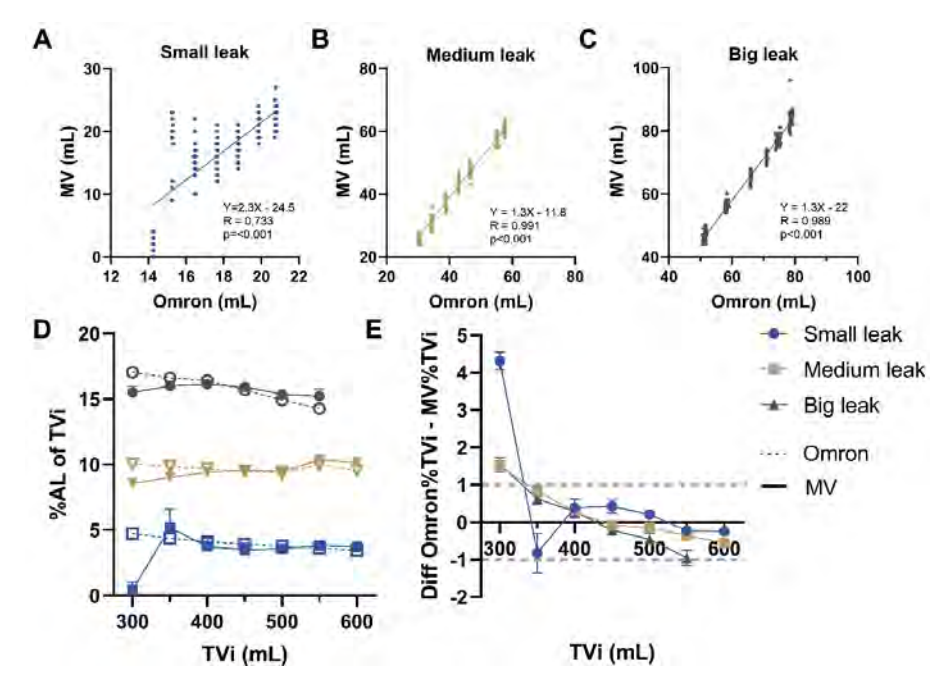


Figure 4: Breath-by-breath analysis results A/B/C) Correlation between standardized AL measurements and the mechanical ventilator readings D) Calculated AL percentage of inspiratory tidal volume (TVi) for standardized measurement (Omron) versus the mechanical ventilator readings (MV) and E) Absolute differences based on D. Dotted lines show borders for a ±1% absolute difference.

Aerostatic efficacy outcome measures

Omron measured an AL reduction of 47.9% (95%-CI: 47.4-48.4%) with a low CV (0.015). When uncorrected for baseline deviations, AL reduction was significantly different between Omron and MV1 (mean -11.5%, 95%-CI -13.8--9.3%, p=0.004), MV5 (mean -10.9%, 95%-CI -11.9- -9.9%, p=0.003) and SERV (mean -118.8%, 95%-CI -160.6- -77.1%, p=0.002) (**Figure 5A**). When corrected for baseline, there were no significant differences (Figure 5B). Consistent with prior results, the highest precision was found for MV5c (48.8±0.9%, CV: 0.018) versus MV1c (49.2±3.0%, CV: 0.062, p=0.03), PROXc (50.9±9.2%, CV: 0.181, p=0.008) and SERVc (47.1±20.6%, CV: 0.437, p=0.005).

The digital chest drain system was found to have a strong and significant correlation to Omron over a measurement range of 0-2000mL/min (R: 0.999, p<0.001). In the Bland-Altman analysis for the digital drain, a mean systemic bias compared to Omron of -11.1% (95% LoA: -18.9% to -3.3%) with homogeneous scatter was observed (Figure 5C/D).

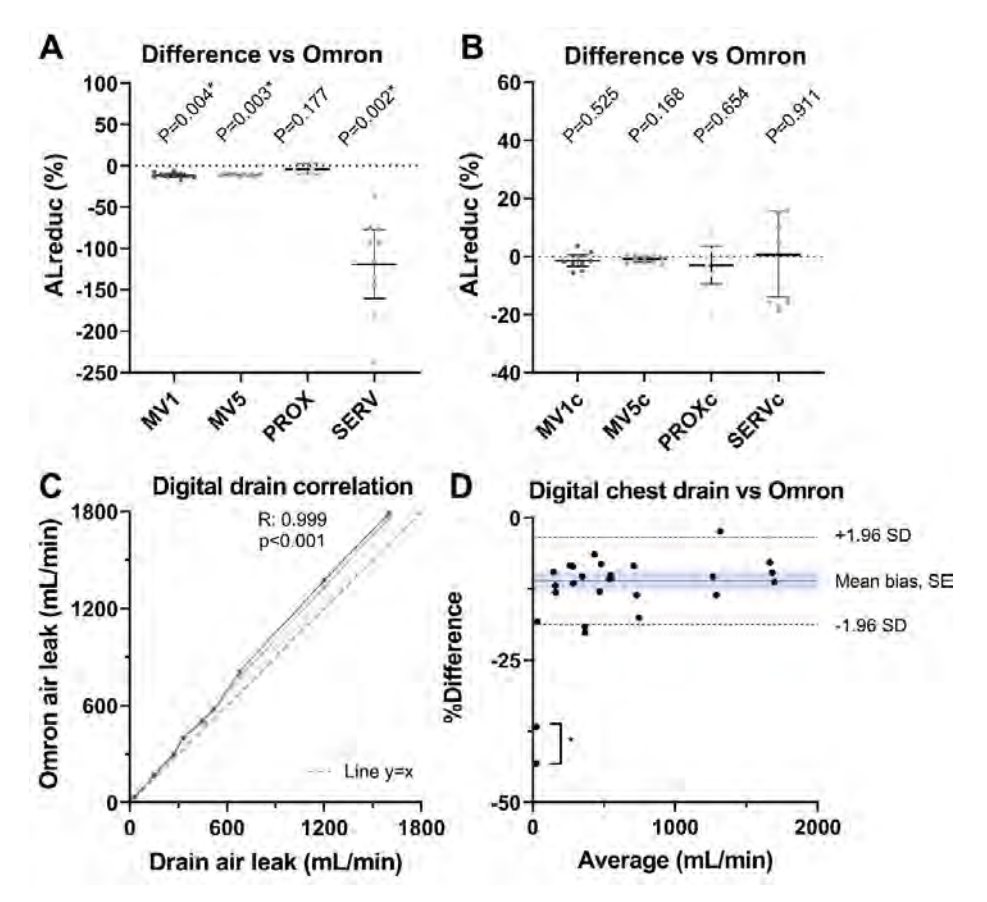


Figure 5: A/B) Air leak reduction (ALreduc%) measurements comparison, standardized measurement (Omron) versus mechanical ventilator methods, uncorrected (A) and corrected (B) for baseline deviations. C) Correlation between digital chest drain readings and standardized flow measurements, each line corresponding to a unique drainage system (N=3). D) Bland-Altman analysis of digital chest drain readings, showing a homogenous scatter. *N=2 outliers excluded for construction of mean and limits of agreement.

Discussion

In this study, we measured AL using several methods, comparing their measurement characteristics. We demonstrate that AL calculations based on flow signal analysis methods (PROX and SERV) were less precise compared to tidal volume data displayed on the mechanical ventilator monitor. Breath-by-breath analysis indicated most accurate measurements when the AL is >20mL/breath, in tidal volume ranges of 350 to 600mL. Measurement of smaller AL resulted in inaccurate measurements, indicative of a detection threshold.

Correction for baseline deviations was shown to improve the accuracy of Al measurements.

Interpretation of results

The direct AL measurement Omron has been volumetrically calibrated and shows a high measurement precision, and is therefore suited as a control for the other methods that were used. MV1 and MV5 are both based on the tidal volumes displayed on the mechanical ventilator, and show the highest measurement precision of all methods. In this regard, MV1 is more sensitive to outliers compared to MV5, due to averaging over less breaths. PROX measures tidal flow proximal to the endotracheal tube in both directions, but was found to have a lower precision compared to MV5. Similarly, SERV calculations were based on tidal flow data extracted from the mechanical ventilator, but these also showed significantly lower precision compared to MV5. An advantage of flow signal analysis methods is that large amounts of data can readily be acquired, which was also achieved in these experiments using a custom OCR tool on the mechanical ventilator screen in the breath-by-breath analysis. Finally, the digital chest drainage system was found to result in reliable measurements of AL, with a systemic measurements bias that should be addressed based on the gas flow measurement conditions and conventions used.

The MV5 measurement exhibits a detection threshold, below which it is unsuited to detect the presence of, or rule out small AL. Based on the breathby-breath analysis, this threshold lies around 20mL/breath. This is likely explained by measurement errors of the inspiratory and expiratory flow channels exceeding the magnitude of the AL. Computer simulations support this hypothesis, revealing a similar funnel shape as seen in the experimental data (Supplement 2C). Thus, for the purpose of intraoperative detection of AL, other techniques are required. Most commonly, a water submersion test is used, but this has disadvantages during thoracoscopic surgery due to limited vision. Here, novel methods such as CO₂ insufflation or indocyanine green aerosols may provide a better alternative. (24,25)

The MV5 measurement can be used for AL quantification and thus stratification of risk groups based on AL size. However, AL still need to surpass the detection threshold associated with mechanical ventilator measurements. A recent Delphi study proposed classification of mild (100mL/min), moderate (100-400mL/min) and severe (>400mL/min) AL.(1) Depending on the respiratory rate and AL/breath, mild and moderate AL might be difficult to distinguish, but

severe AL should be accurately identifiable. This should also be the case for the AL magnitudes of >500mL/min or >9.5% of TVi that were previously found predictive of pPAL. (2,3)

When using different methods for AL characterisation and risk prediction, an empirical correction factor is required and should be obtained for different devices. As we have shown in comparison to Omron, the MV5 method might overestimate AL ~10%, depending on the AL size, while the digital drainage system might underestimate AL~10%, independent of the AL size. Additionally, previous literature shows a large variability for different mechanical ventilators or measurement methods when quantifying tidal volumes. (20,26) It is important that researchers and clinicians use the same calibrations and definitions for AL, to ensure global interoperability between devices, hospitals and research findings.

AL can accurately be measured in an automated fashion, which can easily be implemented in present experimental studies using a simple OCR setup. Experimental studies investigating lung sealing devices and quantifying AL as outcome measure are scarce, while this outcome measure is of high clinical relevance for measuring aerostatic efficacy. (17,27,28) Failure to use clinically relevant outcome measures might contribute to poor translational power of animal studies, raising ethical concerns. (29) This digitalized method is advantageous over methods used previously, such as a water displacement method or aspiration of air from plastic bags using syringes, by reducing interobserver variability. (16,30,31) Other ex-vivo experimental studies have described AL quantification systems, which may be useful for validating further AL measurement methodologies. (32,33)

Clinical implications

Clinical studies investigating lung sealing devices may benefit from accurate measurement of AL, by improving objective subject recruitment. This possibility has been shown in a recent clinical trial, using a standardized mechanical ventilator test and only applying lung sealants to AL 150-400mL/min or to AL >400mL/min that were downgraded first using sutures and staplers, showing cost-effective use. (11) No such positive effect was observed in a retrospective study with the same lung sealant, in which no selection algorithm was applied. (34) Another trial used intra-operative AL severity criteria, but based on the visual Macchiarini air bubble scale. (35) This is more prone to inter-observer variability and can thus be improved using AL quantification methods.

In order to translate the present experimental findings to a clinical surgical setting, several technical factors should be considered. First of all, the system should be free of leaks, except for the leak of the lung. For this, all external connections should be checked carefully and the cuff pressure of the endotracheal tube should be at least above the peak ventilation pressure. However, a constant leak originating from elsewhere may also be solved by continuous measurements and correcting AL for baseline deviations. Secondly, a state of stable ventilation should be reached. When atelectasis is still being reduced, the TVi will be increased compared to the TVe as a consequence of the inflation of previously collapsed alveoli, overestimating the actual AL. The inverse is true when trapped air escapes from the lung. Finally, the AL should preferably be measured over a standardized interval of at least five breaths such as in MV5, with standardized settings, to prevent influence form outliers and errors, thus providing the highest accuracy. (3,36)

When measuring gas flow under clinical conditions, the measurement characteristics may theoretically vary up to ~10% due to the combined gas laws, if unaccounted for. In the mechanical ventilator-patient-drain interface, temperature and pressure are never constant, and therefore the volume of air may vary accordingly. The following equation is derived from the combined das law:

$$\frac{V_2}{V_1} = \frac{T_1 + \Delta T}{P_1 + \Delta P} \times \frac{P_1}{T_1} \tag{5}$$

Assuming the highest pressure conditions ($\Delta P=40 \text{cmH}_2 O=0.0387 \text{atm}$, $P_1=1 \text{atm}$) and lowest temperature conditions ($\Delta T = -17K$, $T_1 = 310.15K$) in the physiological patient/machine interface⁽³⁷⁾, we calculate the highest value of V_2/V_1 to be 91%. To improve interoperability between different measurements in this context, values of all devices should be normalized by also measuring temperature and pressure, using the same conventions.

Limitations

As with all bench studies, the findings might not generalize to clinical situations, and should be further investigated in ventilated lungs. Furthermore, these findings might not translate to other devices using different sensors. Measurement characteristics should be attained empirically, to allow for accurate and interoperable use. The standardized flow sensor used for comparison in this study has a high reliability, and is therefore most suited to assess the precision of the AL measurement. The flow sensor was calibrated

to measure standard volumes of air under ambient conditions, which may not be the best method for assessing validity. This should be improved by applying standardized normalization conventions using temperature and pressure measurements

Future perspective

This study provides an experimental and theoretical basis for further development of intraoperative AL quantification algorithms. Accurate detection of AL with the mechanical ventilator should be ensured by standardized settings and intervals, stable respiration, normalization and suited sensors (i.e. low measurement error). Continuous measurements may improve measurement accuracy, by providing a baseline correction capability. Prediction models for pPAL based on pre- and intraoperative characteristics should be further developed to allow for an integrated digital system which can be used to aid in surgical decision-making. (2,11,38)

Conclusion

In conclusion, AL quantification can be reliably performed based on tidal volume data on the SERVO-I® mechanical ventilator within certain tidal volume ranges (350-600mL), in AL >20mL/breath. To measure smaller AL values and overcome the detection threshold using a mechanical ventilator, flow sensors with smaller measurement errors are required.

References

- Zaraca F, Brunelli A, Pipitone MD, Abdellateef A, Abu Akar F, Augustin F, et al. A Delphi Consensus report from the "Prolonged Air Leak: A Survey" study group on prevention and management of postoperative air leaks after minimally invasive anatomical resections. Eur J Cardiothorac Surg. 2022.
- Kim WH, Lee HC, Ryu HG, Yoon HK, Jung CW. Intraoperative ventilatory leak predicts prolonged air leak after lung resection: A retrospective observational study. PLoS One. 2017;12(11):e0187598.
- Brunelli A, Salati M, Pompili C, Gentili P, Sabbatini A. Intraoperative air leak measured after lobectomy is associated with postoperative duration of air leak. Eur J Cardiothorac Surg. 2017;52(5):963-8.
- Attaar A, Tam V, Nason KS. Risk Factors for Prolonged Air Leak After Pulmonary Resection: A Systematic Review and Meta-analysis. Ann Surg. 2020;271(5):834-44.
- Liang S, Ivanovic J, Gilbert S, Maziak DE, Shamji FM, Sundaresan RS, Seely AJE. Quantifying the incidence and impact of postoperative prolonged alveolar air leak after pulmonary resection. J Thorac Cardiovasc Surg. 2013;145(4):948-54.
- Brunelli A, Xiume F, Al Refai M, Salati M, Marasco R, Sabbatini A. Air leaks after lobectomy increase the risk of empyema but not of cardiopulmonary complications: a case-matched analysis. Chest. 2006;130(4):1150-6.
- Yoo A, Ghosh SK, Danker W, Kassis E, Kalsekar I. Burden of air leak complications in thoracic surgery estimated using a national hospital billing database. Clinicoecon Outcomes Res. 2017;9:373-83.
- Brunelli A, Chapman K, Pompili C, Chaudhuri N, Kefaloyannis E, Milton R, et al. Ninetyday hospital costs associated with prolonged air leak following lung resection. Interact Cardiovasc Thorac Surg. 2020;31(4):507-12.
- Attaar A, Luketich JD, Schuchert MJ, Winger DG, Sarkaria IS, Nason KS. Prolonged Air Leak After Pulmonary Resection Increases Risk of Noncardiac Complications, Readmission, and Delayed Hospital Discharge: A Propensity Score-adjusted Analysis. Ann Surg. 2021;273(1):163-72.
- 10. Goto M, Aokage K, Sekihara K, Miyoshi T, Tane K, Yokoi K, Tsuboi M. Prediction of prolonged air leak after lung resection using continuous log data of flow by digital drainage system. Gen Thorac Cardiovasc Surg. 2019;67(8):684-9.
- 11. Zaraca F, Vaccarili M, Zaccagna G, Maniscalco P, Dolci G, Feil B, et al. Cost-effectiveness analysis of sealant impact in management of moderate intraoperative alveolar air leaks during video-assisted thoracoscopic surgery lobectomy: a multicentre randomised controlled trial. J Thorac Dis. 2017;9(12):5230-8.
- 12. Chang PC, Chen KH, Jhou HJ, Lee CH, Chou SH, Chen PH, Chang TW. Promising Effects of Digital Chest Tube Drainage System for Pulmonary Resection: A Systematic Review and Network Meta-Analysis. J Pers Med. 2022;12(4).
- 13. Hoeijmakers F, Hartemink KJ, Verhagen AF, Steup WH, Marra E, Röell WFB, et al. Variation in incidence, prevention and treatment of persistent air leak after lung cancer surgery. Eur J Cardiothorac Surg. 2021.
- 14. Macchiarini P, Wain J, Almy S, Dartevelle P. Experimental and clinical evaluation of a new synthetic, absorbable sealant to reduce air leaks in thoracic operations. J Thorac Cardiovasc Surg. 1999;117(4):751-8.

- 15. Cerfolio RJ, Bass C, Katholi CR. Prospective randomized trial compares suction versus water seal for air leaks. Ann Thorac Surg. 2001;71(5):1613-7.
- 16. Ranger WR, Halpin D, Sawhney AS, Lyman M, Locicero J. Pneumostasis of experimental air leaks with a new photopolymerized synthetic tissue sealant. Am Surg. 1997;63(9):788-95.
- 17. McCarthy PM, Trastek VF, Bell DG, Buttermann GR, Piehler JM, Payne WS, et al. The effectiveness of fibrin glue sealant for reducing experimental pulmonary ari leak. Ann Thorac Surg. 1988;45(2):203-5.
- 18. Rodriques GG, Freitas US, Bounoiare D, Aguirre LA, Letellier C. Leakage Estimation Using Kalman Filtering in Noninvasive Mechanical Ventilation. IEEE Transactions on Biomedical Engineering. 2013;60(5):1234-40.
- 19. Vicario F, Alkhairy S, Buizza R, Truschel WA, editors. Two-parameter leak estimation in noninvasive ventilation. 2017 39th Annual International Conference of the IEEE Engineering in Medicine and Biology Society (EMBC); 2017 11-15 July 2017.
- 20. Lyazidi A, Thille AW, Carteaux G, Galia F, Brochard L, Richard JC. Bench test evaluation of volume delivered by modern ICU ventilators during volume-controlled ventilation. Intensive Care Med. 2010;36(12):2074-80.
- 21. Diedenhofen B, Musch J. cocor: A Comprehensive Solution for the Statistical Comparison of Correlations. PLOS ONE. 2015;10(4):e0121945.
- 22. Diedenhofen B. cocor comparing correlations 2015 [Available from: http:// comparingcorrelations.org/.
- 23. Aickin M, Gensler H. Adjusting for multiple testing when reporting research results: the Bonferroni vs Holm methods. American Journal of Public Health. 1996;86(5):726-8.
- 24. Kang DY. Intraoperative air leak site detection in spontaneous pneumothorax through carbon dioxide insufflation during thoracoscopic surgery. Surg Endosc. 2020;34(1):312-6.
- 25. Yokota N, Go T, Fujiwara A, Kato A, Otsuki Y, Yokomise H. A New Method for the Detection of Air Leaks Using Aerosolized Indocyanine Green. Ann Thorac Surg. 2021;111(2):436-9.
- 26. Roesthuis LH, van der Hoeven JG, Guérin C, Doorduin J, Heunks LMA. Three bedside techniques to quantify dynamic pulmonary hyperinflation in mechanically ventilated patients with chronic obstructive pulmonary disease. Ann Intensive Care. 2021;11(1):167.
- 27. Zhang R, Bures M, Höffler K, Jonigk D, Haverich A, Krueger M. In vitro comparison of two widely used surgical sealants for treating alveolar air leak. Thorac Cardiovasc Surg. 2014;62(8):705-9.
- 28. Belda-Sanchis J, Serra-Mitjans M, Iglesias Sentis M, Rami R. Surgical sealant for preventing air leaks after pulmonary resections in patients with lung cancer. Cochrane Database Syst Rev. 2010(1):Cd003051.
- 29. van der Worp HB, Howells DW, Sena ES, Porritt MJ, Rewell S, O'Collins V, Macleod MR. Can Animal Models of Disease Reliably Inform Human Studies? PLOS Medicine. 2010;7(3):e1000245.
- 30. Kjaergard HK, Pedersen JH, Krasnik M, Weis-Fogh US, Fleron H, Griffin HE. Prevention of air leakage by spraying vivostat fibrin sealant after lung resection in pigs. Chest. 2000;117(4):1124-7.
- 31. Araki M, Tao H, Sato T, Nakajima N, Sugai H, Hyon SH, et al. Creation of a uniform pleural defect model for the study of lung sealants. J Thorac Cardiovasc Surg. 2007;134(1):145-51.
- 32. Eckert CE, Harris JL, Wong JB, Thompson S, Kassis ES, Tsuboi M, et al. Preclinical quantification of air leaks in a physiologic lung model: effects of ventilation modality and staple design. Med Devices (Auckl). 2018;11:433-42.

- 33. Klassen C, Eckert CE, Wong J, Guyette JP, Harris JL, Thompson S, et al. Ex Vivo Modeling of Perioperative Air Leaks in Porcine Lungs. IEEE Trans Biomed Eng. 2018;65(12):2827-36.
- 34. Gologorsky RC, Alabaster AL, Ashiku SK, Patel AR, Velotta JB. Progel Use is Not Associated with Decreased Incidence of Postoperative Air Leak after Nonanatomic Lung Surgery. Perm J. 2019;23.
- 35. Anegg U, Lindenmann J, Matzi V, Smolle J, Maier A, Smolle-Jüttner F. Efficiency of fleecebound sealing (TachoSil) of air leaks in lung surgery: a prospective randomised trial. Eur J Cardiothorac Surg. 2007;31(2):198-202.
- 36. Zaraca F, Vaccarili M, Zaccagna G, Maniscalco P, Dolci G, Feil B, et al. Can a standardised Ventilation Mechanical Test for quantitative intraoperative air leak grading reduce the length of hospital stay after video-assisted thoracoscopic surgery lobectomy? J Vis Surg. 2017;3:179.
- 37. Marini JJ. Recruitment by sustained inflation: time for a change. Intensive Care Med. 2011;37(10):1572-4.
- 38. Pompili C, Falcoz PE, Salati M, Szanto Z, Brunelli A. A risk score to predict the incidence of prolonged air leak after video-assisted thoracoscopic lobectomy: An analysis from the European Society of Thoracic Surgeons database. J Thorac Cardiovasc Surg. 2017;153(4):957-65.

Supplement 2A - Data acquisition and calibration

Three flow signals were sampled continuously:

i. Standardized AL sensor (Omron)

A mass air flow sensor (model D6F-02A1-110, Omron Electronics, 0-2000mL/min, accuracy $\pm 3\%$ and reliability $\pm 0.3\%$) was calibrated for use with a Simulink data-acquisition model for continuous data recording and monitoring for measuring low-flow ranges. The sensor was connected to a stable 12VDc power supply and the signal wires were connected to an acquisition device (National Instruments, USB-6210), which was connected to a laptop with Matlab (version R2020/2021a). The signals were retrieved using the analog input recorder in Simulink at a sample rate of 1000Hz. This signal was passed through an unbuffer and discrete filter (50Hz bandstop) before being visualized continuously in the data scope.

Initial calibration

A flow regulator valve was connected to a pressurized air source and an air flow was passed through first the TSI 4100 Series Mass Flowmeter (model 41401PHI) and then the Omron Electronics mass air flow sensor. Under ambient conditions, the flow was increased in steps of approximately 200L/min until 2000L/min and the voltage output in the data-scope was recorded. These data-points were non-linear (as also described in the data-sheet), and a polynomial fit (4 degrees) was created using the curve fitting tool in Matlab (adjusted R-square = 0.999). This polynomial fit of flow (mL/min) was then added as a function of voltage in the Simulink data-acquisition model to attain a flow signal in mL/min.

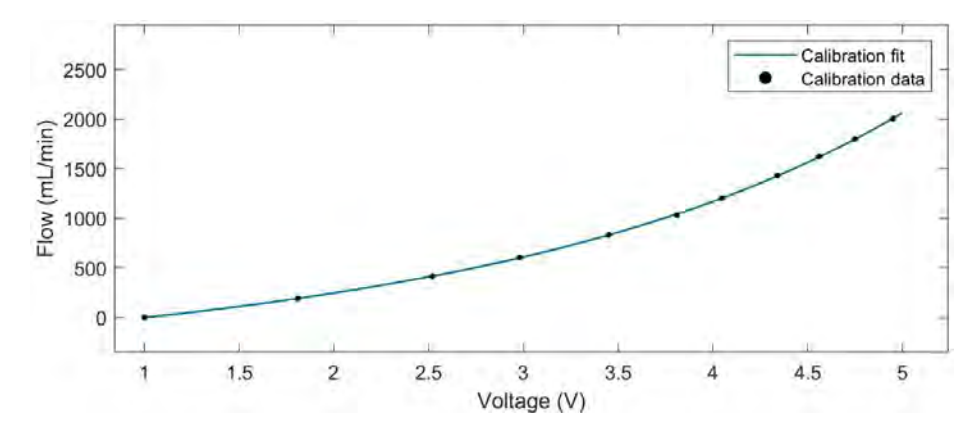


Figure 1: polynomial fit on flow as a function of output voltage for the Omron Electronics mass air flow sensor.

Calibration of a standard volume

Three syringes were used to calibrate a standard volume for further calibration of the flow sensor (10mL BD Emerald, 20mL BD Plastipak and 60mL BD Plastipak). These syringes were tested for gas-tightness by submerging them in water, increasing the pressure and checking for air bubble formation. Pure water at a temperature of 20°C (0.998203 g/mL) was drawn up until the maximum plunger distance (to assure most repeatable volume) in all syringes and weighed 10 times per syringe, using a calibrated Sartorius Entris 4202-1S Balance (4200 x 0.01 g). The maximum plunger volumes were calculated using the aforementioned density to be 11.97mL (95% CI: 11.92-12.03), 21.95mL (95% CI: 21.88-22.02) and 63.98mL (95% CI: 63.93-64.03) for the 10mL, 20mL and 60mL syringes, respectively.

Second calibration

A total of 10 injections were made with each of the calibrated syringes through the flow meter and the resulting flow data was integrated using a cumulative trapezoid function to get the cumulative volumes in Matlab. The mean calculated volumes were divided by the mean injected volumes for the three syringes. The average of these three calculations was added as an additional gain in the Simulink model, since the calculations slightly overestimated the actual injected value (additional gain in the Simulink data-acquisition model = 0.9852).

Validation measurements

Injections were made with the previously calibrated volumes of 11.97mL. 21.95mL and 63.98mL (10 each) through the flow meter. The volumes were determined using the same method as described under 'second calibration' and are plotted in Figure 2. As can be seen, the flow sensor has a high reproducibility. %Difference was calculated as (Calculated volume - average injected volume)/ (Average of calculated volume and injected volume), and was found to be within the accuracy limits provided by the sensor datasheet (accuracy $\pm 3\%$).

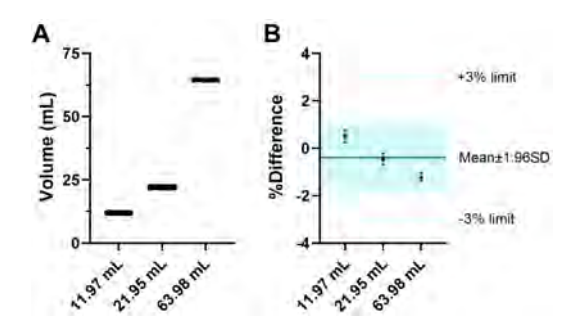


Figure 2: Calibration results of the Omron flow sensor.

Servo-I mechanical ventilator flow signal (SERV):

To acquire the mechanical ventilator (SERVO-I®, Getinge, Gotenburg, Sweden) flow, the ServoTracker software (version 4.1, Maguet Critical Care) was used to generate an analog output (-5 to +5V, sample rate 200Hz), which was recorded into the analog input recorder application in Simulink (Matlab version R2020/2021a) using two input/output devices (NI USB-6229 and NI USB-6210). The gain was given by the ServoTracker software to be linear (q =600) to give a signal in mL/s. All inputs in the Simulink model were filtered (f = 50Hz bandstop) and oversampled at 1000Hz. Calibration of the ventilator flow sensors was ensured by running the internal pre-check at start-up.

iii. Proximal flow sensor (PROX):

For the proximal flow sensor (model SFM3300-D, Sensirion, ±250 slm, accuracy $\pm 3\%$), the ControlCenter software (v1.31.1, Sensirion) was used, and sampled at 1000Hz. This flow sensor was checked for accurate flow measurements using a calibrated flow analyzer before the experiments (IMT Medical, PF300). For this, both devices were connected in series to a pressurized air source using a pressure regulator valve. The calibration results are shown in Table 1.

PROX (SLM) IMT-Medical (l/min)*		Difference	
2.5	2.5	0	
5.1	5	-0.1	
7.5	7.5	0	
10.1	10	-0.1	
15.1	15.1	0	
20	20	0	
29	29	0	

0

Table 1: Calibration results of proximal flow sensor

30.2

30.2

Furthermore, recordings were taken of the digital chest drain systems and the ventilator monitor:

Mechanical ventilator monitor

Initially, values from the ventilator monitor were manually noted. Thereafter, in order to gather and process large amounts of breath-by-breath data from

^{*}Measurement settings: air/standard temperature and pressure (STP).

SLM: standard liter per minute.

the Servo-I ventilator interface, a custom optical character recognition (OCR) application was made using Matlab (R2021a). As shown in Figure 3, this app is used to establish webcam communications with Matlab. The name is entered by the user to allow for saving raw and processed data. The frequency box is used as input for the frequency of image acquisition in the OCR loop based on the ventilator respiratory rate and the measurements box determines how many respiratory cycles are acquired. In the back-end of this application, image data is acquired using the snapshot function from the connected webcam. During the first measurement, the user performs a manual image crop around the tidal volumes, which is automatically used for subsequent snapshots. The green pixel values are fed into the imbinarize function, and the binazired matrix is fed into the ocr function (preset for number recognition). The number outputs of the orr function are displayed besides the binarized image data for the user to check for correctness (Figure 2 in main text).

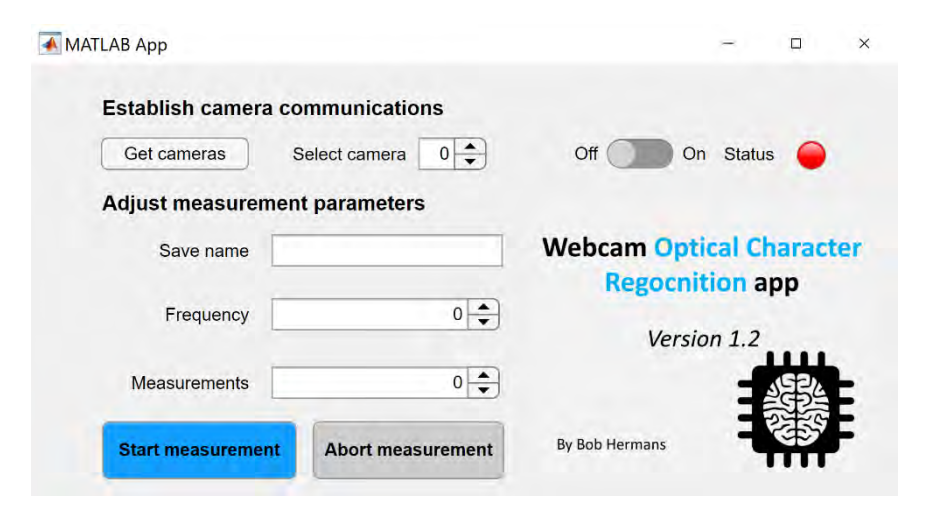


Figure 3: Screenshot from the custom optical character recognition application made using Matlab.

ii. Digital chest drain

Three digital chest drainage systems (Thopaz®, Medela, Baar, Switzerland) were checked for adequate pressure regulation using the pressure measurements of the calibrated flow analyzer (IMT Medical, PF300), by connecting the drainage tubing to the pressure port of the flow analyzer.

Table 2: Calibration of the Thopaz drainage systems

Set pressure	Device 1	Device 2	Device 3
-20	-19.5 to -21.4	-19.1 to -22	-19.5 to -20.3
-15	-14.3 to -15.4	-14.7 to -15.5	-14.4 to -15.1
-10	-9.2 to -10.2	-9.5 to -10.5	-9.3 to -10.1
-5	-4.3 to -5.4	-4 to -5.4	-4.6 to -5.0

Supplement 2B - Statistical analysis

i. Linear regression using Matlab

The "polyfit" function is used to generate a first degree polynomial fit (i.e. a linear fit). The y-residuals are calculated as "original data - fitted data". The residual sum of squares (SS_{resid}) is calculated as the sum over all the residuals squared. The total sum of squares (SS_{total}) is calculated by multiplying the variance of the original data by the number of observations minus one. R² is calculated as $1-(SS_{resid}/SS_{total})$ (see information on https://nl.mathworks.com/ help/matlab/data analysis/linear-regression.html).

Variable variance function using Matlab ii.

First, a Bland-Altman plot is constructed using the same formulas as in Graphpad Prism 9. %difference on the y-asis is calculated as (100*("new method" - "standardized flow measurement"/average of methods)) and the average of the two methods is plotted on the x-axis. The "getpts" function is used to select intervals on which the local means and variances will be calculated. On all points in each interval, the middle index (x-axis) with corresponding mean, standard deviation and standard error and 95% confidence intervals are calculated. A third-degree polynomial fit is generated through these points ("polyfit" function) to estimate the limits of agreement. See Figure 4.

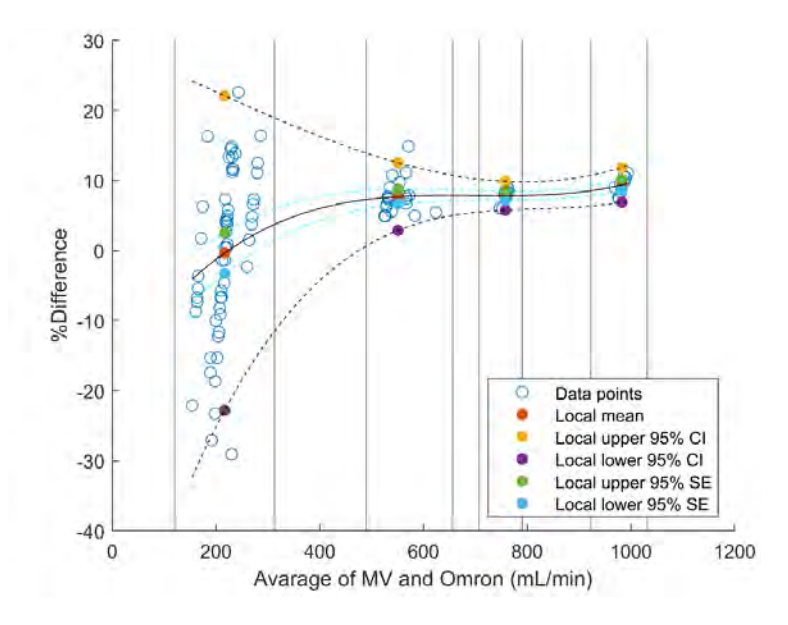


Figure 4: Estimation of variable limits of agreement using a third-degree polynomial fit in a Bland-Altman plot by calculating local means and variances in selected intervals (black lines).

Supplement 2C: Computer simulations of air leak measurements

Methods

In order to improve understanding of the influence of measurement error, tidal volumes, AL size and measurement protocol on the accuracy of AL measurements using a ventilator, a mathematical model was created using Matlab (version R2021a). This model assumes that tidal volumes are measured using two separate sensors (inspiratory and expiratory), each sensor has its own measurement error with respect to measured tidal volume. The model inputs are (27 combinations total): the inspiratory tidal volume (TVi=200/400/600mL), the measurement error (error=2/5/8%) and the number of breaths over which the average AL is calculated (j=10/5/1). The AL size per breath is generated as a random number between 0 and 100mL for every iteration, which is used to calculate the expiratory tidal volume (TVe). With this, the simulated tidal volumes are sampled from a Gaussian distribution (draw n=i samples, 100.000 times per input setting) $TV_{measured} \sim N(\mu, \sigma)$, where μ denotes the input tidal volume (TVi and TVe) and σ the standard deviation calculated as: $\sigma = \frac{TV_{input} \times error}{1.96}$. Then, the measured AL is calculated as the average of the difference between the sampled tidal volumes. Bland-Altman plots are generated from this data, by calculating the average of the input AL and simulated AL values, and the percent difference of the measurements as "(sampled data - input data)/average". To estimate the 95% limits of agreement, local means and standard deviations are calculated in increments of 0.5mL, followed by a smoothing of the interpolated confidence bounds.

Findings

Modelling of AL measurements using a MV revealed a measurement threshold, below which AL cannot accurately be derived from the tidal volumes due to overlapping of the measurement errors of the separate sensors. This threshold could be reduced by measuring larger AL with respect to the TVi, by reducing the measurement errors or by averaging the AL over multiple breaths. Visually, a relevant improvement in measurement certainty is seen for 1 vs 5 breaths. This improvement is more subtle for 5 vs 10 breaths (Figure 5).

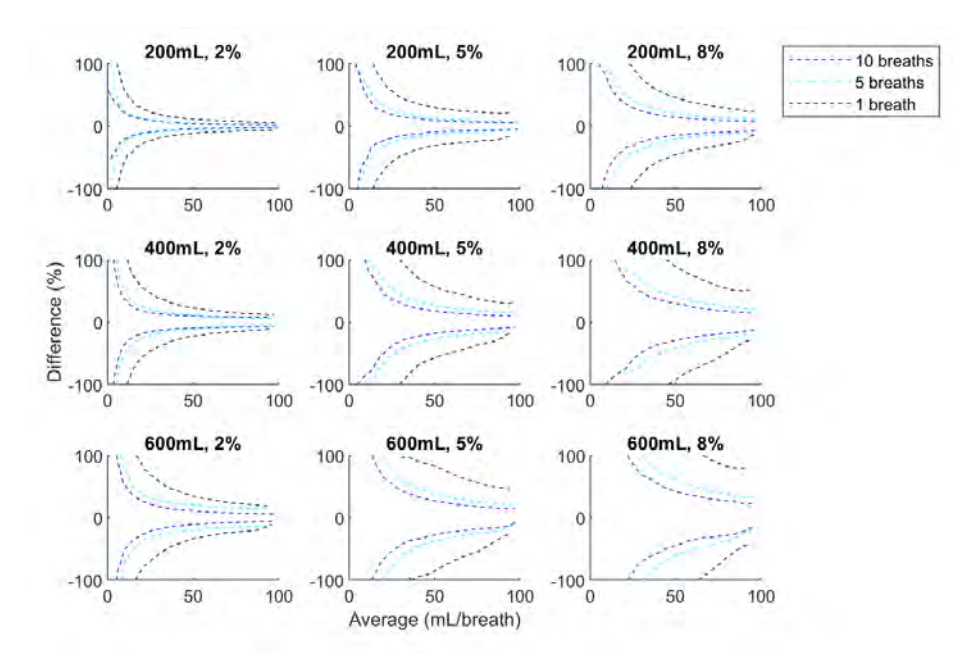


Figure 5: Computer simulation results. The smoothed interpolated 95% limits of agreement generated from 100.000 simulated samples drawn from a Gaussian distribution per setting are shown.



Chapter 3

Evaluating and developing sealants for the prevention of pulmonary air leakage: a systematic review of animal models

Bob P Hermans¹, Steven Poos², Daniël IM van Dort¹, Jort Evers¹, Wilson WL Li¹, Erik HFM. van der Heijden³, Ad FTM Verhagen¹, Harry van Goor², Richard PG ten Broek²

Radboud university medical center, Radboud Institute for Health Sciences, Nijmegen, The Netherlands.

¹Department of Cardio-thoracic surgery

²Department of General surgery

³Department of Pulmonology

Used with permission of SAGE Publications Ltd., from "Hermans BP, Poos SEM, van Dort DIM, et al. Evaluating and developing sealants for the prevention of pulmonary air leakage: A systematic review of animal models. *Laboratory Animals*. 2023;57(5):504-517. doi:10.1177/00236772231164873"; permission conveyed through Copyright Clearance Center, Inc.

ABSTRACT

Sealants may provide a solution for pulmonary air leakage (PAL), but their clinical application is debatable. For sealant comparison, standardized animal models are lacking. This systematic review aims to assess methodology and quality of animal models for PAL and sealant evaluation. All animal models investigating lung sealing devices (e.g. staplers, glues, energy devices) to prevent or treat PAL were systematically retrieved from Embase, Pubmed and Web of science. Methodological study characteristics, risk of bias, reporting quality and publication bias were assessed. 71 studies were included (N=75 experiments, N=1659 animals). Six different species and 18 strains were described. 92% of experiments used healthy animals, disease models were only used in 6 studies. Lesions to produce PAL were heterogenous, and only 11 studies used a previously reported technique, encompassing N=5 unique lesions. Clinically relevant outcomes were used in the minority of studies (imaging 16%, air leak 10.7%, air leak duration 4%). Reporting quality was poor, but revealed an upward trend per decade. Overall, high risk of bias was present, and only 18.7% used a negative control group. All but one study without control groups claimed positive outcomes (95.8%), in contrast to 84.3% using positive or negative control groups, that also concluded equivocal, adverse or inconclusive outcomes. In conclusion, animal studies evaluating sealants for prevention of PAL are heterogenous and have a poor reporting quality. Using negative control groups, disease models, and quantifiable outcomes seem important to increase validity and relevance. Further research is needed to reach consensus for model development and standardization.

Introduction

Pulmonary air leakage (PAL) remains an important cause of complications following pulmonary resection in modern thoracic surgery. Air leaks (AL) persisting for more than 5 days are generally considered to be prolonged (pPAL), and estimates are that 5.6-30% of patients are affected. (1) As a consequence of pPAL, post-operative complications (30% vs 18%) and mortality (OR 1.90, 95% CI 1.42, 2.55) are increased. (2-4) Hospital stay is extended four to eight days and patients are subject to more re-interventions and re-admissions. (5-9) As a result, complications associated with pPAL increase both hospital and societal costs. (8, 9) To mitigate the impact of pPAL, lung sealing devices (LDs) have been proposed for intraoperative use.

LDs are a heterogeneous group of devices and implants (e.g. staplers, glues, energy devices) to establish an aerostatic seal of the resected lung. A large number of LDs have been evaluated with positive results in animal studies. However, currently, only 42% of surgeons find the evidence compelling for routine use of LDs (with the exception of staplers). (10) To summarize the evidence based on several systematic reviews and meta-analysis, there appears to be a positive effect on PAL, but impact on clinically relevant outcomes such as complications and length-of-stay are debatable. (11-14) Furthermore, there is considerable doubt regarding cost-effectiveness. (15) Another important concern is the lack of clinical trials performing head-to-head comparisons of different LDs. (13) So, although there is some evidence for a number of LDs, none seems to work perfectly and the search for better solutions for pPAL continues, requiring a standardized and valid pre-clinical work-up. (10)

The discrepancy between positive results derived from animal studies and the debatable clinical benefits from LDs is noteworthy. In this regard, valid animal models are indispensable for direct comparison or novel product development purposes. However, the current literature of in-vivo studies investigating LDs is heterogenous and there are no widely accepted standards for research of pPAL in animal models. (16-21) This is in contrast to animal studies in different medical fields such as gastro-intestinal anastomosis. (22) This makes standardized preclinical research into novel and existing LDs especially difficult. Considering that conduction of animal research with poor methodological quality (e.g. lack of randomization and blinding) or invalid model designs (e.g. healthy animals and lack of clinically relevant outcomes) may be one of the reasons for insufficient performance of LDs in clinical practice, further investigations are necessary. (23)

Live animals are still required in this field of research due to the complex mechanisms involved, including foreign body reactions, coagulation cascades, local tissue homeostasis and pleural mechanisms in spontaneously breathing mammals, that cannot yet be replaced by animal-free models. (24-26) Due to the ethical and societal concerns associated with animal experiments, it is especially important to only perform research of the highest internal quality, in the best model with the highest external validity and in the most refined manner possible. (23) In order to identify and improve on the described methodological problems, animal systematic reviews are recommended in the translational research phase. (27)

The aim of this systematic review is to provide a comprehensive overview of the methodological characteristics of previous animal models used for the evaluation of LDs for the treatment of PAL, and provide recommendations for future research in this field. Furthermore, the risk of bias and quality of reporting will be assessed, providing a baseline for quality improvements in this field.

Methods

Search strategy

A systematic review study protocol was registered in the International Platform of Registered Systematic Review and Meta-analysis Protocols (INPLASY) under registration number 202270003. A search strategy with three components was devised to identify all animal studies describing the evaluation of LDs as a treatment of parenchymal PAL. In short, one component including terms related to pulmonary surgery and post-operative air leakage and a second component with terms related to LDs were combined using the animal studies search filter designed by Hooimans. (28) Key Mesh terms included: 'Pulmonary surgical procedures', 'Pneumothorax', 'Respiratory tract fistula', 'Pneumonectomy', 'Tissue adhesives' and 'Fibrin tissue adhesive'. This search strategy was deployed in Pubmed, EMBASE and Web of Science on 9-2021 (Supplement 3A). No language or publication date restrictions were applied to the literature search.

Identification of relevant articles

Citation information from each of the database searches was collected in Endnote (version 20), and duplicates were automatically removed. Title and abstract screening was then performed on the collected references in Endnote citation manager by one investigator (BH or JE), and in case of doubt the full-text was

retrieved for screening. Full-text retrieval was then done through 1) university access, 2) online searches and 3) help of our university library contacting national and international universities. Full-text screening of possible relevant studies was performed by consensus between two investigators (BH and SP/ JE). In case of non-English papers, the papers were translated using Google Translate for screening purposes. If this translation was insufficient, papers were screened with help of native speakers. Reference lists of included English studies were screened by one author (BH or JE) to identify potential additional relevant articles. Inclusion criteria were 1) in-vivo study design in mammals. 2) model of parenchymal PAL (small bronchioles within lesions may be included), 3) sealing of the AL with a surgical LD and 4) assessing aerostatic efficacy of the LD. The following exclusion criteria were considered: 1) LD is only used to seal a large bronchus or trachea (such as large segmental or lobar bronchi), 2) LD is a nonsurgical intervention (such as bronchoscopy, pleurodesis, thoracic drainage) and 3) studies only evaluating the hemostatic or biocompatibility characteristics of the LD under investigation. Any article form other than a complete research paper (e.g. conference abstracts) were also excluded. All included non-English full texts were translated using Google Translate, and two Russian papers were translated by a native speaker. In case the translation quality was not enough to reliably perform data-extraction or risk of bias grading, data extraction and quality grading was performed by an academic native speaker (N=4 Japanese studies) and help of one researcher (BH).

Data extraction and quality assessment

In order to generate an overview of the methodologies used in all animal studies, a wide range of characteristics relating to the animal model (age, sex, strain, weight, disease model), air leak model (surgical characteristics, defect descriptions, baseline leak measurements), lung sealing and outcomes (acute sealing testing, histology, bursting pressure, air leak, imaging, macroscopy, adverse events) were extracted from each study. A complete overview is provided in the table in Supplement 3B.

For assessment of trends in reporting quality, a custom score was calculated (18 points max), that was derived from a similar score used by Yauw et. al. in their animal systematic review, designed for surgical animal studies. (29) We chose items that were most appropriate with regard to experimental investigations of lung sealants, and objectively reproducible when scoring (i.e. items do not require any form of reviewer judgement such as in risk of bias scoring). This score was partly based on items from the ARRIVE Guidelines

(strain, sex, age, weight, housing, anesthesia, analgesia post-operatively, antibiotic prophylaxis, sterility during surgery, ethical statement, data access statement, registration of protocol) and additional items added relevant to the study of lung sealants (type of incision to gain access to the lungs, location of defect right or left lung, location of defect lobe used, creation of the lesion on a static lung, application of the sealant on a static lung, defect dimensions). (29, 30) The lung was considered static in case the area of interest was not being ventilated during relevant parts of the procedure (e.g. using a clamp, singlelung ventilation, continuous positive airway pressure or ventilatory arrest). Each item was scored as '1' if reported, and '0' if not reported or not applicable. All variables were extracted by one author (BH), and completely checked for mistakes by a second author (SP). Data was only extracted from text and tables.

For study quality assessment, the SYRCLE Risk of bias tool (RoB) was used, which consists of bias assessment in six domains, specifically designed for use in animal systematic reviews. Items 1-8 on this tool were assessed using signaling questions, which were answered as 'yes', 'no' or 'unclear' (Supplement 3C). Thereafter, items were scored as 'high', 'unclear' or 'low' risk of bias. (31) In the specific case of poorly reported studies, often no mention is made regarding a signaling question, and we considered the subsequent 'probable no' answer similarly as 'no', generally leading to a high risk of bias grading. Furthermore, an additional six questions related to internal validity were formulated (randomization, blinding, power-calculation, use of positive and negative control groups and industry funding) and answered with 'yes', 'no' or 'unclear'. Publication bias is qualitatively assessed based on authors conclusions regarding the LSD efficacy (positive, equivocal, adverse, inconclusive). Funnel plot analysis was not feasible in this regard due to high heterogeneity of interventions and outcomes and poor outcome reporting quality. All quality assessment was initially done by reaching consensus between two authors (BH and SP), except for the papers read by the Japanese native speaker (N=4).

Data analysis

All study characteristics were gathered and analyzed using IBM SPSS Statistics for Windows, Version 27.0 (Armonk, New York; IBM Corp). GraphPad Prism (version 9) was used for graphical presentation of data. Methods of animal models were assessed in a semi-quantitative analysis, describing model characteristics with descriptive statistics. Trends due to date of publishing were investigated using Pearson's correlation. Due to a large heterogeneity between included studies, no meta-analysis or meta-regression was performed.

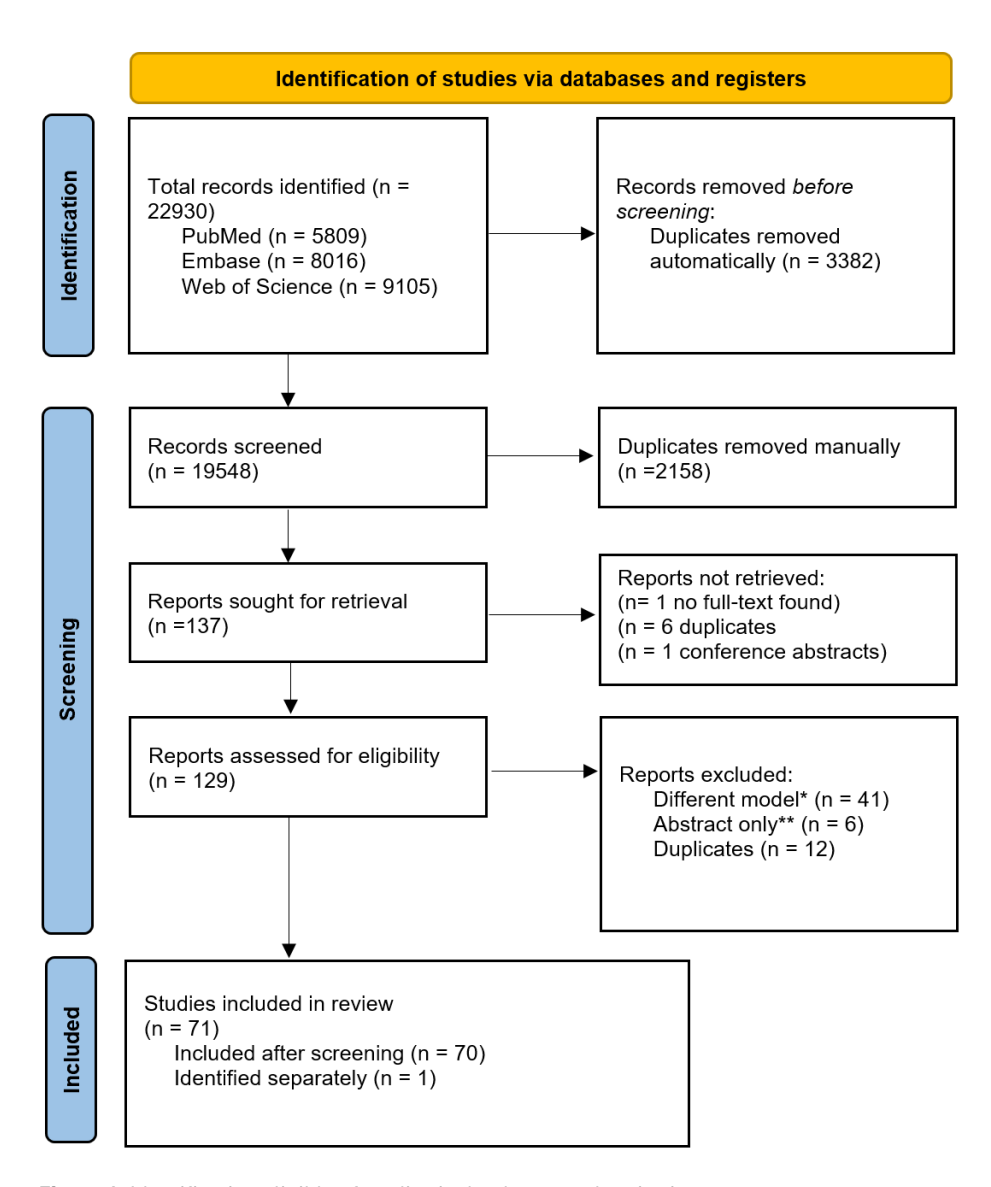


Figure 1: Identification eligible of studies in databases and registries.

^{*}No in-vivo study (such as post-mortem), biocompatibility model, no lung lesion, review article, clinical study, bronchus lesion

^{**}Abstract or paper described so poorly that data extraction and risk of bias grading according to the set criteria was not feasible.

Results

Description of included studies

A total of 71 papers (Supplement 3D) were included in this review, describing 75 experiments (**Figure 1**). Three papers were identified by reference list screening, but were upon inspection also present in the original search and missed during screening. Only one paper was identified completely separate from the initial literature search and refence list screening. Two articles first appeared to meet the inclusion criteria, but were extracted due to very poor descriptions of methodology and results, making reliable data-extraction and risk of bias grading impossible. Study characteristics were extracted per experiment and risk of bias grading was performed per paper. Most experiments were performed after 1990, with 17 experiments dating from the 35 year period between 1955-1989 (**Figure 2**). A total of 1659 animals were used (mean: 23, SD: 29 per experiment, N=3 missing data) with a downward trend per decade (R: -0.140, p=0.241).

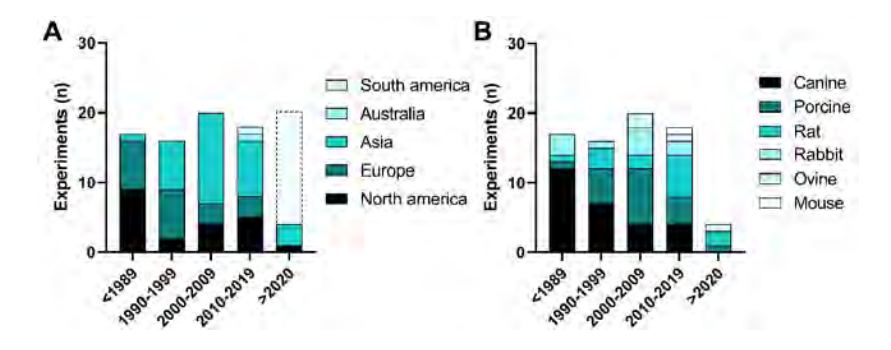


Figure 2: General study characteristics and animal models used. **A)** Study continent of origin grouped per decade. The dotted bar shows an estimate for this decade based on linear extrapolation. **B)** Animal model used grouped per decade.

Quality assessment

Study quality assessment is shown in **Figure 3**. The custom reporting quality score revealed an upward trend through the decades (R: 0.539, P<0.001). Items most frequently left unreported were registration of protocol (100%), data access (96%), housing details (89%), post-operative analgesia (89%), perioperative antibiotic prophylaxis (80%), sterile surgery (76%), description of static lung state during defect creation (75%), ethical approval statement (63%), description of static lung state during LD application (61%), anatomical location of lesion location (53%).

Based on the SYRCLE RoB bias tool, no studies were considered low risk of bias, andinalldomains the majority of studies were graded as high risk of bias (Figure 3, Supplement 3E). In the additional questions, it was noted that negative control groups were only used in 18.7% of studies. Regarding publication bias, all but one of studies without any control groups claimed positive outcomes, in contrast to (15.7%) using either positive or negative control groups, that also concluded equivocal, adverse or inconclusive outcomes.

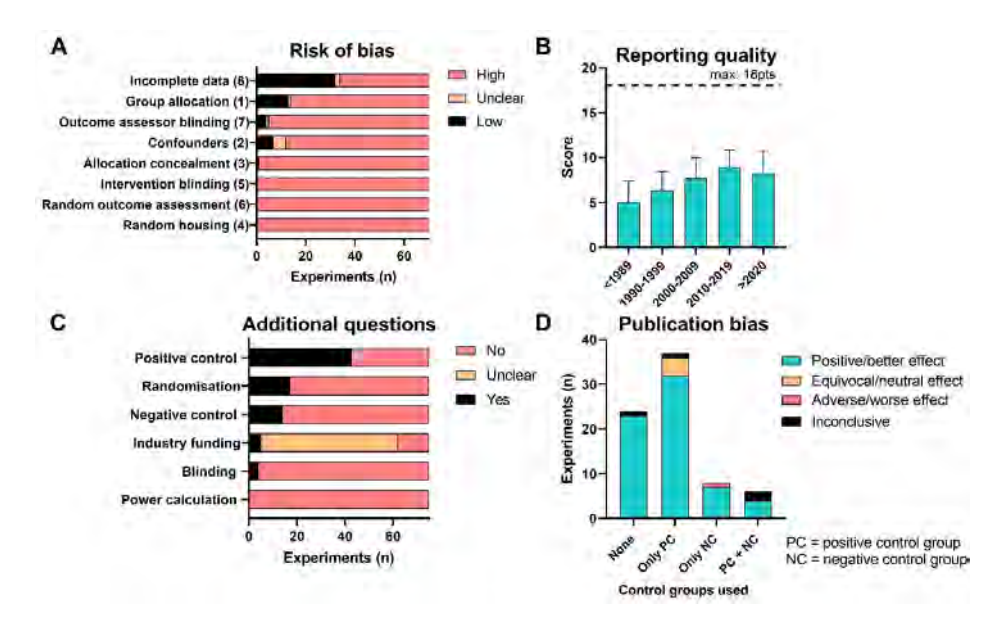


Figure 3: Study quality assessment. A) Risk of bias assessment, based on the SYRCLE risk of bias tool. B) Custom reporting quality score, revealing an upward trend per decade (R: 0.539, P<0.001). C) Additional risk of bias questions. D) Publication bias assessed by collecting authors conclusions, grouped by control groups used.

Animal models

Included experiments had the aim of showing either aerostatic efficacy (30.7%) or both aerostasis and biocompatibility (69.3%), In 24% of studies the animals were sacrificed immediately after surgery. Use of six different species was described (canine 36%, porcine 25.3%, rats 18.7%, rabbits 13.3%, ovine 5.3% and mice 1.3%). Strain was further defined in 68% of studies, revealing a heterogenous pool of animal models (N=18). Of these, most used were Beagle dogs (23.5%), New-Zealand white rabbits (15.7%), Wistar rats (13.7%) and Mongrel dogs (11.8%). Sex, weight and age were described in 48.7%, 39.7% and 74.4% respectively. Both sexes were only used in 11.1% of studies that

specified sex, and animals used were frequently relatively young (64.7% <1 years). Mainly healthy animals were used (92%), and disease models used comprised athymic rats (N=3), coagulopathy (N=2) and emphysema (N=1).(32-36)

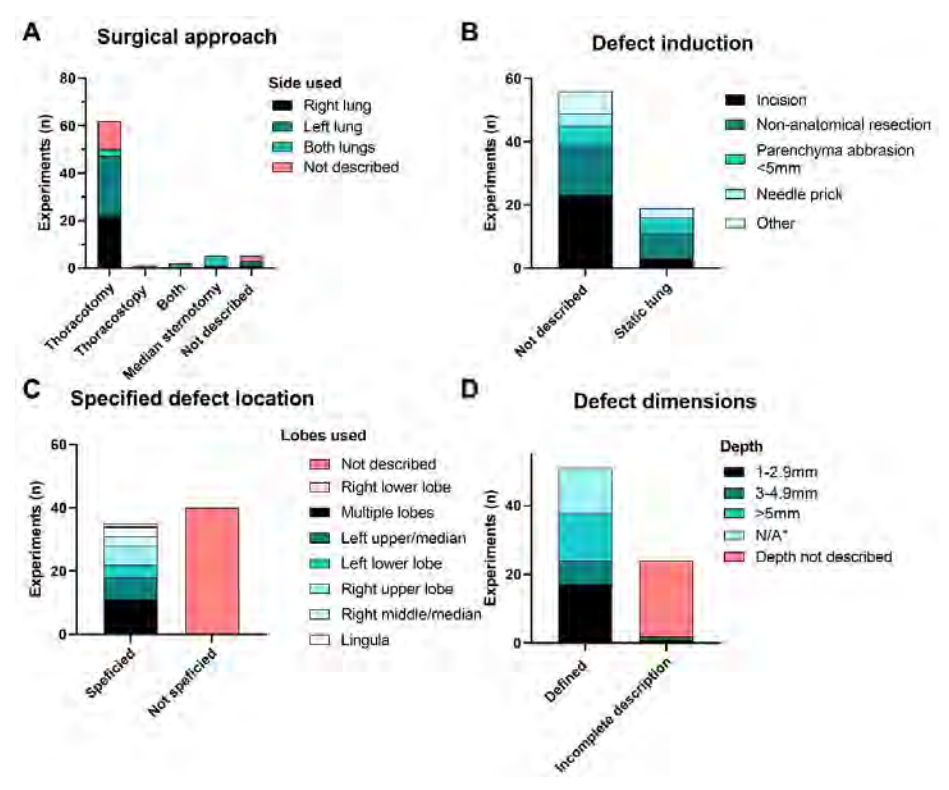


Figure 4: Pulmonary defect models used. A) Surgical technique and lung used. B) Defect type used, grouped by the description of static lung state during defect induction. C) Precise anatomical defect location used. D) Defect depth, grouped by presence or absence of a complete description of defect dimensions. *Defect depth not applicable (e.g. wedge resection or only removal of pleura).

Air leak models

The surgical approach for defect creation consisted of a thoracotomy (82.7%) in most cases, and the left lung (40%) was used more frequently than the right lung (32%). The precise anatomical location of the lung defect was reported in 46.5% of experiments. If described, a heterogenous division of locations was seen (Figure 4), with a median number of defects of 1 per animal (IQR: 1, range: 14). The defect models used were even more heterogenous, with only N=5 defects being used in more than 1 experiments (combined N=11 experiments). Exact defect dimensions were described in 68% of experiments, and these lesions

were made at a varying depth (see **Figure 4**). However, only 25.3% of authors describe the creation of lesions on a static lung, for example with a clamp applied to the lung parenchyma or at a static ventilatory pressure, making this actual number of lesions that can accurately be reproduced, lower.

At baseline, hemostatic measures other than the applied lung sealant were described in 20%. With respect to potential confounding factors, assessment of baseline air leak was described infrequently: 40% of studies included some descriptive indication of baseline air leak (e.g. 'Leaking of blood and air were confirmed' or 'Air leak confirmed by bubble formation') and formal methods with quantifiable outcome measures were used in 15 (20%) studies. (35, 37) Quantifiable measures included a water submersion test with visual grading, bursting pressure/minimal leaking pressure or actual air leak amount (Figure 5). (17, 38-41)

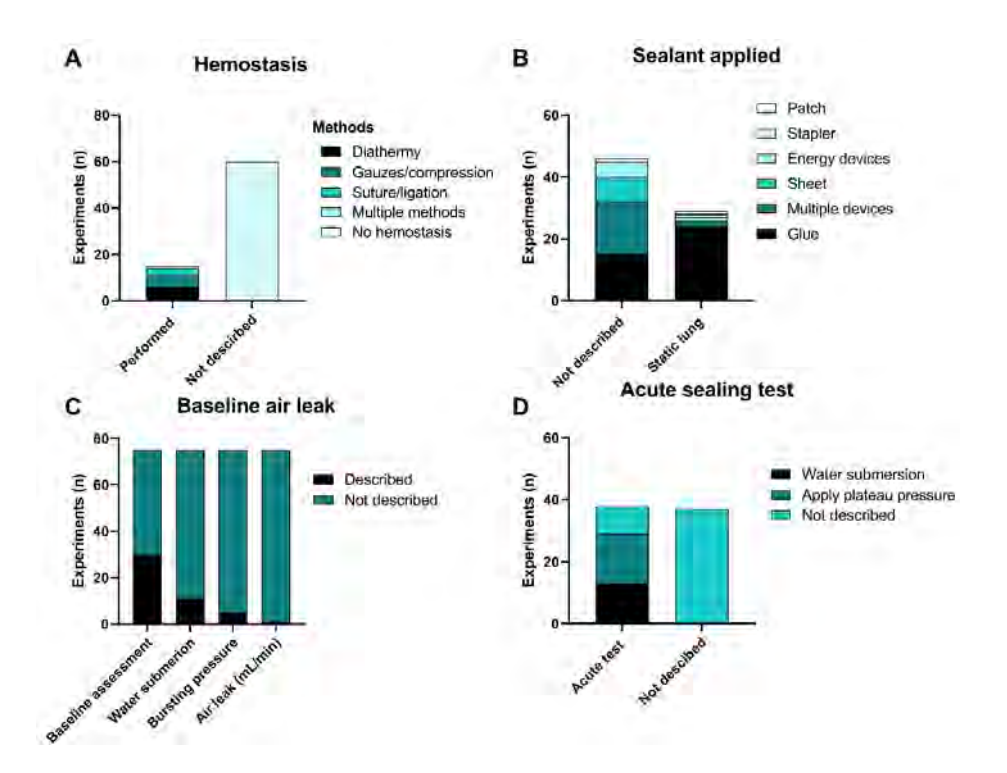


Figure 5: Baseline defect and sealing characteristics. A) Hemostasis techniques used. B) Lung sealant type applied, grouped based on the description of static lung state during sealant application. **C)** Baseline air leak measurements performed. **D)** Acute lung sealing tests performed.

Lung sealing and outcomes

A wide range of LDs has been evaluated in animal experiments, which are grouped according to application category in Figure 5. Regarding methodology, 38.7% describe application on a static lung. In 50.7% of experiments an acute sealing test directly after application was performed, either by water submersion testing or application of a threshold ventilatory pressure (max 45cmH2O). Remarkably, one paper describes pressure resistance of up to 350-400cmH2O, which seems unlikely for the canine lungs to have withstood. (42) LDs were evaluated using only positive pressure ventilation in 22.7% of experiments, and using both mechanical ventilation and physiological breathing in 74.7% of experiments. The most evaluated late outcomes included were histology (77.3%), adverse events (62.7%, such as a post-operative pneumothorax, infections or death), macroscopic observations (52%) and bursting pressures (42.7%). Late evaluation was usually performed at a median follow-up of 30 days (IQR: 46 days). A clinically relevant outcome including pneumothorax detection with imaging (16%), air leak (10.7%) and air leak duration (4%) was measured in a small proportion of experiments.

Discussion

For the purpose of evaluating LDs as a treatment for PAL, no standardized animal model has been described to date. This is supported by this systematic review revealing high heterogeneity regarding methodological characteristics and outcome measures between all previous animal studies. High risk of bias and poor reporting quality complicate further standardization of models. Translatability of results may be further impaired by lack of quantifiable measures of PAL and lack of disease models in the previous animal studies. As such, including a negative control group will help to increase study validity, by assessing the natural healing course of a lesion. Confirming that a lesion results in PAL and not immediate closure from intrinsic healing will help reduce publication bias.

Interpretation and comparison to literature

To the best of our knowledge, this is the first systematic review of literature performed on the use of LDs for treatment of PAL in preclinical animal studies. Nevertheless, the methodological shortcomings illustrated by this systematic review are a common finding in other preclinical systematic reviews, including lack of randomization, allocation concealment, blinding, low reporting quality and the presence of a publication bias. (27, 29) Another common problem is

heterogeneity due to lack of standardized protocols, as was also illustrated in the preclinical systematic review on intestinal anastomosis. (29) Reducing this heterogeneity can allow for better meta-analysis and investigation of external validity by comparison of pooled preclinical findings to clinical data. (29) A recent review article by van der Worp and coworkers described common causes of reduced external validity to be due to insufficient use of disease models, use of a homogenous group of animals, using only male or female animals, insufficient similarity between clinical and experimental disease and difference in outcome measures. (23) All these factors were also identified to lack in the included animal studies. From this perspective, systematic appraisal of preclinical literature can be beneficial, allowing for rationalized recommendations for future research, as will be further discussed. (27)

The current preclinical literature does not provide sufficient evidence to conclude standards for making a lesion that results in relevant and persistent PAL. While many different lesions have been investigated, appraisal of their validity is impossible due to lack of negative control groups or quantifiable outcome measures. Moreover, there is evidence that healthy animal lungs may possess strong intrinsic healing mechanisms that can provide fast sealing of relative large lung lesions. For example, removal of the entire parietal pleural surface at 3mm depth in the healthy dogs was not associated with air leak complications. (43) Another study performed segmental resections with a negative control group, leaving the raw parenchymal area of 9-15cm² untreated. (44) No air leak complications were seen due to this negative control lesion, making interpretation of aerostatic efficacy of evaluated treatments impossible. (44) Yet another study with especially large square defects (9x9x0.5cm) in healthy dogs illustrated intrinsic healing in 4/8 negative control animals within 24 hours, the same proportion as in the fibrin glue treated group. (17) In our own work with healthy sheep, we have observed similar rapid intrinsic healing of parenchymal lesions (unpublished data).

Considering these intrinsic healing mechanisms, a valid model that results in relevant and persistent PAL is required. In the absence of standardized validated models, a negative control group should be included to confirm the presence of PAL when left untreated. For standardized model development, the current literature offers several leads. Several studies have shown that nonanatomical partial resections of the lung are associated with air leaks and air leak complications in healthy animals. (38, 45, 46) The leakage capabilities of such lesions are potentially related to the laceration of bronchioli. In the study by Ranger and colleagues, bronchioli of 1.5-3.0mm diameter were intentionally

included, observing significant air leaks over the 24 hour observation period in the negative control group. (38)

Secondly, from a clinical perspective, a disease model to increase the odds for pPAL could be considered. The healthy animals used in most pre-clinical studies differ from the diseased patients which are at risk of pPAL. In clinical practice, patients undergoing pulmonary resections, especially those at risk for pPAL, are often older, have a history of smoking and chronic obstructive pulmonary disease, take medications (anticoagulation, antiplatelets, steroids) and might have had chemo- and radiotherapy prior to surgery. (1, 47-49) In contrast, laboratory animals are often younger, healthy and have no prior history of disease. Disease models impairing immune function, lung quality or coagulation mechanisms were only used in a minority of studies. (32, 35, 36) This difference might impact the healing course of lung lacerations and modify LD results accordingly.

A promising disease model might be the emphysema model. Gika et. al. reported inferior bursting pressure results for all LDs under investigation applied in their emphysema model compared to the healthy animal model. (36) A drawback of this model is that the induction of emphysema by bronchoscopic elastase instillation is difficult to standardize. (36) Balakrishnan described a disease model that is easy to standardize, based on heparinization. (35) Such a model might reduce intrinsic healing mechanisms, but no negative control group or quantifiable outcomes were used to confirm that this method enhances risk of PAL. (35) In conclusion, the use of disease models seems promising, however it could come at a cost of less standardization, more complexity of the study, and reduced animal welfare. Use of disease models should be ethically weighed in the light of the aforementioned uncertainties and experimental aims.

Considering further standardization of animal models, reproducible lesions should be ensured across animal experiments, and the precise method of induction and lung expansion state should be specified. The lung changes throughout the respiratory cycle with a volumetric strain of 20-50%. (50) Therefore, a lung defect should be created on a set inflation state for valid and reproducible results (e.g. empty lung or 10cmH2O positive pressure). Furthermore, when creating multiple lesions, the influence of anatomical location on PAL should also be considered. For instance, a clinical association has been described between upper lobectomies and occurrence of PAL in humans. (49, 51) Mechanistically, this could possibly be explained by the effects of gravity on the intrapleural pressure gradient, which has a different orientation in quadrupedal animals. (52, 53) The influence of species effects on PAL from a lung lesion and intrinsic healing in animal models is currently unknown.

Recommendations for future research

Because of the lack of standardized preclinical models known to reliably result in PAL, the inclusion of negative control groups is needed to confirm model validity. Ultimately, PAL findings need to be studied across varying lesions, species, anatomical locations and disease models and systematically compared to clinical data to determine the preclinical model with the highest external validity. Previous literature indicates that parenchymal lesions in healthy animal might seal intrinsically, whereas lesions with bronchioli are capable of PAL, but this should be further investigated. (17, 38, 43) When creating lesions, the precise conditions (e.g. lung inflation state, dimensions, location) should be documented to allow for standardization. Finally, specific disease models such as pulmonary emphysema or coagulopathy might be used to enhance translational value. (35, 36)

Air leakage should be objectively quantified, both as a baseline confounder and outcome parameter and an air leak should be of adequate size, at least comparable to clinical cases where a lung sealant might be indicated for use. Recent consensus guidelines advice to classify air leaks as mild (<100mL/min), moderate (100-400mL/min) and severe (>400mL/min). (54) In other studies, intraoperative PAL >500mL/min or >9.5% of the inspiratory tidal volume have been found to be predictive of pPAL. (55, 56) Similar classification might also apply to larger animals, such as sheep and pigs. Classifications of air leakage that are specified or validated for animal species are not available and should further be developed.

Risk of bias can be mitigated by use of randomization, allocation concealment and use of negative control groups. Studies should also be sufficiently powered to detect meaningful outcomes. Although increasing the power of an animal model initially might seem to increase the number of animals needed, it will eventually reduce the amount of animal needed by lowering the need to perform duplicate models. (57) To further improve the methodologies of animal experiments, Delphi consensus quidelines made by an international board of experts could be used to standardize models and improve translational value. (22, 29) To improve internal validity, researchers are encouraged to use the ARRIVE quidelines when designing and publishing animal experiments (see Table 1 for summary of recommendations).(30)

Table 1: Summary of recommendations for future research

Topic	Author recommendations	Knowledge gap
Animal model	Consider large animals for aerostatic efficacy testing (similar biomechanics)	 Species-specific intrinsic pulmonary healing differences Bipedal versus quadrupedal and anatomical location effect- modification
Disease model	Develop disease model that enhances pulmonary air leak and reduces intrinsic healing	 Validity of heparinized disease model⁽³⁵⁾ Validity of emphysema disease model⁽³⁶⁾
Air leak model	 Create lesions on static lung with defined pressure conditions Consider large lesions in healthy animals (extended parenchymal or inclusion of bronchioles 1.5-3.0mm) (17,38) Aim for air leak >400-500mL/min (large animals) or >9.5% of tidal volume (54-56) 	 Dose-response relationship between different lesion types/sizes on air leak (study inter- and intraspecies) Translation factor of animal versus clinically relevant air leaks
Outcome measures	 Ensure baseline measurements (lesion size, air leak, bronchioles, coagulation times) to control between groups Consider similar outcome measures to clinical practice (air leak size and duration, time until drain removal) 	Translational value of animal outcome measure to clinical practice
Reduction & Refinement	 Consider multiple lesions per lung (large animals) to increase power (e.g. animals as own control) and calculate required sample size beforehand Use multimodal analgesia principles from clinical thoracic surgical practice Use transcostal sutures to reduce post-operative pain⁽⁵⁸⁾ 	Mutual influence with multiple lesions per lung (e.g. through pneumothorax, empyema)
Risk of bias	 Use negative controls to adjust for intrinsic healing effects Use randomization and blinding principles Adhere to ARRIVE guidelines⁽³⁰⁾ 	Gather panel of experts to specify and improve recommendations

Limitations

Because of the high number of studies lacking a control group and quantifiable outcome measures, publication bias is difficult to assess, and standard techniques such a funnel plots were insufficient. Therefore, an analysis of author conclusions was performed as a surrogate outcome for publication bias. (29) This analysis showed that publication bias is likely, as the majority of studies reported positive conclusions.

To ensure a valid assessment of risk of bias, this was performed by two investigators independently, after which consensus was reached. Our assessment may be a conservative estimation of the overall study quality and not fully represent the true risk of bias, because there was also a low reporting quality in most studies. Cases were a specific aspect of study design was not reported, were generally treated as high risk of bias (e.g. no mention of randomization), but some uncertainty remains whether the experiments were actually highly biased or poorly reported. (59) Either way, problems with poor reporting or risk of bias are evident in the current body of literature, posing ethical concerns when using laboratory animals and contributing to research waste and poor reproducibility. However, due to the underestimation of the quality of evidence, the results should thus be interpreted with appropriate caution.

The custom reporting quality scoring has two associated limitations. First of all, not applicable items were not accounted for in overall scoring (e.g. sterility or antibiotic prophylaxis in short terminal experiments), which might lead to an underestimation of the reporting quality. Secondly, no complete scoring of all items on the ARRIVE guidelines was performed, which may have further increased the relevance of the reporting quality scoring in the context of animal studies.

Conclusions

This systematic review underlines the methodological gaps in previous studies investigating LDs for the problem of PAL. Overall, lack of standardized methodology and a high risk of bias is a problem for translating results to clinical practice. Low reporting quality further complicates the reproduction of experiments. Despite the limitations of a systematic review to generate conclusive evidence for the best animal model, using negative control groups, disease models, and quantifiable outcomes seem important to increase validity and clinical relevance of results. Improvement in animal models are necessary from a scientific, ethical and societal perspective, and we recommend formation of an international panel of experts to further specify guidelines for this field of research.

References

- 1. Attaar A, Tam V and Nason KS. Risk Factors for Prolonged Air Leak After Pulmonary Resection: A Systematic Review and Meta-analysis. Ann Surg 2020; 271: 834-844. 2019/10/03. DOI: 10.1097/sla.000000000003560.
- Okereke I, Murthy SC, Alster JM, et al. Characterization and importance of air leak after lobectomy. Ann Thorac Surg 2005; 79: 1167-1173. 2005/03/31. DOI: 10.1016/j. athoracsur.2004.08.069.
- Yoo A, Ghosh SK, Danker W, et al. Burden of air leak complications in thoracic surgery estimated using a national hospital billing database. Clinicoecon Outcomes Res 2017; 9: 373-383. 2017/07/20. DOI: 10.2147/ceor.S133830.
- Brunelli A, Xiume F, Al Refai M, et al. Air leaks after lobectomy increase the risk of empyema but not of cardiopulmonary complications: a case-matched analysis. Chest 2006; 130: 1150-1156. 2006/10/13. DOI: 10.1378/chest.130.4.1150.
- Liang S, Ivanovic J, Gilbert S, et al. Quantifying the incidence and impact of postoperative prolonged alveolar air leak after pulmonary resection. J Thorac Cardiovasc Surg 2013; 145: 948-954. 2012/09/18. DOI: 10.1016/j.jtcvs.2012.08.044.
- Singhal S, Ferraris VA, Bridges CR, et al. Management of alveolar air leaks after pulmonary resection. Ann Thorac Surg 2010; 89: 1327-1335. 2010/03/27. DOI: 10.1016/j. athoracsur.2009.09.020.
- Attaar A, Luketich JD, Schuchert MJ, et al. Prolonged Air Leak After Pulmonary Resection Increases Risk of Noncardiac Complications, Readmission, and Delayed Hospital Discharge: A Propensity Score-adjusted Analysis. Ann Surg 2021; 273: 163-172. 2019/03/05. DOI: 10.1097/sla.000000000003191.
- Varela G, Jimenez MF, Novoa N, et al. Estimating hospital costs attributable to prolonged air leak in pulmonary lobectomy. Eur J Cardiothorac Surg 2005; 27: 329-333. 2005/02/05. DOI: 10.1016/j.ejcts.2004.11.005.
- Brunelli A, Chapman K, Pompili C, et al. Ninety-day hospital costs associated with prolonged air leak following lung resection. Interact Cardiovasc Thorac Surg 2020; 31: 507-512. 2020/09/01. DOI: 10.1093/icvts/ivaa140.
- 10. Brunelli A, Bölükbas S, Falcoz PE, et al. Exploring consensus for the optimal sealant use to prevent air leak following lung surgery: a modified Delphi survey from The European Society of Thoracic Surgeons. Eur J Cardiothorac Surg 2020 2020/12/19. DOI: 10.1093/ eicts/ezaa428.
- 11. Belda-Sanchis J, Serra-Mitjans M, Iglesias Sentis M, et al. Surgical sealant for preventing air leaks after pulmonary resections in patients with lung cancer. Cochrane Database Syst Rev 2010: Cd003051. 2010/01/22. DOI: 10.1002/14651858.CD003051.pub3.
- 12. Malapert G, Hanna HA, Pages PB, et al. Surgical sealant for the prevention of prolonged air leak after lung resection: meta-analysis. Ann Thorac Surg 2010; 90: 1779-1785. 2010/11/26. DOI: 10.1016/j.athoracsur.2010.07.033.
- 13. McGuire AL and Yee J. Clinical outcomes of polymeric sealant use in pulmonary resection: a systematic review and meta-analysis of randomized controlled trials. J Thorac Dis 2018; 10: S3728-s3739. 2018/12/07. DOI: 10.21037/jtd.2018.10.48.
- 14. Zhou J, Lyu M, Pang L, et al. Efficiency and safety of TachoSil® in the treatment of postoperative air leakage following pulmonary surgery: a meta-analysis of randomized controlled trials. Jpn J Clin Oncol 2019; 49: 862-869. 2019/05/29. DOI: 10.1093/jjco/hyz076.

- 15. Singhal S and Shrager JB. Should buttresses and sealants be used to manage pulmonary parenchymal air leaks? J Thorac Cardiovasc Surg 2010: 140: 1220-1225, 2010/10/19, DOI: 10.1016/j.jtcvs.2010.06.039.
- 16. Macchiarini P, Wain J, Almy S, et al. Experimental and clinical evaluation of a new synthetic, absorbable sealant to reduce air leaks in thoracic operations. J Thorac Cardiovasc Surg 1999; 117: 751-758. 1999/03/30. DOI: 10.1016/s0022-5223(99)70296-5.
- 17. McCarthy PM, Trastek VF, Bell DG, et al. The effectiveness of fibrin glue sealant for reducing experimental pulmonary air leak. Annals of Thoracic Surgery 1988; 45: 203-205. DOI: http:// dx.doi.org/10.1016/S0003-4975(10)62438-1.
- 18. Lewis KM, Spazierer D, Slezak P, et al. Swelling, sealing, and hemostatic ability of a novel biomaterial: A polyethylene glycol-coated collagen pad. J Biomater Appl 2014; 29: 780-788. 2014/08/03. DOI: 10.1177/0885328214545500.
- 19. Annabi N, Zhang YN, Assmann A, et al. Engineering a highly elastic human protein-based sealant for surgical applications. Sci Transl Med 2017; 9 2017/10/06. DOI: 10.1126/ scitranslmed.aai7466.
- 20. Elvin CM, Vuocolo T, Brownlee AG, et al. A highly elastic tissue sealant based on photopolymerised gelatin. Biomaterials 2010; 31: 8323-8331. 2010/08/03. DOI: 10.1016/j. biomaterials.2010.07.032.
- 21. Araki M, Tao H, Nakajima N, et al. Development of new biodegradable hydrogel glue for preventing alveolar air leakage. J Thorac Cardiovasc Surg 2007; 134: 1241-1248. 2007/11/03. DOI: 10.1016/j.jtcvs.2007.07.020.
- 22. Bosmans J, Moossdorff M, Al-Taher M, et al. International consensus statement regarding the use of animal models for research on anastomoses in the lower gastrointestinal tract. Int J Colorectal Dis 2016; 31: 1021-1030. 2016/03/11. DOI: 10.1007/s00384-016-2550-5.
- 23. van der Worp HB, Howells DW, Sena ES, et al. Can Animal Models of Disease Reliably Inform Human Studies? PLOS Medicine 2010; 7: e1000245. DOI: 10.1371/journal.pmed.1000245.
- 24. Cárdenes N, Sembrat J, Noda K, et al. Human ex vivo lung perfusion: a novel model to study human lung diseases. Sci Rep 2021; 11: 490. 2021/01/14. DOI: 10.1038/s41598-020-79434-4.
- 25. Horvath MA, Hu L, Mueller T, et al. An organosynthetic soft robotic respiratory simulator. APL Bioeng 2020; 4: 026108. 2020/06/23. DOI: 10.1063/1.5140760.
- 26. Klassen C, Eckert CE, Wong J, et al. Ex Vivo Modeling of Perioperative Air Leaks in Porcine Lungs. IEEE Trans Biomed Eng 2018; 65: 2827-2836. 2018/07/12. DOI: 10.1109/ tbme.2018.2819625.
- 27. Ritskes-Hoitinga M, Leenaars M, Avey M, et al. Systematic reviews of preclinical animal studies can make significant contributions to health care and more transparent translational medicine. Cochrane Database of Systematic Reviews 2014. DOI: 10.1002/14651858. ED000078.
- 28. Hooijmans CR, Tillema A, Leenaars M, et al. Enhancing search efficiency by means of a search filter for finding all studies on animal experimentation in PubMed. Lab Anim 2010; 44: 170-175. 2010/06/17. DOI: 10.1258/la.2010.009117.
- 29. Yauw ST, Wever KE, Hoesseini A, et al. Systematic review of experimental studies on intestinal anastomosis. Br J Surg 2015; 102: 726-734. 2015/04/08. DOI: 10.1002/bjs.9776.

- 30. Percie du Sert N, Hurst V, Ahluwalia A, et al. The ARRIVE guidelines 2.0: Updated guidelines for reporting animal research. PLoS Biol 2020; 18: e3000410. 2020/07/15. DOI: 10.1371/ journal.pbio.3000410.
- 31. Hooijmans CR, Rovers MM, de Vries RB, et al. SYRCLE's risk of bias tool for animal studies. BMC Med Res Methodol 2014; 14: 43. 2014/03/29. DOI: 10.1186/1471-2288-14-43.
- 32. Kanzaki M, Sekine H, Takagi R, et al. Bioartificial pleura using allogenic cell sheet for closing of lung air leakage. JTCVS Techniques 2020; 4: 336-340. DOI: http://dx.doi.org/10.1016/j. xitc.2020.09.024.
- 33. Kanzaki M, Takaqi R, Isaka T, et al. Off-the-Shelf Cell Sheets as a Pleural Substitute for Closing Visceral Pleural Injuries. Biopreserv Biobank 2019; 17: 163-170. 2019/02/02. DOI: 10.1089/bio.2018.0105.
- 34. Kanzaki M, Yamato M, Yang J, et al. Dynamic sealing of lung air leaks by the transplantation of tissue engineered cell sheets. Biomaterials 2007; 28: 4294-4302. 2007/07/03. DOI: 10.1016/j.biomaterials.2007.06.009.
- 35. Balakrishnan B, Payanam U, Laurent A, et al. Efficacy evaluation of anin situforming tissue adhesive hydrogel as sealant for lung and vascular injury. Biomed Mater 2021; 16 2021/04/27. DOI: 10.1088/1748-605X/abfbbf.
- 36. Gika M, Kawamura M, Izumi Y, et al. The short-term efficacy of fibrin glue combined with absorptive sheet material in visceral pleural defect repair. Interact Cardiovasc Thorac Surg 2007; 6: 12-15. 2007/08/03. DOI: 10.1510/icvts.2006.139436.
- 37. Kawai N, Suzuki S, Naito H, et al. Sealing Effect of Cross-Linked Gelatin Glue in the Rat Lung Air Leak Model. Ann Thorac Surg 2016; 102: 282-286. 2016/05/23. DOI: 10.1016/j. athoracsur.2016.02.038.
- 38. Ranger WR, Halpin D, Sawhney AS, et al. Pneumostasis of experimental air leaks with a new photopolymerized synthetic tissue sealant. Am Surg 1997; 63: 788-795. 1997/09/18.
- 39. Nomori H, Horio H, Morinaga S, et al. Gelatin-resorcinol-formaldehyde-glutaraldehyde glue for sealing pulmonary air leaks during thoracoscopic operation. Ann Thorac Surg 1999; 67: 212-216. 1999/03/23. DOI: 10.1016/s0003-4975(98)01184-9.
- 40. Servais AB, Valenzuela CD, Kienzle A, et al. Functional Mechanics of a Pectin-Based Pleural Sealant after Lung Injury. Tissue Eng Part A 2018; 24: 695-702. 2017/09/19. DOI: 10.1089/ ten.tea.2017.0299.
- 41. Buyukkale S, Citak N, Isgorucu O, et al. The effect of sodium hyaluronate-carboxymethyl cellulose membrane in the prevention of parenchymal air leaks: an experimental and manometric study in rats. Tuberkuloz Ve Torak-Tuberculosis and Thorax 2017; 65: 265-270. DOI: 10.5578/tt.9681.
- 42. Gigauri VS, Andrianov NG, Got'e SV, et al. [Hemostasis and hermetic sealing of the parenchyma in operations on the lungs]. Voen Med Zh 1975: 23-25. 1975/09/01.
- 43. Poticha SM, Macaladad F and Lewis FJ. THE CONTROL OF AIR LEAKS FOLLOWING SUBSEGMENTAL PULMONARY RESECTIONS. Surg Gynecol Obstet 1965; 120: 803-809. 1965/04/01.
- 44. Kausel HW and Lindskog GE. The healing of raw lung surfaces after experimental segmental resection. J Thorac Surg 1955; 29: 197-211. 1955/02/01.
- 45. Wilder RJ, Playforth H, Bryant M, et al. THE USE OF PLASTIC ADHESIVE IN PULMONARY SURGERY. J Thorac Cardiovasc Surg 1963; 46: 576-588. 1963/11/01.

- 46. Nuchprayoon C, Tamayo AG, Reimann AF, et al. The use and tissue reaction of a biologic adhesive in the prevention of air leak following a transection of the lung. Dis Chest 1968; 53: 445-452. 1968/04/01. DOI: 10.1378/chest.53.4.445.
- 47. Attaar A, Winger DG, Luketich JD, et al. A clinical prediction model for prolonged air leak after pulmonary resection. J Thorac Cardiovasc Surg 2017; 153: 690-699.e692. 2016/12/04. DOI: 10.1016/j.jtcvs.2016.10.003.
- 48. Moon DH, Park CH, Kang DY, et al. Significance of the lobe-specific emphysema index to predict prolonged air leak after anatomical segmentectomy. PLoS One 2019; 14: e0224519. 2019/11/07. DOI: 10.1371/journal.pone.0224519.
- 49. DeCamp MM, Blackstone EH, Naunheim KS, et al. Patient and surgical factors influencing air leak after lung volume reduction surgery: lessons learned from the National Emphysema Treatment Trial. Ann Thorac Surg 2006; 82: 197-206; discussion 206-197. 2006/06/27. DOI: 10.1016/j.athoracsur.2006.02.050.
- 50. Nam S and Mooney D. Polymeric Tissue Adhesives. Chem Rev 2021; 121: 11336-11384. 2021/01/29. DOI: 10.1021/acs.chemrev.0c00798.
- 51. Rivera C, Bernard A, Falcoz PE, et al. Characterization and prediction of prolonged air leak after pulmonary resection: a nationwide study setting up the index of prolonged air leak. Ann Thorac Surg 2011; 92: 1062-1068; discussion 1068. 2011/08/30. DOI: 10.1016/j. athoracsur.2011.04.033.
- 52. Mentzer SJ, Tsuda A and Loring SH. Pleural mechanics and the pathophysiology of air leaks. J Thorac Cardiovasc Surg 2018; 155: 2182-2189. 2018/02/06. DOI: 10.1016/j. itcvs.2017.12.062.
- 53. Pompili C and Miserocchi G. Air leak after lung resection: pathophysiology and patients' implications. J Thorac Dis 2016; 8: S46-54. 2016/03/05. DOI: 10.3978/j.issn.2072-1439.2015.11.08.
- 54. Zaraca F, Brunelli A, Pipitone MD, et al. A Delphi Consensus report from the "Prolonged Air Leak: A Survey" study group on prevention and management of postoperative air leaks after minimally invasive anatomical resections. Eur J Cardiothorac Surg 2022 2022/04/05. DOI: 10.1093/ejcts/ezac211.
- 55. Brunelli A, Salati M, Pompili C, et al. Intraoperative air leak measured after lobectomy is associated with postoperative duration of air leak. Eur J Cardiothorac Surg 2017; 52: 963-968. 2017/04/27. DOI: 10.1093/ejcts/ezx105.
- 56. Kim WH, Lee HC, Ryu HG, et al. Intraoperative ventilatory leak predicts prolonged air leak after lung resection: A retrospective observational study. PLoS One 2017; 12: e0187598. 2017/11/10. DOI: 10.1371/journal.pone.0187598.
- 57. Charan J and Kantharia ND. How to calculate sample size in animal studies? J Pharmacol Pharmacother 2013; 4: 303-306. 2013/11/20. DOI: 10.4103/0976-500x.119726.
- 58. Rooney MB, Mehl M and Monnet E. Intercostal thoracotomy closure: transcostal sutures as a less painful alternative to circumcostal suture placement. Vet Surg 2004; 33: 209-213. 2004/04/24. DOI: 10.1111/j.1532-950X.2004.04031.x.
- 59. de Vries RB, Wever KE, Avey MT, et al. The usefulness of systematic reviews of animal experiments for the design of preclinical and clinical studies. Ilar j 2014; 55: 427-437. 2014/12/30. DOI: 10.1093/ilar/ilu043.

Chapter 3 Supplemental material

Supplements B, D and E are not shown in this thesis and can be accessed online (https://doi.org/10.1177/00236772231164873)

Supplement 3A - Database entries

PUBMED: All fields, no restrictions

((Pulmon*[tw] OR Lung*[tw] OR Lobectom*[tw] OR Pneumectom*[tw] OR Segmentectom*[tw] OR Pleur*[tw] OR "Lung resect*"[tw] OR "Pulmonary surgical procedures"[Mesh] OR "Air Leak*"[tw] OR PAL[tw] OR "Pneumothorax" [Mesh] OR "Alveolar-pleural fist*" [tw] OR "Bronchial "Pleural Diseases"[Mesh] Fistula"[Mesh] OR OR "Subcutaneous Emphysema"[Mesh:NoExp] OR "Lung Diseases"[Mesh] OR "Lung"[Mesh] 0R "Respiratory Tract Fistula" [Mesh: NoExp] OR Pneumothorax[tw] bronch*[tiab] OR "Bronchial Fistula*"[tw] OR OR alveol*[tiab] OR "Pneumonectomy" [Mesh]))

AND

((aerostatic*[tw] OR adhesiv*[tw] OR seal*[tw] OR glue*[tw] OR bioglue*[tiab] OR spray*[tiab] OR patch[tiab] OR sheet*[tiab] OR "Tissue Adhesives" [Mesh] OR "Tissue Adhesives" [Pharmacological Action] OR "Fibrin Tissue Adhesive" [Mesh] OR Mesh[tiab] OR buttressing*[tiab] OR Hydrogel*[tiab]))

AND

Animal studies filter(1)

WEB OF SCIENCE: All fields, no restrictions, Web of Science core collection

ALL=(Pulmon* OR Lobectom* OR Pneumectom* OR segmentectom* OR "Lung" resect*" OR "Pulmonary surg*" OR "Pulmonary alveolar air leak" OR "Air leak" OR "Pneumothorax" OR "Bronchial fistula" OR "Alveolar-pleural fist*" OR "Lung NEAR/1 surg*" OR Lung*) AND ALL=(aerostatic* OR adhesiv* OR seal* OR glue* OR "surgical adhesive" OR bioglue OR spray* OR patch OR sheet* OR Mesh OR "fibrin patch" OR sealant OR "sealing device" OR buttressing OR

hydrogel* OR "tissue adhesive" OR "fibrin tissue adhesive") AND ALL=("Animal experiment" OR "Animal model" OR "in-vivo" OR "experimental setup" OR "exvivo" OR "animal NEAR/1 experimentation" OR vertebrate OR mammal OR porcine OR pig OR ovine OR sheep OR canine OR dog OR hog OR rabbit OR rat OR mouse)

EMBASE: All fields, no restrictions

((Pulmon* or Lung* or Lobectom* or Pneumectom* or Segmentectom* or Pleur* or Lung resect* or Air Leak* or Alveolar pleural fist* or Pneumothorax or Bronchial fistula).mp. or (bronch* or alveol*).ti,ab,kw. or "lung surgery"/ or "lung resection"/ or "lung lobectomy"/ or exp "artificial pneumothorax"/ or exp "pneumothorax"/ or "bronchus fistula"/ or "respiratory tract fistula"/ or "pleura disease"/ or "lung emphysema"/ or "respiratory tract fistula"/)

AND

((aerostatic* or adhesiv* or seal* or glue* or surgical adhesive*).mp. or (bioglue* or spray* or patch or sheet* or Mesh or buttressing* or Hydrogel*). ti,ab,kw. or exp "tissue adhesive"/ or exp "fibrin"/ or exp "fibrin glue"/ or exp "sealant"/)

AND

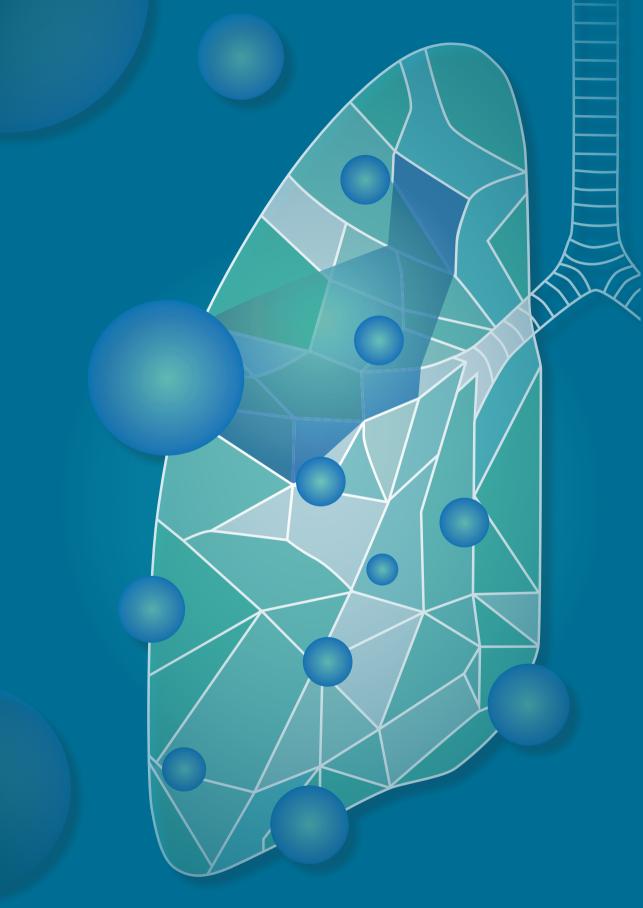
Animal studies filter(1)

References

1. Hooijmans CR, Tillema A, Leenaars M, Ritskes-Hoitinga M. Enhancing search efficiency by means of a search filter for finding all studies on animal experimentation in PubMed. Lab Anim. 2010;44(3):170-5.

Supplement 3C - Risk of bias tool

Nr.	Review authors judgment	Answer question	Risk of bias	Motivation
1	Was the allocation sequence adequately generated and applied?			
2	Were the groups similar at baseline or were they adjusted for confounders in the analysis?			
3	Was the allocation adequately concealed?			
4	Were the animals randomly housed during the experiment?			
5	Were the caregivers and /or investigators blinded from knowledge which intervention each animal received during the experiment?			
6	Were animals selected at random for outcome assessment?			
7	Was the outcome assessor blinded?			
8	Were incomplete outcome data adequately addressed?			



Chapter 4

Sealing effectiveness of a novel NHS-POx based patch: experiments in a dynamic *ex-vivo* porcine lung

Bob P Hermans¹, Wilson WL Li¹, Edwin A Roozen², Daniël IM van Dort¹, Jort Evers¹, Erik HFM van der Heijden³, Stefan M van der Heide¹, Harry van Goor², Ad FTM. Verhagen¹

Radboud university medical center, Radboud Institute for Health Sciences, Nijmegen, The Netherlands.

¹Department of Cardio-thoracic surgery

²Department of General surgery

³Department of Pulmonology

Used with permission of Nancy International Ltd., from "Hermans BP, Li WWL, Roozen EA, van Dort DIM, Evers J, van der Heijden EHFM, van der Heide SM, van Goor H, Verhagen AFTM. Sealing effectiveness of a novel NHS-POx based patch: experiments in a dynamic *ex vivo* porcine lung. *J Thorac Dis.* 2023 Jul 31;15(7):3580-3592. doi: 10.21037/jtd-22-1821."; permission conveyed through Copyright Clearance Center, Inc.

ABSTRACT

Background: Sealants are used to prevent prolonged pulmonary air leakage after lung resections (incidence 5.6-30%). However, clinical evidence to support sealant use is insufficient, with an unmet need for a more effective product. We compared a novel gelatin patch impregnated with functionalized polyoxazolines (NHS-POx) (GATT-Patch) to commercially available sealant products.

Methods: GATT-Patch Single/Double layers were compared to Progel[®], Coseal[®], Hemopatch[®] and TachoSil[®] in an *ex-vivo* porcine lung model (first experiment). Based on these results, a second head-to-head comparison between GATT-Patch Single and Hemopatch[®] was performed. Air leakage (AL) was assessed in three settings using increasing ventilatory pressures (max=70cmH2O): 1. baseline, 2. with 25x25mm superficial pleural defect, and 3. after sealant application. Lungs floating on saline (37°C) were video recorded for visual AL assessment. Pressure and tidal volumes were collected from the ventilator, and bursting pressure (BP), AL and AL-reduction were determined.

Results: Per sealant 10 measurements were performed (both experiments). In the first experiment, BP was superior for GATT-Patch Double (60 ± 24 cmH20) compared to TachoSil® (30 ± 11 cmH20, P<0.001), Hemopatch® (33 ± 6 cmH20, P=0.006), Coseal® (25 ± 13 cmH20, P=0.001) and Progel® (33 ± 11 cmH20, P=0.005). AL-reduction was superior for GATT-Patch Double ($100\pm1\%$) compared to Hemopatch® ($46\pm50\%$, P=0.010) and TachoSil® ($31\pm29\%$, P<0.001), and also for GATT-Patch Single ($100\pm14\%$, P=0.004) and Progel ($89\pm40\%$, P=0.027) compared to TachoSil®. In the second experiment, GATT-Patch Single was superior regarding BP (45 ± 10 vs 40 ± 6 cmH20, P=0.043) and AL-reduction (100 ± 11 vs $68\pm40\%$, P=0.043) when compared to Hemopatch®.

Conclusions: The novel NHS-POx patch shows promise as a lung sealant, demonstrating elevated BP, good adhesive strength and a superior AL-reduction.

Introduction

Pulmonary air leakage (PAL) is an important concern for patients undergoing pulmonary resections. Prolonged PAL (pPAL), defined as PAL lasting longer than five days, affects 5.6-30% of patients.(1) pPAL is the main reason for delayed chest tube removal, prolonged hospital stay and readmissions (2-4), while resulting in more complications including empyema⁽⁵⁾, pneumonia^(6,7) and mortality. (8) Furthermore, 4.8% of patients with pPAL require additional interventions (extra chest tubes, bronchoscopy and reoperation). (6) In an attempt to prevent these postoperative consequences, various sealants have been developed for intraoperative use. (9)

There is a broad variation in surgical management of air leaks. A recent study found significant between-hospital variation for pPAL incidence in the Netherlands (2.6-19.3% adjusted for case-mix), and also important variation regarding intraoperative PAL management, including sealant use. (10) Available evidence supporting intraoperative sealant use in this setting is controversial at best, highlighted by a recent survey in which only 42% of surgeons believed enough evidence exists to support their sealant use. (11) This is in line with a Cochrane review on this subject published in 2010⁽¹²⁾, that does not recommend the routine use of sealants due to unclear benefits, for example on length of hospital stay. However, this study pooled multiple products with varying modes of action into one analysis, but head-to-head comparisons between sealants are scarce. (12,13) Considering some sealants might be more effective than others⁽¹⁴⁾, a comparison of existing and novel products is warranted, to further substantiate sealant selection and use in current surgical practice. Furthermore, there is an unmet need for a single-component and more effective surgical sealant capable of sealing PAL in wet and dynamic biological environments, as stated by Brunelli. (11)

To this end a novel patch based on porcine derived gelatin impregnated with synthetic polymers, may hold promise as a lung sealant. The gelatin-based patch contains poly(2-oxazolines) functionalized with N-hydroxysuccimide ester (NHS-POx) and nucleophilically activated polyoxazoline (NU-POx) (GATT Technologies BV, Nijmegen, The Netherlands). (15-18) After wet tissue contact, the reactive NHS side-chains will form covalent bonds with amines present on tissues, blood, NU-POx and the gelatin carrier itself. The polymers are further functionalized using hydroxyl groups for increased hydrophilicity to ensure adequate blood and water uptake, acting synergistically with

coagulation mechanisms. This results in a strongly adhesive and cohesive polyoxazoline hydrogel with good sealing properties. Positive results have been obtained for hemostatic applications in-vivo (15,17,18) and clinical trials are currently being performed to assess hemostatic efficacy on liver bleeding (ClinicalTrials.gov Identifier: NCT04819945 and NCT05385952).

In this study, we aim to investigate the aerostatic properties of this novel NHS-POx based patch in an ex-vivo porcine lung model compared to other commonly used lung sealants, by measuring bursting pressure (BP), air leak (AL) reduction and conformability to the lung surface.

While the ARRIVE reporting checklist is designed to improve the reporting of in-vivo studies, we decide to follow the ARRIVE 2.0 reporting checklist in this ex-vivo study considering many applicable items for better reporting in the study design, statistical analysis and results.

Methods

Study setup

We performed an ex-vivo study in a dynamic porcine lung model. First, a multigroup comparison was undertaken evaluating the novel patch applied in two ways (GATT-Patch Single and GATT-Patch Double) compared to Progel® (C. R. Bard, Inc., Murray Hill, New Jersey), Coseal® (Baxter International Inc., Deerfield, Illinois), Hemopatch® (Baxter International Inc., Deerfield, Illinois), and TachoSil® (Takeda Pharmaceutical Company Limited, Tokyo, Japan). Sample size (N=10 per group) was chosen based on previous reported experiments. (14) GATT-Patch Single/Double and Hemopatch® groups were randomized (Microsoft Excel, Aselect function) and blinded to the allocated group until the sealant was handed to the researcher, to mitigate unconscious influences on lesion creation. All GATT-Patches were provided by the manufacturer to the researchers, and all control products were commercially ordered.

Secondly, following this multigroup comparison, we performed a randomized head-to-head comparison of the novel GATT-Patch Single compared to the best product with the same mode of application (Hemopatch®). This experiment was undertaken in a similar randomized and blinded fashion after a formal sample size calculation (power=0.8, two-sided alpha=0.05, N=10 per group).

Porcine lung model

No live animals were involved in experimental procedures, and all experiments were performed on ex-vivo porcine lung tissue obtained from a slaughterhouse. Lungs from domestic pigs, used for human consumption and weighing between 90-100kg, were excised in the slaughterhouse, and put on ice as soon as possible for transport. All excess tissue was removed and sutures were used to prevent blood leaking in the setup. Caudal lobes were suctioned and selectively intubated (6.0mm endo-tracheal tube). Lungs were inflated manually, followed by clamping of the tube. Airtightness was ensured before use. Lobes with poor compliance or persistent atelectasis (as visually assessed) were rejected. Rewarming of the included porcine lungs was started approximately fifteen minutes before measurements.

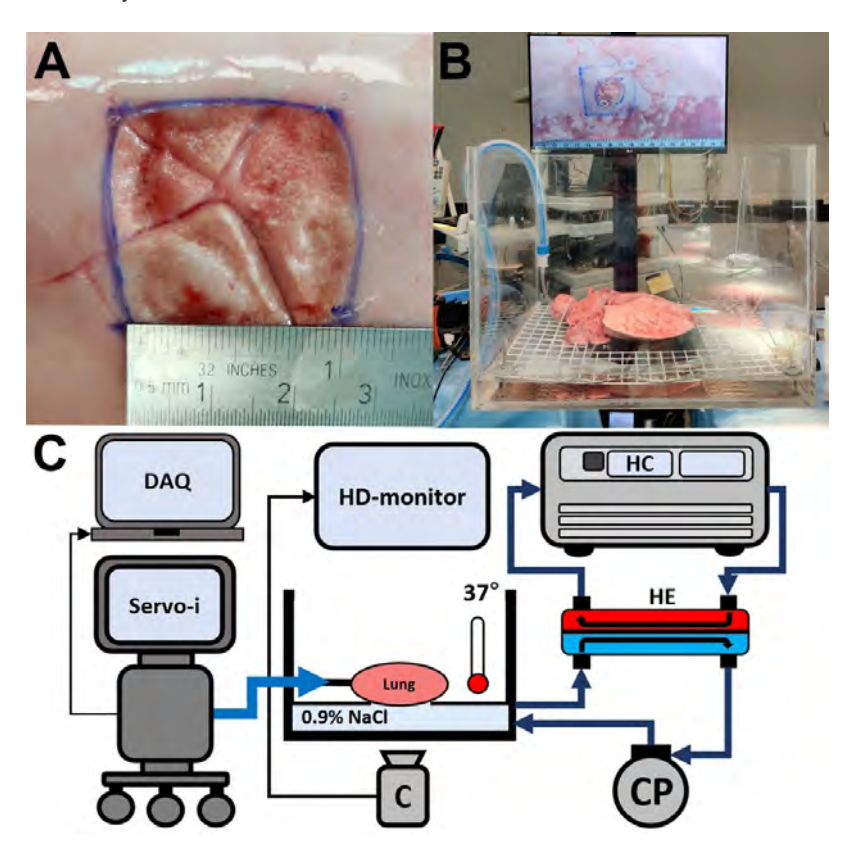


Figure 1: Overview of ex-vivo porcine lung model. A) Standardized pleural defect (25x25mm), made at static lung inflation pressure of 10cmH20. B) Experimental setup C) Schematic of experimental setup.

DAQ: data-acquisition setup; Servo-i: mechanical ventilator; C: camera; HD: high definition; NaCl: physiological saline solution; HC: heater-cooler; HE: heat-exchanger; CP: centrifugal pump. Specimens were examined in a clear container containing 10L 0.9% saline (NaCl) kept at 37°C. A camera positioned under the container and a ruler positioned at water level were used to record PAL and surface area expansion (SAE) (Figure 1 and Video 1). Airway pressures were recorded from the mechanical ventilator (Supplement 4A), and synchronized to the video data by pressing on the lung (visible on both datafiles). Tidal volumes were noted from the mechanical ventilator at the end of each measurement cycle to calculate AL.

Study protocol and outcome measures

Study outcomes were collected during three separate measurement cycles: (1) before and (2) after creating a standardized superficial pleural lesion, and (3) after sealant application. All study outcomes and definitions are presented in **Table 1**. To ensure standardized study measurements, porcine lung specimen were ventilated under increasing pressures with pressure control ventilation (initial settings: respiratory rate 12/min, inspiratory:expiratory ratio 1:2, positive end-expiratory pressure [PEEP] 5cmH2O and pressure above PEEP 5cmH20). Each measurement cycle, the plateau ventilatory pressure (Pplat) was re-started at the initial settings and increased with 5cmH2O every 90 seconds. Pressure was increased until a maximum of 40cmH2O for cycles (1) and (2) and 70cmH2O or upon reaching of grade III leakage (Table 1, Macchiarini scale⁽¹⁹⁾) during cycle (3). These measurement cycles were conducted as follows:

- (1) Baseline SAE measurements were performed after marking a 5x5cm area at static lung inflation of 5cmH20 PEEP on a dorsal non-atelectatic segment of the caudal lobe and measuring 'Baseline SAE', 'Lung compliance' and 'Baseline AL'. The SAE is defined as the percentual increase of this previously marked area at 40cmH20 with respect to 5cmH20 as a measure for lung surface expandability (see Figure 1B);
- (2) Defect AL measurements were performed after creating a standardized superficial pleural lesion (2.5x2.5cm, Figure 1A) using a sanding wheel (Dremel Lite 7760) and tweezers/scissors at static lung inflation of 10cmH20 PEEP. The lesion was made at the minimum depth required to remove the superficial pleura and expose the underlying parenchyma. Measurements included 'Baseline leaking pressures' (using the Macchiarini scale⁽¹⁹⁾) and 'Defect AL';
- (3) BP measurements were performed after sealant application, applying all patches at 5cmH20 PEEP static lung inflation and gels on a deflated lung. (Table 2)

In case of atelectasis following sealant application, 15-25cmH2O PEEP was administered for 5-10s. Measurements included 'BP', 'AL-reduction', 'Mode of failure' and 'expansion area change (EAC)'. BP was defined as the pressure setting at which the first bubbles were visible (i.e. grade I AL), and for values higher than 70cmH20, 75cmH20 was noted as an off-scale value. EAC is the measure of sealant conformability to the lung, defined as the proportion SAE post sealant application with respect to SAE pre sealant application (**Table 1**).

Table 1: Data collection and processing

Variable	Definition
Measurement cycle 1: Baseline	SAE
Baseline SAE	Surface area at 40cmH2O/Surface area at 5cmH2O (ImageJ, version 1.53a, Wayne Rasband)
Baseline AL	Calculated at Pplat=40cmH2O, as "12x(TVi-'expiratory tidal volume') (read from the mechanical ventilator user interface). AL measured during 'Baseline SAE' measurements was subtracted from 'Defect AL' and 'BP measurements' to correct for circuit leakage and bias flow.
Lung compliance	TVi at 40cmH2O/35
Ischemic time	Time from arrival at laboratory until start of experiments.
Measurement cycle 2: Defect AL	
Baseline leaking pressures	Macchiarini scale (grades: I=countable bubbles, II=stream of bubbles, III=coalesced bubbles) (16), assessed by two investigators.
Defect AL	See 'Baseline AL'
Surface and water temperature	Measured before sealant application
Measurement cycle 3: BP measu	rements
Sealed leaking pressures	See 'Baseline leaking pressures' BP = pressure at which first AL occurred (grade I).
AL-reduction	BP measurements AL: see 'Baseline AL' 100%x((Defect AL-BP measurements AL)/Defect AL), capped at 0 and 100% (calculated at Pplat=40cmH20). Always noted as 100% if BP>40cmH20.
EAC	Sealed SAE: see 'Baseline SAE' EAC = Sealed SAE/Baseline SAE EAC=100% indicates perfect conformability of the sealant to lung expansion, EAC <100% indicates reduced SAE after sealant application compared to baseline (Supplement 4A).
Mode of failure	Adhesive failure (leakage between sealant and lung; Figure 3D) Cohesive failure (leakage through the sealant; Figure 3F).

SAE: surface area expansion; AL: air leak; Pplat: plateau ventilatory pressure; TVi: inspiratory tidal volume; BP: bursting pressure; EAC: expansion area change.

Recorded video data was used for independent assessment of leaking pressures and BP by two investigators, noting the timepoints when different leaking grades occurred in the videos (Table 1), followed by reaching consensus and synchronization of the corresponding pressure values. Assessors were blinded to the assigned group for the baseline videos, but not for the sealed samples due to obvious differences in product appearance.

Table 2: Modes of application

Sealant	Application
TachoSil® (4.8x4.8cm)	Saline gauzes: 3 minute compression
Hemopatch® (4.5x4.5cm)	SBB lung priming Dry gauzes: 2 minute compression
GATT-patch Single (5x5cm)	SBB lung priming Diluted SBB gauzes: 2 minutes compression + 60mL diluted SBB irrigation
GATT-patch Double (5x5cm)	SBB lung priming, apply first patch Apply second patch perpendicularly with 60 mL SBB irrigation between patches Saline gauzes: 2 minutes compression + 60mL saline irrigation
Coseal® (2mL)	Spray marked area, dry 60 seconds
Progel® (2mL)	Spray marked area, dry 120 seconds

SBB: sodium-bicarbonate buffer (pH 8.3-8.5); Diluted SBB: SBB with saline (1:2)

Statistical analysis

Statistical analysis was performed using IBM SPSS Statistics for Windows, Version 26.0 (Armonk, New York; IBM Corp). Kolmogorov-Smirnov test was used for assessment of data distribution. Non-normally distributed data and normally distributed data were presented as median±interquartile range (IQR) or mean±standard deviation (SD) respectively. For the first experiment, Kruskal-Wallis test (non-parametric) or analysis of variance (parametric) were used. Bonferroni correction was used during post-hoc analysis (pairwise). For the second experiment, Mann-Whitney-U test (nonparametric) or independent samples T-test (parametric) were used. Fischer's exact test was used for categorical data. Missing data was analyzed by pairwise exclusion. Tests were performed two-tailed and the null-hypothesis was rejected if P<0.05.

Results

First experiment

We performed 60 measurements on 60 lungs, 10 for each group of sealants. Baseline characteristics were similar between groups (Table 3). Four measurements had missing or incomplete video/pressure data, due to technical errors (GATT-Patch Double and Single, TachoSil® and Coseal®). One measurement had missing tidal volumes for baseline AL measurements (GATT-Patch Double).

GATT-Patch Double (60±24cmH20) showed significantly higher BP compared to Progel® (33±11cmH2O, P=0.005), Coseal® (25±13cmH2O, P=0.001), Hemopatch® (33±6cmH2O, P=0.006) and TachoSil® (30±11cmH2O, P<0.001), but no significant differences in BP compared to GATT-Patch Single (40±10cmH20) (P>0.99). Between GATT-Patch Single, Progel®, Coseal®, Hemopatch® and TachoSil® no significant differences in BP were found (Figure 2A, Table 3). AL-reduction was significantly better for GATT-Patch Double compared to Hemopatch® (P=0.010) and TachoSil® (P<0.001). GATT-Patch Single (P=0.004) and Progel® (P=0.027) showed significantly better ALreduction compared to TachoSil® (Figure 2B, Table 3).

The EAC was significantly better for Coseal® (98±13%) compared to TachoSil® (80±11%, P=0.023), GATT-Patch Single (77±9%, P=0.005) and GATT-Patch Double (76±9%, P=0.004) (Table 3). Cohesive failure was observed more often for GATT-Patch Double, GATT-Patch Single, Progel® and Coseal®, while adhesive failure was seen more frequently for Hemopatch® and TachoSil® (P<0.001) (Table 3, Figure 3, Video 1). Interestingly, different failure mechanisms were observed: progression until grade III leakage was generally more gradual for GATT-Patch Double, GATT-Patch Single, Progel® and Coseal®, requiring one or more pressure intervals to reach grade III leakage. For Hemopatch® and TachoSil®, grade III leakage was usually reached in the same pressure interval where first leakage occurred (**Table 3**).

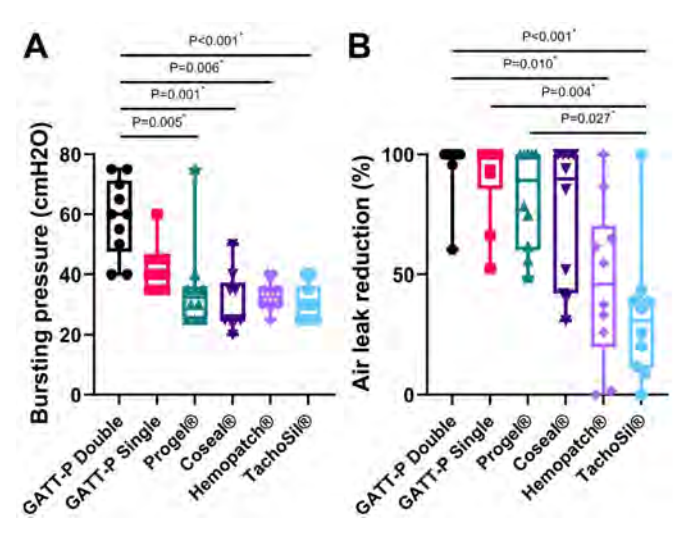


Figure 2: First experiment main results A) Bursting pressure B) Air leak reduction

Presented as median, interquartile range and range. Statistical analysis is performed using a Kruskal-Wallis test (two-tailed) and P-values are adjusted using the Bonferroni correction in post-hoc analysis. *Statistically significant at P<0.05; GATT-P: Gelatin patch impregnated with N-hydroxysuccimide ester functionalized poly(2-oxazolines).

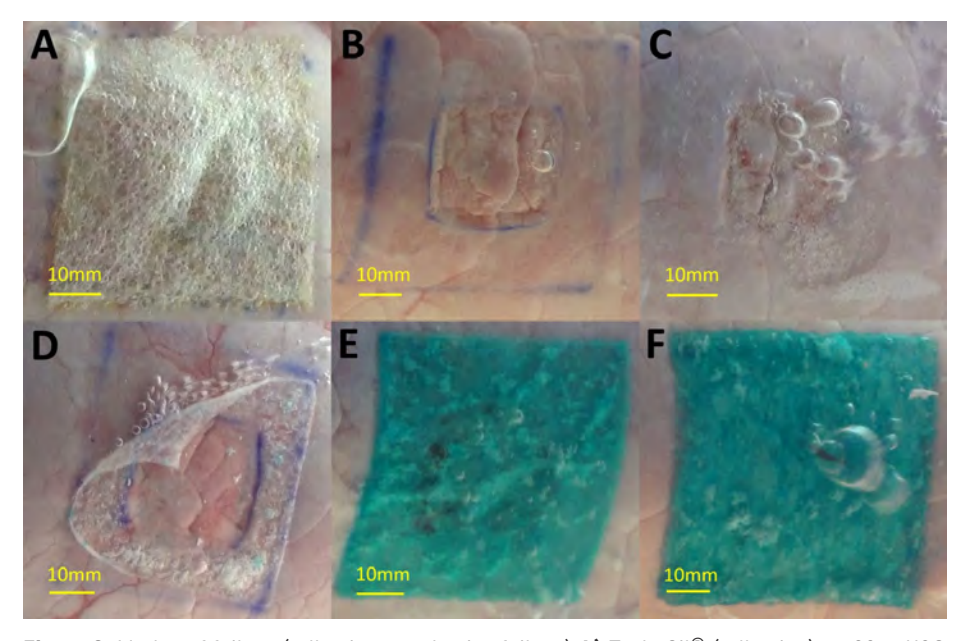


Figure 3: Modes of failure (adhesive or cohesive failure) **A)** TachoSil[®] (adhesive), at 30cmH20 ventilatory pressure. **B)** Coseal[®] (cohesive), at 50cmH20. **C)** Progel[®] (cohesive), at 40cmH20 **D)** Hemopatch[®] (adhesive), at 40cmH20 **E)** GATT-Patch Single (cohesive), at 70cmH20 **F)** GATT-Patch Double (cohesive), at 55cmH20. Note: all lesions (25x25mm) were made at 10cmH20, patches were applied at 5cmH20 and gels on a deflated lung.

S	
Ф	
Ξ	
<u>_</u>	
ō	
≒	
5	
_	
ō	
\equiv	
Ø	
Ś	
\overline{c}	
2	
LIS	
ē	
_	
ပ	
rac	
ë	
č	
\overline{c}	
o e	
≧	
=	
Ф	
2	
a	
1	
ī	
ē	
Ĕ	
⊆	
Ξ	
<u> </u>	
xbe	
â	
ב	
S	
≟	
ī	
e S	
e	
=	
apr	

	Patch sealants				Spray sealants		
	GATT-Patch Double	GATT-Patch Single	Hemopatch [®]	TachoSil [®]	Progel [®]	Coseal®	P-value
BASELINE CHARACTERISTICS							
Sample characteristics							
Ischemic time (minutes)⁺	238±141	233±105	119±66	215±158	213±102	226±164	0.32
Left lower lobe (n, %)	8 (80)	6 (90)	5 (50)	7 (70)	(09) 9	6 (90)	0.33
Physical characteristics							
Surface temperature (°C)†	31.2±1.2	31.8±1.6	31.9±1.3	31.7±2.2	33.0±1.0	31.7±1.2	0.15
Water temperature (°C) ⁴	37.2±0.5	37.2±0.3	37.3±0.3	37.2±0.5	37.2±0.5	37.1±0.2	0.49
Baseline SAE (%)‡	152±13	149±25	153±18	148±20	153±35	151±15	>.99
Lung compliance (mL/cm H20)*	24±7	23±7	27±2	26±7	24±6	26±5.0	0.30
Leakage characteristics							
Baseline leaking pressures							
Grade I (cmH2O)*	10±5	13±11	10±5	15±5	10±1	13±5	0.15
Grade II (cmH2O)*	15±3	18±15	15±1	20±10	18±5	15±5	0.44
Grade III (cmH2O)⁺	23±6	26±8	23±5	24±8	23±6	22±5	0.84
AL							
Amount (L/min)*	1.1±0.6	0.6±1.5	1.2±0.8	0.7±1.4	1.1±1.4	0.9±0.9	0.64
Percent of TVi (%)⁺	10.7±6.2	5.9±11.2	9.6±7.9	9.7±9.6	10.2±12.2	7.9±6.3	0.62

Table 3: Continued

	Patch sealants				Spray sealants	ts	
	GATT-Patch Double	GATT-Patch Single	Hemopatch [®] TachoSil [®]	TachoSil [®]	Progel®	Coseal®	P-value
EXPERIMENT OUTCOMES							
Sealed leaking pressures							
Grade I (cmH20)♯	60±24	40±10	33±6	30±11	33±11	25±13	<.001
Grade II (cmH2O) ♯	60±24	45±15	33±6	30±11	33±15	30±13	<.001
Grade III (cmH20) ‡	65±21	50±29	35±6	30±20	40±19	40±25	<.001
AL-reduction (%)*	100±1	100±14	46±50	31±29	89±40	90±58	<.001
Cohesive failure (n, %)	8 (89)	6 (90)	3 (30)	2 (20)	8 (89)	10 (100)	<.001
EAC (%)†	76±9	77±9	92±13	80±11	88±14	98±13	0.001

Bold P-value indicate statistical significance (P<0.05). $^\dagger \text{Mean} \pm \text{standard deviation (SD)}$

*Median±interquartile range (IQR) SAE: surface area expansion; AL: air leak; TVI: inspiratory tidal volume; EAC: expansion area change.

Second experiment

Twenty measurements were performed on 20 lungs, 10 for each group. Despite adequate randomization, baseline AL was found to be significantly higher in the GATT-Patch Single group compared to the Hemopatch group (1.5±0.8 vs 0.8±0.5 L/min, P=0.03). Other baseline characteristics were not significantly different (Supplement 4A). Despite the larger baseline AL, BP for GATT-Patch Single (45±10cmH20) was significantly higher compared to Hemopatch® (40±6cmH20, P=0.043) (Figure 4A). AL-reduction also reached statistical significance (P=0.043) (Figure 4B). Hemopatch® showed only adhesive failure and GATT-Patch Single only cohesive failure (P<0.001). EAC measurements were not performed due to extensive adhesive failure of Hemopatch[®].

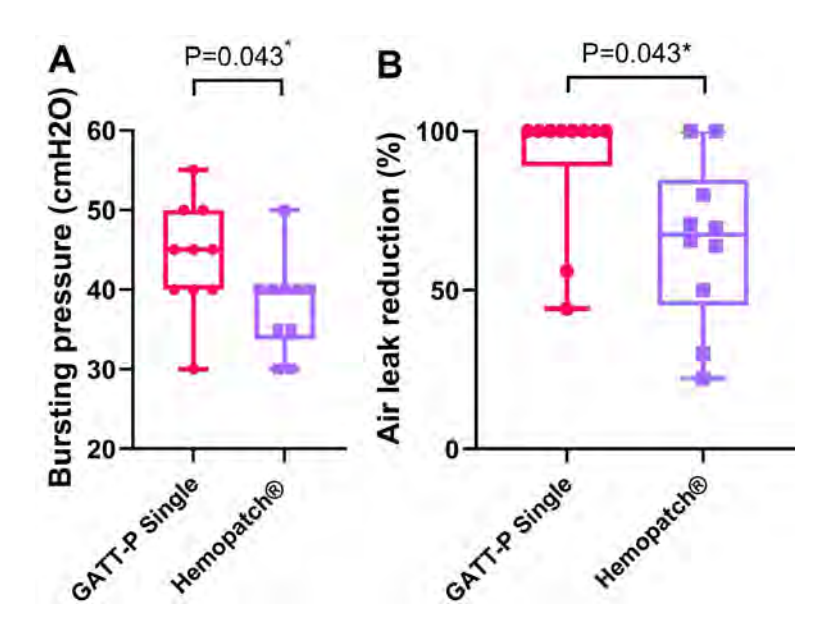


Figure 4: Second experiment main results A) Bursting pressure B) Air leak reduction

Presented as median, interquartile range and range. Statistical analysis is performed using a Mann-Whitney-U test (two-tailed).

GATT-P: Gelatin patch impregnated with N-hydroxy succimide ester functionalized poly (2-oxazolines).

^{*}Statistically significant at P<0.05

Discussion

This *ex-vivo* experimental study demonstrated favorable mechanical properties for the novel NHS-POx based lung sealant (GATT-Patch). The patch exhibited excellent adhesive characteristics to the lung parenchyma, withstanding repetitive lung expansions in a wet and dynamic *ex-vivo* lung environment without tearing or debonding until pressures of at least 30-40cmH2O. Importantly, in the second head-to-head comparative experiment, GATT-Patch Single showed improved performance compared with a commercially available patch used for lung sealing with a similar application method (Hemopatch®).

Interpretation of results

The potentially higher BP which can be achieved with the NHS-POx patch may be of clinical relevance. It has been suggested that the BP of a sealant should be high enough to withstand pressures during coughing (14) or during positive-pressure recruitment maneuvers (up to 40cmH20). (20,21) Physiologically, intra-thoracic pressures during coughing can reach up to 408cmH2O (22) and up to 71cmH2O in the post-thoracotomy state. (23) Pedersen suggested that the actual pressures on the lesion might be lower due to pleural apposition, relieving transpulmonary pressures during coughing (14). In this context, we hypothesize that different modes of failure could make some sealants more effective than others. We observed that TachoSil® and Hemopatch® generally lose their sealing capacities after bursting due to lower adhesive strength. Progel®, Coseal®, GATT-Patch Double and Single remain effective in reducing the AL even after reaching BP and take one or more pressure-intervals to reach higher leakage intensities, due to the strong adhesive properties to the entire parenchymal lung defect (**Table 3**). (24)

As described previously, a lung sealant should have high conformability to the lung surface, to prevent debonding when re-expanding the lung. (24) We hypothesize this is especially true for gel-based sealants, as they cannot be applied to a slightly inflated lung with active leakage (air bubble formation). We observed tears leading to sealant failure for Coseal® and Progel® under increasing lung expansions, which may render these sprays less suitable for coverage of large areas. Patch sealants might not require as much conformability compared to gel sealants, being applicable to a slightly inflated lung surface with an active leak (counterpressure with gauzes). We observed successful applications at PEEP=5cmH2O for the TachoSil®, Hemopatch® and GATT-Patch groups. Debonding was not observed in the GATT-Patch groups during

lung expansions due to strong adhesive properties. Thus, the experimentally measured lower EAC compared to Coseal® might not be of clinical importance.

Ease of use is an important benchmark for a sealants usability in the operating room. GATT-Patch Single has a similar mode of application compared to Hemopatch® and TachoSil®. However, GATT-Patch Double might be more difficult to implement in a clinical setting, especially minimally invasive surgery. In this case, a sprayable sealant might be preferable, which may also be better suited on irregular surfaces such as stapler lines, due to mechanical interlocking. Consequently, different modes of application are required depending on the surgical scenario.

Before clinical use of GATT-Patch as a lung sealant, safety outcomes for implantation in the thoracic cavity need to be assessed in-vivo, including inflammatory properties, influences on wound healing, adhesion formation with the parietal pleura and biodegradation. Roozen et. al. have shown that the histological results of GATT-Patch for intra-abdominal implantation were similar to control patches, showing complete biodegradation within 4-6 weeks. (17) However, no significant conclusions could be drawn with respect to adhesion formation. (17) Chemically, the amide and thioester bonds formed due to NHS reactivity are hydrolysable, and the NHS-POx degradation products have been shown to be effectively renally excreted in a rat model. (16) Porcinederived gelatin, constituting the patch-carrier for NHS-POx, is already being used in other devices such as SURGIFLO® Hemostatic Matrix (Ethicon Inc. Raritan, New Jersey), Gelfoam® and Gelita TUFT-IT® and may be cleared in 3 weeks. (17) A theoretical downside to this material is the potential for antigenicity and allergic reactions, but this is very rare. (25) Finally, GATT-Patch is being investigated in multi-center clinical trials of liver surgery (ClinicalTrials.gov Identifier: NCT04819945 and NCT05385952), suggestive of a promising safety profile in humans.

Comparison to literature

The extent of intra-operative PAL has previously been used to predict the occurrence of pPAL. Kim found an AL percentage of inspiratory tidal volume (TVi) >9.5% is predictive of pPAL, while Brunelli showed this for AL >500 mL/min. (26,27) Furthermore, a recent consensus survey has proposed that AL >400mL/min is classified as severe. (28) Therefore, the amount of AL observed in our study as a result of the created pleural lesions in porcine lungs (median 0.6-1.2L/min at Pplat=40cmH2O, **Table 3**) seems clinically relevant.

In previously published *ex-vivo* experiments, defect AL wasn't always determined, making interpretation of those results more troublesome. Pedersen and Zang/Bures found higher BP for TachoSil® (median=35cmH2O, range=30-55cmH2O and mean=36.0cmH2O, SD=4.9cmH2O, respectively) when compared to our finding (median 30, range 25-40 cmH2O).^(14,29) This may be due to differences in defect used. Fibrin glues, commonly used in thoracic surgery⁽⁹⁾, were also investigated by Pedersen. However, Tisseel® and Evicel® both performed significantly worse when compared to TachoSil®, and were therefore not included in our study.⁽¹⁴⁾

In current literature, comparative clinical studies evaluating effectiveness between sealants are scarce. In a recent systematic review⁽¹³⁾, only 2/21 included studies compared one sealant to another. In these two randomized clinical trials (RCTs) (BioGlue vs Vivostat⁽³⁰⁾ and Tisseel vs Vivostat⁽³¹⁾), no significant differences were found in postoperative PAL duration. A more recent RCT not included in this systematic review compared TachoSil and Neoveil, showing no significant differences.⁽³²⁾ Since 2018, a new clinical trial has been started (ClinicalTrials.gov Identifier: NCT03450265), aiming to compare Hemopatch[®] to TachoSil[®] in a non-inferiority study. Based on a favourable trend in AL-reduction seen in our study (**Figure 2**), the capabilities of Hemopatch[®] for intraoperative AL management and preventing pPAL may be superior when compared to TachoSil[®] clinically, but results of this trial have to be awaited.

Limitations

For AL quantification, the tidal volumes displayed by the ventilator were used, and corrected for baseline deviations which could be caused by system leaks or bias flow. The last breath of each pressure setting was used, to ensure the measurement was not influenced by resolving atelectasis (overestimation) or escaping trapped air (underestimation). However, despite the use of similar AL measurements in previous studies^(26,27,29), the most optimal air leak quantification approach remains to be validated.

With our SAE measurements, we attempted to integrate a conformability measurement in the BP setup. Due to possible influences by tears forming in the sealant (Progel® and Coseal®), debonding of the sealant (Hemopatch®) and camera angle, results should be interpreted cautiously (Supplement 4A). The method used by Yamaoka may have advantages in this perspective, not being influenced by different tearing/debonding characteristics. (24)

Difficulties were observed while applying Coseal® with the standard applicator, leading to inhomogeneous coverage, and higher BP may be reached with a more homogenous layer (e.g. dedicated spray set). Due to cohesive failure in Progel® and Coseal® groups, a thicker layer may lead to higher BP. Due to adhesive failure in TachoSil® and Hemopatch® groups, higher BP may be obtained with a larger adhesive overlap around the defect.

In the first experiment, randomization was not performed in the Progel® and Coseal® groups due to the limited shelf life of the prepared syringes (4mL) and not in the TachoSil® group using the same allocation scheme. Influence of possible unconscious biases are expected to be low, due to the demonstrated statistically similar baseline measurements in the first experiment. Sample sizes were not large enough to detect all significant differences. Due to a significantly larger air leak in the GATT-Patch Single group in the second experiment, the actual effect size between GATT-Patch Single and Hemopatch may have been underestimated.

Recommendations for future research

While the porcine lung has been found to be comparable to the human lung⁽³³⁾, ex-vivo results should be interpreted cautiously, as they may not translate accordingly to in-vivo situations (e.g. due to pleural mechanisms, coagulation, immune response, physiological breathing). The NHS-POx patch mode of application should be further optimized to improve usability in a clinical setting while maximizing mechanical cohesive strength (e.g. by creating a thicker single-layer patch). Before clinical use can be established, safety outcomes for implantation of the GATT-Patch in the thoracic cavity need to be assessed in-vivo. Fundamentally, mechanisms of sealant failure and BP should be further studied in relation to critical moments such as coughing or recruitment maneuvers, to establish threshold values for product development.

Conclusion

In conclusion, the novel NHS-POx based patch shows promise as a lung sealant due to favorable mechanical properties, demonstrating elevated BP and good adhesive strength to the lung. The gradual leakage pattern may provide superior reduction of an AL, especially in challenging clinical scenario's such as coughing or mechanical recruitment. The mode of sealant application should be optimized, and further in-vivo research is required to validate our findings and establish a safety profile for intra-thoracic implantation.

- 1. Attaar A, Tam V, Nason KS. Risk Factors for Prolonged Air Leak After Pulmonary Resection: A Systematic Review and Meta-analysis. Ann Surg 2020;271:834-44.
- 2. Seely AJ, Ivanovic J, Threader J, et al. Systematic classification of morbidity and mortality after thoracic surgery. Ann Thorac Surg 2010;90:936-42; discussion 42.
- 3. Brunelli A, Chapman K, Pompili C, et al. Ninety-day hospital costs associated with prolonged air leak following lung resection. Interact Cardiovasc Thorac Surg 2020;31:507-12.
- 4. Liu J, Yang X, Liu X, et al. Predictors of Readmission After Pulmonary Resection in Patients With Lung Cancer: A Systematic Review and Meta-analysis. Technol Cancer Res Treat 2022;21:15330338221144512.
- Brunelli A, Xiume F, Al Refai M, et al. Air leaks after lobectomy increase the risk of empyema but not of cardiopulmonary complications: a case-matched analysis. Chest 2006;130:1150-6.
- Liang S, Ivanovic J, Gilbert S, et al. Quantifying the incidence and impact of postoperative prolonged alveolar air leak after pulmonary resection. J Thorac Cardiovasc Surg 2013;145:948-54.
- 7. Singhal S, Ferraris VA, Bridges CR, et al. Management of alveolar air leaks after pulmonary resection. Ann Thorac Surg 2010;89:1327-35.
- 8. Yoo A, Ghosh SK, Danker W, et al. Burden of air leak complications in thoracic surgery estimated using a national hospital billing database. Clinicoecon Outcomes Res 2017;9:373-83.
- 9. Rocco G, Rendina EA, Venuta F, et al. The use of sealants in modern thoracic surgery: a survey. Interact Cardiovasc Thorac Surg 2009;9:1-3.
- 10. Hoeijmakers F, Hartemink KJ, Verhagen AF, et al. Variation in incidence, prevention and treatment of persistent air leak after lung cancer surgery. Eur J Cardiothorac Surg 2021.
- 11. Brunelli A, Bölükbas S, Falcoz PE, et al. Exploring consensus for the optimal sealant use to prevent air leak following lung surgery: a modified Delphi survey from The European Society of Thoracic Surgeons. Eur J Cardiothorac Surg 2020.
- 12. Belda-Sanchis J, Serra-Mitjans M, Iglesias Sentis M, et al. Surgical sealant for preventing air leaks after pulmonary resections in patients with lung cancer. Cochrane Database Syst Rev 2010:Cd003051.
- 13. McGuire AL, Yee J. Clinical outcomes of polymeric sealant use in pulmonary resection: a systematic review and meta-analysis of randomized controlled trials. J Thorac Dis 2018;10:S3728-s39.
- 14. Pedersen TB, Honge JL, Pilegaard HK, et al. Comparative study of lung sealants in a porcine ex vivo model. Ann Thorac Surg 2012;94:234-40.
- Boerman MA, Roozen E, Sánchez-Fernández MJ, et al. Next Generation Hemostatic Materials Based on NHS-Ester Functionalized Poly(2-oxazoline)s. Biomacromolecules 2017;18:2529-38.
- Boerman MA, Roozen EA, Franssen GM, et al. Degradation and excretion of poly(2oxazoline) based hemostatic materials. Materialia 2020;12:100763.
- 17. Roozen E, Lomme R, Calon N, et al. Efficacy of a novel polyoxazoline based hemostatic patch in liver and spleen surgery. 2023.
- 18. Roozen EA, Warlé MC, Lomme R, et al. New polyoxazoline loaded patches for hemostasis in experimental liver resection. J Biomed Mater Res B Appl Biomater 2021.

- 19. Macchiarini P, Wain J, Almy S, et al. Experimental and clinical evaluation of a new synthetic, absorbable sealant to reduce air leaks in thoracic operations. J Thorac Cardiovasc Surg 1999:117:751-8.
- 20. Marini JJ. Recruitment by sustained inflation: time for a change. Intensive Care Med 2011;37:1572-4.
- 21. Annabi N, Zhang YN, Assmann A, et al. Engineering a highly elastic human protein-based sealant for surgical applications. Sci Transl Med 2017;9.
- 22. McCool FD. Global physiology and pathophysiology of cough: ACCP evidence-based clinical practice guidelines. Chest 2006;129:48s-53s.
- 23. Byrd RB, Burns JR. Cough dynamics in the post-thoracotomy state. Chest 1975;67:654-7.
- 24. Yamaoka M, Maki N, Wijesinghe A, et al. Novel Alaska Pollock Gelatin Sealant Shows High Adhesive Quality and Conformability. Ann Thorac Surg 2019;107:1656-62.
- 25. White RZ, Kerr L, White TJ, et al. Review of topical gelatin-based haemostatic agents; an insidious culprit of intraoperative anaphylaxis? ANZ J Surg 2021;91:2002-7.
- 26. Kim WH, Lee HC, Ryu HG, et al. Intraoperative ventilatory leak predicts prolonged air leak after lung resection: A retrospective observational study. PLoS One 2017;12:e0187598.
- 27. Brunelli A, Salati M, Pompili C, et al. Intraoperative air leak measured after lobectomy is associated with postoperative duration of air leak. Eur J Cardiothorac Surg 2017;52:963-8.
- 28. Zaraca F, Brunelli A, Pipitone MD, et al. A Delphi Consensus report from the "Prolonged Air Leak: A Survey" study group on prevention and management of postoperative air leaks after minimally invasive anatomical resections. Eur J Cardiothorac Surg 2022.
- 29. Zhang R, Bures M, Höffler K, et al. In vitro comparison of two widely used surgical sealants for treating alveolar air leak. Thorac Cardiovasc Surg 2014;62:705-9.
- 30. Belcher E, Dusmet M, Jordan S, et al. A prospective, randomized trial comparing BioGlue and Vivostat for the control of alveolar air leak. J Thorac Cardiovasc Surg 2010;140:32-8.
- 31. Kılıç B, Erşen E, Demirkaya A, et al. A prospective randomized trial comparing homologous and autologous fibrin sealants for the control of alveolar air leak. J Thorac Dis 2017;9:2915-22.
- 32. Bachmann H, Dackam SVC, Hojski A, et al. Neoveil versus TachoSil in the treatment of pulmonary air leak following open lung surgery: a prospective randomized trial. Eur J Cardiothorac Surg 2022;63.
- 33. Rogers CS, Abraham WM, Brogden KA, et al. The porcine lung as a potential model for cystic fibrosis. Am J Physiol Lung Cell Mol Physiol 2008;295:L240-63.

Chapter 4 Supplemental material

Supplemental Video 1 is published online (https://doi.org/10.21037/jtd-22-1821).

Supplement 4A

Data-acquisition setup

Pressure data is retrieved from the mechanical ventilator (SERVO-I, Maquet Critical Care) through a RS232 link connected to a laptop using the ServoTracker software (version 4.1, Maquet Critical Care). The analog output of this software (-5 to +5V, sample rate 200/s) was then routed through two input-output devices (NI USB-6229 and NI USB-6210), which was then recorded into the analog input recorder application in Simulink (Matlab version R2020a) and oversampled at 1000/s. Before this signal was saved, it was gained (g = 40) and put through a discrete filter (f = 50Hz bandstop) to attain a clean signal in cmH20.

Conformability measurements

Surface area expansion calculation

For the surface area expansion (SAE) measurements, marked area (baseline) or sealant covered area (after sealing) of screenshots taken at airway pressures of 5 and 40 cmH20 were calculated using ImageJ (version 1.53a, Wayne Rasband). The ruler was used to determine the scale in the program. In the case of extensive debonding (mainly in Hemopatch® group), the SAE of the remaining adhesive portion was measured, while tears within sealants (Progel®/Coseal®) were included in the SAE measurements. SAE was calculated as (surface area at 40 cmH20)/(surface area at 5 cm H20) and the area expansion change (EAC was calculated as (sealed SAE)/(baseline SAE). An EAC of 100% indicates perfect conformability of the sealant to the lung, while <100% indicates a reduced expansion after sealing compared to baseline.

Surface area expansion examples

Examples of how a SAE and consequent EAC measurement was performed. First, at ventilatory pressure settings of PEEP = 5 cmH20 and Pc = 35 cmH20, screenshots were taken at 5 cmH20 and 40 cmH20 (figure 1A and B). Then, using ImageJ (version 1.53a, Wayne Rasband), the scale was determined using the ruler and the baseline areas and subsequently sealed areas were

calculated. As can be seen in figure 1, these measurements may be influenced by: tears in the sealant, as was mainly seen in the Progel® and Coseal® gels (figure 1C and D) and debonding of the sealant, as seen in Hemopatch® (1F). In the case of debonding, only the adhesive area was measured. In the case of tears, the entire area was still measured. Also, the lung was positioned manually above the camera and the exact angle between camera and measured surface was not measured, so some unknown factor of optical distortion may be of influence on these measurements.

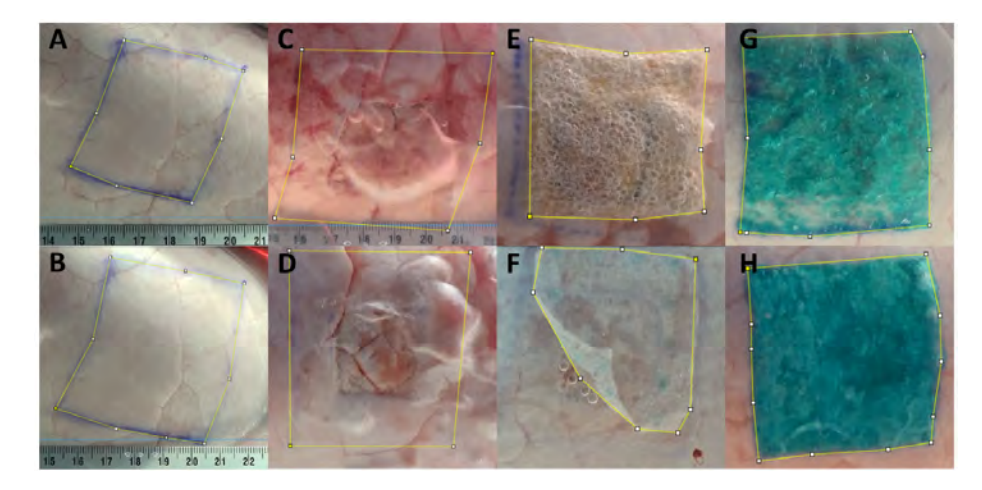


Figure 1) Surface area expansion measurement examples. A) Baseline surface area measurement at 5 cmH20 B) Baseline surface area measurement at 40 cmH20 C) Coseal® example with tears **D)** Proqel[®] example with tears **E)** TachoSil[®] example **F)** Hemopatch[®] example with debonding **G)** GATT-Patch Single example **H)** GATT-Patch Double example.

Supplementary Table

Table S1: second experiment baseline characteristics and outcomes

	GATT-Patch Single	Hemopatch®	P-value
BASELINE CHARACTERISTICS			
Sample characteristics			,
Ischemic time (minutes)†	173±104	180±130	0.90
Left lower lobe (n, %)	8 (80%)	7 (70%)	P>.99
Physical characteristics			
Surface temperature (°C)†	31.9±1.7	32.1±1.2	0.70
Water temperature (°C)‡	37.3±0.1	37.3±0.2	P>.99
Baseline SAE (%) [‡]	154±23	157±7	0.53
Lung compliance (mL/cm H2O)†	25±4	24±6	0.47
Leakage characteristics			
Baseline leaking pressures			
Grade I (cmH2O)‡	15±10	20±3	0.08
Grade II (cmH2O)‡	20±8	25±11	0.11
Grade III (cmH2O)‡	23±11	30±11	0.32
AL			
Amount (L/min)†	1.5±0.8	0.8±0.5	0.03
Percent of TVi (%)†	12.4±5.1	7.1±3.9	0.02
EXPERIMENT OUTCOMES			
Sealed leaking pressures			
Grade I (cm H2O)‡	45±10	40±6	0.04
Grade II (cm H2O)‡	45±10	40±6	0.04
Grade III (cm H2O)‡	50±11	40±6	0.002
AL reduction (%)‡	100±11	68±40	0.04
Cohesive failure (n, %)	10 (100%)	0 (0%)	P<.001
Adhesive failure (n, %)	0 (0%)	10 (100%)	P<.001

Bold P-value indicate statistical significance (P<0.05).

SAE: surface area expansion; AL: air leak; TVi: inspiratory tidal volume.

[†]Mean±standard deviation (SD)

[†]Median±interquartile range (IQR)



Chapter 5

Intrinsic pulmonary sealing, its mechanisms and impact on validity and translational value of lung sealant studies: a pooled analysis of animal studies

Bob P Hermans¹, Wilson WL Li¹, Edwin A Roozen², Daniël IM van Dort¹, Shoko Vos³, Stefan M van der Heide¹, Erik HFM van der Heijden⁴, Richard PG ten Broek², Harry van Goor², Ad FTM Verhagen¹

Radboud university medical center, Radboud Institute for Health Sciences, Nijmegen, The Netherlands.

¹Department of Cardio-thoracic surgery

²Department of General surgery

³Department of Pathology

⁴Department of Pulmonology

Used with permission of Nancy International Ltd., from "Hermans BP, Li WWL, Roozen EA, van Dort DIM, Vos S, van der Heide SM, van der Heijden EHFM, Ten Broek RPG, van Goor H, Verhagen AFTM. Intrinsic pulmonary sealing, its mechanisms and impact on validity and translational value of lung sealant studies: a pooled analysis of animal studies. *J Thorac Dis.* 2023 Sep 28;15(9):4703-4716. doi: 10.21037/jtd-23-180."; permission conveyed through Copyright Clearance Center, Inc.

ABSTRACT

Background: No validated and standardized animal models of pulmonary air leakage (PAL) exist for testing aerostatic efficacy of lung sealants. Lack of negative control groups in published studies and intrinsic sealing mechanisms of healthy animal lungs might contribute to a translational gap, leading to poor clinical results. This study aims to address the impact of intrinsic sealing mechanisms on the validity of PAL models, and investigate the conditions required for an ovine model of PAL for lung sealant testing.

Methods: An ovine acute aerostasis model was developed, consisting of a bilateral thoracotomy with lesion creation, chest tube insertion and monitoring of air leaks using digital drains (\geq 80 minutes), under spontaneous respiration. Healthy mixed-breed adult female sheep were used and all *in-vivo* procedures were performed under terminal anesthesia. Superficial parenchymal lesions were tested *post-mortem* and *in-vivo*, extended lesions including bronchioles (deep bowl-shaped and sequential lung amputation lesions) were tested *in-vivo*. Experiment outcomes include air leakage, minimal leaking pressure and histology.

Results: Two *post-mortem* (N=4 superficial parenchymal lesions) and 10 *in-vivo* experiments (N=5 superficial parenchymal and N=16 lesions involving bronchioles) were performed. In contrast to the *post-mortem* model, superficial parenchymal lesions *in-vivo* showed less air leak (mean flow±SD: 760±693mL/min vs 42±33mL/min, P=0.055). All superficial parenchymal lesions *in-vivo* sealed intrinsically within a median time of 20 minutes (IQR: 10-75). Histology of the intrinsic sealing layer revealed an extended area of alveolar collapse below the incision with intra-alveolar hemorrhage. Compared to superficial parenchymal lesions *in-vivo*, lesions involving bronchioles induced significantly higher air leak post-operatively (normalized mean flow±SD: 459±221mL/min, P=0.003). At termination, 5/9 (55.6%) were still leaking (median drain time: 273 minutes, IQR: 207-435 minutes), and intrinsic sealing for the remaining lungs occurred within a median of 115 minutes (IQR: 52-245 minutes).

Conclusions: Lung parenchyma of healthy sheep shows a strong intrinsic sealing mechanism, explained pathologically by an extended area of alveolar collapse, which may contribute to a translational gap in lung sealant research. A meaningful ovine model has to consist of deep lesions involving bronchioles of >Ø1.5mm. Further research is needed to develop a standardized PAL model, to improve clinical effectiveness of lung sealants.

Introduction

Prolonged pulmonary air leak (pPAL) occurs in up to 30% of lung resections, causing increased morbidity (empyema and post-operative complications), reinterventions (4.8%), readmissions (odds-ratio [OR] = 2) and mortality (OR)= 1.9). (1-7) Preclinical animal studies with lung sealants have shown promising results, and 74% of surgeons use sealants in their high-risk patients. (8-10) Results of lung sealants in preventing pPAL in clinical studies, however, are mixed and guidelines do not recommend their routine use. (11-16) Recently, in a European Society of Thoracic Surgeons (ESTS) survey, the majority of the 258 responding thoracic surgeons affirmed the lack of sufficient evidence for lung sealants, and an unmet clinical need for more effective lung sealants was described. (17) The marked discrepancy between the more positive preclinical studies and often unsatisfactory clinical results indicate a potential translational gap.

For effective clinical use, the performance of lung sealants should be investigated during their development in properly validated animal models. For a valid model, pulmonary air leakage (PAL) needs to be present of sufficient magnitude and without the capacity to resolve spontaneously for the study duration, ensuring accurate assessment of both acute and prolonged aerostatic efficacy of applied lung sealants. Furthermore, in contrast to patients undergoing lung resections, animals used in lung sealing experiments are healthy in 92% of cases and may poses enhanced intrinsic sealing and regenerative capacities, which can possibly invalidate positive study findings if unaccounted for. (18-20) In the present literature, no standardized animal model exists that guarantees clinically significant pPAL, and negative control groups were only used in 18.7% of preclinical studies. (20,21) Therefore, the validity of many previously tested lesions for pPAL in animal models is unknown. (20,22,23)

Several enhancements to animal models for lung surgery research have been described, that might reduce the translational gap. First of all, the type of lesion might impact PAL, as larger lesions and lesions involving bronchioles seem more likely to result in pPAL. (21,24) Secondly, disease models have been described, including models for emphysema and heparinized models. (25,26) Although these disease models increase the risk of pPAL, these models may come at the cost of increased variation and decreased animal welfare. In the present study, we assessed the impact of different types of lesions on PAL from the results of negative controls (untreated lesions) in three animal experiments. These results provide insight in the impact of intrinsic sealing mechanisms on the validity and translational value of animal models for lung sealant research. We present this article in accordance with the ARRIVE 2.0 reporting checklist.

Methods

Study setup

The intrinsic sealing capacities of both superficial parenchymal lesions and lesions involving bronchioles are investigated in *in-vivo* and *post-mortem* ovine models, by measuring air leakage (AL) and characterizing the responsible mechanisms histopathologically. To simulate a real post-operative scenario, an ovine acute aerostasis model with both mechanical ventilation and spontaneous breathing was used, based on previous models. (21,24) A bilateral thoracotomy was performed sequentially and varying standardized lung lesions were created in an explorative study design, after which AL was measured on both lungs after chest closure with a digital drainage system.

The sheep included in the analysis were used in three experiments, one *post-mortem* study and two *in-vivo* studies. First, superficial parenchymal lung lesions were tested in mechanically ventilated *post-mortem* sheep (N=2 cadavers), to test the hypothesis that pleural apposition diminishes AL for superficial lesions after chest closure. (27,28) Then, such lesions were created in a live sheep model (*in-vivo*), testing their natural healing course in the presence of intact coagulation (N=3 sheep). Finally, based on the previous results, more extensive lesions involving macroscopically visible bronchioles were tested (N=7 sheep). Part of the lesions made in the *in-vivo* studies were treated with a sealant. For the present study, we only pooled results for untreated lesions, as the focus of this investigation was to study the mechanisms of intrinsic sealing.

Lung lesions

Lesions were made to simulate the clinical problem of an alveolar-pleural fistula, defined as PAL arising distal to the segmental bronchus. Three different lung lesions were tested: superficial parenchymal, deep bowlshaped and sequential lung amputation lesions. Superficial parenchymal lesions were made by creating $n \times n$ perpendicular cuts in a 25x25mm square with a scalpel limited to 1-3mm depth (**Figure 1A/B**). Deep bowl-shaped lesions were made by cutting a \emptyset 25mm bowl lesion using biopsy punches and

scissors (Figure 1C/D). Sequential lung amputations were made by cutting away tissue perpendicularly to the expected bronchiole branching pattern, at a width of 3-5cm in steps of 1cm until either bronchioles of \emptyset >1.5 or \emptyset 0.5mm were encountered, on the ventral tips of the middle lobe (RML) and lower lobe (RLL) on the right, plus the upper lobe (LUL) and the lower lobe (LLL) on the left side (Figure 1E/F). This method for inducing lesions involving bronchioles was found to be the most repeatable in our ex-vivo investigations (Supplement 5A) and is based on the model of Ranger. (21) All lesions were made on a static lung with a positive end-expiratory pressure (PEEP) of 10cmH2O. Precise lesion types per experiment are explained in Table 1.

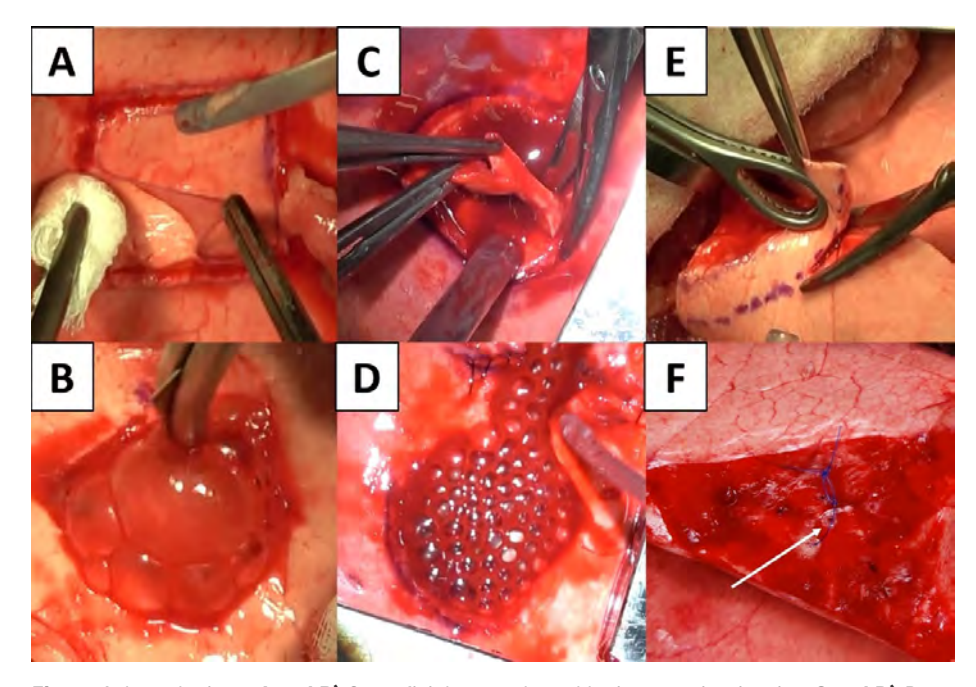


Figure 1: Lung lesions. A and B) Superficial parenchymal lesion creation in-vivo. C and D) Deep bowl-shaped lesion creation in-vivo. **E and F)** Seguential lung amputation lesion in-vivo. White arrow points at a macroscopically visible bronchiole (marked with a suture for recognition at obduction).

Outcome measures

In all experiments, after lesion creation and chest closure, AL was measured using a digital chest drainage system (Thopaz®, Medela, Baar, Switzerland). The time point since start of drainage when AL was <20mL/min, was noted as time until intrinsic sealing. For lesions involving bronchioles, the AL was measured using a mechanical ventilator (SERVO-I®, Getinge, Gotenburg, Sweden), based on the inspiratory (TVi) and expiratory (TVe) tidal volumes, right before and after lesion induction. The minimal leaking pressure (MLP) was determined for these lesions by dialing down the PEEP in steps of 1cmH2O until leakage disappeared or increasing in steps of 1cmH2O until leakage appears. In the *in-vivo* series, the *post-mortem* measurements of MLP were performed either ex-situ after lung explantation, or in-situ using selective intubation (in E4-E6, **Table 1**). Bronchial diameters (lumen, \emptyset) were measured using a ruler with markings every 0.5mm (Aesculap AA804R), and approximated in 0.5mm increments. Finally, macroscopy was recorded descriptively, paying attention to mechanisms of sealing of sealing, hemostasis and atelectasis.

Animal procedures

experiments were performed under a project license (NO.: AVD10300202114869) aranted bν national authorities ('Centrale Commissie Dierproeven', CCD) after review by an independent ethics board ('Dierexperimentencommissie', DEC) in the Netherlands, in compliance with institutional guidelines for the care and use of animals. Humane care and anesthesia were provided throughout the experiments. Experimental protocols were approved by the animal welfare body and registered internally at our institute (NO.: 2021-0012-001 and 2021-0012-002).

Adult mixed-breed female sheep (N=2) which were previously utilized for the production of antibodies in an unrelated project were euthanized using an overdose of pentobarbital, and the cadavers were directly re-used in the postmortem pilot model. Healthy adult mixed-breed female sheep (N=10) were used in the *in-vivo* animal model. Anesthetic protocols *in-vivo* involved deep surgical anesthesia during surgery and lighter sedation during a spontaneous ventilation observation period (Supplement 5B). Mechanical ventilation was guided by the visual presence of atelectasis on lung surfaces and ventilation and oxygenation requirements in the live animals. Reduction of ruminal tympany was ensured throughout the procedure.

A thoracotomy was performed on both sides of in the fifth intercostal space sequentially, always beginning with the right lung. After lesion creation, hemostasis was performed if required using gauzes and diathermy, and time until hemostasis was recorded. If necessary, fibrin plugs were removed using a small tweezers from the bronchiole lesions following hemostasis. Following all measurements, a silicone drainage tube (size Ch30) was placed apically

and exited the thorax ventrally on both sides. The thoracotomy was closed in layers to ensure air-tightness for accurate AL measurements. After an observation period in a back position (post-mortem model, minimum of one hour) or abdominal position (in-vivo model, minimum of three hours) under mechanical or spontaneous ventilation, the live animals were euthanized using pentobarbital. The lungs were explanted through a median sternotomy for inspection, post-mortem measurements and histology.

Histoloav

For histological analysis, samples were taken from the created defects after MLP determination and stored in 4% formaldehyde. Subsequently, they were embedded in paraffin and 4um thick sections were cut and stained with hematoxylin-eosin staining. These coupes were digitalized and assessed by an experienced pathologist (SV).

Statistical analysis

ThopEasy+ software (Medela, Baar, Switzerland) was used to import AL data, giving mean AL values (mL/min) every 10 minutes. For all lesions (postmortem and in-vivo), the mean AL was calculated over the first 80 minutes of drainage (minimum drainage time across all groups). In-vivo, mean AL was calculated over the first 180 minutes of drainage, and in 30 minute intervals for the first 5 hours of drainage. For statistical comparison, drainage AL data was normalized as: $AL_{normalized} = \ln\left(\frac{AL}{N_{leaks}}\right)$, were N_{leaks} denotes the number of effective ALs on the drained side. Normalized values were then compared using an analysis of variance (ANOVA) with Bonferroni-Holm post-hoc test (α =0.05/3). Intraoperative AL (mL/min) based on the mechanical ventilator was calculated as: $AL = \frac{\sum_{k=1}^{5} (TVi_k - TVe_k)}{5} \times RR$, were RR denotes respiratory rate. This AL was corrected for AL measured before the lesion was created as: $AL_{corrected} = AL_{lesion} - AL_{baseline}$. In case this calculation resulted in a negative AL, an AL of OmL/min was noted. MLP, time until hemostasis and AL data were compared between lesions involving bronchioles (\emptyset 0.5mm vs \emptyset >1.5mm using a Mann-Whitney-U test (two-tailed α =0.05). IBM SPSS Statistics 27 (Armonk, New York; IBM Corp) was used for statistical testing.

Results

Summary of experiment characteristics

In twelve animals, 25 untreated lesions were created and analyzed (N=4 superficial parenchyma post-mortem, N=5 superficial parenchyma in-vivo, N=16 lesions involving bronchioles, N=4 \emptyset 0.5mm and N=11 \emptyset 1.5mm bronchioles, N=1 missing diameter). One animal in the in-vivo group (P2) did not regain spontaneous ventilation and was kept on the mechanical ventilator during the observation period, another (P6) died due to acute cardiac arrest right after closure of the left thoracotomy, resulting in missing left lung drainage data and a shorter follow-up period. All experiment characteristics are displayed in **Table 1.**

Air leak characteristics for lesion subtypes

75% of superficial parenchymal lesions resulted in AL after thorax closure in the *post-mortem* model (mean \pm SD: 760 \pm 693mL/min, N=4). One lesion did not exhibit AL, likely due to extensive atelectasis of the affected lobe seen at obduction. For the *in-vivo* superficial parenchymal lesions, only minimal and rapidly decreasing post-operative AL was observed (mean \pm SD: 42 \pm 33mL/min, N=5, **Figure 2A**). All of these lesions stopped leaking within a median time of 20 minutes (IQR: 10-75 minutes, N=5). The average AL at 80 minutes showed a trend towards statistical significance between the *post-mortem* and *in-vivo* groups (p=0.055).

In comparison to superficial parenchymal lesions in-vivo, all lesions involving bronchioles (pooled $\emptyset 0.5 \text{mm}$ and $> \emptyset 1.5 \text{mm}$ lesions) led to significantly higher AL post-operatively (normalized flow mean $\pm SD$: $459\pm221 \text{mL/min}$, p=0.003, N=9, **Figure 2A/B**). Despite relevant AL initially, the magnitude of the AL still decreased over the observation period (**Figure 2C**). At termination of the experiment, 5/9 (55.6%) of these lungs were still leaking (median drain time: 273 minutes, IQR: 207-435 minutes, N=5), and intrinsic sealing for the remaining lungs occurred within a median of 115 minutes (IQR: 52-245 minutes, N=4). The shortest time until intrinsic sealing was observed for the lung affected with a $\emptyset 0.5 \text{mm}$ bronchiole lesion (50 minutes, N=1).

ts	
ె	
Ф	
Ε	
e	
Ď	
×	
Θ	
Φ	
Ē	
-	
ō	
_	
S	
-≍	
S	
÷	
ā	
÷	
ЭС	
_	
Ф	
드.	
C	
Ф	
\subseteq	
≒	
še	
3	
ä	
_	
e	
₹	
읖	
ű	

₽	Weight, age	Mode of ventilation		Tot. (n)	Eff. (n)	Type	Eff. Lobe and lesion	Drainage duration
POST-	POST-MORTEM							
Т3	68.5kg 9y1mo	MV: PC, Pmax 40cmH20	_	<u></u>	-	Par.	LUL: 25x25x1mm visceral pleura removal with 10x10 incisions at 1mm depth	1:20h
			2	1	1	Par.	RML: 25x25x3mm cube excision	4:10h
1 4	75.5kg 6y4mo	MV: PC, Pmax 50cmH20	7	-	-	Par.	LUL: same as T3/L	1:20h
			~	-	—	Par.	RLL: same as T3/L	3:30h
IN-VIVO	0/0							
P1	73kg 3y6mo	MV: VC, Pmax 38cmH20 SV: 2h	_	-	-	Par.	LUL: same as T3/L + additional 10x10 incisions at 3mm depth	3:10h
			~	_	_	Par.	RLL: same as T3/L	7:40h
P2	60.3kg 2y8mo	MV: VC, Pmax 36cmH20 SV: -	7	2	1	Par.	LUL: same as T3/L but 3mm depth incisions	3:30h
			œ	2	-	Br.	RLL: \$25mm/1mm depth, 2x \$10mm/5mm depth, cut bowl + 10x10 incisions at 1mm depth	7:40h
P4	50kg 1y7mo	MV: PC, Pmax 40cmH20 SV: 4:30h	7	5	-	Par.	LUL: same as T3/L but 6x6 incisions at 3mm depth	5:10h
			~	2	1	Par.	RML: same as T3/L but 6x6 incisions at 3mm depth	8:00h
P5	71kg, 2y9mo	MV: PC, Pmax 30cmH20 SV: 3:00h	_	2	2	Br.	LUL/LLL: sequential amputations until bronchioles of \emptyset 1.5mm	3:10h
			~	2	2	Br.	RML/RLL: same as P5/L	6:50h

OI	Weight, age	Mode of ventilation		Tot. (n)	Tot. (n) Eff. (n)	Type	Eff. Lobe and lesion	Drainage duration
P6	67.5kg, 2y10mo	MV: PC, Pmax 40cmH20 SV: -	_	2	2	Br.	LUL/LL: sequential amputations until bronchioles of Ø0.5mm	1
			~	2	2	Br.	RML/LLL: same as P6/L	4:40h
E2	82kg, 2y11mo	82kg, 2y11mo MV: PC, Pmax 25cm H20 SV: 4:09h	~	2	2	Br.	RML/RLL: same as P5/L	10:09h
E3	79.8kg, 1y2mo	79.8kg, 1y2mo MV: PC, Pmax 25cmH20 SV: 4:07h	_	2	2	Br.	LUL/LL: same as P5/L	4:33h
E4	66.3kg, 3y2mo	66.3kg, 3y2mo MV: PC, Pmax 25cmH20 SV: 3:24h	~	-	-	Br	RLL: same as P5/L	7:08h
E5	67kg 3y5mo	MV: PC, Pmax 25cmH20 SV: 3:01h	_	-	-	Br	LLL: same as P5/L	3:27h
E6	66kg 1y8mo	MV: PC, Pmax 25cmH20 L SV: 3:08h	_	-	-	Br	LLL: same as P5/L	3:45h

mo: months; kg: kilograms; h: hours; Par.: superficial parenchymal type lesions; Br.: deeper lesions involving bronchioles; L: left; R: right; RML: right middle lobe; LUL: left upper lobe; RLL/LLL: right/left lower lobe; MV: mechanical ventilation; SV: spontaneous ventilation; PC: pressure control; VC: volume ID: identifier; Tot.: total lesions; Eff.: effective number of lesions leaking on one side, other created lesions were sealed before thorax closure; y: years; control; Pmax: maximum pressure

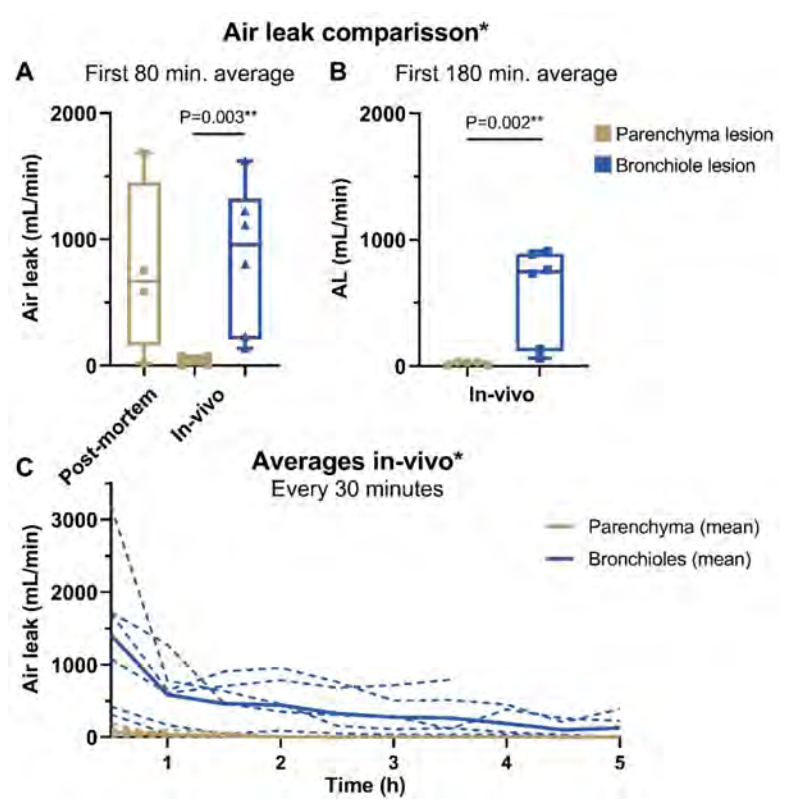


Figure 2: Air leak (AL) results for parenchymal and bronchiole lesions. A) Average AL from first 80 minutes of thoracic drainage. B) Average AL from the first 180 minutes of thoracic drainage C) Average AL values per 30 minutes from in-vivo experiments. Dashed lines show individual drain measurements.

Min. = minutes, h = hours.

Bronchiole diameter and leakage capabilities

Comparing both sizes of bronchioles, $\emptyset > 1.5$ mm lesions (N=11) were found to require longer time until hemostasis then \emptyset 0.5mm lesions (N=4) (mean \pm SD: 6.0±2.7 vs 2.0±0 minutes, P=0.012). However, no significant difference was found between \$\phi > 1.5mm \psi 0.5mm lesions for MLP (median \pm IQR: 5\pm 2cm H20 vs 7±5cmH20, P=0.226) nor mechanical ventilator AL (median±IQR: 581±1012mL/ min vs 140±305mL/min, P=0.104) during the live observation. Furthermore, post-mortem MLP did not differ significantly between \$1.5mm/\$0.5mm (median±IQR: 6±13cmH20 vs 10±41cmH20, P=0.199) A trend was seen for

^{*}Absolute AL values for left or right drains, uncorrected for number of leaks per side (Table 1).

^{**}Statistical testing performed using ANOVA (α =0.05) on log-normalized AL values and Bonferroni-Holm correction for post-hoc testing (only significant comparisons shown).

higher AL alive and lower MLP *post-mortem* for the \emptyset >1.5mm lesions. Of note, N=2 lesions were excluded from MLP analysis in the \emptyset >1.5mm subgroup due to blood contact during obduction, which possibly influenced the MLP (15 and 45cmH2O).

Macroscopy and histology

A rapid intrinsic sealing of the *in-vivo* superficial parenchymal lesions was observed intraoperatively (illustrated in video 1). At obduction, all superficial parenchymal lesions of the *in-vivo* model were covered with a coagulated fibrin sealing layer (**Figure 3A/B**). For the lesions involving bronchioles, the bronchioles appeared contracted or were no longer macroscopically visible (**Figure 3C/D**).

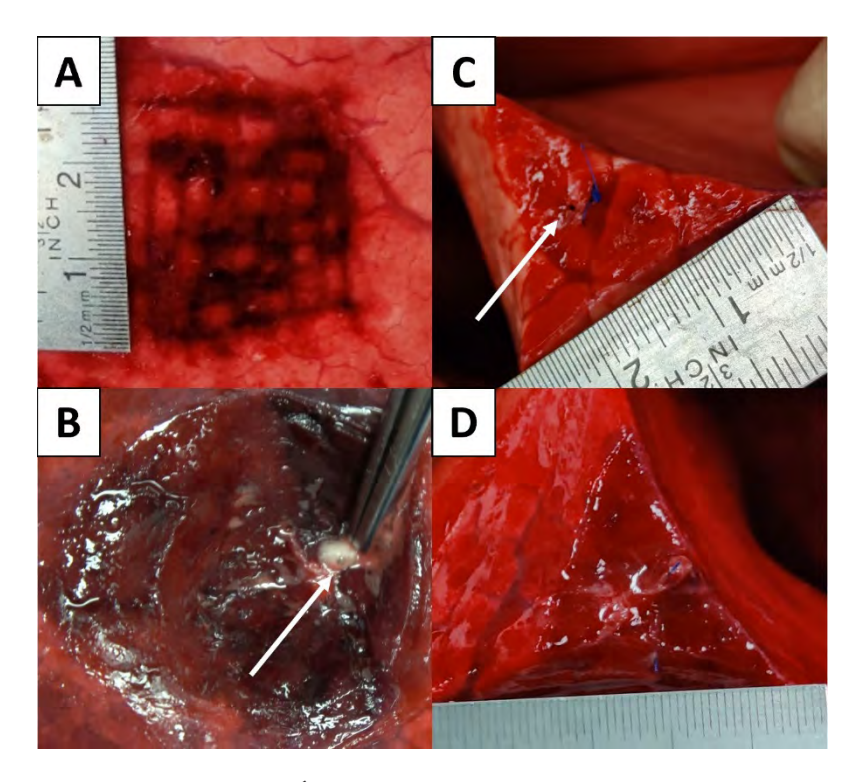


Figure 3: Macroscopic findings. **A)** Intrinsically sealed superficial parenchymal lesion, with a coagulated fibrin layer over the lesion. **B)** Small bronchiole (white arrow) as air leak focus of a deep bowl-shaped lesion with some secretions. Note the intrinsic sealing layer over the lung parenchyma. **C)** Macroscopic aspect of sequential amputation *in-vivo* and **D)** the same lesion at obduction. Note that the bronchiole (white arrow) is no longer visible at obduction and that a coagulated sealing layer is present on top of the parenchyma.

Histology for the superficial parenchymal lesions (N=2 lesions after <12h) revealed an area of alveolar collapse surrounding the injured sites, extending beyond the coagulated parenchymal incisions. Within this area of alveolar collapse, intra-alveolar hemorrhage was observed. Going further proximally, the normal air contents of the parenchyma gradually returned. Minimal influx of immune cells was seen, but no notable immune response was noted (Figure 4). The histological response for the lesions involving bronchioles was similar to the parenchymal lesions in-vivo (Supplement 5C).

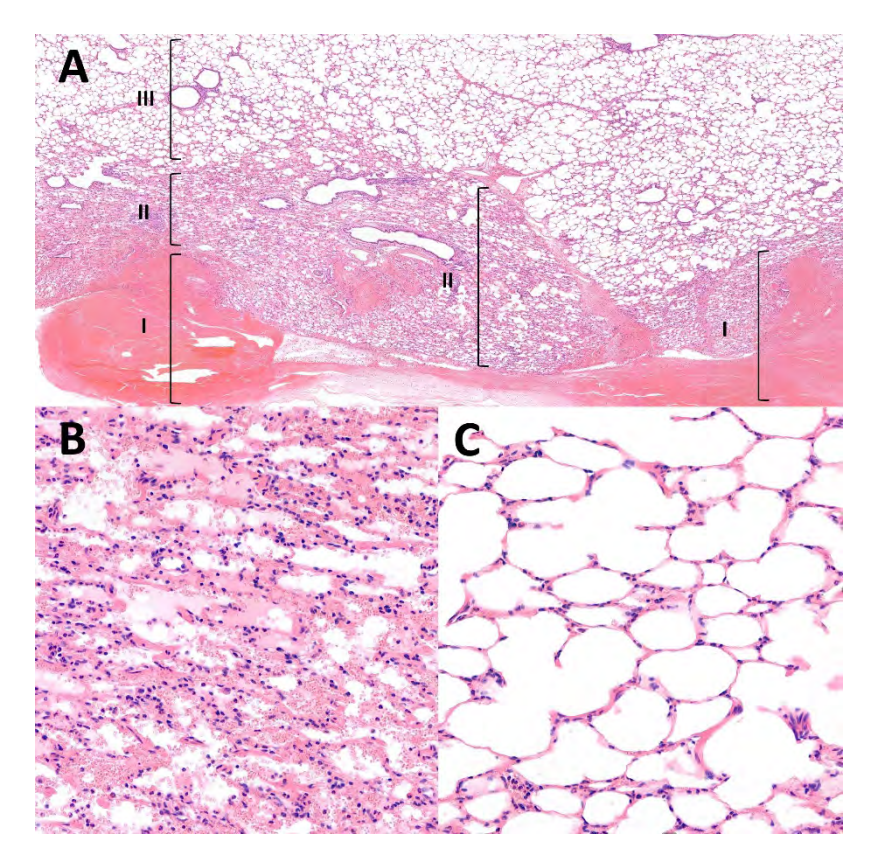


Figure 4: Histology of intrinsically sealed lung parenchyma. A) Aspect of a 3mm deep parenchymal incision (5x magnification). Three areas can be distinguished in the intrinsic sealing layer: area I shows coagulation in the incision itself; area II shows alveolar collapse and intraalveolar hemorrhages extending beyond the actual incision site (detailed at 40x magnification in B) and area III shows the return of normal air containing alveoli. C) Uninjured lung site shows normal air containing parenchyma (40x magnification).

Discussion

This study revealed that superficial parenchymal defects are unsuited for lung sealant testing in a healthy ovine model of PAL, due to rapid intrinsic sealing. Sequential amputation lesions involving bronchioles do result in AL in 56% of cases (median observation time: 4:33h), but with 44% of cases sealing intrinsically in a median time of 1:55h. Bronchioles of Ø1.5mm are preferable over Ø0.5mm, due to a trend towards a longer time to sealing. These lesions can be created in a reproducible manner and therefore seem valid for acute lung sealant testing. Nevertheless, the time to sealing is still too short for analysis of pPAL. These observed intrinsic sealing mechanisms could explain a translational gap in lung sealant research, especially in studies lacking negative control groups to demonstrate pPAL.

Comparison to literature

Presently, many clinical studies have been performed, testing numerous different sealant products. Some sealants were shown to be effective, but there were fluctuating results and no clear evidence based recommendations. As we suggest, disappointing results in clinical studies may be a consequence of a translational gap when negative controls are not used in the preclinical phase to ensure significant PAL. For example, effectiveness of fibrin glue was seen in an animal study that compared bursting pressures of fibrin glue with sutures in a rabbit model, without a negative control group (i.e. lesion with no treatment). In contrast, the animal study by McCarthy et. al., which included a negative control group to demonstrate significant PAL, showed no real effect of fibrin glue. 50% of the animals in their study were free of AL after 24h in both the fibrin glue and negative control groups (i.e. similar effectiveness to natural healing). This study is in line with clinical literature, as fibrin glue has not been found significantly effective for reducing the length of hospital stay in the clinical trials by Fleisher, Wong and Mourirtzen. (31-33)

Our study confirms the hypothesis that it is only possible to induce PAL in healthy animal lungs when creating lesions with adequate depth, lacerating terminal bronchioli. Previous studies with negative control groups had similar findings, as amputations of lung lobes or deep incisions, likely resulting in bronchiolar leaks, resulted in AL complications (Supplement 5D). $^{(21,34-36)}$ As an example, Ranger et. al. produced similar bronchiolar leaks of \emptyset >1.5mm and found higher AL (mean 1.4L/min, range 0.6-3.5L/min) in small dogs with similar drainage settings, as compared to our finding. These differences may

be explained by sampling variation or lobe/species effects. (21) In contrast, various superficial lesions did not lead to AL problems. (18,37-39) Also in larger parenchymal lesions, AL may persist, although in small dogs and pigs (17-35kg) it is unclear whether this is due to some degree of bronchiolar laceration at depths of ~5mm. (24,40)

Intrinsic sealing mechanisms

Pathologically, the intrinsic sealing layer is hypothesized to be more than just superficial coagulation, an extended area of alveolar collapse might be an explanation for the strong and rapid intrinsic sealing seen in this study. Similar mechanisms have previously been described, including compressed or partially aerated alveoli, subpleural alveolar edema, intra-alveolar bleeding and intra-alveolar deposition of fibrin strands. (19,41-43) Based on these studies and the findings in our study, the following mechanisms are proposed to be principally responsible: first, alveolar collapse is physically initiated by air escaping from the subpleural alveolar layer, by direct impression of the surgical instrument and a lower resistance to flow of this distal AL path. (41) Simultaneously, hemorrhage spreads through the pores of Kohn and channels of Lambert. (43) Blood proteins and lipids are known to cause an inhibition of surfactant function, increasing alveolar surface tension (Laplace's law, $P = \frac{2T}{r}$) and thereby attenuating alveolar collapse biophysically. (44-48) This results in a reduction of the common radius of the subpleural alveoli, increasing the resistance and reducing the AL by Poiseuille's law. This attenuates coagulation mechanisms analogous to vasoconstriction in a bleeding wound. (41,43) Inflammatory mechanisms were not seen in our sample (due to the short follow-up period), but may further enhance sealing through alveolar compression, due to capillary enlargement and edema as previously described. (19,42,43) Pleural apposition may also reduce AL, but we hypothesize this to play a small role based on our post-mortem observations and rapid sealing seen intra-operatively. (27)

These micromechanics could also provide a biophysical explanation for the lower intrinsic sealing capabilities in diseased human lungs. Pulmonary emphysema is a major risk factor for pPAL, and emphysema scores have shown to be predictive of pPAL. (1,49-51) Conceptually, in emphysematous lungs, lower pressures are required to prevent alveolar collapse, due to the larger radius of emphysematous alveoli (Laplace's law). Therefore, it is hypothesized that the proposed biophysical intrinsic sealing mechanisms will not induce the same degree of intrinsic sealing by alveolar collapse as seen in the healthy, nonemphysematous ovine lungs. Further study of intrinsic sealing mechanisms in emphysematous lungs might help us understand mechanisms of pPAL, which may improve treatment of these lesions.

The reduction in bronchiole diameter which was observed macroscopically post-mortem, may be due to sympathetic nervous system activation or bronchiole collapse due to absence of hyaline cartilage supporting structures. Especially bronchioles <1mm lack supporting hyaline cartilage, which was also seen histologically in our study (Supplement 5C). (52) In this case, as surrounding alveolar tissues collapse due to a steal phenomenon from the leaking orifice, especially bronchioles without cartilage support could collapse and seal intrinsically (as shown in **Figure 3D**). A bronchiole of \emptyset >1.5mm appears preferable over \emptyset 0.5mm to prevent rapid and strong intrinsic sealing in the acute aerostasis model from this perspective. (21)

There might be species specific considerations for sheep, which explain the strong and rapid intrinsic sealing. These include intra-vascular macrophages and an increased white blood cell count, which may cause immune mediated attenuation of intrinsic sealing mechanisms. (53-55) Coagulation times are comparable to those of humans. (55) High doses of intravenous propofol (dissolved in lipids) were sometimes required during surgical anesthesia, and it was hypothesized that this might result in hyperlipidemia and subsequently increased blood viscosity and coagulability. However, previous in-vitro and *in-vivo* experiments have shown no effect on blood viscosity, and even describe a reduced platelet aggregation. (56)

Translational value of air leak models

The face validity of a bronchiolar AL model is reduced, as clinical pPAL mostly arises from the alveoli in superficial parenchymal injury, such as from the dissection of fissures or pleural adhesions. As an acute aerostasis model, the construct validity remains preserved. PAL >500mL/min intraoperatively was found to predict pPAL, and AL sizes of 150-400mL/min have been used for sealant application in a clinical trial, with positive results. (57,58) Thus, the bronchiole AL seems sufficient for acute sealant testing. The model allows testing on an actively leaking lung, after thoracic closure, at least before intrinsic sealing of specific bronchiole lesion occurs. Thereby, other important mechanisms such as coagulation, immune response, pleural mechanisms and physiological breathing can be replicated, which is presently not feasible in animal-free alternatives. (59,60)

Disease models may be suitable to induce pPAL, but it remains unclear how long PAL should last in a model for sealant testing. Based on the hypothesized micromechanics, emphysema may result in longer pPAL, while heparinization seems a less effective disease model, as this would not inhibit alveolar collapse, and might even enhance spreading of blood through the alveoli. One study found significantly lower bursting pressures for sealants applied to emphysematous lungs, but did not measure PAL postoperatively. (26) The lower bursting pressures could be biochemically ascribed to a lower crosslink density on emphysematous lungs, which may be another explanation for a translational gap. (26) When developing disease models, disease induction might be associated with an increased baseline variation, higher sample size requirement and decreased animal welfare, which needs to be weighed against the potential added benefit of these models.

Limitations

These experiments offer a valuable addition to the present preclinical literature, by confirming the possibility of a translational gap and offering novel insights into intrinsic sealing mechanisms. However, based on these experiments, it is not possible to define a global standardized model for pPAL and lung sealant research. For this, further investigations are needed. First of all, it needs to be studied how long PAL needs to be present in a model for sealant testing to ensure accurate translation. Formulated differently, the time until intrinsic sealing of human lungs when a sealant is applied needs to be studied. Disease models are hypothesized to be suitable options for developing longer leaking PAL, but remain entirely unconfirmed, and come with added costs (higher sample size, decreased animal welfare). Another option might be to create leaks in large bronchi (e.g. segmental bronchi), but this further decreases the face validity. Finally, due to small sample size and heterogenous methods in the present study, all findings described here should be interpreted with appropriate caution and need to be confirmed in a-priori statistically powered experiments.

Recommendations for further research

Clinicians and experimental researchers should be aware of the intrinsic sealing mechanisms of healthy animal lungs. Success of sealants in animal studies should therefore be interpreted cautiously. In new experimental design, negative control groups should always be considered to measure the actual treatment effect. PAL may be created in animal models by creating especially large defects or lacerating bronchioles of \emptyset >1.5mm. $^{(21,24)}$ For

development of a global standardized pPAL model, further research is required into the requirements of valid pPAL models (e.g. duration of PAL), and methods for inducing longer PAL (e.g. emphysema or heparinization). (25,26) Such disease models could also be used to study mechanisms of PAL in clinical scenario's, such PAL arising from stapler lines. The understanding of PAL sealing mechanisms is still incomplete, and the proposed mechanisms should be further investigated. With a thorough understanding hereof, a clinical solution for the problem of pPAL might be discovered, for example by making the surgical treatment better synergize with the underlying mechanisms of the specific lesion type. The conduction of animal systematic reviews and adherence to ARRIVE guidelines should be encouraged to further improve scientific rigorousness of animal studies. (20,61)

Conclusions

Superficial parenchymal lesions exhibit an intrinsic sealing mechanism in a healthy ovine lung model, explained pathologically by an extended area of alveolar collapse attenuating coagulation mechanisms. These mechanisms may reduce model validity and contribute to a translational gap in lung sealant research, especially when negative control groups are not used. Experimental researchers should account for these mechanisms when designing experiments, to improve clinical applicability. One such approach for acute lung sealant testing in an ovine model, is to create deep parenchymal defects involving at least bronchioles of \emptyset >1.5mm. Further study into PAL models is required to develop and validate a universal standardized acute aerostasis model.

References

- Attaar A, Tam V, Nason KS. Risk Factors for Prolonged Air Leak After Pulmonary Resection: A Systematic Review and Meta-analysis. Ann Surg 2020;271:834-44.
- Attaar A, Luketich JD, Schuchert MJ, et al. Prolonged Air Leak After Pulmonary Resection Increases Risk of Noncardiac Complications, Readmission, and Delayed Hospital Discharge: A Propensity Score-adjusted Analysis. Ann Surg 2021;273:163-72.
- Brunelli A, Xiume F, Al Refai M, et al. Air leaks after lobectomy increase the risk of empyema but not of cardiopulmonary complications: a case-matched analysis. Chest 2006;130:1150-6.
- Liang S, Ivanovic J, Gilbert S, et al. Quantifying the incidence and impact of postoperative prolonged alveolar air leak after pulmonary resection. J Thorac Cardiovasc Surg 2013;145:948-54.
- Yoo A, Ghosh SK, Danker W, et al. Burden of air leak complications in thoracic surgery estimated using a national hospital billing database. Clinicoecon Outcomes Res 2017;9:373-83.
- Singhal S, Ferraris VA, Bridges CR, et al. Management of alveolar air leaks after pulmonary resection. Ann Thorac Surg 2010;89:1327-35.
- 7. Okereke I, Murthy SC, Alster JM, et al. Characterization and importance of air leak after lobectomy. Ann Thorac Surg 2005;79:1167-73.
- Zaraca F, Brunelli A, Pipitone MD, et al. A Delphi Consensus report from the "Prolonged Air Leak: A Survey" study group on prevention and management of postoperative air leaks after minimally invasive anatomical resections. Eur J Cardiothorac Surg 2022.
- Kobayashi H, Sekine T, Nakamura T, et al. In vivo evaluation of a new sealant material on a rat lung air leak model. J Biomed Mater Res 2001;58:658-65.
- 10. Yanagihara T, Maki N, Wijesinghe AI, et al. Efficacy of Alaska pollock gelatin sealant for pulmonary air leakage in porcine models. Ann Thorac Surg 2021.
- 11. Belda-Sanchis J, Serra-Mitjans M, Iglesias Sentis M, et al. Surgical sealant for preventing air leaks after pulmonary resections in patients with lung cancer. Cochrane Database Syst Rev 2010:Cd003051.
- 12. Singhal S, Shrager JB. Should buttresses and sealants be used to manage pulmonary parenchymal air leaks? J Thorac Cardiovasc Surg 2010;140:1220-5.
- 13. Zhou J, Lyu M, Pang L, et al. Efficiency and safety of TachoSil® in the treatment of postoperative air leakage following pulmonary surgery: a meta-analysis of randomized controlled trials. Jpn J Clin Oncol 2019;49:862-9.
- 14. McGuire AL, Yee J. Clinical outcomes of polymeric sealant use in pulmonary resection: a systematic review and meta-analysis of randomized controlled trials. J Thorac Dis 2018;10:S3728-s39.
- 15. Malapert G, Hanna HA, Pages PB, et al. Surgical sealant for the prevention of prolonged air leak after lung resection: meta-analysis. Ann Thorac Surg 2010;90:1779-85.
- 16. Aprile V, Bacchin D, Calabrò F, et al. Intraoperative prevention and conservative management of postoperative prolonged air leak after lung resection: a systematic review. J Thorac Dis 2023;15:878-92.
- 17. Brunelli A, Bölükbas S, Falcoz PE, et al. Exploring consensus for the optimal sealant use to prevent air leak following lung surgery: a modified Delphi survey from The European Society of Thoracic Surgeons. Eur J Cardiothorac Surg 2020.

- 18. Poticha SM, Macaladad F, Lewis FJ. THE CONTROL OF AIR LEAKS FOLLOWING SUBSEGMENTAL PULMONARY RESECTIONS. Surg Gynecol Obstet 1965;120:803-9.
- 19. Kausel HW, Lindskog GE. The healing of raw lung surfaces after experimental segmental resection. J Thorac Surg 1955;29:197-211.
- Hermans BP, Poos SEM, van Dort DIM, et al. Evaluating and developing sealants for the prevention of pulmonary air leakage: A systematic review of animal models. Lab Anim 2023:236772231164873.
- 21. Ranger WR, Halpin D, Sawhney AS, et al. Pneumostasis of experimental air leaks with a new photopolymerized synthetic tissue sealant. Am Surg 1997;63:788-95.
- 22. Annabi N, Zhang YN, Assmann A, et al. Engineering a highly elastic human protein-based sealant for surgical applications. Sci Transl Med 2017;9.
- 23. Elvin CM, Vuocolo T, Brownlee AG, et al. A highly elastic tissue sealant based on photopolymerised gelatin. Biomaterials 2010;31:8323-31.
- 24. McCarthy PM, Trastek VF, Bell DG, et al. The effectiveness of fibrin glue sealant for reducing experimental pulmonary air leak. Annals of Thoracic Surgery 1988;45:203-5.
- 25. Balakrishnan B, Payanam U, Laurent A, et al. Efficacy evaluation of anin situforming tissue adhesive hydrogel as sealant for lung and vascular injury. Biomed Mater 2021;16.
- 26. Gika M, Kawamura M, Izumi Y, et al. The short-term efficacy of fibrin glue combined with absorptive sheet material in visceral pleural defect repair. Interact Cardiovasc Thorac Surg 2007;6:12-5.
- 27. Pedersen TB, Honge JL, Pilegaard HK, et al. Comparative study of lung sealants in a porcine ex vivo model. Ann Thorac Surg 2012;94:234-40.
- 28. Mentzer SJ, Tsuda A, Loring SH. Pleural mechanics and the pathophysiology of air leaks. J Thorac Cardiovasc Surg 2018;155:2182-9.
- 29. Clark JM, Cooke DT, Brown LM. Management of Complications After Lung Resection: Prolonged Air Leak and Bronchopleural Fistula. Thoracic Surgery Clinics 2020;30:347-58.
- 30. Bergsland J, Kalmbach T, Balu D. Fibrin seal An alternative to suture repair in experimental pulmonary surgery. Journal of Surgical Research 1986;40:340-5.
- 31. Wong K, Goldstraw P. Effect of fibrin glue in the reduction of postthoracotomy alveolar air leak. Ann Thorac Surg 1997;64:979-81.
- 32. Mouritzen C, Drömer M, Keinecke HO. The effect of fibrin glueing to seal bronchial and alveolar leakages after pulmonary resections and decortications. Eur J Cardiothorac Surg 1993;7:75–80.
- 33. Fleisher AG, Evans KG, Nelems B, et al. Effect of routine fibrin glue use on the duration of air leaks after lobectomy. Ann Thorac Surg 1990;49:133-4.
- 34. Wilder RJ, Playforth H, Bryant M, et al. THE USE OF PLASTIC ADHESIVE IN PULMONARY SURGERY. J Thorac Cardiovasc Surg 1963;46:576-88.
- 35. Nuchprayoon C, Tamayo AG, Reimann AF, et al. The use and tissue reaction of a biologic adhesive in the prevention of air leak following a transection of the lung. Dis Chest 1968;53:445-52.
- 36. Kanzaki M, Yamato M, Yang J, et al. Dynamic sealing of lung air leaks by the transplantation of tissue engineered cell sheets. Biomaterials 2007;28:4294-302.
- 37. Feito BA, Azorin J, Rath AM, et al. Experimental study on the in vivo behaviour of a new collagen glue in lung surgery. European Journal of Cardio-thoracic Surgery 2000;17:8-13.

- 38. Getman V, Wolner E, Mueller MR, et al. Fleece bound sealing prevents pleural adhesions. Interactive Cardiovascular and Thoracic Surgery 2006;5:243-6.
- 39. Buyukkale S, Citak N, Isgorucu O, et al. The effect of sodium hyaluronate-carboxymethyl cellulose membrane in the prevention of parenchymal air leaks: an experimental and manometric study in rats. Tuberkuloz Ve Torak-Tuberculosis and Thorax 2017;65:265-70.
- 40. Luh SP, Chou HH, Tsai TP, et al. Effect of Surgecel coverage with topical electrocauterization for preventing and sealing pulmonary air leakage. Int Surg 2004;89:190-4.
- 41. Joannides M, Hesse AL, Joannides M, Jr. Surgical wounds of the lung; the mode of healing of pulmonary tissue. J Thorac Surg 1949;18:695-706.
- 42. Findlay CW, Jr. The healing of surgical wounds of the lung with particular reference to segmental lobectomy. J Thorac Surg 1950;20:823-34.
- 43. Wheeldon EB, Mariassy AT, McSporran KD. The pleura: a combined light microscopic and scanning and transmission electron microscopic study in the sheep. II. Response to injury. Exp Lung Res 1983;5:125-40.
- 44. Zuo YY, Veldhuizen RA, Neumann AW, et al. Current perspectives in pulmonary surfactant inhibition, enhancement and evaluation. Biochim Biophys Acta 2008;1778:1947-77.
- 45. Raghavendran K, Willson D, Notter RH. Surfactant therapy for acute lung injury and acute respiratory distress syndrome. Crit Care Clin 2011;27:525-59.
- 46. Holm BA, Keicher L, Liu MY, et al. Inhibition of pulmonary surfactant function by phospholipases. J Appl Physiol (1985) 1991;71:317-21.
- 47. Holm BA, Wang Z. Notter RH. Multiple mechanisms of lung surfactant inhibition. Pediatr Res 1999;46:85-93.
- 48. Walter F. Boron ELB. Medical Physiology Medical Physiology 3rd edition. Chapter 27: Mechanics of ventilation. Elsevier 2017.
- 49. DeCamp MM, Blackstone EH, Naunheim KS, et al. Patient and surgical factors influencing air leak after lung volume reduction surgery; lessons learned from the National Emphysema Treatment Trial. Ann Thorac Surg 2006;82:197-206; discussion -7.
- 50. Moon DH, Park CH, Kang DY, et al. Significance of the lobe-specific emphysema index to predict prolonged air leak after anatomical segmentectomy. PloS One 2019;14:e0224519.
- 51. Murakami J, Ueda K, Tanaka T, et al. Grading of Emphysema Is Indispensable for Predicting Prolonged Air Leak After Lung Lobectomy. Ann Thorac Surg 2018;105:1031-7.
- 52. Ball M, Hossain M, Padalia D. Anatomy, Airway. [Updated 2023 Jul 25]. In: StatPearls [Internet]. Treasure Island (FL): StatPearls Publishing; 2024 Jan-. Available from: https:// www.ncbi.nlm.nih.gov/books/NBK459258/
- 53. Delano ML, Mischler SA, Underwood WJ. Biology and Diseases of Ruminants: Sheep, Goats, and Cattle. Laboratory Animal Medicine. 2002:519-614. Doi: 10.1016/B978-012263951-7/50017-X. Epub 2007 Sep 2.
- 54. Matute-Bello G, Frevert CW, Martin TR. Animal models of acute lung injury. Am J Physiol Lung Cell Mol Physiol 2008;295:L379-99.
- 55. Wilhelmi MH, Tiede A, Teebken OE, et al. Ovine blood: establishment of a list of reference values relevant for blood coagulation in sheep. Asaio j 2012;58:79-82.
- 56. Reinhart WH, Felix C. Influence of propofol on erythrocyte morphology, blood viscosity and platelet function. Clin Hemorheol Microcirc 2003;29:33-40.
- 57. Brunelli A, Salati M, Pompili C, et al. Intraoperative air leak measured after lobectomy is associated with postoperative duration of air leak. Eur J Cardiothorac Surg 2017;52:963-8.

- 58. Zaraca F, Vaccarili M, Zaccagna G, et al. Cost-effectiveness analysis of sealant impact in management of moderate intraoperative alveolar air leaks during video-assisted thoracoscopic surgery lobectomy: a multicentre randomised controlled trial. J Thorac Dis 2017;9:5230-8.
- 59. Klassen C, Eckert CE, Wong J, et al. Ex Vivo Modeling of Perioperative Air Leaks in Porcine Lungs. IEEE Trans Biomed Eng 2018;65:2827-36.
- 60. Horvath MA, Hu L, Mueller T, et al. An organosynthetic soft robotic respiratory simulator. APL Bioeng 2020;4:026108.
- 61. Percie du Sert N, Hurst V, Ahluwalia A, et al. The ARRIVE guidelines 2.0: Updated guidelines for reporting animal research. PloS Biol 2020;18:e3000410.

Chapter 5 Supplemental material

Supplemental Video 1 is published online (https://doi.org/10.21037/jtd-23-180)

Supplement 5A - Ex-vivo characterization of sequential amputation lesions

Study setup

Using an ex-vivo setup with ovine lungs, the repeatability of sequential lung edge amputations or lung incisions for attaining bronchioles of ≥1.5mm but lower than 3.0mm was investigated (same inclusion criteria as the model used by Ranger et. al. in 1997). Next, the defect which was found most optimal was investigated in an in-vivo acute aerostasis experiment and the intrinsic sealing capabilities were tested, by measuring minimal leaking pressures (MLP) at obduction and air leakage using a digital drain (see main manuscript).

Outcome measures

Bronchial diameters (lumen) were measured using a ruler with markings every 0.5mm (Aesculap AA804R), and approximated in 0.5mm increments. Bronchioles <0.5mm but approximately larger than 0.25mm were noted as 0.5mm. If the bronchial lumen was approximately smaller than 0.25mm or if no bronchiole lumen could be identified macroscopically, this was noted as Omm. MLP was determined using a Servo-I mechanical ventilator (Maguet critical care). Under pressure control settings, positive end-expiratory pressure (PEEP) was put on 10cmH20 while air leakage was assessed using water immersion or dripping water over the lesion. PEEP was gradually dialed down in steps of 1cmH2O until air leakage disappeared and the last plateau ventilatory pressure (Pplat) at which air leakage was still present was noted as MLP. In the case of MLP>10cmH20, the pressure was gradually increased until leakage was observed. The dimensions (length and width) of sequential amputation lesions were measured in whole millimeters (figure S1).

Sequential amputations versus incisional defects

First, two methods for attaining bronchiole lesions were compared ex-vivo: sequential amputations versus lung incisions. For this, lungs of two sheep (54 and 84kg) sacrificed for a different experiment were harvested immediately after death. Sequential lung amputations perpendicular to bronchial branching were compared with lung incisions regarding repeatability and leaking capability. Right upper (RUL), right middle (RML), right lower (RLL), left upper (LUL) and left lower lobes (LLL) were selectively intubated and fully recruited until Pmax=40-50cmH20. All lesions were marked and created on a static lung with PEEP=10cmH20. First, sequential amputations (figure S1) were performed starting at 1cm from the edge and measuring maximum bronchiole diameter and MLP during each increment until bronchioles of ≥ 1.5 mm were encountered. Then, a large clamp was placed across the defective area and the procedures were repeated on the same lobe for incisional defects (25mm long, 5mm deep and increasing depth in steps of 5mm).

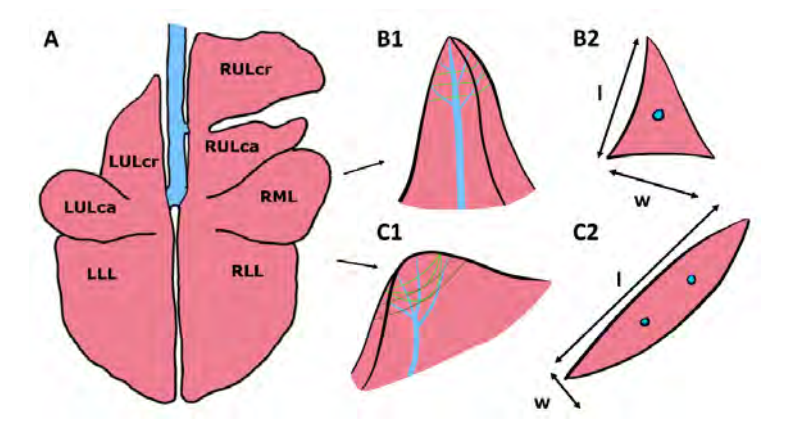


Figure S1: A) Sequential amputation lesions are best performed on the RML/LULca/LLL/RLL in the in-vivo situation, and are roughly made perpendicular to bronchial branching. **B1)** Lesions on the RML/LULca are performed by sequentially increasing the cut line with 1cm from the previous cut line (green lines), resulting in a triangular defect **(B2)**. **C1)** Lesions on the RLL/LLL are performed by increasing the cut depth, but limiting the cut width to allow for future patch placement in the model (light green lines, corresponds to the maximum defect width of 5cm). This results in a roughly oval shaped defect **(C2)**. In the initial ex-vivo characterization experiment, the dark green cut lines were followed, leading to increased defect lengths.

On the two lung specimens, a total of N=31 variations of the sequential amputation defect (N=10 1cm from edge, N=10 2cm from edge, N=7 3cm from edge and N=4 4cm from edge) and N=34 variations of the incision defect (N=10 at 5mm depth, N=9 at 10mm depth, N=10 at 15mm depth, N=4 at 20mm depth and N=1 at 30mm depth) were created, N=2 for each RUL, RML, RLL, LUL and LLL. For the sequential amputations, a significant strong positive correlation was found between distance from the edge (1-4cm) and maximum bronchiole diameter in the defect (Pearson correlation coefficient = 0.635, P<0.001). This was also the case for incisional defects between incisional depth (5-30mm) and maximum

bronchiole diameter (Pearson correlation coefficient = 0.678, P<0.001). However, the incisional defect produced outliers in maximum bronchiole diameter of 3-5mm, while the sequential amputations showed a more predictable pattern of bronchiole diameter increase upon further amputations. In both cases, the maximum bronchiolar diameter showed a significant strong negative correlation with the MLP. For sequential amputations, the Pearson correlation coefficient was -0.739 (P<0.001) and for incisional defects -0.678 (P<0.001). These relations are shown visually in figure S2. Based on this experimental data, it was decided that sequential amputation lesions will result in a more repeatable model regarding bronchiole diameters, and this defect was used in the following experiments. The RUL was no longer considered for further experiments, due to limited access and to increase comparability between right and left lung lesions in-vivo (RML/LUL and RLL/LLL lesions are more comparable regarding their geometry).

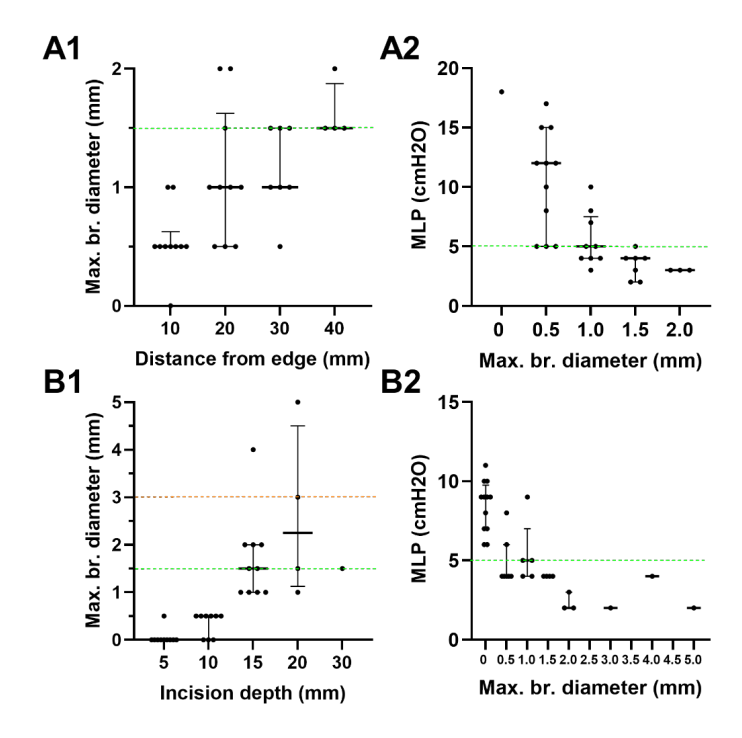


Figure S2: Sequential amputations versus incisional defects characterization. A1) Sequential amputations defect shows a positive correlation between cut distance from edge, which follows a roughly linear and predictable pattern. From 2cm distance from edge on, the 1.5mm threshold for a suited model is passed (green line). A2 and B2) The bronchiole diameter in the defect is negatively correlated with the MLP. From 1.5mm on, the MLP is consistently 5cmH2O or lower (green line). B1) Incisional defect show a positive correlation with the incision depth, cut following a less predictable pattern. As can be seen, from 15mm depth on, the 1.5mm threshold for bronchial diameter is passed (green line), but the 3.0mm upper limit (orange line) may also be exceeded.

Supplement 5B - Anesthesia protocol in-vivo studies

Housing remarks

Animals were transported to the research facility from a farm one day before the experiment together with two buddy sheep. Housing was in accordance with institutional protocols, and animals were fed ad-libitum up until the surgery.

Anesthesia

In these model development studies, anesthetic protocols were being optimized for the acute aerostasis model, which lead to some heterogeneity in used methods. P1 and P2 were pre-medicated using midazolam and carprofen, followed by induction of anesthesia using propofol in the jugular vein. P4, P5, P6, E2 and E3-E6 were pre-medicated using midazolam, ketamine and carprofen and anesthesia was induced using remifentanil and propofol through an intra-venous canula. They were then intubated and put on isoflurane during shaving and placement of a urinary catheter. Mechanical ventilator settings were adjusted based on the ventilation and oxygenation requirements. Propofol and remifentanil titrated for adequate blood pressure regulation (target mean arterial blood pressure during surgery: 50-100mmHg) were used for an esthetic maintenance during surgery in P1 and P4, P5, P6, E2 and E3-E6, and propofol and sufentanil in P2. In P2, propofol was swapped out for pentobarbital halfway through the surgery to achieve a more stable blood pressure. Additionally, an arterial blood pressure line and ventilation line in the rumen (through a small epigastric incision in P1 and P2 and trans-esophageal in the remaining) were placed. The first sheep (P1) received a percutaneous tracheotomy canula to facilitate insertion of an endo-bronchial blocker (EZ-blocker) for single-lung procedures. Intermitted hyperoxygenation followed by apnea to facilitate defect creation on the lung was utilized for P2 and P4, P5, P6, E2 and E3-E6 as a less complicated alternative. An intercostal block was placed in all animals at three levels with a combination of lidocaine and bupivacaine. After surgery, the sheep were placed in an abdominal position, buprenorphine was administered and ketamine and midazolam were infused continuously to allow the sheep to breath spontaneously while still under anesthesia, and propofol was administered if required to maintain a deep anesthetic plane. During this spontaneous observation period, the animal was continuously monitored by an experienced biotechnician. Anesthetic monitoring throughout the procedure included end-tidal CO2, oxygen saturation, pulse, blood pressure, arterial blood gasses and reflexes. At the end of the experiment, the sheep was euthanized by an overdose of pentobarbital.

Supplement 5C - Histology of bronchiolar lesions

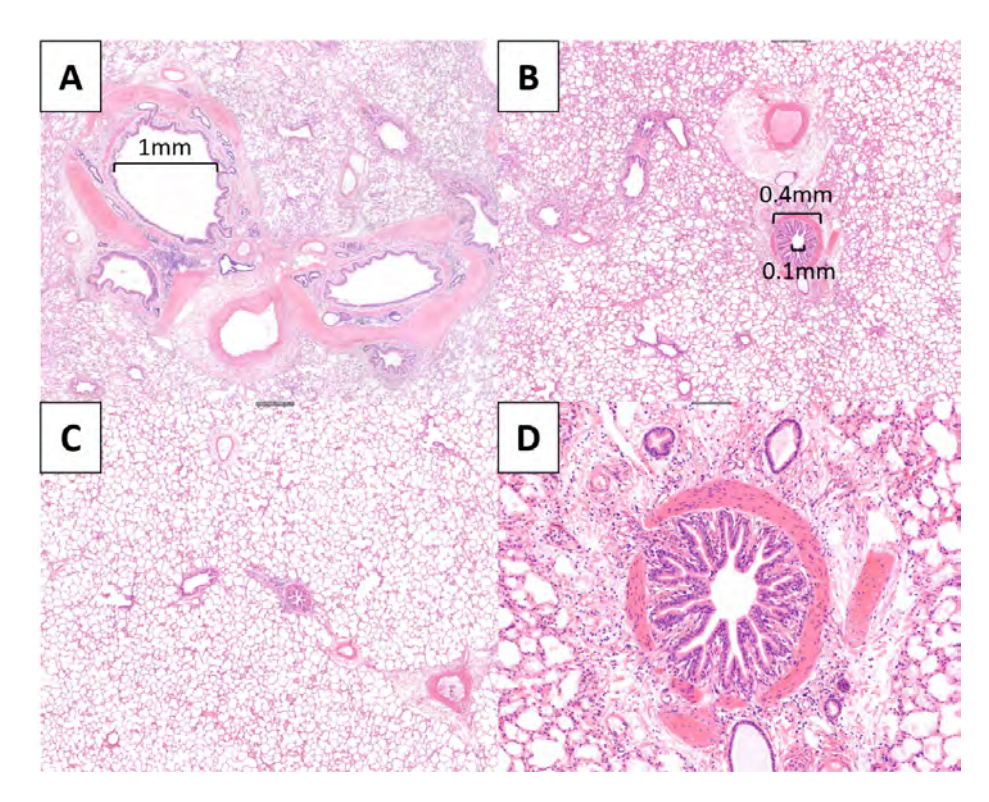


Figure S3: A) Large bronchi are noted in this section, corresponding to macroscopic bronchi of Ø1.5mm. Note the hyaline cartilage around the lumen. Compared to normal parenchyma (C, control section), the alveoli in this section appear less aerated due to intra-alveolar bleeding and alveolar collapse. B) Small bronchioles are seen, which appear contracted, and only a very small part of hyaline cartilage is seen (detail in D). However, the bronchioles in the normal parenchyma also have this similar contracted appearance (C).

Supplement 5D - Literature table of previous animal studies with negative control groups

Table S1: Intrinsic sealing mechanisms from untreated pulmonary parenchymal lesions described in previously literature (based on comprehensive

literature survey)				
Author, year	Species, N	Lesion	Intrinsic sealing findings	Histology (intrinsic sealing)
Joannides, 1948[41]	Dogsª, ND	Crushing, punctures, tears, incisions, wedges, resection of lung tissue	Secretion plugging bronchioles Alveolar compression due to air leak collapsing the lung after injury or after gentle compression ^b	Extended intra-alveolar bleeding Compressed alveoli
Findlay, 1950 [42]	Cats, ND	Segmental lobectomy, residual parenchymal defect 2x1.5x1.5cm Middle lobe tip amputated and rotated into wound	Minimal air leak or pneumothorax One animal died from BPF	Partial aeration of alveoli Widening of the septa Inflammatory response Intra-alveolar blood
Kausel, 1955[19]	Dogs, N=8	Segmental lobectomy, residual parenchymal defect 9-15cm²	No pneumothorax or air leaks One animal died from BPF	Compressed alveoli Intra-alveolar bleeding Massive capillary enlargement Alveolar cell enlargement
Wilder, 1963[34]	Dogs, N=9	5x2cm amputation of upper lobe	No drains left in place, 6/9 animals survived (compared to 3/9 in glue-treated group). In survivors, lesions were adherent to chest wall.	ΩN
Poticha, 1965[18]	Dogs, N=6	Removal of entire parietal surface of lobe at 3mm depth	No drains left in place, no air leak complications. One death due to other pulmonary complications Exudate of blood and fibrin sealed all air leaks, at one week leading to fibrin adhesions to chest wall and atelectasis adjacent the injury.	Q

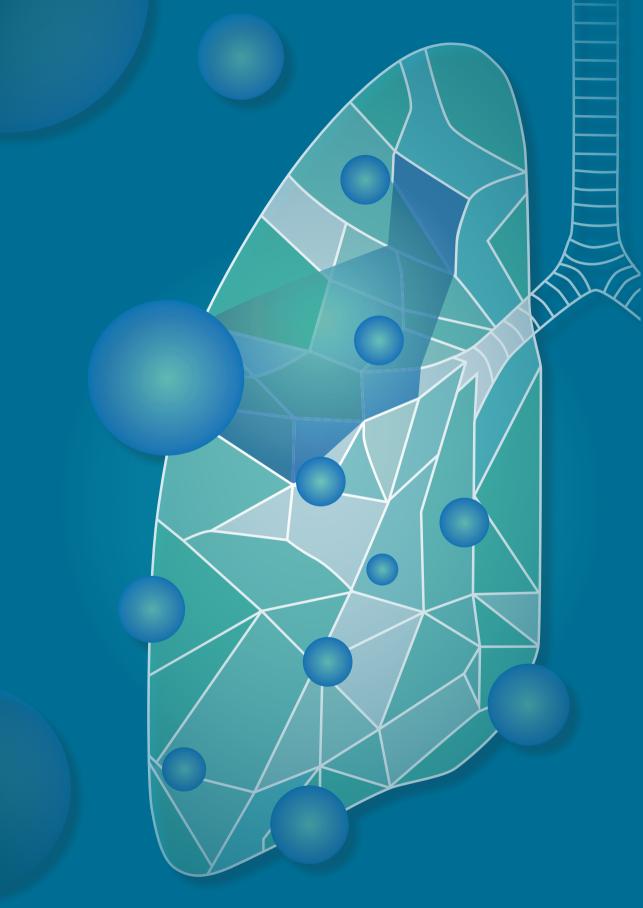
$\overline{}$
2
×
=
٠Ħ
Ħ
5
ŏ
~
∺
S1:
§ S1: (
le S1: (
ble S1: (
able S1: (

Author, year	Species, N	Lesion	Intrinsic sealing findings	Histology (intrinsic sealing)
Nuchprayoon, 1968[35]	Dogs, N=8	Removal of lung tissue at costophrenic margin at 1.5-2cm depth, inducing 12x1.5cm raw surface.	Bronchi > 1.0mm suture ligated and three hours thoracic drainage postoperatively. 6/8 animals died due to tension pneumothorax. 2/8 developed chronic lower lobe atelectasis due to air leak	Alveolar congestion
McCathy, 1988[24]	Dogs, N=8	9x9cm defect at 0.5cm depth on left lower lobe	Air leak sealed on thoracic drainage in 4/8 control animals (also in 4/8 sealed animals)	ND
Feito, 2000[37]	Rabbits, N=10	Several superficial incisions (average 7) at 1.5mm depth	Uneventful postoperative course in all animals At day 0-1, mean 19.4% pneumothorax, reduced to 3.3% at day 6-7. Adhesions present at obduction.	ND
Luh, 2004[40]	Pigs, N=5	Bilateral 5x5cm <0.5cm depth lesions on left and right upper lobes	Critical leak pressure <5mmHg at 0.5 and 72h Air leakage on thoracic drain until 72h	Poor pleural coverage
Getman, 2006[38]	Rats, N=10	5mm parietal defects	Uneventful postoperative course Adhesions of defect area to chest wall	ND
Kanzaki 2007[36]	Rats, N=4	5mm long incision at 3mm depth	4/4 animals died due pneumothorax within 1h	ND
Büyükkale, 2017[39]	Rats, N=8	Linear incision left upper zone 0.2x0.1cm (length x height)	No postoperative complications Air leak pressure mean 43.5mmHg at day 7.	ND

^aSpecies used not well described in paper

^bSince sutures were used, healing cannot be attributed to intrinsic sealing. However, histology findings were representative of intrinsic sealing mechanisms

in this study. ND: not described; BPF: broncho-pleural fistula



Chapter 6

Proof-of-principle of a lung sealant based on functionalized polyoxazolines: experiments in an ovine acute aerostasis model

Bob P Hermans¹, Richard PG ten Broek², Wilson WL Li¹, Edwin A Roozen², Shoko Vos³, Erik HFM van der Heijden⁴, Harry van Goor², Ad FTM Verhagen¹

Radboud university medical center, Radboud Institute for Health Sciences, Nijmegen, The Netherlands.

¹Department of Cardio-thoracic surgery

²Department of General surgery

³Department of Pathology

⁴Department of Pulmonology

Reprinted by permission of Oxford University Press on behalf of the European Association for Cardio-Thoracic Surgery from: "Hermans BP, Ten Broek R, Li WWL, Rooen EA, Vos S, Van Der Heijden E, Van Goor H, Verhagen AFTM. Proof-of-principle of a lung sealant based on functionalized polyoxazolines: experiments in an ovine acute aerostasis model. *Interdiscip Cardiovasc Thorac Surg.* 2024 Jun 4:ivae113. doi: 10.1093/icvts/ivae113.". The version in this thesis differs slightly from the published version, after processing following peer review comments.

ABSTRACT

Objectives: More effective lung sealants are needed to prevent prolonged pulmonary air leakage (AL). Polyoxazoline impregnated gelatin patch (NHS-POx) was promising for lung sealing ex-vivo. The aim of this study is to confirm sealing effectiveness in an in-vivo model of lung injury.

Methods: An acute aerostasis model in healthy adult female sheep was used, performing bilateral thoracotomy, amputation lesions (bronchioles Ø>1.5mm), sealant application, digital chest tube for monitoring AL, spontaneous ventilation, obduction and bursting pressure (BP) measurement. Two experiments were performed: 1) Three sheep with two lesions per lung (N=4 NHS-POx double-layer, N=4 NHS-POx single-layer, N=4 untreated) and 2) three with one lesion per lung (N=3 NHS-POx single-layer, N=3 untreated). In pooled linear regression, AL was analyzed per lung (N=7 NHS-POx, N=5 untreated) and BP per lesion (N=11 NHS-POx, N=7 untreated).

Results: Baseline AL was similar between groups (mean 1.38-1.47L/min, p=0.90). NHS-POx achieved sealing in one attempt in 8/11 (72.7%) and in 10/11 (90.9%) in >1 attempt. Application failures were only observed on triangular lesions requiring three folds around the lung. No influences of methodological variation between experiments was detected in linear regression (p>0.9). AL over initial 3h of drainage was significantly reduced for NHS-POx (median: 7mL/min, IQR: 333mL/min) versus untreated lesions (367mL/min, IQR: 680mL/min, p=0.036). BP was higher for NHS-POx (mean: 33, SD: 16cmH20) versus untreated lesions (mean: 19, SD: 15cmH20, p=0.081).

Conclusions: NHS-POx was effective for reducing early AL, and a trend was seen for improvement of bursting strength of the covered defect. Results were affected by application characteristics and lesion geometry.

Introduction

Prolonged pulmonary air leakage (pPAL), an air leak that persists for more than five days, occurs in five to thirty percent of patients after lung resection. (1) pPAL is associated with an increased risk of postoperative complications (i.e. empyema), re-interventions, readmissions and mortality. (2-5) Hospital stay is on average extended with four days and hospital costs are fifty percent higher compared to patients without pPAL. (6) Lung sealants to prevent pPAL are advocated, however current sealants have not been satisfactorily proven to be effective on clinically relevant outcomes such as length of hospital stay, despite good preclinical results. (7-10) An unmet clinical need exists for a better product which is easily applicable, capable of hermetic lung sealing in a wet environment and sufficiently compliant for lung expansion. (8)

Polyoxazolines are a novel polymer group that holds promise for a lung sealant due to its strong adhesive and cohesive characteristics. (11-14) A specific formulation containing amine-functionalized and N-hydroxysuccimide ester functionalized poly(2-oxazoline)s (NHS-POx, GATT Technologies BV, Nijmegen, The Netherlands) was a highly effective hemostat when impregnated in a porcine gelatin carrier. (11, 12, 14) NHS-POx reacts with proteins on tissue and blood within the patch to form covalent bonds, creating a strong sealing hydrogel within minutes. (11) We have previously demonstrated lung sealing effectiveness with these patches ex-vivo, showing superior aerostatic efficacy compared to sprays based on polyethylene glycol (Progel®, Coseal®) and collagen patches with polyethylene glycol (Hemopatch®) or fibrin/ thrombin coating (TachoSil®).(15)

We aim to further confirm the effectiveness of the NHS-POx patch as an aerostatic lung sealant using a clinically relevant sheep lung injury model.

Methods

Ethical statement

Experiments were performed under a project license (AVD10300202114869) granted by national authorities (4-10-2021) after review by an ethics board. Protocols were approved by the animal welfare body and registered at our institute (2021-0012-002).

Study design

The *in-vivo* study was performed in two phases, comparing the NHS-POx patch to a control group (**Figure 1**). Lung lesions resulting in clinically relevant PAL were made in anesthetized sheep, treated with NHS-POx and observed during spontaneous ventilation, followed by measuring air leak (AL) and bursting pressure (BP).⁽¹⁶⁾ The first experiment was performed in three animals (E1-E3) with four lesions per animal, two lesions in each lung, based on a sample size calculation. An additional three animals (E4-E6) with two lesions per animal, one lesion in each lung, were included in the second experiment. Randomization was performed at the level of each lung, ensuring the following conditions: one group per lung, no two same groups per animal and each group once to each lung. Allocation sequence was concealed until the moment of application.

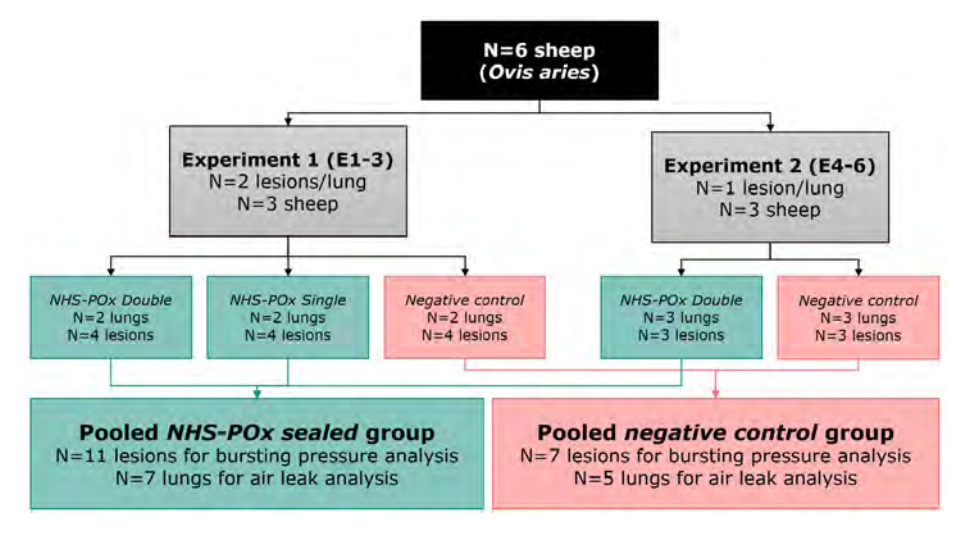


Figure 1: Study flowchart.

Anesthesia and surgery

Adult female sheep (*Ovis aries*) were housed with buddy sheep at least one day prior to surgery, and fed *ad libitum*. Pre-medication (ketamine and midazolam) was administered before induction of anesthesia (remifentanil, propofol, carprofen). Anesthesia was maintained using remifentanil, propofol and isoflurane (no isoflurane with active AL). An endo-tracheal tube, urinary catheter and blood pressure catheter (femoral artery) were placed.

Mechanical ventilation settings were adjusted to match ventilation and oxygenation requirements, maintaining pressure <25cmH2O. A right and left

lateral thoracotomy was performed in the fifth intercostal space, starting with the right lung. An intercostal block was placed on three levels with lidocaine/ bupivacaine. After lesion creation and sealing, a chest tube was positioned apically in the thorax. In the second experiment, an additional chest tube was placed ventrally in the thorax. Incisions were closed airtight in layers.

Spontaneous ventilation was observed for three to four hours, under ketamine, midazolam and buprenorphine anesthesia. Monitoring of vital signs was ensured throughout the procedure and recorded every thirty minutes during surgery and every hour during spontaneous ventilation. Arterial blood gas was measured at baseline, after each lung incision and twice during the observation period. After observation, euthanasia was performed using a pentobarbital. Obduction was performed and general observations were noted. The lungs were further used for BP measurements (E1-E3: ex-situ after lung explantation, E4-E6: in-situ), and samples were taken of lesions for histological processing.

Defect creation and sealing

Strips of tissue at a maximum width of 5cm were removed from the right middle (RML), right lower (RLL), left upper (LUL) and left lower (LLL) lobes in steps of 0.5-1cm, until bronchioles of 1.5mm were encountered (Video 1, Figure 2). Hemostasis was achieved using diathermy and compression. Fibrin plugs were removed from the bronchiole to ensure PAL. No further treatment was performed in the control group. In the NHS-POx group, the lung was primed using phosphate-buffered saline (PBS), which improves crosslinking and adhesive strength. The patch was applied with overlap of at least 0.5cm on healthy pleura and pressure was applied for two minutes using gauzes drenched in PBS or saline solution. For the double layer, a second patch was applied, irrigating with 20cc PBS or saline solution in between the patches, before applying pressure. In case of application failure, remnants were removed and a new patch was applied (application fluids: **Table 2**).

After the first experiment, we observed that the RML/LUL lesions were more triangular in shape, causing application difficulties. These lesions are not clinically representative in shape and location compared to the lesions that generally result from lung surgery for which a sealant would be used. Therefore, only RLL/LLL lesions were included in the second experiment.

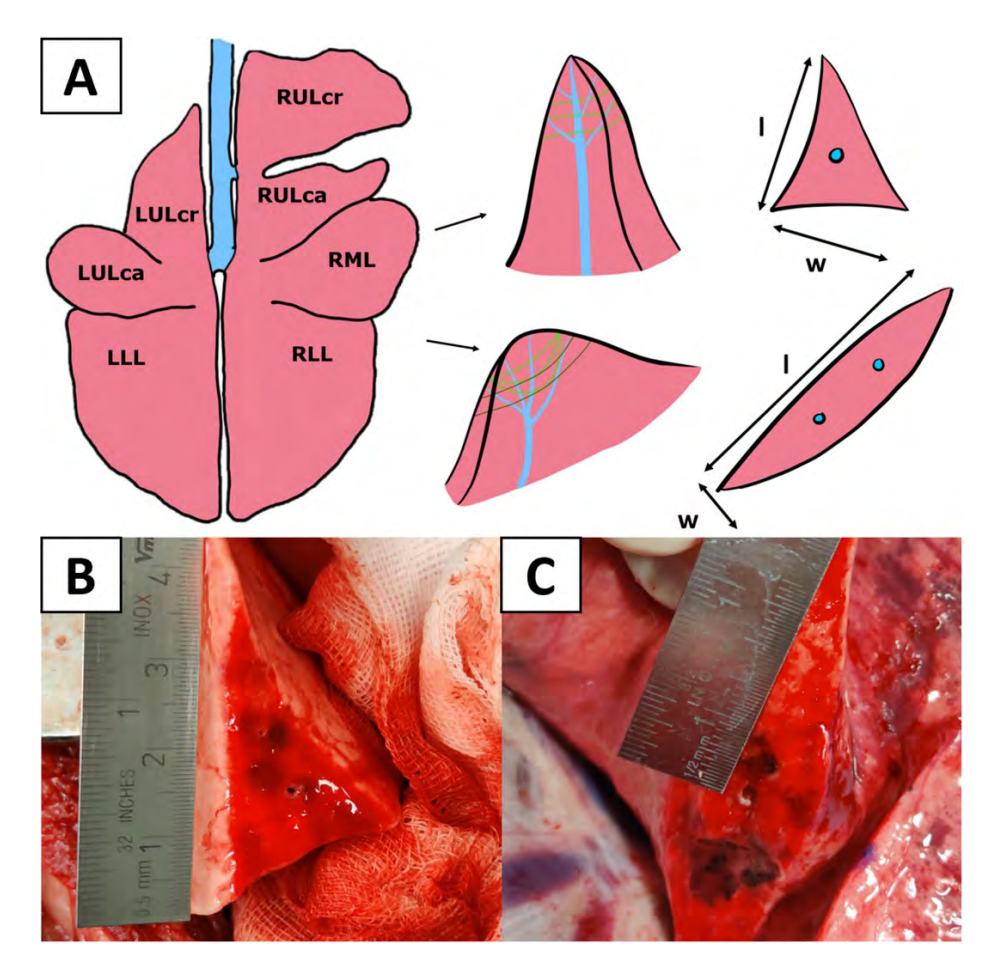


Figure 2: A) Middle/upper lobe (RML/LULca) lesions are more triangular (B) and lower lobe (RLL/LLL) lesions are more oval (C). Reused/adapted with permission from AME Publishing Company. [16]

Outcome measures

Baseline AL was measured by registering tidal volumes for fifteen breaths (RR 15/min, PEEP 5cmH20, PPlat 15-20cmH20). Minimal leaking pressure (MLP) was determined by adjusting PEEP (steps of 1cmH20, starting at 10cmH20). Sealing success was defined by absence of bubbles after irrigation with saline directly after application. Postoperative AL was measured using a digital drainage system (Thopaz®, Medela, Baar, Switzerland). BP (pressure at first visual bubbles) is determined post-mortem, by increasing ventilation pressure with 5cmH20 every sixty seconds (respiratory rate 12/min, PEEP 5cmH20, I:E 1:2, Pc 15cmh20). (15) For control lesions or sealed lesions with persistent leakage,

MLP was determined and analyzed as a BP value. Failure mechanism was noted as adhesive (leakage between the sealant and lung) or cohesive (leakage within the sealant). Histology samples were stored in 4% formaldehyde, embedded in paraffin, sliced in (4µm) and stained with hematoxylin-eosin. The slices were analyzed for signs of acute adverse inflammatory response.

Data analysis

Postoperative AL data was imported using ThopEasy+ software (Medala, Baar, Switzerland), giving mean AL values (mL/min) every ten minutes. Mean postoperative AL was calculated over the first three hours. This asynchronous interval was chosen to facilitate interpretation in the context of time-dependent intrinsic sealing. (16) Intraoperative baseline AL (mL/min) based on the mechanical ventilator was calculated as: $AL = \frac{\sum_{k=1}^{5} (TVi_k - TVe_k)}{5} \times RR^{(17)}$ This was corrected for AL measured before lesion creation as: $AL_{corrected} = AL_{lesion} - AL_{baseline}$. As the sample size was small and possible differences are detectable with more power on a continuous scale, we used linear regression to estimate differences in mean postoperative AL and BP between sealing and non-sealing while correcting for experiment heterogeneity (using the intervention group and experiment number as predictors). NHS-POx samples were pooled and compared to control lesions (Figure 1). Log- and square root transformations were considered if this made the regression residuals better normally distributed. Significance was considered if p<0.05 for predictors in the analysis. Baseline values were compared between groups using an independent samples T-test or Fischer's exact test with a significance level of 0.05. IBM SPSS Statistics 27 (Armonk, New York; IBM Corp) was used for statistical testing.

Results

At baseline, lesions resulted in similar intraoperative AL (mean 1.38-1.47 L/ min, p=0.90; all Macchiarini grade 3) and bleeding (mean grade 3.3-3.8, p=0.27). A tension pneumothorax developed in one animal (E2) during the second thoracotomy and resolved by putting the sheep in an abdominal position and finishing the procedure in this position. Baseline characteristics are shown in Table 1.

Sealing using NHS-POx was achieved in 8/11 (72.7%) cases in one attempt (p=0.004) and in 10/11 (90.9%) cases in >1 attempt (p<0.001) compared with negative controls. Failures to apply the patch in one attempt occurred on lesions

Table 1: Baseline characteristics

	NHS-POx sealed (N=11)	Control (N=7)	P-value
GENERAL CHARACTERISTICS			
Animal			
Weight (kg)	73.6±6.2	74.7±7.8	0.75
Age (months)	23±11.5	28±11.7	0.37
Timing			
Spontaneous ventilation (hh:mm)	3:51±0:26	3:43±0:31	0.58
Drainage duration (hh:mm)	6:12±2:04	6:15±2:55	0.96
Lesion side (n)			
RML	2	1	p>0.99
RLL	4	2	
LUL	2	1	
LLL	3	3	
LESION CHARACTERISTICS			
Visual assessment			
Bleeding (SBSS grade) [28]	3.8±0.9	3.3±1.1	0.27
Air leak (Macchiarini grade)[29]	3±0	3±0	-
Minimal leaking pressure (cmH2O)	5±2	5±1	0.85
Lesion dimensions			
Cut distance from edge (cm)	3.4±1.0	3.9±1.1	0.31
Bronchiole diameter (mm)	1.5±0.2	1.6±0.2	0.75
Length (mm)	57±17	59±15	0.79
Width (mm)	18±5	23±6	0.052
Mechanical ventilator measurement			
Baseline AL (L/min)	1.38±0.98	1.47±2.09	0.90
ANESTHESIA PARAMETERS			
During surgery			
Heart rate (bpm)	107±5	105±6	0.53
Mean arterial blood pressure (mmHg)	89±6	90±8	0.65
Temperature (°C)	37.7±0.4	37.9±0.2	0.11
Observation period			
Heart rate (bpm)	115±9	114±12	0.81
Mean arterial blood pressure (mmHg)	106±17	102±21	0.66
Temperature (°C)	38.5±0.4	38.2±0.3	0.17
Respiratory rate (bpm)	54±5	54±7	0.77
Tidal volume (mL)	197±44	191±56	0.81
BIOCHEMICAL PARAMETERS			
Coagulation ACT (s)	115±10	117±12	0.71
			J., 1
Blood gas	7.35±0.07	7.34±0.09	0.71
pH pO2 (kPa)	7.35±0.07 21.9±7.8	7.34±0.09 23.5±9.6	0.71
pCO2 (kPa)	6.9±0.5	6.9±0.7	0.71
POOL (KI U)	J. /±0.J	J. / ±0. /	0.77

Analysis per sample, multiple samples tested in one animal. Presented as mean and standard deviation. Statistical testing with independent samples T-test or Fischer's exact test.

with a triangular shape (RML/LUL lesions, Figure 2, Table 2). Saline seemed to result in less unwanted sticking of the patch to the gauzes compared to PBS application fluid (Table 2, no application failures with saline). Compression atelectasis was observed after application (Figure 4).

Sealing with NHS-POx was associated with a lower postoperative AL (median: 7mL/min, IQR: 333mL/min) compared to the control group (median: 367mL/ min, IQR: 680mL/min, p=0.036) in multivariable linear regression analysis. There were no effects of heterogeneity between the experiments in this analysis (i.e. one versus two lesions per lung) (p=0.936) (Figure 3). Average postoperative AL was <20mL/min in 5/7 (71.4%) of NHS-POx sealed lungs, while always (5/5) being >20mL/min in the control lungs. Control lungs showed intrinsic sealing (cessation of leakage with AL <10mL/min) during the observation period in 3/5 (60%) cases, within a mean of 2:57h (SD: 1:45h) after start of drainage.

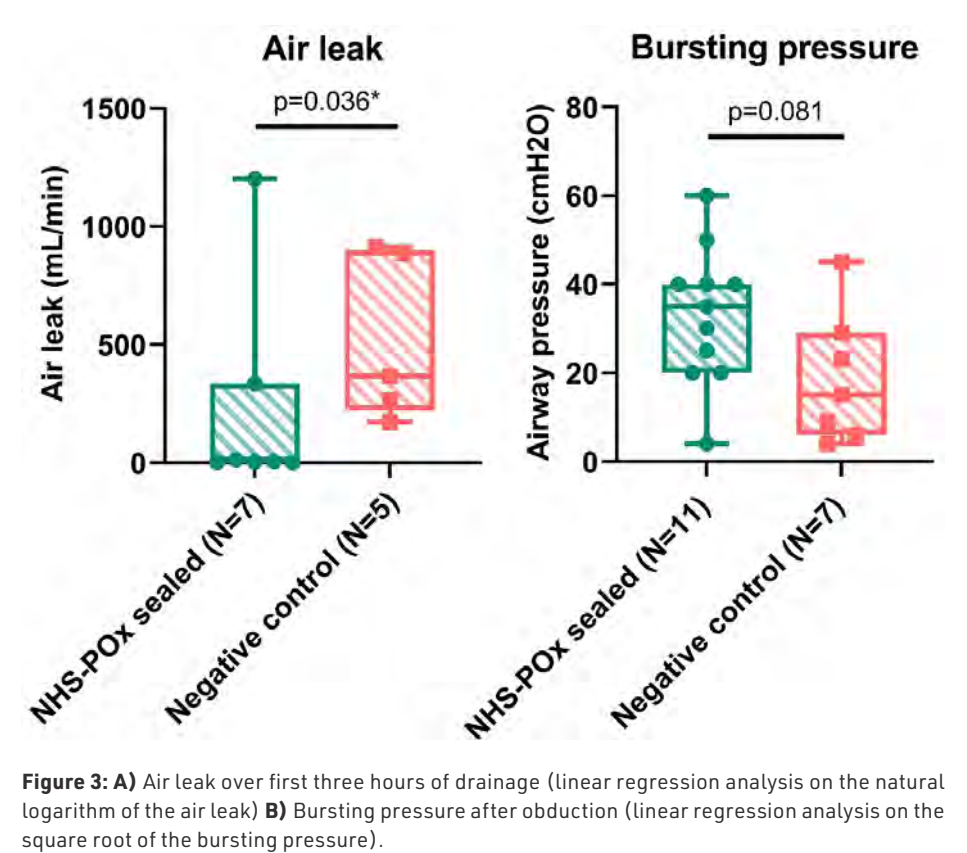


Figure 3: A) Air leak over first three hours of drainage (linear regression analysis on the natural logarithm of the air leak) B) Bursting pressure after obduction (linear regression analysis on the square root of the bursting pressure).

^{*}p<0.05.

Table 2: Aerostatic findings

ID	G	roup	AL (mL/min) ^a	Lobe(s)	Sealant	Fluids	Acute sealing	BP (cmH2O)b
					EXPERIMENT	1		
E1	R	Seal.	3	RML	NHS-P0x single	PBS	Yes, 2 nd attempt	50
				RLL	NHS-P0x single	PBS	Yes	30
	L	Seal.	2	LUL	NHS-P0x double	PBS	Yes	35
				LLL	NHS-P0x double	PBS	Yes	20
E2	R	Cont.	886	RML	Untreated	N/A	N/A	9 ^d
				RLL	Untreated	N/A	N/A	4 ^d
	L	Seal.	336	LUL	NHS-P0x single	PBS / saline	No, 4 th attempt	20
				LLL	NHS-P0x single	Salinec	Yes	40
E3	R	Seal.	14	RML	NHS-P0x double	PBS / saline	Yes, 2 nd attempt	40
				RLL	NHS-P0x double	PBS / saline	Yes	25
	L	Cont.	913	LUL	Untreated	N/A	N/A	15
				LLL	Untreated	N/A	N/A	45
					EXPERIMENT	2		
E4	R	Cont.	267	RLL	Untreated	N/A	N/A	29 ^d
	L	Seal.	7	LLL	NHS-P0x double	Saline ^c	Yes	60
E5	R	Seal.	6	RLL	NHS-P0x double	Saline ^c	Yes	40
	L	Cont.	173	LLL	Untreated	N/A	N/A	23^{d}
E6	R	Seal.	1202	RLL	NHS-P0x double	Saline ^c	Yes	4 ^d
	L	Cont.	367	LLL	Untreated	N/A	N/A	6 ^d

^aNot normalized for number of leaks.

BP was higher for the NHS-P0x group (mean: 33, SD: 16cmH20) compared to the control group (mean: 19, SD: 15cmH20), without reaching statistical significance in the linear regression analysis (p=0.081) (**Figure 3**). There were no effects of methodological differences (i.e. ex-situ versus in-situ measurements) between experiments in this analysis (p=0.985). BP was >30cmH20 in 7/11 (63.6%) of NHS-P0x cases and in 1/7 (14.3%) control cases (**Table 2**). Mode of failure was cohesive in 10/11 (90.9%) NHS-P0x sealed cases (examples **Figure 4B/D**).

bE1-E3 ex-situ measurements, E4-E6 in-situ measurements

^cCombined with PBS priming

dMeasured using minimal leaking pressure protocol by adjusting PEEP in 1cmH20 steps AL: average air leak over first 3h of drainage; BP: bursting pressure; L: left; R: right; RML: right middle lobe; LUL: left upper lobe; RLL/LLL: right/left lower lobe; PBS = phosphate-buffered saline.

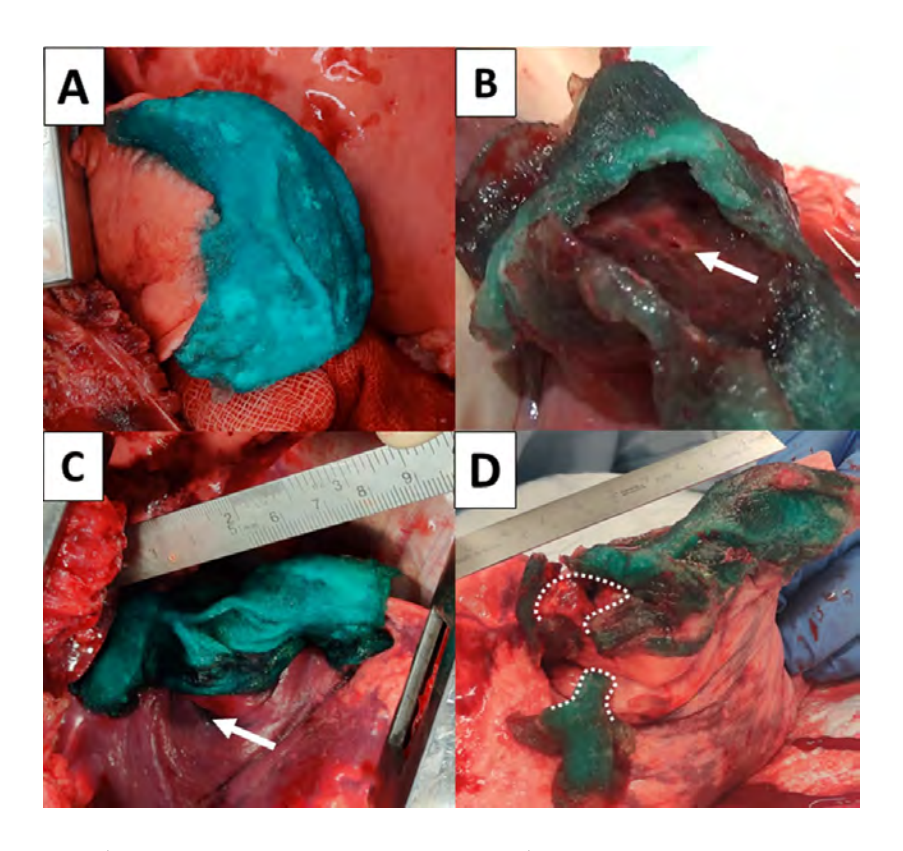


Figure 4: A) Patch on a middle/upper lobe lesion. B) Mode of failure double patch. Dome formation was seen, with cohesive tear through the dome (half of dome cut away). Arrow pointing at bronchiole. C) Double patch after application, showing atelectasis and folding of lung parenchyma (white arrow). D) Mode of failure of patch in (C), showing cohesive failure due to lung expansion (dotted lines).

At sacrifice, intra-thoracic migration of a small piece was seen in three NHS-POx samples (E3R and E4L). In one sheep (E2), a small encapsulated abscess was seen at obduction distant from the lesions, without clinical symptoms. Some swelling of the patch was observed, and appeared lower in the second experiment due to the ventral chest tube (which prevented pooling of fluids around the patch). The patch could be removed using manual dissection or tweezers without tearing the underlying lung, and appeared less adhesive and cohesive compared to right after application. Intra-thoracic bleeding was observed during lung explantation procedures in the first experiment. Morphological analysis revealed a response consistent with the created lung injury (collapsed parenchyma, fibrin depositions, neutrophile infiltration). No major acute inflammatory reactions to the foreign body were observed (Figure 5).

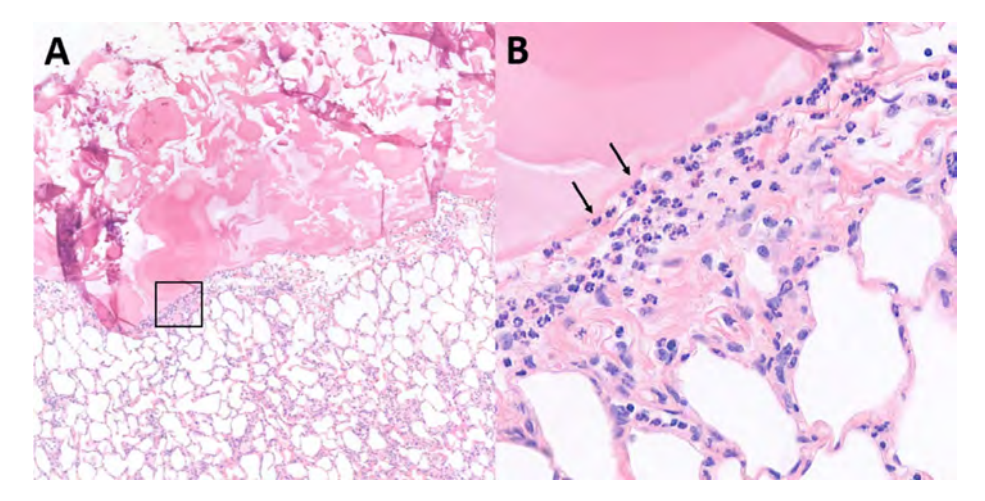


Figure 5: A) Example of pleural interface, showing tight adhesion and normal alveoli. **B)** Detail of **(A)**, showing influx of neutrophilic granulocytes (arrows).

Discussion

We have investigated the performance of novel NHS-POx coated gelatin patches, demonstrating proof-of-principle for lung sealing applications in anesthetized sheep mimicking the clinical situation. In the majority of cases, clinically severe baseline ALs, on average measuring >400mL/min on the mechanical ventilator, could be sealed with only one application of the patch. (18) Postoperative AL during the follow-up period was significantly reduced compared to non-treated lung lesions, and the bursting strength of the covered lesions tended to be better than the controls, indicative of treatment effectiveness.

The patch could be effectively molded around a single lung edge and proved compatible with thoracotomy based application to the lung. Only one adhesive failure was noted, confirming adequate adhesion to the tissue. (a) In contrast, the currently most studied lung sealing patch (TachoSil®) showed mainly adhesive failures in preclinical studies. (15, 19, 20) For lung sealing, an optimal balance is required between adhesive and cohesive forces, but a cohesive failure mechanism may be advantageous. In our previous study, we noted patches with an adhesive failure mechanism generally lost all sealing potential upon bursting, while samples with cohesive failure mechanisms show gradual loss of sealing potential due to strong adhesion to the leaking surface. (15)

Issues regarding surgical application need to be addressed. Firstly, excessive adhesion of the application gauzes to the patch were seen, and the application fluids were adjusted consequently (Table 2). Secondly, double layer patch application was associated with sealant failure. As irrigation is required between the patches to ensure cohesion, no immediate pressure is applied, allowing an air pocket to form and ultimately causing dome formation and cohesive tearing. (15) Thus, while aerostatic proof-of-principle has been shown, optimizations are still required in the precise application method to resolve these problems.

Application failures were only seen on triangular lesions, which is an unconventional geometry in clinical practice. (19) Comparison of sealant efficacy on various geometries is not well studied, but lesions requiring several folds around edges seem inherently less suited for patch application. Conceptually, spray based sealants with high viscosity might be a better alternative in such cases. (21) The sealing efficacy of the patch might be higher on other lesion geometries which were not studied in the current experiment, such as superficial pleural lesions and dissected fissures. (15)

A higher BP was observed for the NHS-POx samples, without reaching statistical significance. During lung explantation for ex-situ measurements, intra-thoracic bleeding and blood contact of the control lesions was observed, which may have increased BP, while the manipulations required to explant the lung might have caused damage to the sealants, lowering the BP. As a consequence, we hypothesize that a significant difference would have been demonstrated, when all measurements were performed in-situ.

Comparison of current findings to relevant literature is difficult, due to many studies lacking a standardized model of PAL, appropriate control groups and quantitative outcome measures. (22, 23) Intrinsic healing mechanisms in healthy animals may invalidate results if no control groups are used. (16) Because AL is mainly due to alveolar leakage in patients with emphysema, the translational value from healthy animal lungs remains unclear, and lung sealing results may be overestimated due to a lower crosslink density in emphysema. (1, 16, 24)

In the present study, the primary aim was to investigate the effectiveness of the novel patch to seal AL in-vivo. No comparison to similar devices was performed, but superior BP was previously measured ex-vivo. (15) Further in-vivo comparison to gold-standard products should be performed for benchmarking. Clinically, the best studied patch is the fibrinogen-thrombin

coated collagen patch (TachoSil[®]). Call Gel/spray sealants, such as the novel human serum albumin/polyethylene glycol spray (Progel[®]) appear less suited for comparison to a patch, due to the aberrant mode of application.

We showed that 5/7 (71.4%) patches had <20mL/min postoperative AL. For comparison, several studies with negative control groups and AL measurements should be pointed out, showing on the whole comparable results. Ranger et. al. used similar lesions in healthy dogs, testing a photopolymerizable gel, which remained aerostatic in 80% over a 24h period. (22) Kjaergard et. al. measured AL for two hours over a bilateral upper lobe wedge resection, demonstrating average 92% AL reduction for an autologous fibrin sealant. (9) McCarthy et. al. used large parenchymal lesions in dogs, which were either left untreated or sealed with a fibrin glue, demonstrating average 19.8% vs 80.8% AL reduction from baseline. (25)

With regard to safety, no major acute adverse inflammatory or allergic reactions were observed. Other studies have shown biocompatibility and biodegradability within six weeks for intra-abdominal use, and the polymers are renally excreted. (12-14) However, the present experiment has limited value with regard to demonstrating safety for intra-thoracic use. Organ-specific safety considerations should be further scrutinized in longer-term experiments, relating to biodegradation as a function of underlying tissue healing, material migration, foreign body response and impact on adhesion formation, lung expansion and atelectasis.

Macroscopically, swelling appeared to impact the adhesive-cohesive matrix integrity at sacrifice, which could be indicative of rapid degradation. This might pose a safety issue in the direct post-operative period for re-leakage. Swelling occurs due to the hydrophilicity designed to enhance blood uptake for hemostatic purposes, but will be mainly due to water uptake in primary air leaks. (11) This increases the polymer chain separation which weakens the secondary intermolecular forces, and enhances hydrolysis of amide and thioester bonds. (13, 26, 27) The specifications with regard to degradation speed as a function of underlying tissue healing are unknown in the context of pPAL, and should be further investigated in longer-term models.

These experiments consist both model development as well proof-of-principle of a new lung sealant in a live animal model, forming the basis for further investigations. Methodological variation between the experiments and a small sample size are inherent limitations to this approach. By use of linear regression

analysis and pooling of all NHS-POx samples, we were able to account for this variation. This approach is in our opinion most appropriate ethically, ensuring optimal research returns while reducing the amount of animals required.

Postoperative AL data was analyzed per lung over the first three hours of drainage, to allow for meaningful interpretation of AL in the context of rapid intrinsic sealing mechanisms. Consequently, right lung lesions were mainly exposed to positive pressure ventilation in lateral decubitus positions, and left lung lesions to physiological breathing in abdominal position, which could impact AL. These effects appear to have been mitigated by use of randomization, as no clear AL differences are seen as a consequence (**Table 2**).

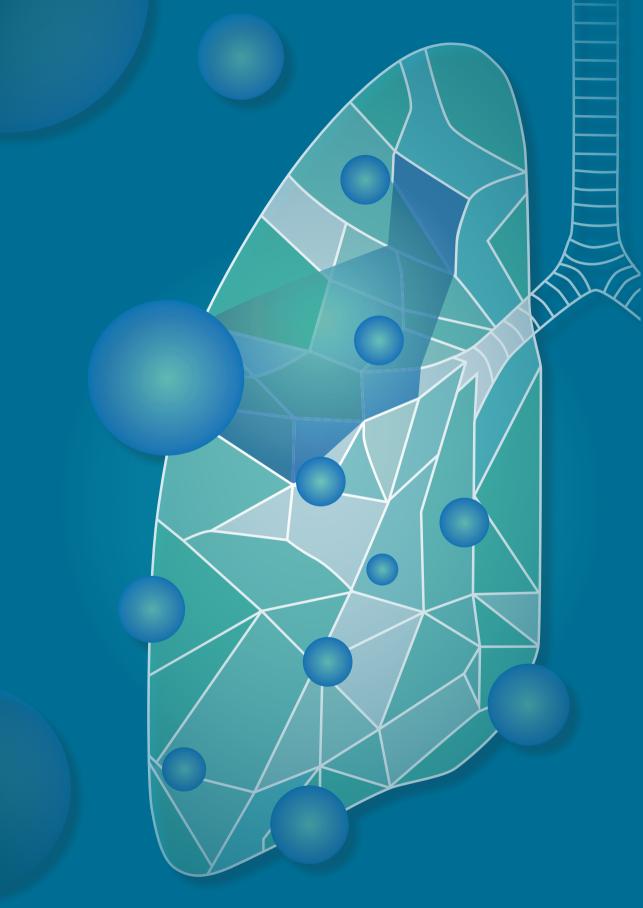
Treatment options for severe AL remain limited to sutures or staplers, which might be insufficient due to tissue tearing in lungs with compromised integrity (e.g. emphysema, advanced age, corticosteroid use). (10) The capabilities of this patch for sealing clinically severe AL without the additional support of sutures or staplers are therefore promising. However, before clinical applications, further study is required. The single-patch should be improved to replace the double patch, and application method should be optimized to minimize sticking to gauzes. Carrier materials which resemble the lung regarding elasticity and compressibility may be considered. Comparison to currently available similar devices is required for benchmarking. Finally, in-vivo biodegradability, safety and healing of underlying tissue should be studied in longer-term survival models.

Conclusions

In conclusion, NHS-POx technology may be a potent lung sealant, based on effective reduction of severe ALs in a subacute model. The mode of application needs to be optimized to meet the specific demands of a lung sealant. Further research is required for longer-term aerostatic efficacy, biodegradability and safety, before clinical use.

- 1. Attaar A, Tam V, Nason KS. Risk Factors for Prolonged Air Leak After Pulmonary Resection: A Systematic Review and Meta-analysis. Ann Surg. 2020;271(5):834-44.
- 2. Brunelli A, Xiume F, Al Refai M, Salati M, Marasco R, Sabbatini A. Air leaks after lobectomy increase the risk of empyema but not of cardiopulmonary complications: a case-matched analysis. Chest. 2006;130(4):1150-6.
- 3. Yoo A, Ghosh SK, Danker W, Kassis E, Kalsekar I. Burden of air leak complications in thoracic surgery estimated using a national hospital billing database. Clinicoecon Outcomes Res. 2017;9:373-83.
- Attaar A, Luketich JD, Schuchert MJ, Winger DG, Sarkaria IS, Nason KS. Prolonged Air Leak After Pulmonary Resection Increases Risk of Noncardiac Complications, Readmission, and Delayed Hospital Discharge: A Propensity Score-adjusted Analysis. Ann Surg. 2021;273(1):163-72.
- 5. Liang S, Ivanovic J, Gilbert S, Maziak DE, Shamji FM, Sundaresan RS, Seely AJE. Quantifying the incidence and impact of postoperative prolonged alveolar air leak after pulmonary resection. J Thorac Cardiovasc Surg. 2013;145(4):948-54.
- Brunelli A, Chapman K, Pompili C, Chaudhuri N, Kefaloyannis E, Milton R, et al. Ninetyday hospital costs associated with prolonged air leak following lung resection. Interact Cardiovasc Thorac Surg. 2020;31(4):507-12.
- 7. Belda-Sanchis J, Serra-Mitjans M, Iglesias Sentis M, Rami R. Surgical sealant for preventing air leaks after pulmonary resections in patients with lung cancer. Cochrane Database Syst Rev. 2010(1):Cd003051.
- 8. Brunelli A, Bölükbas S, Falcoz PE, Hansen H, Jimenez MF, Lardinois D, et al. Exploring consensus for the optimal sealant use to prevent air leak following lung surgery: a modified Delphi survey from The European Society of Thoracic Surgeons. Eur J Cardiothorac Surg. 2020.
- 9. Kjaergard HK, Pedersen JH, Krasnik M, Weis-Fogh US, Fleron H, Griffin HE. Prevention of air leakage by spraying vivostat fibrin sealant after lung resection in pigs. Chest. 2000;117(4):1124-7.
- 10. Singhal S, Shrager JB. Should buttresses and sealants be used to manage pulmonary parenchymal air leaks? J Thorac Cardiovasc Surg. 2010;140(6):1220-5.
- Boerman MA, Roozen E, Sánchez-Fernández MJ, Keereweer AR, Félix Lanao RP, Bender J, et al. Next Generation Hemostatic Materials Based on NHS-Ester Functionalized Poly(2oxazoline)s. Biomacromolecules. 2017;18(8):2529-38.
- Roozen EA, Warlé MC, Lomme R, Félix Lanao RP, van Goor H. New polyoxazoline loaded patches for hemostasis in experimental liver resection. J Biomed Mater Res B Appl Biomater. 2021.
- 13. Boerman MA, Roozen EA, Franssen GM, Bender JCME, Hoogenboom R, Leeuwenburgh SCG, et al. Degradation and excretion of poly(2-oxazoline) based hemostatic materials. Materialia. 2020;12:100763.
- 14. Roozen E, Lomme R, Calon N, Broek R, Goor H. Efficacy of a novel polyoxazoline based hemostatic patch in liver and spleen surgery2023.
- 15. Hermans BP, Li WWL, Roozen EA, van Dort DIM, Evers J, van der Heijden EHFM, et al. Sealing effectiveness of a novel NHS-POx based patch: experiments in a dynamic ex-vivo porcine lung. Journal of Thoracic Disease. 2023.

- 16. Hermans BP, Li WWL, Roozen EA, van Dort DIM, Vos S, van der Heide SM, et al. Intrinsic pulmonary sealing, its mechanisms and impact on validity and translational value of lung sealant studies: a pooled analysis of animal studies. Journal of Thoracic Disease. 2023.
- 17. Brunelli A, Salati M, Pompili C, Gentili P, Sabbatini A. Intraoperative air leak measured after lobectomy is associated with postoperative duration of air leak. EUROPEAN JOURNAL OF CARDIO-THORACIC SURGERY, 2017:52(5):963-8.
- 18. Zaraca F, Brunelli A, Pipitone MD, Abdellateef A, Abu Akar F, Augustin F, et al. A Delphi Consensus report from the "Prolonged Air Leak: A Survey" study group on prevention and management of postoperative air leaks after minimally invasive anatomical resections. Eur J Cardiothorac Surg. 2022.
- 19. Zhang R, Bures M, Höffler K, Jonigk D, Haverich A, Krueger M. In vitro comparison of two widely used surgical sealants for treating alveolar air leak. Thorac Cardiovasc Surg. 2014;62(8):705-9.
- 20. Zhou J, Lyu M, Pang L, Gao Y, Ning K, Wang Z, Liu L. Efficiency and safety of TachoSil® in the treatment of postoperative air leakage following pulmonary surgery: a meta-analysis of randomized controlled trials. Jpn J Clin Oncol. 2019;49(9):862-9.
- 21. Zaraca F, Vaccarili M, Zaccagna G, Maniscalco P, Dolci G, Feil B, et al. Cost-effectiveness analysis of sealant impact in management of moderate intraoperative alveolar air leaks during video-assisted thoracoscopic surgery lobectomy: a multicentre randomised controlled trial. J Thorac Dis. 2017;9(12):5230-8.
- 22. Ranger WR, Halpin D, Sawhney AS, Lyman M, Locicero J. Pneumostasis of experimental air leaks with a new photopolymerized synthetic tissue sealant. Am Surg. 1997;63(9):788-95.
- 23. Hermans BP, Poos SEM, van Dort DIM, Evers J, Li WWL, van der Heijden E, et al. Evaluating and developing sealants for the prevention of pulmonary air leakage: A systematic review of animal models. Lab Anim. 2023:236772231164873.
- 24. Gika M, Kawamura M, Izumi Y, Kobayashi K. The short-term efficacy of fibrin glue combined with absorptive sheet material in visceral pleural defect repair. Interact Cardiovasc Thorac Surg. 2007;6(1):12-5.
- 25. McCarthy PM, Trastek VF, Bell DG, Buttermann GR, Piehler JM, Payne WS, et al. The effectiveness of fibrin glue sealant for reducing experimental pulmonary ari leak. Ann Thorac Surg. 1988;45(2):203-5.
- 26. Nam S, Mooney D. Polymeric Tissue Adhesives. Chem Rev. 2021;121(18):11336-84.
- 27. William D. Callister DGR. Chapter 18: Corrosion and Degredation of Materials Materials Science and Engineering Ninth Edition ed: Wiley; 2011. p. 670.
- 28. Ardehali A, Spotnitz WD, Hoffman RW, Olson SA, Bochicchio GV, Hermann MC, et al. Evaluation of the safety and efficacy of a new hemostatic powder using a quantitative surface bleeding severity scale. J Card Surg. 2019;34(1):50-62.
- 29. Macchiarini P, Wain J, Almy S, Dartevelle P. Experimental and clinical evaluation of a new synthetic, absorbable sealant to reduce air leaks in thoracic operations. J Thorac Cardiovasc Surg. 1999;117(4):751-8.



Chapter 7

Biocompatibility of a novel lung sealant based on functionalized polyoxazolines in an ovine model of parenchymal lung injury

Bob P Hermans¹, Shoko Vos³, Wilson WL Li¹, Erik HFM van der Heijden⁴, Harry van Goor², Ad FTM Verhagen¹, Richard PG ten Broek²

Radboud university medical center, Radboud Institute for Health Sciences, Nijmegen, The Netherlands.

¹Department of Cardio-thoracic surgery

²Department of General surgery

³Department of Pathology

⁴Department of Pulmonology

ABSTRACT

A lung sealant based on a porcine gelatin carrier impregnated with N-hydroxysuccimide ester functionalized (NHS-POx) and nucleophilically activated (NU-POx) poly(2) oxazolines was shown to be efficacious ex-vivo and in-vivo. We investigate the local biocompatibility. Three groups, NHS-POx, fibrin patch (TachoSil®) and untreated control, are randomly applied to lesions on the right lung (n=3/lung) of adult female domestic sheep, which are sacrificed for blinded histological assessment at 5, 14 and 42 days (n=4animals per term). Semi-quantitative scoring (scale 0-4) was performed on immune cell subtypes (polymorphonuclear cells, lymphocytes, plasma cells, macrophages, giant cells, necrosis) and biomaterial response (fibrosis, neovascularization, fatty infiltrate). Post-hoc analysis was performed for a suspected labeling mistake and adapted datasets were obtained (6 weeks). The total cell response score was significantly higher for NHS-POx versus control (score: 11.5 [9-13] vs 7 [6-8], p=0.005) at five days, and for fibrin patch versus control (score: 14 [12-17] vs 7 [5-8], p=0.022) at 2 weeks. At 6 weeks, cell response was similar between groups (p=0.22), with outliers due to granulomatous inflammation to residual patch (n=1 fibrin patch and n=1 mixup sample likely fibrin patch). Wound healing, fibrosis and neovascularization were similar across groups, showing local pleural thickening. NHS-POx patch showed mesothelial coverage at 2 weeks and was macro- and microscopically completely degraded at 6 weeks with replacement of the patch material with extracellular matrix (adapted data). In conclusion, NHS-POx patch shows a comparable to favorable biocompatibility profile compared to fibrin patch, and is a potent candidate for clinical lung sealing applications.

Introduction

Lung resections can result in pulmonary air leakage (PAL) after surgery, especially in patients with diseased lungs, such as in emphysema. (1, 2) Prolonged PAL (pPAL), defined as PAL lasting longer than five days, occurs in up to 30% of patients. (1) pPAL is associated with a more adverse postoperative course, including increased risk of infections (e.g. empyema: odds-ratio [OR] = 8.5), re-admissions (OR = 2), re-interventions (4.8%) and a higher mortality (OR = 1.9). (3-8)

A potential solution to pPAL is the intraoperative application of lung sealants, but their routine use is not recommended. (9, 10) There is some evidence for potential benefits, for example, a reduction in hospital stay of ~2 days has been shown in a meta-analysis for a fibrin-thrombin patch (fibrin patch, TachoSil®).(11) However, there are still improvements to be made with regard to adhesive strength and efficacy. As an example, the average length of stay increase is four days in patients with pPAL, indicating a possible gap in effectiveness. (8) Another downside is the use of humane fibrin and thrombin. which is a costly process that requires plasma donors. So, there currently is an unmet clinical need for a more effective lung sealant, preferably based on synthetic components that are easy to produce, with a favorable biodegradation profile while not causing an excessive immune response. (12)

A novel bio-adhesive patch, based on a *porcine* gelatin carrier impregnated with N-hydroxysuccimide ester functionalized poly(2)oxazolines (NHS-POx) and nucleophilically activated polyoxaxolines (NU-POx), might be promising (NHS-POx patch, GATT-Technologies B.V., Nijmegen, The Netherlands). (13-15) Initial preclinical investigations have demonstrated effective use on liver bleedings. and the patch is currently being tested in clinical trials for this indication (ClinicalTrials.gov Identifier: NCT04819945 and NCT05385). (16) The mechanism of action is based on covalent bonds between NHS-POx and tissue amines, crosslinking of NHS-POx with amines within the gelatin carrier and NU-POx, and synergistic action with coagulation mechanisms due to blood uptake. (13, 15)

Our research group has previously tested the effectiveness of the NHS-POx patch for lung sealing purposes in an ex-vivo porcine lung model, showing superior aerostatic properties compared to commercially available sealants such as the fibrin-thrombin patch (TachoSil®) and favorable mechanical properties. (17) Further investigations confirmed the sealing capabilities in a translational animal model of large air leaks (>400mL/min) (unpublished data). Therefore, the NHS-POx patch might be a promising solution to the problem of pPAL.

However, the specific safety profile for intra-thoracic application of the NHS-POx patch, in terms of biodegradation and inflammation, is unknown. Previous safety experiments in a rat model have shown that the NHS-POx polymer degradation products are renally excretable. (18) Experiments in a porcine model of intra-abdominal application showed complete degradation of NHS-POx impregnated gelatin patches in 4-6 weeks, with comparable histological response to control patches (including TachoSil®). (16)

The aim of the present study will be to assess the biocompatibility and safety characteristics of the novel NHS-POx patch for lung sealing applications, compared to a clinically used control patch (fibrin patch, TachoSil®), by examining local tissue inflammatory (foreign body) response, healing and material biodegradation.

Materials and methods

Study design

Experimental layout

A translational large animal (*ovine*) model of superficial parenchymal lung injury was used, comparing the novel NHS-POx patch to a positive control group (fibrin patch, TachoSil®, Takeda Pharmaceutical Company Limited, Tokyo) and an untreated negative control group. Animals were sacrificed at five days, two weeks and six weeks. Primary outcomes include histological response, healing and material biodegradation. Secondary outcomes include adhesion formation, material migration and adverse events. Three groups are tested per animal, ensuring each group is applied at least once on each predefined injury location per survival term. Researchers are blinded to group allocation until the moment of biomaterial application. A sample size of four per group per survival term is chosen for feasibility purposes, resulting in a total of 36 lesions in 12 sheep (**Figure 1**).

Lung lesions and biomaterial application

Standardized lesions are created in the same order: the right middle lobe (RML), right lower lobe ventral aspect (RLLv) and right lower lobe dorsal aspect (RLLd) (**Figure 1**). At a constant inflation pressure of 10cmH2O, a

25x25mm square is cut using a scalpel (#15) limited to 3mm depth in a clamp, followed by visceral pleura removal and an additional 6x6 perpendicular cuts in this square. Baseline air leakage (Macchiarini scale, minimal leakage pressure [MLP]) and bleeding (surface bleeding severity scale [SBSS]) are recorded, and hemostasis is reached with gauze compression. (19-21) For the NHS-POx patch (5x5cm), the lung is primed using phosphate-buffered saline solution, followed by applying pressure with saline-wetted gauzes for 30s, removal of the gauzes and reapplying pressure for another 90s. The fibrin patch is applied using saline-wetted gauzes for three minutes. The lung is kept at 5cmH20 static pressure during patch application, but ventilation is resumed if required.

Based on prior experiments, it is known that the lesions do not result in PAL due to intrinsic sealing, which facilitates the use of untreated lesions to compare the pathological mechanisms without necessitating prolonged chest drainage. (19)

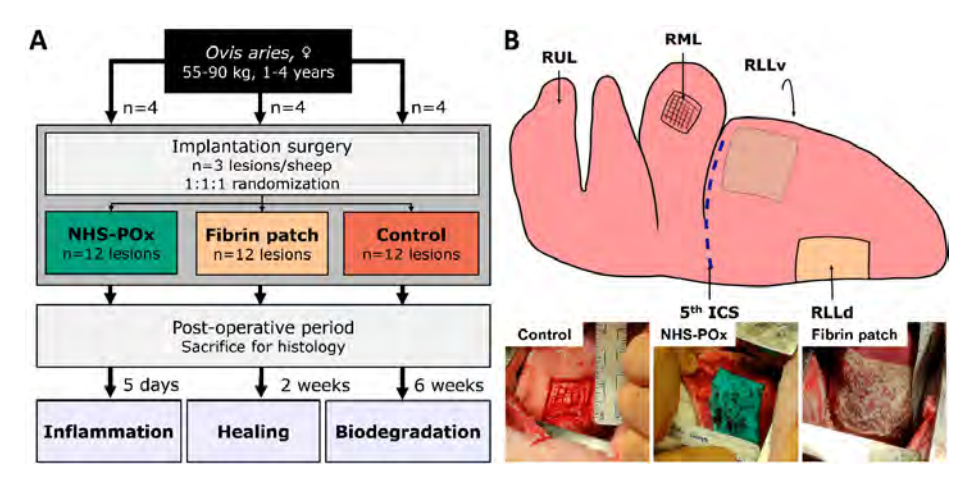


Figure 1: A) Study design. B) Anatomical locations ensure adequate distance from the 5th intercostal space incision (blue dotted line). Lesions are made on the right middle lobe (RML), right lower lobe, ventral diaphragmatic segment (RLLv) and the right lower lobe, dorsal-caudal segment (RLLd).

Animal procedures

Ethical statement

All animal experiments were performed under a project license granted by national authorities after review by an independent ethics board. Protocols were approved by the animal welfare body and registered at our institute, in accordance with relevant national and international legislation (EU Directive 2010/63/EU). The experiments were carried out using the ARRIVE 2.0 guidelines.

Animals and housing

Adult female domestic sheep (Ovis aries, weight 55-90kg, age 23-52 months) are hoof trimmed, sheared, treated with Spotinor Pour-On (to prevent ectoparasites) and housed in standard laboratory pens with a thick layer of sawdust bedding (4.5x2.5m for two animals, ambient temperature ~18-21°C, 12h light/dark cycles). They are fed hay ad libitum and have continuous access to drinking water, and are additionally fed standard pellets. During housing and transportation, animals are always accompanied by at least one buddy sheep. Animals are transported to the laboratory at least one day before surgery, and in the 2 and 6 week groups, transported back to the farm at least five days postoperatively, and housed with a flock of sheep until being transported back for sacrifice. The housing conditions at the farm included a large stable (12x5m, hay bedding, large open doors and natural ventilation, willow branches as cage enrichment), ad libitum hay and water, and are fed additionally pellets, beet pulp and mineral lick. Female sheep were chosen because they are not aggressive when housed in groups, and no relevant influences of sex are expected on biocompatibility outcome measures.

After histologically encountering a parasitic lung infection following the first two experiments, the remaining animals were separated from the larger flock to a clean stable and treated prophylactically with ivermectin subcutaneously (20mg).

Anesthesia, analgesia and antibiotic prophylaxis

Pre-medication included midazolam (0.7 mg/kg) and ketamine (10 mg/kg) intramuscularly. Anesthesia was induced using propofol (2 mg/kg), methadone (0.2 mg/kg) and ketamine (1 mg/kg) intravenously, and maintained using propofol, ketamine (0.2 mg/kg/h), remifentanil (0.06 mg/kg/h) and isoflurane. Doses were titrated to maintain the mean arterial pressure between 50-100mmHg. Antibiotic prophylaxis included amoxicillin (10 mg/kg) intravenously thirty minutes before incision, and ampicillin (15 mg/kg) intramuscularly after surgery and again after 48 hours. Multi-modal analgesia included meloxicam (0.5 mg/kg) intramuscularly during induction and daily for the first five days postoperatively (orally 0.4mg/kg), magnesium sulphate (40mg/kg) intravenously during surgery, fentanyl (100 μ g/h) applied trans-dermally during induction and an intercostal block at three levels using ropivacaine (1.5mg/kg). In case of

discomfort post-operatively, additional ketamine (0.5 mg/kg) was administered intramuscularly (Supplement 7A, Table A1). In the first animal, a slightly different variant of this anesthesia protocol was used (Supplement 7A, Table A2).

Surgical procedures

Animals were shaven, washed with soap containing chlorhexidine gluconate (40 mg/ml. HiBiSCRUB®) and disinfected using povidone-iodine solution (100 mg/ml, Betadine®). Blood pressure was measured using a percutaneous or surgically placed intra-arterial line in the groin. Surgery was performed by a board-certified surgeon (R. ten Broek). After sterile draping, an incision was made in the right hemithorax in the fifth intercostal space through skin, subcutaneous muscle and subcutaneous fat. The latissimus dorsi muscle was split in the direction of the muscle fibers and the serratus anterior muscle was mobilized (muscle sparing approach). The thorax was entered in the fifth intercostal space and two perpendicular retractors were used for exposure. After experimental procedures, airtight closure was obtained in layers: transcostal sutures (2 Vicryl), latissimus dorsi (0 Vicryl), subcutaneous muscle (2-0 Vicryl) and skin (4-0 Monocryl). (22) A silicone chest tube was placed apically in the thorax (size Ch30). The anesthetic depth was lowered to allow for spontaneous ventilation, and the chest tube was removed when there was no relevant air leak (<10-20mL/min), as assessed by digital chest drainage (Thopaz®, Medela, Baar, Switzerland). Wounds were sprayed with chlortetracycline hydrochloride (2.45% w/W, CTC spray) for prevention of wound-infections and the sheep was allowed to recover in the pen.

Post-operative monitoring and euthanasia

Post-operatively, animals are checked using welfare monitoring lists, by scoring activity, social interaction, fur, dehydration, breathing, nose, eyes, feces, movement/gait, grimace, posture, eating/drinking and wound healing (0: normal, 1: slightly abnormal, 2: abnormal, max 26 points total). In case of aberrant breathing, lung auscultation is performed in combination with pulse oximetry to assess for a significant pneumothorax. For euthanasia at different timepoints, animals are administered ketamine and midazolam for anxiolysis, followed by an overdose of pentobarbital intravenously. Humane endpoints were defined in the institutional protocol and included severe weight loss (>20%), fever or infections (>3 days), apathic behavior (>1 day), diminished food or fluid intake (1-2 days), changes in defecation (>3 days), aberrant breathing (>3 days), prolonged air leak (>5 days) or pneumothorax and prolonged need for analgetic medication (>7 days).

Post-mortem procedures

Obduction and macroscopy

Obduction is performed through a median sternotomy, with right subcostal extension for exposure of all lesions. Macroscopic findings are systematically recorded and photographed. Presence of biomaterial migration is inspected before and after manipulation of the lung. Adhesions of the lesions are graded using the Zühlke classification (scale 0-4). $^{(23)}$ Any other adverse findings are recorded. Pictures and histology were taken after lung explantation or *insitu* after further incision extension, as determined *ad hoc* by the method that would results in the least risk of manipulating the tissue around the lesions.

Histology: sampling, processing and scoring

Histology samples are taken for systematic scoring: two per sealant (centrally through lesion and with healthy pleural overlap), one centrally through lesion for negative control (Supplement 7B, Figure B1). Additional samples were taken for qualitative analysis, including sections of unaffected lung tissue, parietal pleura, lymph nodes and other macroscopically relevant lesions. All samples were stored in 4% formaldehyde, embedded in paraffin, sliced in 4µm thick sections and stained with hematoxylin-eosin staining. Slices were digitalized using the Pannoramic 1000 (3DHISTECH, Budapest, Hungary) and assessed using CaseViewer software (3DHISTECH, version 2.4).

Sections for systematic scoring were assessed in a randomized and blinded fashion by a researcher (B. Hermans) and a board-certified pathologist (S. Vos), and consensus was reached after independent grading. In or directly adjacent to the pleura and biomaterial, cell response (polymorphonuclear cells, lymphocytes, plasma cells, macrophages, giant cells, necrosis) and biomaterial response (neovascularization, fibrosis, fatty infiltrate) were graded semi-quantitatively (scale 0-4) (Supplement 7B, Table B1, based on ISO 10993-6:2016). (24) Total response is calculated as the sum of cell response and biomaterial response. Healing was graded according to the Shafer criteria (1: very light healing, 2: moderate healing, 3: advanced healing, 4: wellorganized). (25) Biodegradation was assessed semi-quantitatively (on central slides and macroscopic photos), estimating the proportion of the patch remaining at the application site (0: no material remaining, 1:1-10%, 2:11-25%, 3: 26-50%, 4: 51-75%, 5: 76-100%) in comparison to control samples of both patches right after application. Qualitative pathological descriptions were obtained.

Due to the unexpected encounter of chronic granulomatous inflammation due to a parasitic infection in the lung parenchyma, additional scoring was obtained to assess impact on the primary study outcomes. These were assessed in the lung parenchyma and included: granulomatous inflammation and associated presence of eosinophils and parasites, smallest distance from granuloma to pleura (mm) and eosinophilia at the pleural interface (scale 0-4: absent, rare, minimal, moderate, packed). Granulomas were sometimes located right below the pleura. In these cases, the inflammatory response associated with this granulomatous reaction was not counted towards the protocolar histological scoring, which was possible due to clear histological distinguishability (Supplement 7C, Figure C3).

Data analysis

Primary outcome measures, including histological (cell response, biomaterial response, total response), healing and biodegradation scores, are compared between groups within each survival term. Histological scores are compared between central and pleural overlap slides within sealant groups, while all comparisons between groups are made based on central histological slides. Relevant qualitative findings in the pathological descriptions are counted and presented as frequencies.

Dichotomous data is presented as frequencies and comparisons are made using Fisher's exact test (between animal comparisons) or Cochran's Q test (within-animal comparisons between groups). Interval or continuous data is presented as median and range and comparisons are made using Kruskal-Wallis test (between animal comparisons) or Friedman's test (within-animal comparisons between groups). Tests are performed two-tailed at an alpha of 0.05. A closed testing procedure is used for pairwise comparisons, so pairwise comparisons are only performed in case the overall test for the three groups is significant. Pairwise comparisons are performed using a Wilcoxon Signed-Rank test at an alpha of 0.05. Statistical testing is performed using SPSS (version 29, Armonk, New York, USA; IBM Corp).

Post-hoc analysis

Because residual patch material in a sample from the NHS-POx group at six weeks showed typical histological resemblance to the fibrin patch, additional post-hoc analysis (after blinded grading) was performed to identify whether an accidental mix-up could have occurred based on: 1) analysis of notes taken during experiment and photos taken during obduction, 2) additional staining based on 'Elastin according to Masson (EvM)' staining, resulting in blue/

green staining of collagen fibers such as in the fibrin patch and 3) blinded histological sample grouping task by an independent pathologist not related to the study project based on H&E and EvM staining. Results from this analysis were combined in an 'adjudication report' which was also assessed by an independent surgeon not related to the study project.

Results

General observations: surgery, post-operative course, obduction

The surgical procedure was successful in all twelve animals, creating a total of 36 lesions. Characteristics were similar over all time points, except weight gain and estimated operative blood loss (**Table 1**). In two animals (5 day and 6 week groups), dense adhesions were found during surgery, resulting in iatrogenic lung lacerations during mobilization that were sutured (Supplement 7C, Table C5). Lesions produced similar baseline bleeding and air leaks across groups, but air leak varied significantly based on lesion location (Supplement 7C, Table C1-C2). Chest tubes were removed in the operating room and post-operative recovery was prosperous (**Table 1**). All animals survived the follow up period, and there were no major complications that were attributed to the tested biomaterials. Several complications that did not require additional interventions were noted (**Table 1**, Supplement 7C, Table C3). Other minor protocol deviations are described in Supplemental 7C (Table C5).

Table 1: Animal baseline characteristics

	5 days (n=4)	14 days (n=4)	42 days (n=4)	P-value
Procedure characteristics				
Weight (kg)				
Baseline	74.6 (56.3-87.6)	76.6 (61.3-89.4)	71.5 (67.5-79)	0.78
Obduction	73.6 (55.8-85.5)	78.2 (62-89.4)	77.6 (71.9-78.8)	0.78
Change	-1.0 (-2.1, -0.5)	0.9 (0-2.3)	4.7 (-0.2 - 7.4)	0.018
Age (months)	37 (23-48)	33 (25-51)	38 (28-52)	0.87
Disease symptoms (n, %)1				
Any	2 (50%)	2 (50%)	2 (50%)	>0.99
Lung related	0 (0%)	0 (0%)	0 (0%)	
Surgery characteristics				
Surgery duration (min.)	182 (152-193)	128 (116-160)	129 (117-257)	0.16
Pmax (cmH20)	28 (20-31)	20 (20-22)	21 (20-22)	0.14
Estimated blood loss (mL) ²	250 (50-300)	15 (10-20)	70 (50-350)	0.023
Rib fracture (n, %)	2 (50%)	1 (25%)	1 (25%)	>0.99
latrogenic lung laceration (n, %)	1 (25%)	0 (0%)	1 (25%)	>0.99

Table 1: Continued

	5 days (n=4)	14 days (n=4)	42 days (n=4)	P-value
Physiological values				
Systolic blood pressure	101 (89-126)	118 (100-128)	102 (93-122)	0.40
(mmHg)	120 (05 1/1)	105 (110 155)	1///122 172\	0 / /
Baseline ACT (sec.)	138 (95-161)	125 (113-155)	146 (133-173)	0.44 0.60
pH	7.35 (7.33-7.51)	7.38 (7.35-7.43)	7.38 (7.36-7.40)	
Lactate (mmol/L)	2.1 (0.9-2.7)	1.5 (1.4-2.7)	1.8 (1.6-3.2)	0.44
HCO3- (mmol/L)	28.8 (24.2-32.7)	29.9 (29.1-30.5)	27.4 (26.7-30.4)	0.62
Intra-operative findings				
Adhesions (n, %)	1 (25%)	0 (0%)	1 (25%)	>0.99
Infiltrates (n, %)	1 (25%)	0 (0%)	2 (50%)	0.71
Biopsied (n, %)	0 (0%)	0 (0%)	2 (50%)	0.27
Post-operative				
Welfare score				
Day 0	3 (0-5.5)	1.5 (1-2)	1.3 (0.5-2)	0.92
Day 1	0.6 (0-1)	1 (0.5-2)	0.3 (0-0.5)	0.074
Day 2	0 (0-1)	0 (0-1)	0 (0-1)	0.96
Adverse events (n, %)				
No complication	2 (50%)	2 (50%)	3 (75%)	>0.99
Any deviation, no	2 (50%)	2 (50%)	1 (25%)	>0.99
interventions ³				
General obduction				
Macroscopic infiltrates				
(n, %)				
Any ²	3 (75%)	1 (25%)	4 (100%)	0.20
Under patch	1 (25%)	0 (0%)	0 (0%)	>0.99
Pleural effusion (n, %)				
Serous	1 (25%)	3 (75%)	3 (75%)	0.46
Serosanguinous	3 (75%)	1 (25%)	1 (25%)	
Incisional adhesion (n, %)	4 (100%)	3 (75%)	2 (50%)	0.71

¹ Minor pre-operative symptoms, including mastitis, paw infection, asymptomatic swelling

Pmax = maximum ventilatory pressure applied during surgery

Data presented as median ± range.

Statistical testing performed with Kruskall-Wallis test or Fischer exact test, two-sided with alpha=0.05.

Analysis of suspected mix-up

The results of the independent mix-up analysis of a sample in the six week group are shown in Supplement 7D, showing converging evidence that a mix-up occurred during biopsy and labeling. The mix-up has some consequences for the histological analysis, and no consequences for macroscopic outcomes. For

² Gross estimate of total blood loss made by the operating surgeon.

³ Minor complications including elevated respiratory rate, groin hematoma, low appetite, seroma, thickened udder. In one sheep, a gauze was left behind in the thorax (found at obduction), without causing any clinical symptoms. This gauze was encapsulated and not directly related to any patch in the thorax.

the histological analysis both original and adapted data were analyzed. There were no noteworthy changes in statistical significances between original and adapted data for between-group comparisons, except lymphocytes and fatty infiltrate barely reaching significance (p=0.05) (Supplement 7C, Table C7). Descriptively, adapted data demonstrated a lower phagocyte response, chronic inflammation and necrosis in NHS-POx, as a result of remnant patch material in the suspected mix-up group (**Figure 2 and 3**). In the adapted data, this remnant patch material is identified as fibrin patch instead of NHS-POx.

Histology: inflammation, healing, biodegradation

Within-group comparisons for central versus pleural overlap slides revealed no significant differences (Supplement 7C, Table C6). Central slides are used for further between-group comparisons. Cell response was significantly higher for NHS-POx versus control (score: $11.5\ [9-13]\ vs\ 7\ [6-8]\ p=0.005)$ at five days, and for fibrin patch versus control (score: $14\ [12-17]\ vs\ 7\ [5-8]\ p=0.022)$ at 2 weeks. At 6 weeks, cell response was similar between groups (p=0.22), with outliers due to granulomatous chronic inflammation to residual patch material (n=1 fibrin patch and n=1 suspected mix-up sample likely fibrin patch). Biomaterial response scores were similar across groups. The total histological score was significantly higher for the fibrin patch versus control group at 2 weeks (score: $19.5\ [17-22]\ vs\ 11\ [10-12]\ p=0.008)$, but were similar at 42 days across groups (p=0.53) (**Figure 2A-C**, Supplement 7C, Table C7).

Sub-analysis revealed similar patterns of classical wound healing, starting with acute inflammation, followed by chronic and phagocytotic inflammation and scar formation. Acute inflammation was similar across groups (polymorphonuclear cells, **Figure 3A**). Signs of chronic inflammation (lymphocytes and plasma cells) were higher in the fibrin patch group (score 6.5 [5-7]) compared to NHS-POx (score: 3.5 [3-5], p=0.034) and control (score: 3.5 [3-4], p=0.034) at 2 weeks. At 6 weeks, adapted data showed higher chronic inflammation associated with necrotizing granulomatous reaction to remnant fibrin patch material, albeit not statistically significant (p=0.082, Figure 3B, Supplement 7C, Figure C4). Phagocyte response (macrophages and giant cells) was higher in the NHS-POx group (score: 4.5 [4-6]) compared to control (score: 2.5 [2-3], p=0.013) and fibrin patch (score: 3.5 [2-4], p=0.077) at five days, while NHS-POx (score: 5.5 [4-7], p=0.034) and fibrin patch (score: 6 [4-7], p=0.034) both had a significantly higher phagocyte response compared to control (score: 2.5 [2-3]) at 14 days (Figure 3C). There was up to moderate necrosis at 2 weeks in both NHS-POx and fibrin

patch groups (p=0.20), and up to severe necrosis in fibrin patch group (adapted data) at 6 weeks (p=0.14) (Figure 3D). Groups showed a similar increase in neovascularization and fibrosis across until 6 weeks (Figure 3E). Minimal fat was found associated with fibrosis in NHS-POx at 6 weeks (p=0.050), but this was also found in pleural overlap slides of the fibrin patch group at 6 weeks (Supplement 7C, Figure C1).

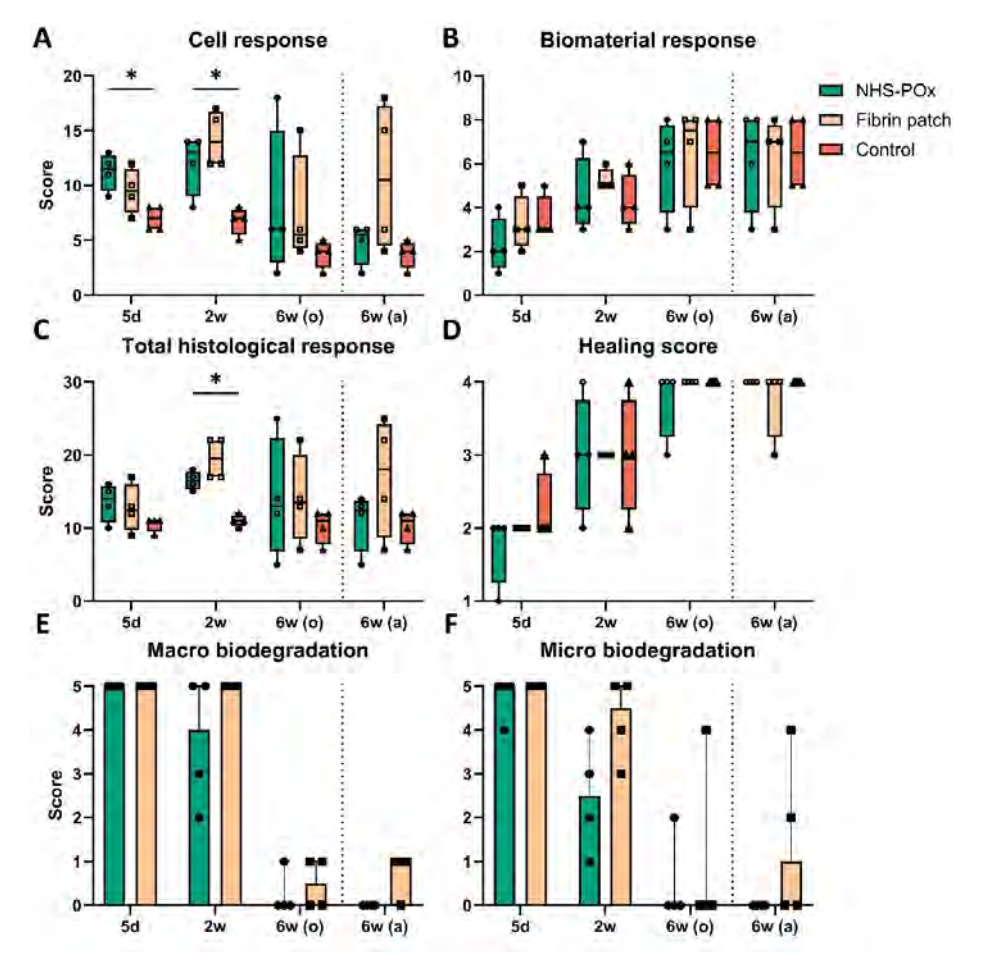


Figure 2: Between-group comparisons on main study outcomes at different timepoints based on central histological sections. A) Total cell response score (sum of semiquantitative scores [0-4] on polymorphonuclear cells, lymphocytes, plasma cells, macrophages, giant cells, necrosis, max 24 points). B) Total biomaterial response score (sum of semiguantitative scores [0-4] on neovascularization, fibrosis, fatty infiltrate, max 12 points). C) Total histological response score (sum of cell and biomaterial response, max 36 points). D) Healing score, according to Shafer criteria (scale 1-4). E) Estimated macroscopic and F) estimated microscopic biodegradation (scale 0-5). Statistical testing performed with Friedman's test or Wilcoxon Signed-Rank test. *p<0.05. d = day; w = week; o = original data; a = adapted data.

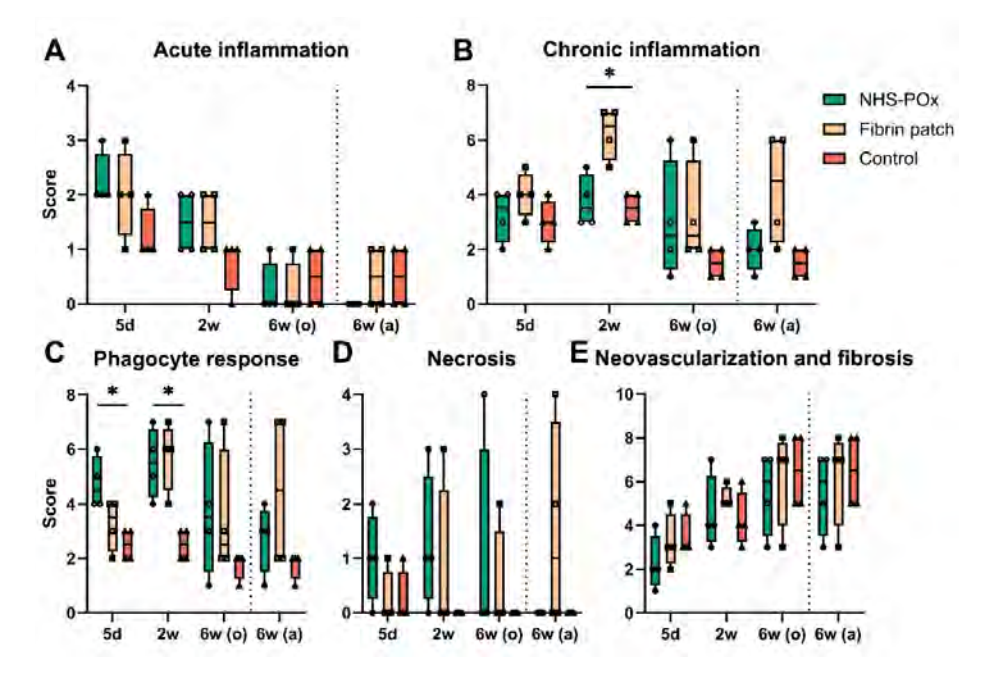


Figure 3: Between-group sub-analysis of histological parameters at different timepoints based on central histological sections. All individual items are scored on a semi-quantitative scale 0-4. **A)** Measure of acute inflammation based on polymorphonuclear cell score (max 4 points). **B)** Measure of chronic inflammation, based on the sum of lymphocyte and plasma cell scores (max 8 points). **C)** Measure of phagocytic response, based on the sum of macrophage and giant cell scores (max 8 points). **D)** Necrosis (max 4 points). **E)** Sum of neovascularization and fibrosis scores (max 8 points).

Statistical testing performed with Friedman's test. *p<0.05. d = day; w = week; o = original data; a = adapted data.

Healing scores were similar across groups (**Figure 2D**), showing overall well-organized healing at 6 weeks in both groups (p=0.368). At 2 weeks, fibrous and mesothelial coverage of the patch material could be observed (**Figure 4A-C**). At 6 weeks, local pleural thickening could be seen at the prior patch location (**Figure 4D-F**). Subpleural type II hyperplasia was noted at 5 days (Supplement 7C, Figure C4). Microscopically, based on adapted data, the NHS-POx patch was degraded at 6 weeks, while in two cases, there were microscopic remnants in the fibrin patch group with associated granulomatous reaction (**Figure 5**). Macrophages with a foamy aspect were observed adjacent degrading material in NHS-POx, and also within the pleura at 6 weeks in both NHS-POx and fibrin patch groups (Supplement 7C, Figure C4). Qualitative overview of histological findings is provided in Supplement 7E.

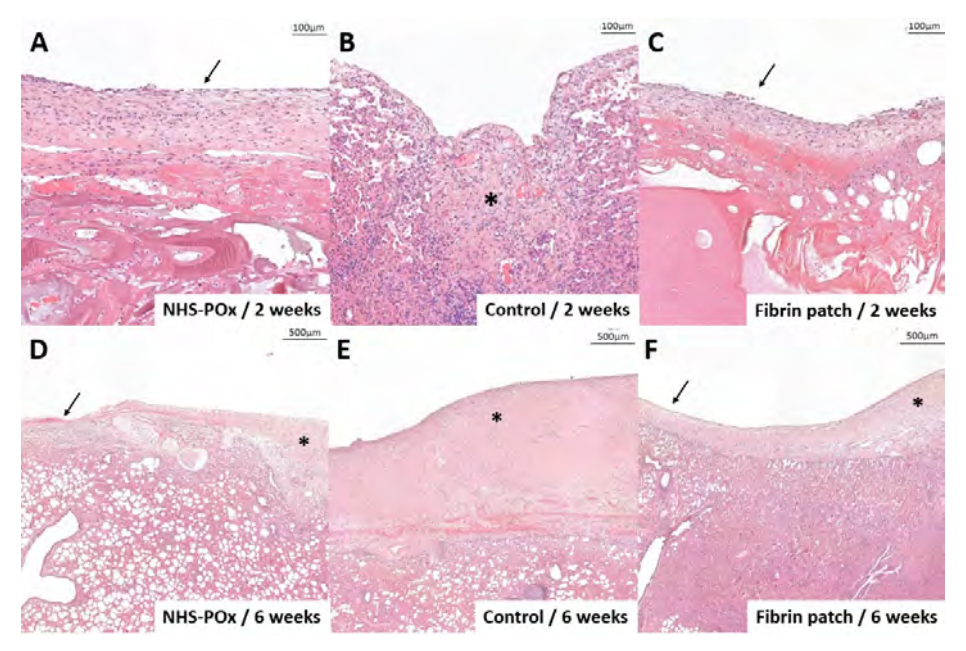


Figure 4: Aspects of healing mechanisms. A layer of fibrosis and mesothelial cells can be seen covering the patch material in A and C (indicated by arrow). B) Granulation tissue formation in a control lesion at 2 weeks. In the slides with healthy pleura overlap \mathbf{D} and \mathbf{E} , localized pleural thickening can be seen (indicated by asterisk), where the pleura gradually becomes thinner (indicated by arrow). E) Fibrous thickening of pleura in a control lesion at 6 weeks. All sections are stained with hematoxylin-eosin.

Additional polarized light microscopy in a sample of slides revealed no birefringence in the patch material or in the foamy macrophages. Birefringence was seen in a previously unidentified non-staining structure in a NHS-POx sample (adapted data) and in a giant cell in in a fibrin patch sample at 6 weeks. Second look of a sample of lymph nodes revealed foamy macrophages in a lymph node at 6 weeks, with a single birefringent needle-like structure of unknown significance (Supplement 7C, Figure C5).

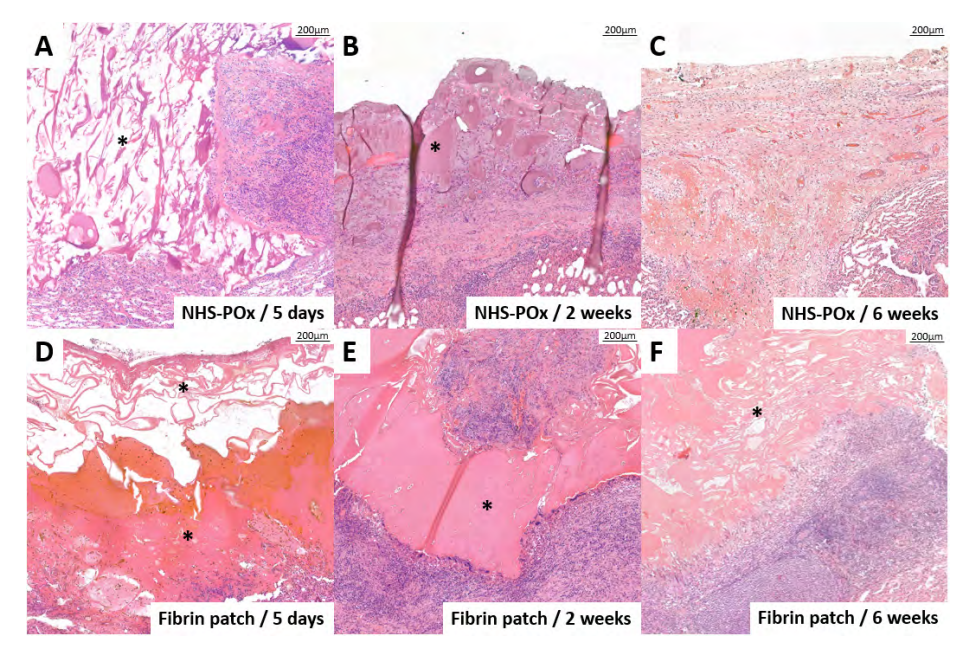


Figure 5: Histological aspect of biodegradation. NHS-POx patch at 5 days **(A)** and 2 weeks **(B)** (shown by asterisk), with no more remnant at 6 weeks **(C)**. The biomaterial is extensively infiltrated with mainly macrophages at 2 weeks **(B)**. Fibrin patch at 5 days **(D)**, 2 weeks **(E)** and 6 weeks **(F)** (shown by asterisk). A granulomatous reaction can be seen surrounding the biomaterial in **E** and **F**.

All sections are stained with hematoxylin-eosin.

Macroscopy: obduction, adhesions and migration

At obduction, pleural effusion was seen in all cases (estimated <150mL), which appeared more serosanguinous at 5 days and more serous at 14 days and 6 weeks. There were adhesions between the incision and the lung in 9/12 (75%) animals, without relation to any of the lesions (**Table 1**). In the two animals with pre-existing adhesions during surgery, there also were extensive generalized adhesions during obduction, making adhesion grading difficult (Supplement 7C, Table C5). In one animal, an encapsulated gauze that was left behind during surgery was found. This gauze was used to control bleeding from extensive adhesiolysis to mobilize the lung during the initial procedure, at a site remote from any of the lesions. Another animal at 2 weeks showed marked pleural thickening.

Adhesions up to Zühlke grade 3 were found in the NHS-POx and untreated control groups, and up to grade 2 in the fibrin patch group (**Figure 6A-D**). There were no significant differences between groups regarding adhesion

presence or severity (Supplement 7C, Table C8). Migration of a small material segment was noted in 2/4 NHS-POx and 1/4 fibrin patch cases at 5 days without additional adverse findings, but these migrations were only observed after the lung had been manipulated during obduction. Macroscopically, based on the adapted data, NHS-POx patch showed no more remnants at 6 weeks, while 3/4 (75%) fibrin patch cases showed grade 1 remnants (estimated 1-10%) (p=0.083) (Figure 2E). Complete overview of macroscopic findings is provided in Supplement 7F.

Qualitative histology: additional findings, pleural reaction and chronic granulomatous inflammation

Additional qualitative analysis (Supplement 7C, Table C4) of unaffected lung and parietal pleura biopsies revealed signs of pleural irritation in 20/28 (71.4%) of samples at 2 weeks, but only in 3/27 (11.1%) at 6 weeks. In 12/27 (44.4%) of samples at 6 weeks, pleural thickening was seen, especially in samples across prior patches/lesions (**Table 2**). Histological signs of bronchopneumonia were noted in one animal at 2 weeks, but this animal was otherwise asymptomatic. Lymph nodes were unremarkable besides signs of chronic granulomatous inflammation due to parasitic infections.

Table 2: additional analysis of pleural fibrosis and irritation on extra histology samples

	5 days	14 days	42 days
Pleural thickening			
Lung without lesion	1/4 (75%)	4/4 (100%)	4/4 (100%)
Parietal pleura ¹	0/9 (0%)	4/12 (33.3%)	1/12 (8.3%)
Across NHS-P0x	N/A	2/4 (50%)	2/4 (50%)
Across fibrin patch	N/A	3/4 (75%)	2/3 (66.7%)
Across control lesion	N/A	2/4 (50%)	3/4 (75%)
Total	1/13 (7.7%)	15/28 (53.6%)	12/27 (44.4%)
Pleural irritation ²			
Lung without lesion	2/4 (50%)	3/4 (75%)	0/4 (0%)
Parietal pleura ¹	3/9 (33.3%)	6/12 (50%)	0/12 (0%)
Across NHS-P0x	N/A	4/4 (100%)	0/4 (0%)
Across fibrin patch	N/A	4/4 (100%)	1/3 (33.3%)
Across control lesion	N/A	3/4 (75%)	2/4 (50%)
Total	5/13 (38.5%)	20/28 (71.4%)	3/27 (11.1%)

¹Apical, lateral, costodiaphragmatic recess samples.

²Based on immune cell infiltration, fibrinoid pleuritis, reactive mesothelial cells, neovascularization.

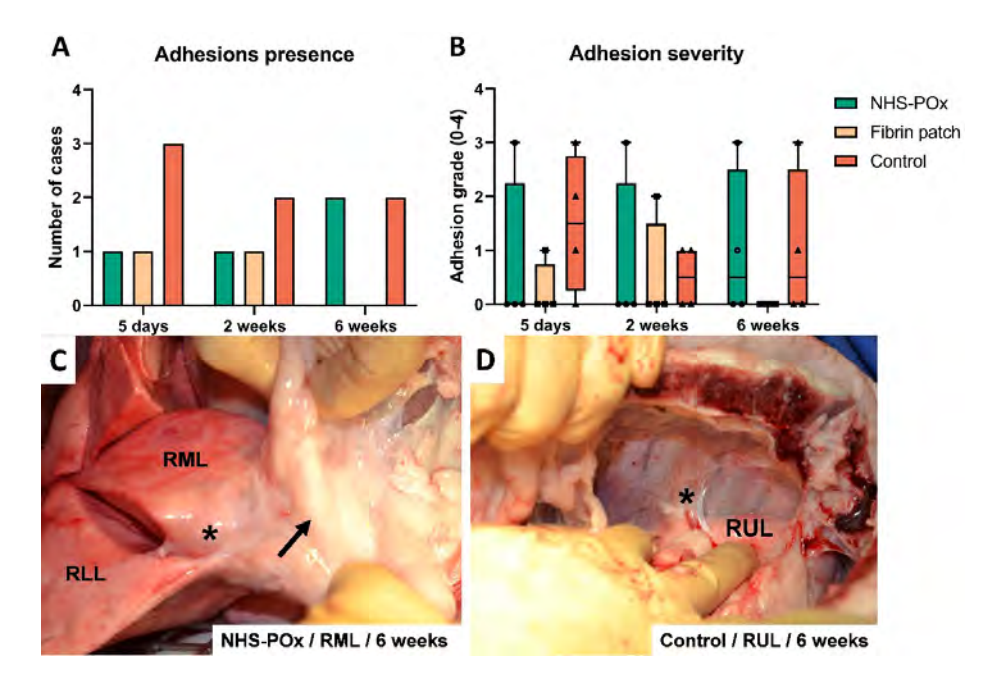


Figure 6: Between-group comparisons of adhesions directly associated with each lesion location. Adhesions due to surgical procedures (i.e. incisional) or pre-existing adhesions not included. A) Presence of adhesions. B) Severity of adhesions, measured by Zühlke classification (scale 0-4). Between-group comparisons revealed no statistically significant differences. C) Example of a dense adhesion (grade 3) of a prior NHS-POx allocated lesion on the right middle lobe (RML), showing extension to the right lower lobe (RLL, asterisk) and mediastinum (arrow). D) Example of a dense adhesion (grade 3, indicated by asterisk) associated with a control lesion that was made on the right upper lobe (RUL) during index surgery.

Original and adapted data at 6 weeks are identical.

A range of granulomatous reactions (eosinophilic, necrotizing, calcified) was seen in the lung parenchyma or lymph nodes of all animals. In 5/12 (41.7%) of animals, parasites were also found to be associated with this reaction (Supplement 7C, Figure C2-C3). Veterinary consultation revealed the most suspected causative agent to be *Muellerius capillaris*. Animals were generally asymptotic. No typical infectious symptoms were recorded, possibly related symptoms were elevated respiratory rate and low appetite in 2/12 (16.7%) (Supplement 7C, Table C3). Macroscopic infiltrates were seen in 8/12 (66.7%) of animals at obduction, and in one case right below a fibrin patch, which were histologically confirmed to be a granulomatous inflammation. Biopsies taken in two animals at index surgery also confirmed the presence of this inflammation before patch application.

There were no statistically significant differences between distribution of granulomas and parasites between animals at different time points or between the pathological samples of the groups (Supplement 7C, Figure C2, Table C9-C10). There was minimal eosinophilia associated with the biomaterial in the pleura, and this was not significantly different between groups. Minimal distance from the granuloma to pleura was not significantly different between groups (Supplement 7C, Figure C2).

Discussion

The biocompatibility and safety of the novel NHS-POx patch as a lung sealant were investigated in a long-term translational animal model up to 6 weeks. We demonstrate that complete degradation of the NHS-POx patch at 6 weeks is highly likely. Application causes an acute inflammatory and foreign body response with predominantly polymorphonuclear cells, macrophages and giant cells at 5 and 14 days. At 6 weeks inflammation was comparable between NHS-POx and fibrin patch in the original data, in the adapted data no significant residual inflammation was seen at 6 weeks for NHS-POx. Healing is observed with mesothelial coverage at 14 days and localized visceral and parietal pleural thickening at 6 weeks. Overall, these findings point towards a favorable biocompatibility profile for the novel NHS-POx patch for lung sealant use.

Comparison to previous literature

In comparison to the fibrin patch (TachoSil®), the NHS-POx patch showed favorable biodegradability, with highly likely no remaining material or significant immune response at 6 weeks. The fibrin patch is a valid control group from a translational perspective, being the most studied lung sealant clinically. (11) In our study, patch remnants were found in 2/4 (50%) of the fibrin patch group at 6 weeks (adapted data), with associated granulomatous inflammation. These findings are consistent with data from previous pre-clinical investigations, supporting the validity: the Food and Drug Administration described remnants up to 4 months, and the European Medicine Agency up to 20 weeks. (26, 27) Getman and colleagues had similar findings, applying TachoSil® to the rat lung, describing residual lymphocyte infiltrations adjacent the applied patch at 6 weeks, which resolved at 12 weeks with no more remaining patch material. (28)

Biocompatibility of NHS-POx on a gelatin carrier patch was directly compared to TachoSil® in two previous animal studies. In a rat model of liver application, no clear differences in inflammatory cells were found at 7 days. (15) In a porcine model of liver application, both patches degraded within 3-4 weeks, and the histological patterns were considered comparable, however, a comprehensive sub-analysis was not performed, examining individual cell types. (16) In our study, albeit not statistically significant, the total histological response score showed a trend towards being higher in the fibrin patch group at 2 and 6 weeks (adapted data). At least, these findings indicate that the novel NHS-POx patch does not result in a more adverse local tissue response compared to the current gold standard lung sealant.

Mechanisms involved in biodegradation and healing

The NHS-POx patch was diffusely infiltrated with immune cells, indicating replacement of the prior biomaterial with extracellular matrix material, while the visceral surface of the patch was covered with a mesothelial lining. In the biodegradation process, the amide and thioester bonds formed by NHS-esters are hydrolyzed, while the *porcine* gelatin carrier is degraded by hydrolysis, matrix metalloproteases (gelatinases, collagenases) and phagocytosis. (29-31) While the release and excretion pathways of the polyoxazoline polymers from the application site are unknown, they are renally cleared once in the bloodstream. (18)

The specific release mechanism from the application site requires further study, as macrophages with a 'foamy' aspect were identified at 6 weeks with unknown contents, raising the question whether all polymers are excreted, or whether there is a degree of local retention in macrophage phagosomes. For example, such foamy macrophages were reported in a rat study testing poly-Lactide implants, but these contained birefringent granules. (32) In our study, no significant birefringence was noted in the foamy macrophages (except a single birefringent structure in a lymph node). Because the macrophages were also present in a fibrin patch sample, the precise causal relation is unclear.

The degradation mechanisms of the fibrin patch are well understood, as its composed entirely of endogenous components. *Humane* fibrinogen and thrombin form a fibrin cloth upon wet tissue contact, with an *equine* collagen carrier as structural support. (27) These components are degraded by plasmin and collagenases, respectively. (33, 34) A previous document from the European Medicine Agency describes the degradation process as 'layer by layer by absorptive granulation tissue and conversion into a pseudo-capsule', which is similar to the observed degradation mechanism in our study. (27) A chronic inflammatory response was observed in association with the fibrin patch in our study, with a high number

of plasma cells. This could be indicative of a humoral immunity response to the xenogeneic components in the ovine species, but requires further investigation. (35)

Model validity

Ovis aries is a realistic surgical application model for biomaterials with a high translational value, due to similar anatomy, respiratory physiology and coagulation mechanisms. (36-42) However, species-specific immune system differences should be considered. Pulmonary intravascular macrophages (PIMs) are present in up to 20% of the capillary endothelium in sheep lung, while only present in humans under specific conditions, and sheep lung house less alveolar macrophages. (43, 44) PIMs are thought to have a phagocytic function of blood borne particles, and also seem to play an important role in mediation of the immune response. (44) But, the extent and impact of these cells on the current study findings is unknown.

Chronic granulomatous inflammation with associated parasites was found in the lung parenchyma and lymph nodes of the sheep in this study. Causative agents in the Netherlands include Muellerius capillaris, Protostrongylus rufescens, Protostrongylus brevispiculum, Neostrongylus linearis and Cystocaulus ocreatus. (45) These infections are generally asymptomatic and a high prevalence has been described (36.1-73%). (46, 47) Histologically, chronic (eosinophilic) granulomatous pneumonia has been described, consistent with our findings. (48-51) Ivermectin treatment was used after the first two sheep, but may be ineffective for complete eradication due to inhibited larval stages and the possibility of re-infestation, as seen in the sheep at 6 weeks. (47)

Our findings do not support the notion that the biomaterial itself is the cause of (eosinophilic) granulomatous inflammation. We confirmed histologically its presence during the index surgery, observed a limited eosinophilic response within the pleura, and noted an apparently equal distribution of granulomas across histological sections which were associated with parasites in 41.7% of animals. There is no evident pathology consistent with our findings in previous clinical and preclinical literature. Other adverse histological reactions that have been described include destructive parenchymal fibrosis, abscesses with leukocytes and debris, and nonspecific bronchopneumonia in preclinical lung sealant studies⁽⁵²⁻⁵⁴⁾. Clinical literature also documents eosinophilic reactions (like pleural effusion and eosinophilia) to fibrin glue, poly-glycolic acid, polyethylene glycol, and foreign body reactions/granulomas to previously implanted biomaterials. (55-66)

Chronic infections may skew the immune response, but influences are considered limited due to equal distribution of granulomas, and the testing of each group per animal. (67) The biomaterial immune response may be overestimated in case of granulomas proximal to the pleura, but was accounted in the grading process (Supplement 7C, Figure C3). Application of biomaterials may provide a favorable environment for infections, but no evident local increase in granulomas was seen in NHS-POx and fibrin patch samples compared to control across group, with exception of the fibrin patch sample at 5 days (Supplement 7C, Figure C2).

Limitations

The mix-up analysis to identify the contents of the remnant patch material in a sample at six weeks shows strong converging evidence based on additional staining, independent and blinded histological analysis and analysis of obduction photos that a mix-up in biopsy and labeling has occurred, accidentally labeling a fibrin patch sample as NHS-POx. Therefore, we think that adapting the data is justified as the collected converging evidence seems to indicate a near certainty probability. However, it should be acknowledged that there are no previously validated methods to distinguish the remnant material with absolute certainty.

The main limitation of this study is the small sample size, and lack of *a priori* power calculations on the primary outcomes. Therefore, the findings where no statistical differences (e.g. adhesions, adverse events) were encountered should be interpreted with caution, due to possible type II errors. Histological grading was performed using semi-quantitative scales, which may have some subjectivity (e.g. difference between minimal and moderate classifications), but was accounted for using two assessors and consensus meetings. These scales have inherent statistical limitations, being less powerful for detection of differences as compared to continuous measures. Finally, while all assessments of primary outcome measures were performed blinded, there were evident histological differences between groups and survival terms which may have biased assessment.

Because the inter-subject variability were expected to be lower than the intra-subject variability, each animal was taken as its own control to lower the total sample size required. Some inter-subject variability was observed (baseline leak capacity based on lesion location), but this is likely negligible on biocompatibility related outcome measures. A downside to this approach are cross-over effects due to whole-pleura responses. For example, signs of generalized pleural irritation were seen at 14 days, but this could also be a consequence of the surgery itself. Finally, root-cause analysis of adverse

events affecting the whole animal is difficult, but the experiment was not powered for this outcome measure.

Some limitations to macroscopic outcome measures should also be noted. Adhesion assessment of specific lesions was sometimes difficult, especially in cases of diffuse intra-thoracic adhesions (i.e. in the animals with extensive pre-existing adhesions), and the RLLd location was sometimes difficult to expose. Migration was only found in this study after lung manipulation during obduction, which may have confounded this outcome measure. Biodegradation was sometimes difficult to assess on the photos, especially at 6 weeks.

Recommendations for future research

Extensive diffuse adhesions found during obduction can be sign of a serious adverse event, but this seems due to pre-existing adhesions. However, further study is required to assess the impact of NHS-POx on adhesion formation, preferably in a study design without potential cross-over effects of different groups within the same pleural cavity. The lesions in this study exhibit intrinsic sealing, so no air leak related parameters were measured, but further study is required into the sealing capabilities of the NHS-POx patch in relation to wound healing, in order to prevent pneumothorax as a safety endpoint (e.g. in emphysematous lungs). (19) This study only primarily looked at local biocompatibility parameters, and further study with a higher sample size is required to study systemic effects and adverse events, such as impact on incidence of post-operative infections (i.e. bacteriostatic properties of the patch in a realistic environment). Also, this study did not look at the impact of local pleural thickening on the pulmonary function, but should be further investigated. Finally, further investigations are required to confirm the findings of our study, and investigations into the local immunogenic effects can be further specified by looking at influences on pro-versus anti-inflammatory cytokines and macrophages differentiation (M1/M2 subtypes). (68)

Conclusions

The novel NHS-POx patch applied to the lung shows comparable to favorable local biocompatibility properties compared to existing fibrin patch. Complete biodegradation and no significant residual tissue response at 6 weeks are highly likely. Further research is required to study the impact on aerostatic efficacy and adverse events.

References

- 1. Attaar A, Tam V, Nason KS. Risk Factors for Prolonged Air Leak After Pulmonary Resection: A Systematic Review and Meta-analysis. Ann Surg. 2020;271(5):834-44.
- 2. DeCamp MM, Blackstone EH, Naunheim KS, Krasna MJ, Wood DE, Meli YM, McKenna RJ, Jr. Patient and surgical factors influencing air leak after lung volume reduction surgery: lessons learned from the National Emphysema Treatment Trial. Ann Thorac Surg. 2006;82(1):197-206; discussion -7.
- 3. Yoo A, Ghosh SK, Danker W, Kassis E, Kalsekar I. Burden of air leak complications in thoracic surgery estimated using a national hospital billing database. Clinicoecon Outcomes Res. 2017;9:373-83.
- 4. Brunelli A, Xiume F, Al Refai M, Salati M, Marasco R, Sabbatini A. Air leaks after lobectomy increase the risk of empyema but not of cardiopulmonary complications: a case-matched analysis. Chest. 2006;130(4):1150-6.
- Liang S, Ivanovic J, Gilbert S, Maziak DE, Shamji FM, Sundaresan RS, Seely AJE. Quantifying the incidence and impact of postoperative prolonged alveolar air leak after pulmonary resection. J Thorac Cardiovasc Surg. 2013;145(4):948-54.
- Attaar A, Luketich JD, Schuchert MJ, Winger DG, Sarkaria IS, Nason KS. Prolonged Air Leak After Pulmonary Resection Increases Risk of Noncardiac Complications, Readmission, and Delayed Hospital Discharge: A Propensity Score-adjusted Analysis. Ann Surg. 2021;273(1):163-72.
- Ponholzer F, Ng C, Maier H, Lucciarini P, Öfner D, Augustin F. Risk factors, complications and costs of prolonged air leak after video-assisted thoracoscopic surgery for primary lung cancer. J Thorac Dis. 2023;15(2):866-77.
- 8. Brunelli A, Chapman K, Pompili C, Chaudhuri N, Kefaloyannis E, Milton R, et al. Ninety-day hospital costs associated with prolonged air leak following lung resection. Interact Cardiovasc Thorac Surg. 2020;31(4):507-12.
- 9. Aprile V, Bacchin D, Calabrò F, Korasidis S, Mastromarino MG, Ambrogi MC, Lucchi M. Intraoperative prevention and conservative management of postoperative prolonged air leak after lung resection: a systematic review. Journal of Thoracic Disease. 2023;15(2):878-92.
- Belda-Sanchis J, Serra-Mitjans M, Iglesias Sentis M, Rami R. Surgical sealant for preventing air leaks after pulmonary resections in patients with lung cancer. Cochrane Database Syst Rev. 2010(1):Cd003051.
- 11. Zhou J, Lyu M, Pang L, Gao Y, Ning K, Wang Z, Liu L. Efficiency and safety of TachoSil® in the treatment of postoperative air leakage following pulmonary surgery: a meta-analysis of randomized controlled trials. Jpn J Clin Oncol. 2019;49(9):862-9.
- 12. Brunelli A, Bölükbas S, Falcoz PE, Hansen H, Jimenez MF, Lardinois D, et al. Exploring consensus for the optimal sealant use to prevent air leak following lung surgery: a modified Delphi survey from The European Society of Thoracic Surgeons. Eur J Cardiothorac Surg. 2020.
- Boerman MA, Roozen E, Sánchez-Fernández MJ, Keereweer AR, Félix Lanao RP, Bender J, et al. Next Generation Hemostatic Materials Based on NHS-Ester Functionalized Poly(2oxazoline)s. Biomacromolecules. 2017;18(8):2529-38.
- Boerman MA, Van der Laan HL, Bender JCME, Hoogenboom R, Jansen JA, Leeuwenburgh SC, Van Hest JCM. Synthesis of pH- and thermoresponsive poly(2-n-propyl-2-oxazoline) based copolymers. Journal of Polymer Science Part A: Polymer Chemistry. 2016;54(11):1573-82.

- 15. Roozen EA, Warlé MC, Lomme R, Félix Lanao RP, van Goor H. New polyoxazoline loaded patches for hemostasis in experimental liver resection. J Biomed Mater Res B Appl Biomater, 2021.
- 16. Roozen E, Lomme R, Calon N, Broek R, Goor H. Efficacy of a novel polyoxazoline based hemostatic patch in liver and spleen surgery 2023.
- 17. Hermans BP, Li WWL, Roozen EA, van Dort DIM, Evers J, van der Heijden EHFM, et al. Sealing effectiveness of a novel NHS-POx based patch: experiments in a dynamic ex vivo porcine lung. Journal of Thoracic Disease. 2023;15(7):3580-92.
- 18. Boerman MA, Roozen EA, Franssen GM, Bender JCME, Hoogenboom R, Leeuwenburgh SCG, et al. Degradation and excretion of poly(2-oxazoline) based hemostatic materials. Materialia. 2020;12:100763.
- 19. Hermans BP, Li WWL, Roozen EA, van Dort DIM, Vos S, van der Heide SM, et al. Intrinsic pulmonary sealing, its mechanisms and impact on validity and translational value of lung sealant studies: a pooled analysis of animal studies. Journal of Thoracic Disease. 2023.
- 20. Ardehali A, Spotnitz WD, Hoffman RW, Olson SA, Bochicchio GV, Hermann MC, et al. Evaluation of the safety and efficacy of a new hemostatic powder using a quantitative surface bleeding severity scale. J Card Surg. 2019;34(1):50-62.
- 21. Macchiarini P, Wain J, Almy S, Dartevelle P. Experimental and clinical evaluation of a new synthetic, absorbable sealant to reduce air leaks in thoracic operations. J Thorac Cardiovasc Surg. 1999;117(4):751-8.
- 22. Rooney MB, Mehl M, Monnet E. Intercostal thoracotomy closure: transcostal sutures as a less painful alternative to circumcostal suture placement. Vet Surg. 2004;33(3):209-13.
- 23. Zühlke HV, Lorenz EM, Straub EM, Savvas V. [Pathophysiology and classification of adhesions]. Langenbecks Arch Chir Suppl II Verh Dtsch Ges Chir. 1990:1009-16.
- 24. ISO 10993-6:2016 Biological evaluation of medical devices. Part 6: Tests for local effects after implantation 2009.
- 25. Deyhimi P, Khademi H, Birang R, Akhoondzadeh M. Histological Evaluation of Wound Healing Process after Photodynamic Therapy of Rat Oral Mucosal Ulcer. J Dent (Shiraz). 2016;17(1):43-8.
- 26. Filing of Final Pre-Clinical Review of STN 125351-0 TachoSil. In: Administration FaD, editor. https://www.fda.gov/vaccines-blood-biologics/approved-blood-products/tachosil.
- 27. Scientific discussion for the approval of TachoSil. . In: Agency EM, editor. https://www.ema. europa.eu/en/medicines/human/EPAR/tachosil#ema-inpage-item-authorisation-details.
- 28. Getman V, Devyatko E, Wolner E, Aharinejad S, Mueller MR. Fleece bound sealing prevents pleural adhesions. Interact Cardiovasc Thorac Surg. 2006;5(3):243-6.
- 29. Raphael Rubin DSS. Rubin's Pathology: Clinicopathologic Foundations of Medicine. Chapter 2: Inflammation. Sixth edition ed: Wolters Kluwer; 2012.
- 30. Nam S, Mooney D. Polymeric Tissue Adhesives. Chem Rev. 2021;121 (18):11336-84.
- 31. Ullm S, Krüger A, Tondera C, Gebauer TP, Neffe AT, Lendlein A, et al. Biocompatibility and inflammatory response in vitro and in vivo to gelatin-based biomaterials with tailorable elastic properties. Biomaterials. 2014;35(37):9755-66.
- 32. De Jong WH, Eelco Bergsma J, Robinson JE, Bos RRM. Tissue response to partially in vitro predegraded poly-L-lactide implants. Biomaterials. 2005;26(14):1781-91.

- 33. Brown AC, Barker TH. Fibrin-based biomaterials: modulation of macroscopic properties through rational design at the molecular level. Acta Biomater. 2014;10(4):1502-14.
- 34. Helling AL, Tsekoura EK, Biggs M, Bayon Y, Pandit A, Zeugolis DI. In Vitro Enzymatic Degradation of Tissue Grafts and Collagen Biomaterials by Matrix Metalloproteinases: Improving the Collagenase Assay. ACS Biomaterials Science & Engineering. 2017;3(9):1922-32.
- 35. Massaro MS, Pálek R, Rosendorf J, Červenková L, Liška V, Moulisová V. Decellularized xenogeneic scaffolds in transplantation and tissue engineering: Immunogenicity versus positive cell stimulation. Mater Sci Eng C Mater Biol Appl. 2021;127:112203.
- 36. Gray ME, Meehan J, Sullivan P, Marland JRK, Greenhalgh SN, Gregson R, et al. Ovine Pulmonary Adenocarcinoma: A Unique Model to Improve Lung Cancer Research. Front Oncol. 2019;9:335.
- 37. Weisskopf M, Kron M, Giering T, Walker T, Cesarovic N. The sheep as a pre-clinical model for testing intra-aortic percutaneous mechanical circulatory support devices. Int J Artif Organs. 2021;44(10):703-10.
- 38. Zhou K, Niu S, Bianchi G, Wei X, Garimella N, Griffith BP, Wu ZJ. Biocompatibility assessment of a long-term wearable artificial pump-lung in sheep. Artif Organs. 2013;37(8):678-88.
- 39. Scheerlinck JP, Snibson KJ, Bowles VM, Sutton P. Biomedical applications of sheep models: from asthma to vaccines. Trends Biotechnol. 2008;26(5):259-66.
- 40. Hemingway A, Hemingway C. Respiration of sheep at thermoneutral temperature. Respir Physiol. 1966;1(1):30-7.
- 41. Wilhelmi MH, Tiede A, Teebken OE, Bisdas T, Haverich A, Mischke R. Ovine blood: establishment of a list of reference values relevant for blood coagulation in sheep. Asaio j. 2012;58(1):79-82.
- 42. Elvin CM, Vuocolo T, Brownlee AG, Sando L, Huson MG, Liyou NE, et al. A highly elastic tissue sealant based on photopolymerised gelatin. Biomaterials. 2010;31(32):8323-31.
- 43. Bouljihad M, Leipold HW. An ultrastructural study of pulmonary bronchiolar and alveolar epithelium in sheep. Zentralbl Veterinarmed A. 1994;41(8):573-86.
- 44. Schneberger D, Aharonson-Raz K, Singh B. Pulmonary intravascular macrophages and lung health: what are we missing? Am J Physiol Lung Cell Mol Physiol. 2012;302(6):L498-503.
- 45. Different wurm species in sheep (Dutch): Royal GD; [03-06-2023]. Available from: https://www.gddiergezondheid.nl/nl/Diergezondheid/Management/Wormen/Schapen/Algemeen-maagdarmwormen/verschillende-wormsoorten.
- 46. Hanks JE, Campbell AJD, Larsen JWA. Severity and prevalence of small lungworm infection on three South Australian farms and associations with sheep carcass characteristics. Veterinary Parasitology. 2021;296:109503.
- 47. Panuska C. Lungworms of Ruminants. Veterinary Clinics of North America: Food Animal Practice. 2006;22(3):583-93.
- 48. Beresford-Jones WP. Observations on Muellerius capillaris (Müller, 1889) Cameron, 1927: III.—Experimental Infection of Sheep*. Research in Veterinary Science. 1967;8(3):272-81.
- 49. Berrag B, Rhalem A, Sahibi H, Dorchies P, Cabaret J. Bronchoalveolar cellular responses of goats following infections with Muellerius capillaris (Protostrongylidae, Nematoda). Veterinary Immunology and Immunopathology. 1997;58(1):77-88.
- 50. Mansfield LS, Gamble HR. Alveolar mastocytosis and eosinophilia in lambs with naturally acquired nematode infections of Protostrongylus rufescens and Haemonchus contortus. Veterinary Immunology and Immunopathology. 1995;49(3):251-62.

- 51. Gulbahar MY, Davis WC, Yarim M, Guvenc T, Umur S, Kabak YB, et al. Characterization of local immune response against lungworms in naturally infected sheep. Veterinary Parasitology. 2009;160(3):272-8.
- 52. Ennker IC, Ennker J, Schoon D, Schoon HA, Rimpler M, Hetzer R. Formaldehyde-free collagen glue in experimental lung gluing. Ann Thorac Surg. 1994;57(6):1622-7.
- 53. Daniel P, Wehner DW, Morgenstern R, Neumann A, Müller W, Fritzsch G, et al. [Ultrasonic sealing of the lung parenchyma after atypical resection]. Z Exp Chir Transplant Kunstliche Organe. 1987;20(2):117-21.
- 54. Levashev Iu N, Bobkov AG, Varlamov VV, Egorov VI. [Experimental evaluation of different methods of intraoperative aerostasis in surgery of the lungs]. Grud Serdechnososudistaia Khir. 1990(8):63-6.
- 55. Kawamoto N, Okita R, Hayashi M, Okada M, Ito K, Ikeda E, Inokawa H. Suspected fibrin glueinduced acute eosinophilic pneumonia after pulmonary resection: A case report. Thorac Cancer. 2021;12(14):2126-9.
- 56. Kawamoto N, Okita R, Okada M, Ito K, Hirazawa K, Inokawa H. Fibrin glue-induced eosinophilic pleural effusion after pulmonary resection: A case report. Int J Surg Case Rep. 2021;85:106239.
- 57. Kambayashi T, Suzuki T. [Eosinophilic pleural effusion possibly induced by fibrin sealant]. Kyobu Geka. 2012;65(2):141-4.
- 58. Miyahara E, Ueda D, Kawasaki Y, Ojima Y, Kimura A, Okumichi T. Polyglycolic acid mesh for preventing post-thoracoscopic bullectomy recurrence. Surg Today. 2021;51(6):971-7.
- 59. Doğan R, Uysal S, Kumbasar U, Köksal D, Ancın B, Tuncel M. Can surgical adhesives may cause false positivity in follow-up positron emission tomography after lung cancer resection? Tuberk Toraks. 2021;69(1):59-64.
- 60. Kurian EM, Abu-Hijleh M, Lowrey TR, De Las Casas LE. Oxidized Regenerated Cellulose (Surgicel®) on Cytology/Histology. Acta Cytol. 2022;66(6):556-9.
- 61. Okazaki M, Sano Y, Mori Y, Sakao N, Yukumi S, Shiqematsu H, Izutani H. Two cases of granuloma mimicking local recurrence after pulmonary segmentectomy. J Cardiothorac Surg. 2020;15(1):7.
- 62. Suemitsu R, Tokito T, Ichiki M, Takeo S, Momosaki S, Furuya K. Complication of bovine pericardial buttress: pulmonary pseudotumor. Asian Cardiovasc Thorac Ann. 2011;19(1):64-5.
- 63. Sawada T, Watanabe Y, Oura H, Handa M. [Pulmonary staple granuloma mimicking lung cancer; report of a case]. Kyobu Geka. 2008;61(7):591-4.
- 64. Badenes D, Pijuan L, Curull V, Sánchez-Font A. A foreign body reaction to Surgicel(®) in a lymph node diagnosed by endobronchial ultrasound-guided transbronchial needle aspiration. Ann Thorac Med. 2017;12(1):55-6.
- 65. Yousem SA, Amin RM, Levy R, Baker N, Lee P. Pulmonary pathologic alterations associated with biopsy inserted hydrogel plugs. Hum Pathol. 2019;89:40-3.
- 66. Butnor KJ, Bodolan AA, Bryant BRE, Schned A. Impact of Histopathologic Changes Induced by Polyethylene Glycol Hydrogel Pleural Sealants Used During Transthoracic Biopsy on Lung Cancer Resection Specimen Staging. Am J Surg Pathol. 2020;44(4):490-4.
- 67. Ouaissi A. Regulatory Cells and Immunosuppressive Cytokines: Parasite-Derived Factors Induce Immune Polarization. Journal of Biomedicine and Biotechnology. 2007;2007:094971.
- 68. Chandorkar Y, K R, Basu B. The Foreign Body Response Demystified. ACS Biomaterials Science & Engineering. 2019;5(1):19-44.

Chapter 7 Supplemental material

Supplements $\it E/F$ are not shown in this thesis and will be published later online alongside the article.

Supplement 7A - Anesthesia, analgesia and antibiotic prophylaxis

Table A1: Anesthesia protocol in experiment two until experiment twelve

Moment	Medication	Route	Dose	Frequency
Pre-medication	Midazolam	Intra-muscular	0.7 mg/kg	Once
	Ketamine	Intra-muscular	10 mg/kg	Once
Induction	Propofol	Intra-venous	2 mg/kg	Once
	Ketamine	Intra-venous	1 mg/kg	Once
	Methadone	Intra-venous	0.2 mg/kg	Once
Multimodal	Meloxicam	Intra-muscular	0.5 mg/kg	Once during induction
anesthesia during surgery	Magnesium sulphate	Intra-venous	40 mg/kg	Once (in 20 minutes)
	Fentanyl	Trans-dermal	100 μg/h	Continuous for 72h
	Ropivacaine	Intercostal block at three levels	1.5mg/kg	Once right after thoracotomy
Maintenance	Remifentanil	Intra-venous	0.06 mg/kg/h ¹	Continuous during surgery
	Propofol	Intra-venous	Titrated ¹	Continuous during surgery
	Ketamine	Intra-venous	0.2 mg/kg/h	Continuous during surgery
	Isoflurane	Inhalation	Titrated ¹	Continuous during surgery ²
Post-operative	Fentanyl	Trans-dermal	100 μg/h	Continuous for 72h, repeat if required
	Ketamine	Intra-muscular	0.5 mg/kg	In case of discomfort: max 2x/day.
	Meloxicam	Oral	0.4 mg/kg	1x/day for five days, phase out if possible
Antibiotic	Amoxicillin	Intra-venous	10 mg/kg	Once before incision
prophylaxis	Ampicillin	Intra-muscular	15 mg/kg	Right after surgery and again after 48h

¹Doses were titrated to maintain the mean arterial pressure between 50-100mmHg. Noradrenaline is additionally titrated in case of hypotension.

²Inhalation anesthesia is switched of when a lesion is made on the lung.

Table A2: Anesthesia protocol in the first experiment

Moment	Medication	Route	Dose	Frequency
Pre-medication	Midazolam	Intra-muscular	0.7 mg/kg	Once
	Ketamine	Intra-muscular	10 mg/kg	Once
Induction	Propofol	Intra-venous	2 mg/kg	Once
	Remifentanil	Intra-venous	0.01 mg/kg	Once
Multimodal anesthesia	Meloxicam	Intra-muscular	0.5 mg/kg	Once during induction
during surgery	Lidocaine/ bupivacaine 20/5mg/ml	Intercostal block at three levels	0.4 ml/kg	Once right after thoracotomy
Maintenance	Remifentanil	Intra-venous	0.06 mg/kg/h ¹	Continuous during surgery
	Propofol	Intra-venous	Titrated ¹	Continuous during surgery
	Isoflurane	Inhalation	Titrated ¹	Continuous during surgery ²
Post-operative	Buprenorphine	Intra-muscular	0.05 mg/kg	Every 12h for five doses total
	Meloxicam	Oral	0.4 mg/kg	1x/day for five days, phase out if possible
Antibiotic prophylaxis	Amoxicillin	Intra-venous	10 mg/kg	Once before incision
	Ampicillin	Intra-muscular	15 mg/kg	Right after surgery and again after 48h

¹Doses were titrated to maintain the mean arterial pressure between 50-100mmHg. Noradrenaline is additionally titrated in case of hypotension.

 $^{^{2}}$ Inhalation anesthesia is switched of when a lesion is made on the lung.

Supplement 7B - Histological methods

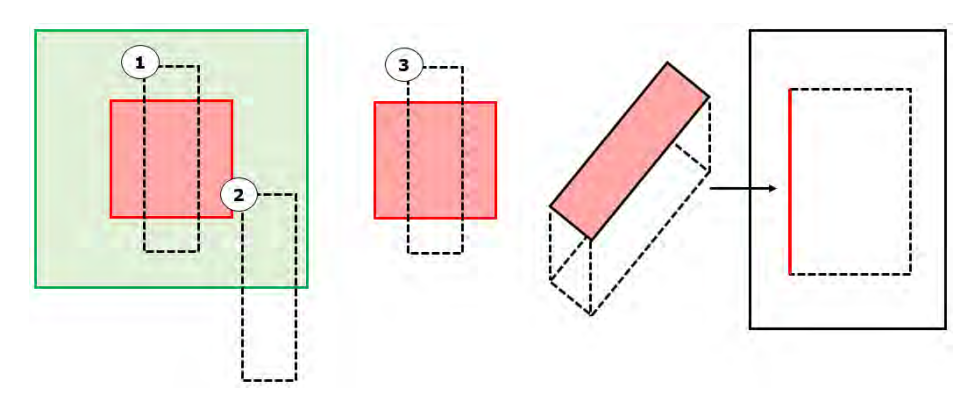


Figure B1: Standardized methodology for cutting histological samples. *Left image:* From the samples with a lung sealant applied, two standardized samples are taken: 1) Through the middle of the lesion and 2) With half of the sample comprising healthy, uncovered pleura. *Middle image:* From the negative control samples, a single sample is taken: 3) Straight through the lesion. *Right image:* All samples are embedded with the pleural side to one direction.

Green = patch; red = lesion.

Table B1: Scoring system to asses cellular and biomaterial response, based on ISO 10993-6:2016 with adjustments made for a semi-quantitative analysis

Cell type/response		Score							
	0	1	2	3	4				
Polymorphonuclear cells	Absent	Rare	Minimal	Moderate infiltrate	Packed infiltrate				
Lymphocytes	Absent	Rare	Minimal	Moderate infiltrate	Packed infiltrate				
Plasma cells	Absent	Rare	Minimal	Moderate infiltrate	Packed infiltrate				
Macrophages	Absent	Rare	Minimal	Moderate infiltrate	Packed infiltrate				
Giant cells	Absent	Rare	Minimal	Moderate infiltrate	Packed infiltrate				
Necrosis	None	Minimal	Mild	Moderate	Severe				
Biomaterial	Score		e						
response	0	1	2	3	4				
Neovascularization	None	Minimal capillary proliferation	Groups of capillaries with supporting fibroblastic structures	Broad band of capillaries with supporting fibroblastic structures	Extensive band of capillaries with supporting fibroblastic structures				
Fibrosis	None	Narrow band	Moderately thick band	Thick band	Extensive band				
Fatty infiltrate	None	Minimal fat associated with fibrosis	Several layers of fat and fibrosis	Elongated and broad accumulation of fat cells	Extensive fat completely surrounding implant				

Supplement 7C - Additional tables, figures, analysis

Additional tables

Table C1: Lesion characteristics at baseline

	NHS-POx (n=12)	Fibrin patch (n=12)	Control (n=12)	P-value
Location (n, %)				n/a
RML	3 (25%)	4 (33%)	4 (33%)	
RLLv	5 (42%)	3 (25%)	3 (25%)	
RLLd	4 (33%)	5 (42%)	3 (25%)	
Other	0 (0%)	0 (0%)	2 (17%)	
SBSS grade (n, %)				0.17
Minimal	1 (8%)	0 (%)	2 (17%)	
Mild	9 (75%)	12 (100%)	10 (83%)	
Moderate	2 (17%)	0 (0%)	0 (0%)	
Hemostasis time (min.)	2,5 (2-8)	2 (2-5)	2 (2-4)	0.17
Macchiarini scale (n, %)				0.97
0	7 (58%)	7 (58%)	6 (50%)	
I	0 (0%)	1 (8%)	2 (17%)	
II	2 (17%)	1 (8%)	2 (17%)	
III	3 (25%)	3 (25%)	2 (17%)	
MLP				
Measured (n, %)	5 (42%)	4 (33%)	5 (42%)	0.91
Value (cmH2O)	8 (6-22)	11 (5-22)	14 (7-17)	n/a

RML = right middle lobe, RLLv = right lower lobe ventral, RLLd = right lower lobe dorsal, SBSS = bleeding scale, MLP = minimal leakage pressure

Data presented as median ± range.

Statistical testing performed with Friedman's test or Cochran's Q test. Not performed on lesion location (equal assignment in randomized allocation) and MLP value (Friedman's test not possible because MLP could not be measured on all lesions per animal).

Table C2: Leakage capacity based on lesion location

	MLP measured ¹	P-Value
RML (n, %)	10/11 (91%)	<0.001
RLLv (n, %)	4/11 (36%)	
RLLd (n, %)	0 /12(0%)	
Other (n, %)	0/2 (0%)	

 $^{^1 \}text{MLP}$ can only be measured in case the lesion shows leakage at normal ventilation pressures. MLP = minimal leakage pressure, RML = right middle lobe, RLLv = right lower lobe ventral, RLLd = right lower lobe dorsal.

Statistical testing with Fischer's Exact test.

Table C3: Description of adverse events and causality to implanted patches

	Adverse event	Causality	Explanation
5 days (n=4)	Groin	Unrelated	Caused by arterial line placement
	hematoma (n=1)	Possible Possible	Parasitic pneumonia, might be exacerbated by patch(es)
	Elevated respiratory rate (n=1)	1 0331010	Unknown cause, differential diagnosis: opioids, surgical trauma, anesthetics, systemic inflammation effects of patches, parasitic
	Low appetite (n=1)		infection
14 days	Incisional	Unrelated	Surgical wound complication
(n=4)	seroma (n=2) Thickened udder (n=1)	Unrelated	Possibly mastitis
42 days (n=4)	Encapsulated intrathoracic gauze, asymptomatic (n=1)	Unrelated	Gauze left behind during index surgery

Table C4: Quantitative synthesis of qualitative histological findings on additional histological samples

Term	Sample location	N	Qualitative finding(s)
5 days	Lung biopsy without lesion	4	Thickening / fibrosis of pleura (n=1, 25%) Irritated pleura² (n=2, 50%) Granuloma (n=3, 75%)
	Lymph node ¹	8	Granuloma (n=3, 37.5%) Parasites associated with granuloma (n=1, 12.5%)
	Parietal pleura biopsy ³	9	Irritated pleura ² (n=3, 33.3%)
	Infiltrate (obduction)	3	Thickening / fibrosis of pleura (n=1, 33%) Irritated pleura² (n=1, 33%) Granuloma (n=2, 67%)
	Extra patch biopsy	1	NHS-POx patch with underlying granulation tissu and fibrinous exudate (n=1, 100%)
14 days	Lung biopsy without lesion	4	Thickening / fibrosis of pleura (n=4, 100%) Irritated pleura ² (n=3, 75%) Granuloma (n=1, 25%) Bronchopneumonia (n=1, 25%)
	Lymph node ¹	3	Granuloma (n=2, 67%)
	Parietal pleura biopsy³	24	Thickening / fibrosis of pleura (n=11, 45.8%) Irritated pleura² (n=17, 70.8%)4
	Infiltrate (obduction)	5	Thickening / fibrosis of pleura (n=5, 100%) Irritated pleura ² (n=5, 100%) Granuloma (n=2, 40%) Parasites associated with granuloma (n=1, 20%)
	Extra patch biopsy	1	NHS-POx patch with lymphohistiocytic reaction. Presence of necrotic fatty and striated muscle tissue, likely originating from parietal pleura (n=1
42 days	Lung biopsy without lesion	4	Thickening / fibrosis of pleura (n=4, 100%) Granuloma (n=2, 50%) Parasites associated with granuloma (n=1, 25%)
	Lymph node ¹	8	Granuloma (n=4, 50%) Parasites associated with granuloma (n=2, 25%)
	Parietal pleura biopsy³	23	Thickening / fibrosis of pleura (n=8, 34.8%) ⁴ Irritated pleura ² (n=3, 13%)
	Infiltrate (obduction)	9	Thickening / fibrosis of pleura (n=3, 33%) Granuloma (n=8, 89%). One sample was not a granuloma, but necrotic / bloody tissue with macrophages Parasites associated with granuloma (n=2, 22%)
	Infiltrate (index surgery)	2	Granuloma (n=2, 100%)

¹Relevant nodes of 2/4/10/11R. ²Based on immune cell infiltration, fibrinoid pleuritis, reactive mesothelial cells, neovascularization. ³Apical, lateral, costodiaphragmatic recess, across NHS-POx, fibrin patch and control lesion samples. ⁴In two parietal pleura samples (n=1 at 14 and n=1 at 42 days), the inflammatory response was also noted in the intercostal muscles.

Tables C5: Description of minor deviations from protocol

Term	Pre-operative symptom
5 days (n=4)	Mastitis (n=1) Paw infection (n=1)
14 days (n=4)	Swelling of paw (n=1) and parasternal (n=1)
42 days (n=4)	Swelling mammary glands (n=1) and parasternal (n=1) $$
Term	Deviation (index procedure)
5 days (n=4)	No ivermectin prophylaxis (n=2) Increased blood loss from pulmonary ligament laceration (n=1) Pre-existing adhesions (grade 2-3), torn upper lobe which was sutured, bone wax on rib fracture (E4, n=1)
14 days (n=4)	N/A
42 days (n=4)	Pre-existing adhesions, torn middle lobe which was sutured, re-thoracotomy before drain removal for suspected tension pneumothorax (E9, n=1) Biopsy of infiltrate during index surgery (n=2) Delayed anesthesia recovery (n=1)
Group	Deviation (lesion/group)
NHS-POX (n=12)	Ventilator on during lesion creation (n=1) Imprecise lesions due to difficult exposure (n=1) Ventilation on during first seconds of application (n=1)
Fibrin patch (n=12)	Ventilator resumed early during application (n=5) Bubble under patch after application (n=1) Extra pressure applied (n=1) New patch applied after inadequate placement (n=2)
Negative control (n=12)	Aberrant MLP measurement (n=1) Right middle lobe not usable due to laceration, placed on right upper lobe (n=1) Accidental aberrant lesion location (right middle lobe instead of right lower lobe ventral) due to complicated procedure (n=1)
Term	Deviation (obduction)
5 days (n=4)	Mechanical sample manipulation due to extensive bleeding during obduction (n=1) Difficult obduction due to severe adhesions, also present at index surgery (n=1)
14 days (n=4)	N/A
42 days (n=4)	Difficult obduction due to severe adhesions, also present at index surgery (n=1) Serosanguinous effusion possibly caused by bleeding during obduction (n=1)

Additional figures

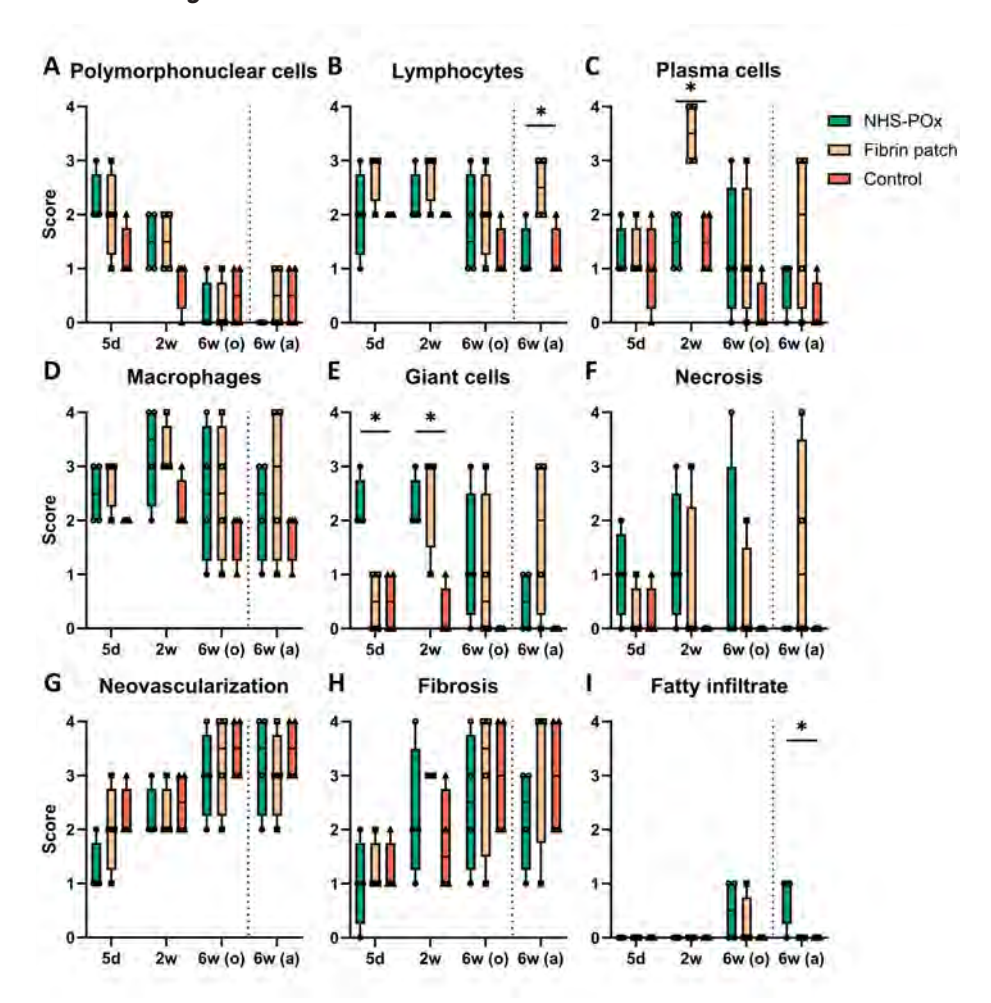


Figure C1: Between-group sub-analysis of histological parameters at different timepoints based on central histological sections.

All items are scored on a semi-quantitative scale 0-4. In or directly adjacent to the pleura, cellular response is scored, based on polymorphonuclear cells (A), lymphocytes (B), plasma cells (C), macrophages (D), giant cells (E) and necrosis (F), and biomaterial response is scored based on neovascularization (G), fibrosis (H), and fatty infiltrate (I).

Statistical testing performed with Friedman's test. *p<0.05. d = day; w = week; o = original data; a = adapted data.

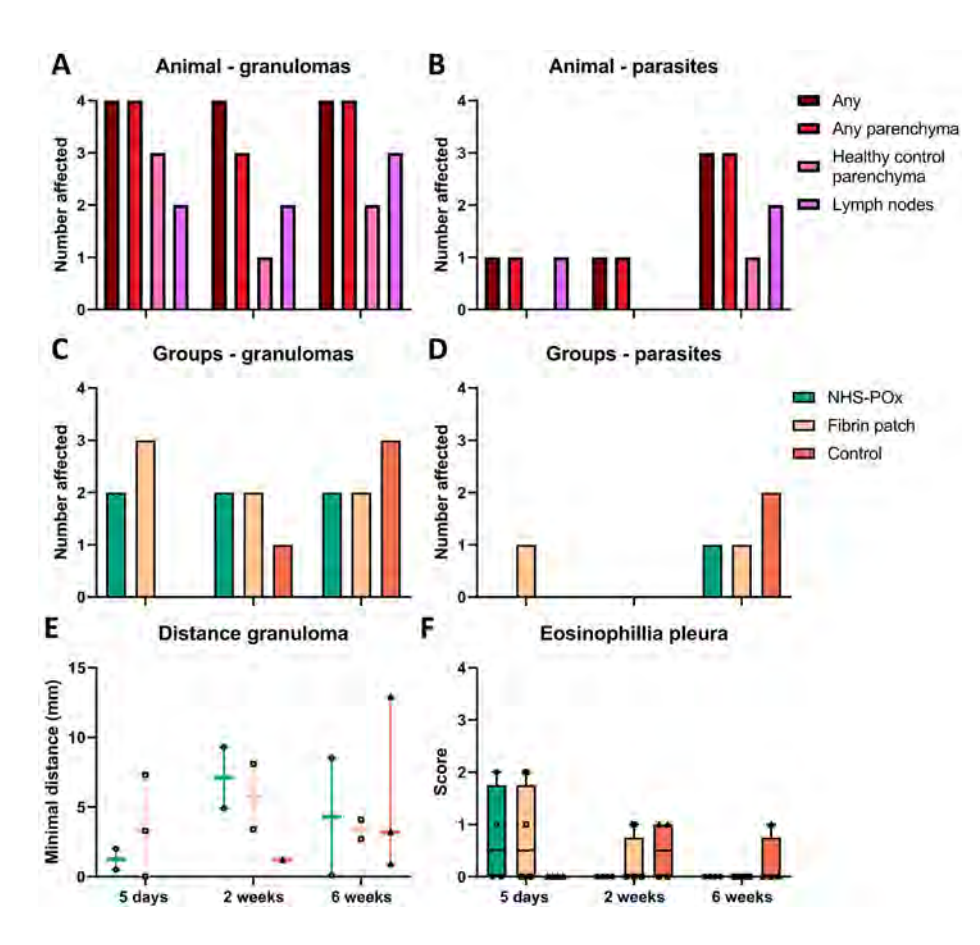


Figure C2: Distribution of chronic granulomatous inflammation and parasitic infestation.

A) Number of animals with presence of (eosinophilic) granulomas per survival term based on different histological sections (any section, any lung parenchyma section, any healthy control parenchyma section, any lymph node section). B) Number of animals also affected by parasites associated with this granulomatous inflammation in A. C) Distribution of (eosinophilic) granulomatous inflammation in central slides of the lesion samples. D) Number of central slides that also show parasites associated with granulomatous inflammation. E) Minimal distance from granuloma to pleural interface in central slides. In case of close proximity to pleura, the immune response of the granuloma is not counted towards the histological scoring of the slide (see Figure C3). F) Eosinophilia within the pleural interface. Original and adapted data at 42 days are identical.

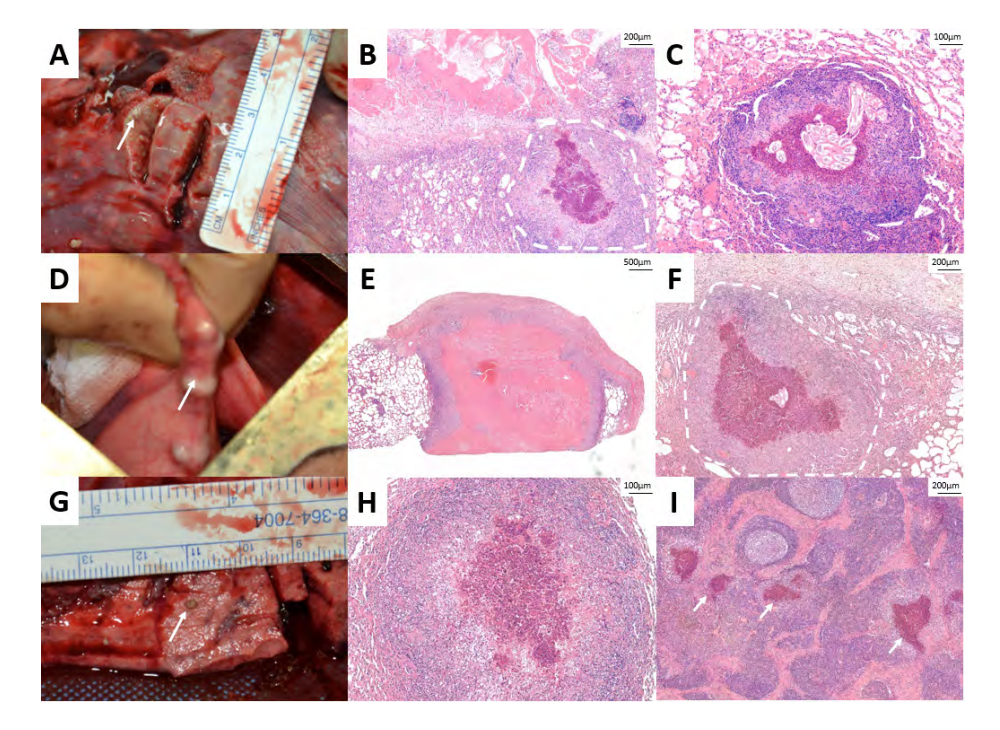


Figure C3: Macro- and microscopic aspects of infiltrates, granulomas and parasitic infestations.

A) Macroscopic infiltrates below fibrin patch sample at 5 days. B) Aspect of infiltrate of A on histology, showing an eosinophilic granuloma with close relation to the pleura. The immune response of this granuloma, encircled by the white dotted line, is not counted towards the inflammatory response of the sample. C) Eosinophilic granuloma with associated parasites.

D) Aspect of macroscopic infiltrates during surgery. E) Aspect of necrotizing granuloma (biopsy of D). F) Aspect of eosinophilic granuloma close to pleural surface. Immune response in white dotted area is not counted towards the inflammatory response of the sample. G) Aspect of macroscopic infiltrate found during lung sectioning, confirmed to be an eosinophilic granuloma in H. I) Aspect of eosinophilic granulomas (arrows) in lymph node.

All samples are stained with hematoxylin-eosin.

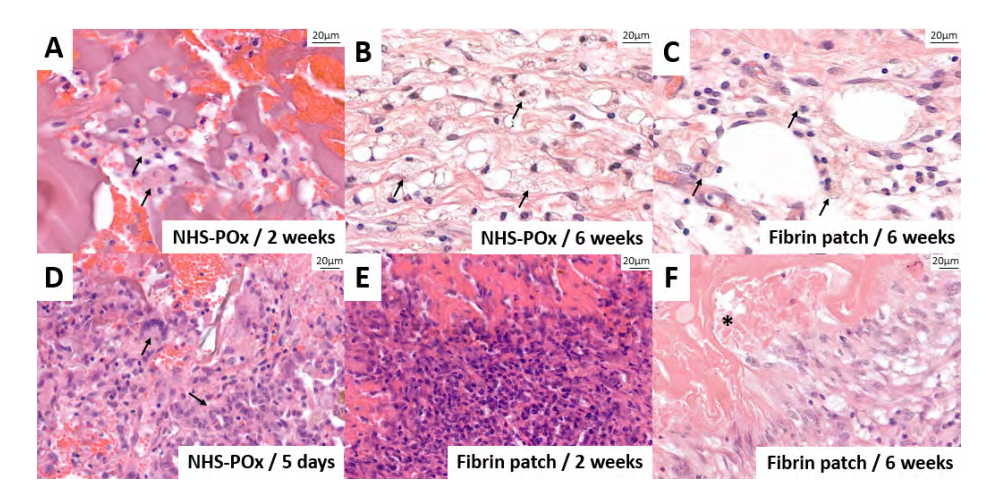


Figure C4: Detailed aspects of histological findings.

A) Aspect of several foamy macrophages associated with NHS-POx remnant material at 2 weeks (arrows). B) Aspect of foamy macrophages (arrows) and fatty tissue in the pleural scar at 6 weeks in the NHS-POx patch group, no associated material remnants. C) Aspect foamy macrophages in a fibrin patch sample at 6 weeks. D) Aspect of horseshoe shaped giant cell (top arrow) and type II pneumocyte proliferation (lower arrow), as seen just below an NHS-POx sample at 5 days. E) Aspect of adaptive immune response with lymphocytes and plasma cells to a fibrin patch sample at 2 weeks. F) Aspect of granulomatous reaction with necrosis to fibrin patch remnant (asterisk) at 6 weeks.

All samples are stained with hematoxylin-eosin.

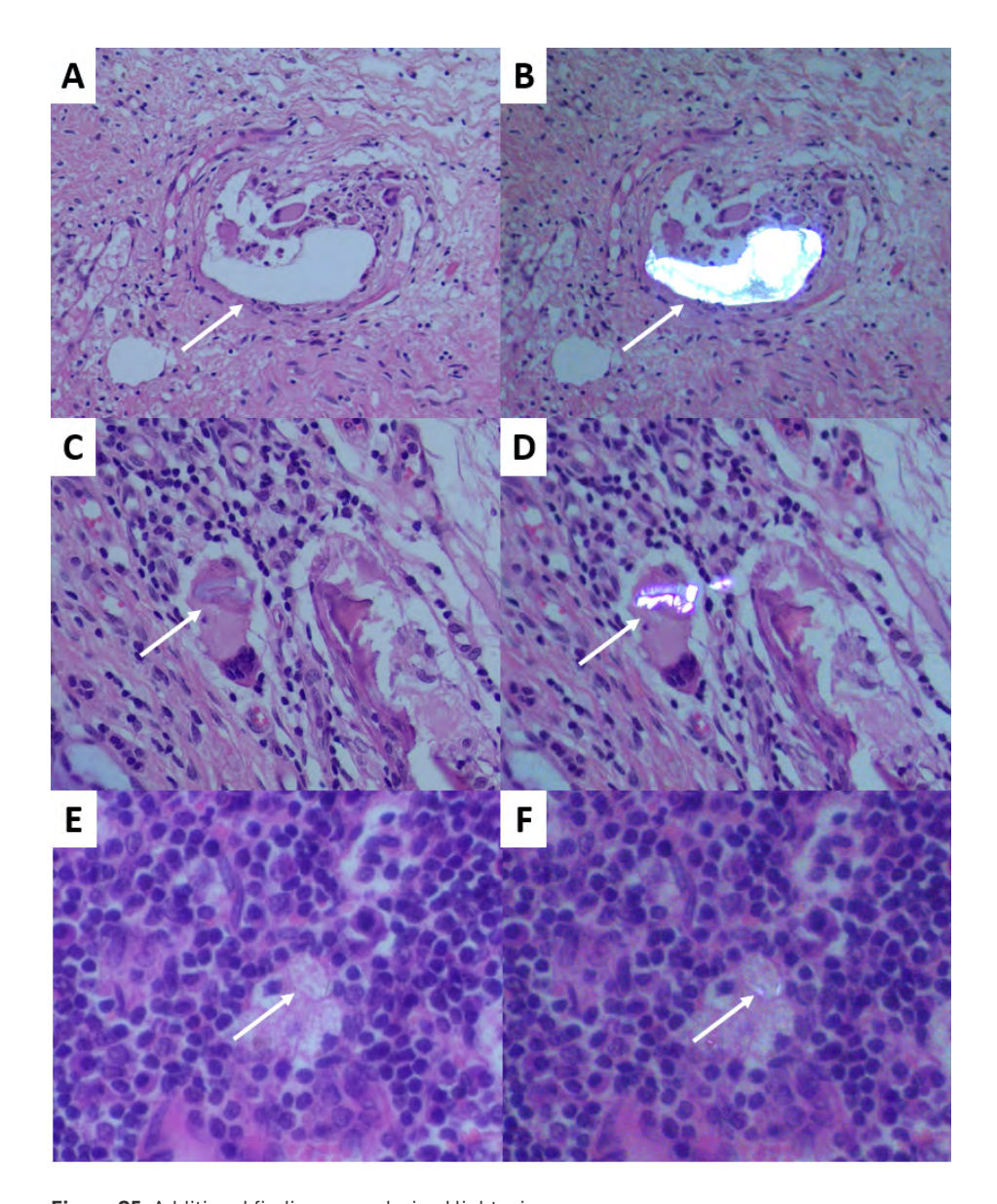


Figure C5: Additional findings on polarized light microscopy.

A) NHS-POx sample at 6 weeks, demonstrating a foreign-body structure with associated giant cells, not clearly visible in the hematoxylin and eosin staining, but showing evident birefringence in (**B**) (after mix-up correction). **C)** Fibrin patch sample at 6 weeks, demonstrating a giant cell containing birefringent foreign body material (**D**). **E)** Lymph node at 6 weeks that demonstrates a needle-like birefringent structure in a foamy macrophage (**F**).

Statistical analysis

Table C6: Within-group comparisons based on central versus pleural overlap slides on main histological outcome measures

		NHS-PO	x		Fibrin patch			
	5d	14d	42d (o)	42d (a)	5d	14d	42d (o)	42d (a)
Polymorphonuclear cells	0.157	0.083	0.317	0.317	0.655	>0.99	0.102	0.102
Lymphocytes	0.564	>0.99	0.157	0.157	0.102	0.317	0.317	0.317
Plasma cells	>0.99	>0.99	0.317	0.317	0.317	0.157	0.180	0.180
Macrophages	0.564	0.157	0.317	>0.99	0.414	0.317	>0.99	0.655
Giant cells	0.414	0.414	0.564	>0.99	0.655	0.317	>0.99	0.317
Necrosis	0.102	0.180	0.317	>0.99	0.317	0.564	0.317	0.157
Neovascularization	>0.99	0.157	0.157	0.564	0.102	0.157	>0.99	0.317
Fibrosis	>0.99	0.180	0.276	0.157	0.317	0.157	0.655	>0.99
Fatty infiltrate	>0.99	>0.99	0.157	0.083	>0.99	>0.99	>0.99	0.317
Cell response	0.197	0.063	0.414	0.414	0.461	>0.99	0.581	0.581
Biomaterial response	>0.99	0.180	0.461	0.581	0.102	>0.99	0.655	0.655
Total response	0.461	0.276	0.414	0.593	0.285	0.655	0.854	0.705
Chronic inflammation (plasma cells + lymphocytes	0.564	>0.99	0.102	0.180	0.102	0.564	0.180	0.180
Phagocytosis (macrophages + giant cells)	0.414	0.102	>0.99	>0.99	0.785	0.180	>0.99	0.414
Neovascularization + fibrosis	>0.99	0.180	0.276	0.276	0.102	>0.99	>0.99	>0.99
Healing score	0.564	0.317	>0.99	>0.99	0.317	>0.99	>0.99	0.317

P-values shown. d = day; w = week; o = original data; a = adapted data.

Cell response = polymorphonuclear cells + lymphocytes + plasma cells + macrophages + giant cells + necrosis. Biomaterial response = neovascularization + fibrosis + fatty infiltrate. Total response = cell response + biomaterial response.

Table C7: Between-group comparisons based on central slides of main histological outcomes

	5d	14d	42d (o)	42d (a)
Polymorphonuclear cells	0.223	0.232	0.717	0.264
Lymphocytes	0.105	0.097	0.368	0.050
Plasma cells	0.779	0.032	0.368	0.368
Macrophages	0.097	0.178	0.717	0.717
Giant cells	0.032	0.038	0.174	0.174
Necrosis	0.232	0.202	0.607	0.135
Neovascularization	0.150	0.368	0.807	0.807
Fibrosis	0.905	0.223	0.936	0.627
Fatty infiltrate	>0.99	>0.99	0.368	0.050
Cell response	0.018	0.038	0.257	0.223
Biomaterial response	0.424	0.420	0.936	0.936
Total response	0.368	0.022	0.607	0.526
Chronic inflammation (plasma cells + lymphocytes	0.116	0.032	0.150	0.082
Phagocytosis (macrophages + giant cells)	0.039	0.050	0.319	0.424
Neovascularization + fibrosis	0.424	0.420	0.936	0.936
Healing score	0.223	0.905	0.368	0.368
Microscopic biodegradation	0.317	0.141	0.655	0.180

P-values shown. Statistically significant values (p<0.05) are shown in bold. d=day; w=week; o=original data; a=adapted data.

Cell response = polymorphonuclear cells + lymphocytes + plasma cells + macrophages + giant cells + necrosis. Biomaterial response = neovascularization + fibrosis + fatty infiltrate. Total response = cell response + biomaterial response.

Giant cells at 5 days	P-value	Total response at 14 days	P-value	Chronic at 14 days	P-value
NHS-POx - Fibrin patch	0.034	NHS-POx - Fibrin patch	0.289	NHS-P0x - Fibrin patch	0.034
NHS-Pox - Control	0.034	NHS-Pox - Control	0.112	NHS-Pox - Control	>0.99
Control - Fibrin patch	>0.99	Control - Fibrin patch	0.008	Control - Fibrin patch	0.034
Cell response at 5 days		Lymphocytes at 42 days		Phago at 5 days	
NHS-POx - Fibrin patch	0.157	NHS-POx - Fibrin patch	0.112	NHS-POx - Fibrin patch	0.077
NHS-Pox - Control	0.005	NHS-Pox - Control	>0.99	NHS-Pox - Control	0.013
Control - Fibrin patch	0.157	Control - Fibrin patch	0.112	Control – Fibrin patch	0.480
Giant cells at 14 days		Fatty infiltrate at 42 days		Phago at 14 days	
NHS-POx - Fibrin patch	0.724	NHS-POx - Fibrin patch	0.112	NHS-P0x - Fibrin patch	>0.99
NHS-Pox - Control	0.052	NHS-Pox - Control	0.112	NHS-Pox - Control	0.034
Control - Fibrin patch	0.022	Control - Fibrin patch	>0.99	Control - Fibrin patch	0.034
Cell response at 14 days		Plasma cells at 14 days			
NHS-POx - Fibrin patch	0.724	NHS-POx - Fibrin patch	0.034		
NHS-Pox - Control	0.052	NHS-Pox - Control	>0.99		
Control - Fibrin patch	0.022	Control - Fibrin patch	0.034		

Cell response = polymorphonuclear cells + lymphocytes + plasma cells + macrophages + giant cells + necrosis. Biomaterial response = neovascularization + fibrosis + fatty infiltrate. Total response = cell response + biomaterial response.

Table C8: Between group comparisons based on macroscopic findings

	5d	14d	42d (o)	42d (a)
Adhesion presence	0.264	0.368	0.264	0.264
Adhesion severity	0.264	0.867	0.264	0.264
Macroscopic biodegradation	>0.99	0.180	0.564	0.083

P-values shown. d = day; w = week; o = original data; a = adapted data.

Table C9: Between animal comparisons of chronic granulomatous infections and parasitic infestations

	Granuloma	Parasites
Any section	n/a	0.455
Any parenchyma	>0.99	0.455
Healthy parenchyma	0.766	>0.99
Lymph node	>0.99	0.709

P-values shown.

Table C10: Between group comparisons of chronic granulomatous infections and parasitic infestations

	5d	14d	42d (o)	42d (a)
Granuloma	0.097	0.607	0.607	0.607
Parasites	0.368	n/a	0.717	0.717
Distance (granuloma - pleura)	0.655	0.368	0.368	0.368
Eosinophilia	0.135	0.223	0.368	0.368

P-values shown. d = day; w = week; o = original data; a = adapted data.

Supplement 7D - Adjudication report

Background

There is a suspicion that two patch groups have been mixed-up during biopsy in experiment 9 (6 weeks survival term) of the biocompatibility study of a novel lung sealant and consequently received the wrong naming on the cassettes.

Experiment design:

- Four sheep at each survival term: 5 days, 2 weeks and 6 weeks.
- Three groups per sheep: GATT-Patch (G), TachoSil (T) and untreated control (C).

Initial assessment based on available data

Findings

- Slides that are named E9-G1 and E9-G2 show an aspect of remaining 1. fibrinoid patch material that does not correspond to the remaining patch material in other GATT-Patch slides on 6 weeks. See evidence #1.
- 2. The aspect of this remaining patch material shows more resemblance to another sample of the TachoSil group at 6 weeks: E11-T1 and E11-T2. See evidence #2.
- 3. Other slices of the GATT-Patch group show no more remaining patch material at 6 weeks. At two weeks, the GATT-Patch looks distinctly different on histology compared to the sections E9-G1/2 and E11-T1/2. See evidence #3.
- Analysis of the cassettes and slices has shown that a mix-up could not have occurred in the naming process.
- In experiment 9, according to the forms and confirmed on the implantation 5. photos: TachoSil was applied to the right lower lobe, ventral part (diaphragmatic). See evidence #4.
- 6. GATT-Patch was applied to the right lower lobe, dorsal part. In the photo we can see the implantation process during which the lung is lifted using two gauzes in clamps. See evidence #5.
- 7. In experiment 9, pictures were marked with a paper that denoted T (for TachoSil) or G (for GATT-Patch).
- In the pictures at obduction, the G-form is put next to a scar on the right 8. lower lobe, ventral segment. See evidence #6.
- 9. It is not as clear from the photos what the location is, but the T-form is evidently not the same scar as seen in the ventral segment. See evidence #7.
- 10. The control lesion C-form is put next to a lesion on the right upper lobe. See evidence #8.

Reasoning / deduction

- 1. Based on findings 1-3, the question arises whether the GATT-Patch and TachoSil samples have been mixed up in E9.
- 2. Based on finding 4, if there is a mix-up, this must have occurred during the obduction, putting a tissue sample in the wrong cassette. In experiment 9 the sacrifice term was 6 weeks, and therefore, both patches are not macroscopically distinguishable anymore, making a mix-up of biopsies in the named cassettes possible. The only way to correctly identify lesions, is to take a biopsy of the right location on the lobe, as has been noted in the forms during index surgery.
- 3. Based on findings 5-10, we can synthesize that:
 - a. The NHS-POx patch was applied to the right lower lobe (dorsal segment).
 - b. At obduction the G-form (for NHS-POx) is put next to the right lower lobe (ventral segment).
 - c. The fibrin patch is applied to the right lower lobe (ventral segment) during index surgery.
 - d. The C-form is put next to a lesion on the right upper lobe, which is consistent with the location described on the forms of the original implantation surgery.
- 4. Therefore, based on the converging evidence of the histological aspects (finding 1-2) and the mix-up of forms at obduction (finding 5-10), we can deduce that a mix up has likely occurred while samples the tissues for histology at obduction between the NHS-POx samples (E9-G1/G2) and fibrin patch samples (E9-T1/T2) but not the control samples (E9-C3).

Additional independent analysis to support the suspicion

Method:

- Additional staining was obtained using 'Elastine volgens Masson' (EvM).
- As additional analysis, a blinded grouping task has been performed of various sections of patch material based on Hemotoxylin-Eosin (HE) and EvM staining by an independent pathologist, using baseline example slides of patch material groups.

Findings

• EvM staining also indicates that the patch remnant of E9-G1/G2 shows more resemblance to TachoSil than GATT-Patch. See evidence #9.

• The findings of the independent analysis also support the notion that the remannt material in E9-G1/G2 is TachoSil instead of GATT-Patch. See supplemental evidence.

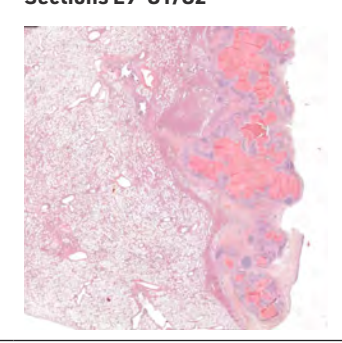
Conclusion

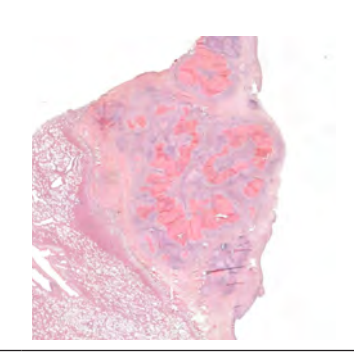
There is strong converging evidence based on macroscopic images, notes taken during the experiment and independent and blinded histological analysis (based on protocolar and additional staining) that the samples E9-G1/G2 and E9-T1/T2 have been mixed up during biopsy.

Evidence

Evidence

Sections E9-G1/G2





2 Sections E11-T1/T2







4 Form E9 / TachoSil implantation





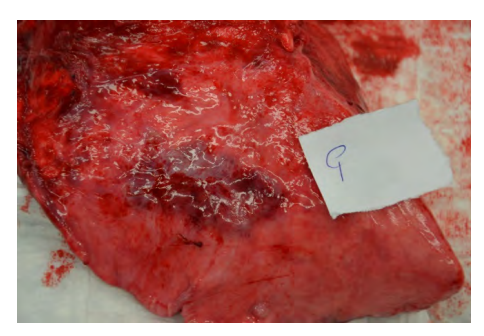
5 Form E9 / GATT-Patch implantation photo



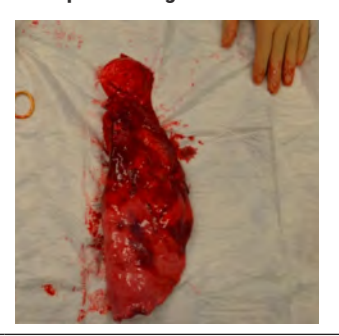


6 E9 aspect during obduction / ventral segment





E9 aspect during obduction / dorsal segment

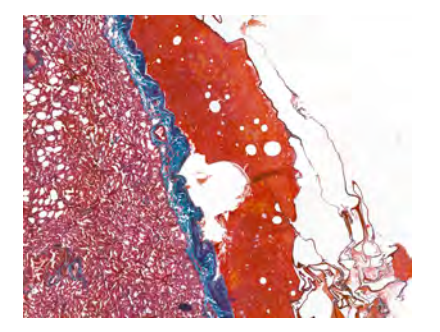




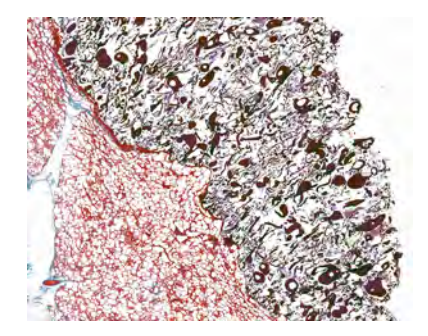
E9 aspect during obduction / control lesion



9 TachoSil baseline



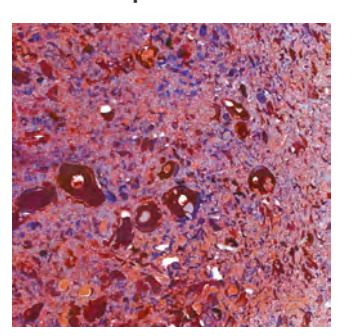
GATT-patch baseline



E9-G1/G2 aspect of remnant material, detail on EvM stain



E8-G1/G2 aspect of remnant material, detail on EvM stain



Supplemental evidence: blinded and independent histological assessment

Aim:

- To confirm that the histological aspects of the patch remnants are distinctly different.
- Substantiate the correction of the histological mix-up.

Method:

- Assessment by independent pathologist.
- Hemotoxylin-Eosin (HE) and 'Elastine volgens Masson' (EvM) staining.
- Two baseline slides are shown to the pathologist, corresponding to the patches at baseline.
- Six other slides are shown per staining method, at 2 and 6 weeks.
- Slides are randomized and blinded.
- The task is to organize the randomized slides according to the suspected patch group, or 'no remnant on pleural surface'.

Results:

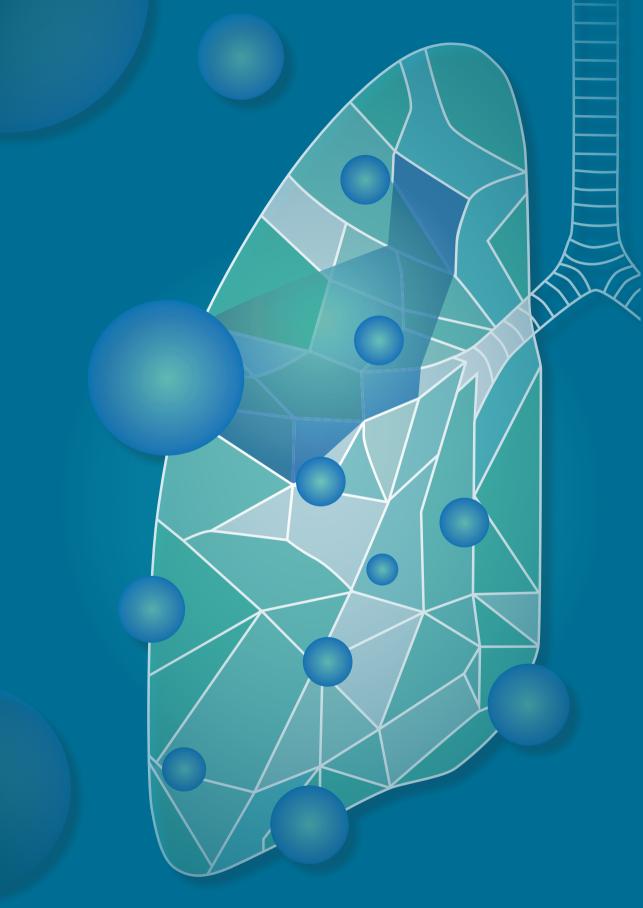
• After unblinding the grouped sections, the results show that the section E9-G1 was grouped in the TachoSil group instead of the GATT-Patch group on both HE and EvM staining.

Assessment based on HE-staining:

Group 1: TachoSil Group 2: GATT-Patch		No remnant on pleural surface			
Code	Key	Code	Key	Code	Key
1	E9-G1	4	E8-G1	3	E11-G1
2	E8-T2			5	E9-T1
6	E11-T1				

Assessment based on EvM-staining:

Group 1: TachoSil Group 2: GATT-Patch		No remnant on pleural surface			
Code	Key	Code	Key	Code	Key
2	E8-T2	1	E8-G1	3	E11-G1
4	E9-G1			5	E9-T1
6	E11-T1				



Chapter 8

General discussion

A significant problem with experimental research, is the external validity of the model used, causing problems when translating the findings to clinical practice. This thesis incorporated several studies to investigate and substantiate the used methodologies. The best method for measurement of pulmonary air leak (PAL) was validated in **Chapter 2** and used in **Chapter 4**, 5 and 6. Previous animal models of PAL were systematically investigated in **Chapter 3**, which were combined with the investigations of **Chapter 5** to improve understanding of intrinsic sealing mechanisms in healthy animal lungs and pathophysiology of clinical PAL. These findings formed the basis for developing the acute aerostasis and long term biocompatibility models.

In order to fill the unmet clinical need for more effective lung sealants, a novel NHS-POx based patch was investigated in a series of experiments aimed at translational value. (6) Three models were used: the *ex-vivo* dynamic porcine lung model (**Chapter 4**), the *in-vivo* acute aerostasis model (**Chapter 6**) and the *in-vivo* long term biocompatibility model (**Chapter 7**). The studies demonstrated superior aerostatic efficacy for the NHS-POx patch in comparison to currently used products, proof-of-principle for aerostatic sealing in a realistic surgical model and biocompatibility and biodegradability up to six weeks after application. The main findings are summarized in **Table 1**.

Here, the findings relating to efficacy, applicability and safety of the NHS-POx patch will be discussed in an integrative way by considering translational value, relevance to clinical practice and knowledge gaps. Then, a perspective is given on future research and development towards clinical application.

Table 1: summary of main findings of translational experiments with NHS-POx in this thesis.

	Design	Application	Main findings
Dynamic porcine lung model (Chapter 4)	Ex-vivo (n=60 caudal lobes) NHS-POx single and double, Progel®, Coseal®, Hemopatch®, TachoSil® multigroup comparison n=10 per group	Flat application Single and double layer	Bursting pressure: NHS-POx double (60±24 cmH20) higher vs TachoSil® (30±11 cmH20, P<0.001), Hemopatch® (33±6 cmH20, P=0.006), Coseal® (25±13 cmH20, P=0.001) and Progel® (33±11 cmH20, P=0.005). Air leak reduction: NHS-POx Patch double (100%±1%) higher vs Hemopatch® (46%±50%, P=0.010) and TachoSil® (31%±29%, P<0.001) NHS-POx single (100%±14%) higher vs TachoSil (p=0.004)
	Ex-vivo (n=20 caudal lobes) NHS-POx single vs Hemopatch [®] , n=10 per group	Flat application Single layer	Bursting pressure:NHS-POx single higher vs Hemopatch $^{\otimes}$ (45±10 vs. 40±6 cmH2O, P=0.043) Air leak reduction:NHS-POx single higher vs Hemopatch $^{\otimes}$ (100%±11% vs.68%±40%, P=0.043)
Ovine acute aerostasis model (Chapter 6)	In-vivo (n=6 sheep) pooled analysis Air leak: n=7 NHS-POx vs n=5 untreated control Bursting pressure: n=11 NHS-POx vs n=7 untreated control	Thoracotomy Folding application Single and double layer	Air leak: Lower for NHS-POx (median: 7mL/min, IQR: 333mL/min) versus untreated lesions (367mL/min, IQR: 680mL/min, p=0.036) Bursting pressure: Higher for NHS-POx (mean: 33, SD: 16cmH2O) versus untreated lesions (mean: 19, SD: 15cmH2O, p=0.081)
In-vivo biocompatibility model (Chapter 7)	In-vivo (n=12 sheep) Intra-animal comparisons: NHS-POx vs TachoSil® vs untreated control n=4 per group, sacrifice at 5 days, 2 and 6 weeks	Muscle sparing thoracotomy Flat application Single layer	Biodegradation within 6 weeks* No significant adverse immune response* Healing by mesothelial covering and replacement of biomaterial with extracellular matrix with localized visceral and parietal pleural thickening.

*based on data adapted for mix-up

The underlying pathophysiological mechanisms of PAL are relevant with respect to face validity for testing lung sealants. First of all, there is hypothesized to be a difference in intrinsic sealing mechanisms between healthy animal lungs and diseased human lungs (**Chapter 5**). Secondly, due to emphysematous destruction of alveoli that is often present in patients at risk for pPAL, there will be a lower tissue density, resulting in a lower crosslink density and lower adhesive strength (as also discussed in **Chapter 5** and **6**). (10, 12, 13) Finally, the distance between alveoli may place a different requirement on the balance between adhesive and cohesive forces within a lung sealant. (14)

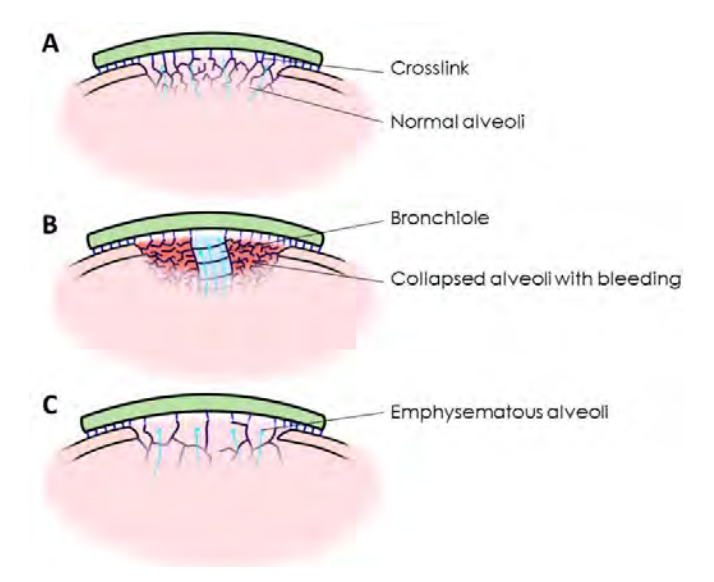


Figure 1: Illustrations of face validity of different air leak models used in this thesis (not to scale). **A)** The ex-vivo porcine lung model consists of an adhesive interface between normal alveoli and the patch, without intrinsic sealing mechanisms. **B)** The acute aerostatit model consists of sealing an air leak from a bronchiole (\emptyset 1.5-2mm) adjacent intrinsically sealed lung parenchyma. **C)** Possible example of the clinical situation in pulmonary emphysema. There is a lower crosslink density and the intrinsic sealing mechanisms are reduced.

The aerostatic efficacy of the NHS-POx patch was investigated in two preclinical models of PAL. The *ex-vivo porcine* lung model (**Chapter 4**) provides a platform of parenchymal PAL without intrinsic sealing mechanisms, but with a high crosslink density due to absence of emphysema. Other considerations are ischemic tissue necrosis that may influence pH and crosslinking, and positive pressure ventilation without pleural mechanisms. Superior bursting pressures were demonstrated for the NHS-POx patch in this model

compared to currently used tissue adhesives, and a second powered and randomized experiment demonstrated superior bursting pressure and air leak reduction for the NHS-POx patch as a single layer compared to Hemopatch[®].

The ovine acute aerostasis model (Chapter 6) provides a model of bronchiolar PAL, with rapid intrinsic sealing of lung parenchyma and a high crosslink density. (10) The large gap that the sealant has to cross (\emptyset 1.5-2mm) puts a different requirement on the adhesive and cohesive forces required. Other considerations are realistic surgical application, presence of negative pressure ventilation, pleural mechanics, local homeostasis of pH, coagulation and immune mechanisms. (19) The sealing capability of the NHS-POx patch was confirmed in this model (proof-of-principle), in comparison to an untreated control group.

Both models provided clinically relevant PAL flow, as confirmed using mechanical ventilator measurements that were validated in Chapter 2. (4, 20-22) A summary of the models compared to the clinical situation is provided in **Table 2** and Figure 1.

	Porcine lung model	Acute aerostasis model	Clinical situation
Intrinsic sealing	No	Yes	May be inhibited
Crosslink density	†	1	1
Air leak orifice ¹	Comparable to healthy human	ø1.5-2.0mm	Healthy: ø200-500µm Emphysematous: †
Lesion	Superficial pleural	Sequential amputation	Varies ²
Air leak size	0.6-1.2 L/min	1.4-1.5 L/min	Severe: >400 mL/min ³
Ventilation mechanics	PPV	PPV / NPV	PPV / NPV
Pleural mechanisms	No	Yes	Yes
Biochemistry	Not controlled	Homeostasis	Homeostasis
Coagulation	No	Yes	May be inhibited
Immune mechanisms	No	Yes	May be inhibited
Timeframe	Minutes	Hours	Days

Table 2: Side-by-side comparison of face validity of air leak models used in this thesis, compared to the clinical situation. Red indicates estimated poor comparability, yellow/orange moderate comparability, green high comparability.

¹Diameter of alveoli for parenchymal leak model based on (1, 2)

²Lesions include staple lines, pulmonary hilum dissections, fissures, iatrogenic lesions, traumatic lesions (3)

³Classification based on (4)

The main knowledge gap to clinical practice for aerostatic efficacy, is the comparative effectiveness on clinically relevant emphysema models, with the research question:

"What is the aerostatic efficacy of the novel NHS-POx patch, in comparison to similar patches (e.g. Hemopatch® and TachoSil®), on the emphysematous human lung?"

Several approaches can be considered: rejected *human* donor lungs on *exvivo* lung perfusion (EVLP), an emphysema animal model or a randomized clinical trial $^{(12,23)}$

Use of human tissue could provide a model with high face validity for emphysema. During the research for this thesis, this approach was explored by use of fresh frozen cadavers, but seemed unsuited due to disrupted pH, which influences NHS ester reactivity (data not shown). (16, 24, 25) Fresh frozen cadavers may be suited for mechanical methods of aerostasis, such as the use of staple line reinforcement as investigated by Murray et. al. (26) Human EVLP lungs can provide an excellent alternative. A model on human EVLP lungs was described in 2021 by Cárdenes, perfusing lungs with various conditions including emphysema. Stable physiology was described for up to six hours. This can be an ideal step between *in-vivo* and clinical research, providing the final test for efficacy. Important downsides are low availability and no study of wound healing. (23)

Simulation of lung emphysema has only been attempted by one author in lung sealant research (**Chapter 3**). (9) Gika et. al. instilled elastase into the right lung of beagles, and performed lung sealant application after six weeks. This resulted in heterogenous emphysema, but samples could be tested specifically on diseased areas. (12) In other fields, various models of emphysema are described as outlined in the review by Liang et. al., including chronic smoke inhalation, chemicals (e.g. NO_2 , lipopolysaccharide) and genetic manipulation. (27) In lung sealant research, the most important characteristic appears to be the low tissue density. So, methods that disrupt the elastase/anti-elastase balance to produce alveolar destruction seem most reasonable, compared to long time required for chronic smoke inhalation models or high costs of genetic modification models. (27)

Handling and applicability

A lung sealant needs to be applicable under various surgical scenarios, as outlined in **Chapter 1**. (6, 28) The NHS-POx patch was surgically applied during a regular thoracotomy (**Chapter 6**), and through smaller muscle-sparing incisions (**Chapter 7**). No difficulties were seen due to insufficient flexibility and material breakage, such as in the trial by Homma using TissuePatchTM. (29) For TachoSil[®], Gondé et. al. described sometimes challenging application for aerostasis due to friable composition. (30) In contrast, the NHS-POx patch was successfully folded around 'oval' lesions (**Chapter 6**), and the flexibility required for this may be similar to folding the patch around a stapler line. As a next step, efficacy should be confirmed on more heterogenous lesions that are routinely encountered clinically, including stapler lines, areas of dissected pulmonary hilum, fissures and iatrogenic lesions (e.g. resulting from manipulation during surgery) (**Chapter 1**). (3)

Applicability of the NHS-POx patch through thoracotomy incisions is a step in the right direction, but compatibility with video-assisted thoracic surgery (VATS) is essential, since this is routinely performed. (31) The NHS-POx patch seems usable under these conditions, as it has recently been used on liver bleeding in a robotic surgery model after introduction of a rolled-up patch through a 12mm trocar. (32) However, this needs to be verified on the lung due to differences in tissue characteristics. (14) It should be noted that prior lung sealants are scarcely tested in VATS. In the systematic review of McGuire, only 2/21 clinical trials tested application through VATS, and both were spray sealants. (33, 34) In clinical practice, patches such as TachoSil® are routinely applied in minimally invasive settings. (30, 35, 36) Surgeons are generally inventive, as also illustrated by the report of Kajiwara et. al., describing a new technique for easier laparoscopic application of TachoSil® during liver resections. (37) However, it is preferred if products are optimized for such applications in the pre-market phase, which may also prevent overestimation of efficacy when only testing in open surgery due to better analogy to clinical practice. (38)

NHS-POx was tested as a single and double layer. Application of the single layer is comparable to other patches (e.g. TachoSil® and Hemopatch®). (15) The double layer application is primarily of experimental interest, to test the capabilities of the NHS-POx technology. This application does not seem clinically usable due to complicated steps required, especially during VATS. (6, 15, 28) So further optimization, for instance in a thicker single layer design, is needed.

A specific advantage of the NHS-POx patch design is homogenous impregnation with the functional polymer, that facilitates application of both sides. (39) TachoSil® and Hemopatch® both have an active side (coated design), that could increase the chances for application failures in stressful clinical scenarios. (40, 41) For example, Homma described difficulty to distinguish the active side in TissuePatch™ in their clinical trial during minimally invasive applications. (29) In the experiments of **Chapter 7**, application failure for TachoSil® was also observed by the investigating surgeon due to accidental application of the non-active side (data not shown).

Biocompatibility, biodegradability and safety

The local biocompatibility of the NHS-POx patch was investigated in **Chapter 7** on a healthy *ovine* lung model of superficial parenchymal injury. This model provides a platform to solely study healing mechanisms, as these lesions do not result in pPAL (**Chapter 5**). (10) By sacrificing the animals at various terms, the mechanisms associated with healing, inflammation and biodegradation can be studied and directly compared to untreated lung injuries and injuries treated with a control patch (fibrin-thrombin patch, TachoSil®). (42) The main finding of this study was that after lung application, the NHS-POx patch degrades within 6 weeks without a significant adverse inflammatory response in comparison to the control patch, while permitting local healing with visceral and parietal pleural thickening and fibrosis.

This model comes with various limitations with regard to the translational value to clinical practice. Patients undergoing lung resections may have one or more risk factors that influence local wound healing and inflammation mechanisms, such as emphysema, corticosteroid use, prior radiation and chemotherapy, anticoagulant use, advanced age and a reduced body-mass-index. (43, 44) In addition, the patch will be applied to significant PAL in clinical practice and not intrinsically sealed lesions, which may modify the wound healing process. (21)

Analogous to bone/cartilage scaffold biomaterials, overall mechanical strength should be sufficient over the healing duration to ensure the specific function. (45) For the lung, the seal integrity is a sum of the underlying tissue healing and the lung sealant strength. Due to degradation, the NHS-POx patch will lose mechanical strength over time, whereas the underlying tissue healing and replacement of the biomaterial with extracellular matrix will increase over time (as seen in

Chapter 7). These mechanisms should be studied in a clinically realistic PAL scenario, in order to prevent the occurrence of a secondary pneumothorax after chest tube removal (**Figure 2**). For example, such a premature sealant failure was seen in **Chapter 6**, associated with double-layer application.

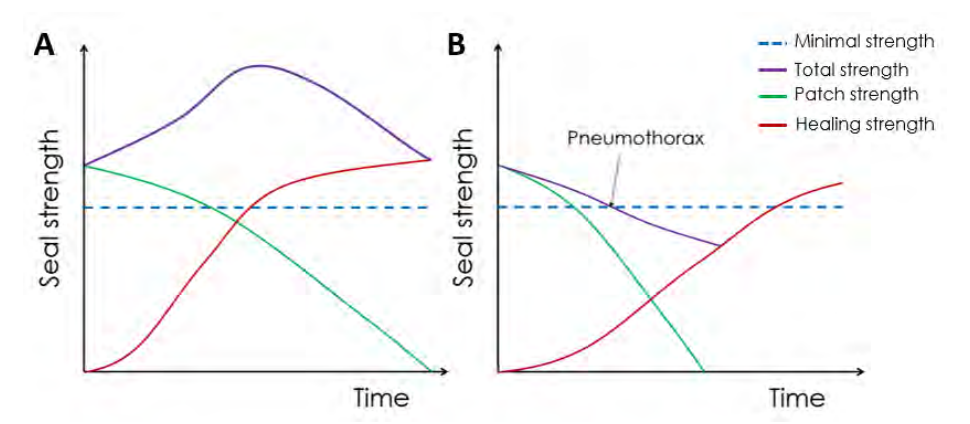


Figure 2: Temporal aerostasis mechanisms (theoretical examples). **A)** The total seal strength remains higher than the minimal strength required to prevent air leakage. **B)** The total seal strength is lower than the minimal required seal strength, resulting in a pneumothorax. This may be due to prolonged healing mechanisms or too rapid biodegradation.

Further study is also required into the impact of the NHS-POx patch on adverse events, since cross-over effects and small sample size limit drawing strong conclusions on adverse events (**Chapter 7**).⁽³⁹⁾ First of all, it needs to be investigated whether the patch does not result in excessive adhesion formation in comparison to other used lung sealants, which can pose a problem during re-operations or restrict pleural sliding.^(46, 47) Secondly, the impact of the pleural thickening should be studied in the context of pulmonary function in applications of lung patches larger then 5x5cm (i.e. lung expansion should not be significantly inhibited).⁽⁴⁸⁾ Thirdly, the influence of the patch on infectious complications is unknown for intrathoracic application.⁽⁴⁹⁾ Finally, the precise uptake pathways of the NHS-POx polymer from the tissue are unknown, and this should be further studied to ensure that there is no degree of local retention of the polymer, of which the long term consequences are unknown (**Chapter 7**).⁽⁵⁰⁾

In summary, the following research questions can be formulated:

 "Is the total sealing strength capable of providing an aerostatic seal over the entire healing duration of the lung, in the context of factors affecting healing in clinical practice?"

- "How does the NHS-POx patch influence adverse events, such as intrapleural infections, adhesions and pulmonary function, as compared to other used sealant products?"
- "What are the local uptake pathways of NHS-POx polymers from the application site, and is there a degree of local retention?"

The first two questions could be studied in a realistic *in-vivo* model mimicking the clinical situation, or a randomized clinical trial. (12, 51) In wound healing research, various pathophysiological models have been applied, including ischemia, infection, diabetes mellitus and obesity. (52) In research on bowel anastomosis, induction of ischemia in attempt to reduce wound healing is described. (53) Conversely, in lung sealant research, such animal models are not routinely applied, as seen in **Chapter 3**. (9) To simulate reduced lung healing, an emphysema model (as described above) could be combined with factors inhibiting wound healing (e.g. cigarette smoking, corticosteroid exposure), but validity of this should be established. (43)

Boerman et. al. has studied the excretion of radioactively labeled polyoxazolines after intravenous injection, by using single-photon emission computed tomography (SPECT/CT). (50) But, tracing of the NHS-POx after application to local tissue has not been performed. Local uptake, distribution and excretion of radiolabeled polyoxazolines after implantation in extravascular space (e.g. pleura, peritoneum, subcutaneous space) could be further investigated (e.g. with SPECT/CT), but isotopes with appropriate half-life need to be selected with respect to the biodegradation times. (54, 55)

From bench to bedside: considerations for clinical studies

Perspectives from current literature: number needed to treat

For a new technology to benefit patients, evidence from randomized clinical trials is required for market implementation. Clinical use can then be scaled up and guideline recommendations formulated for sustainable use. (56) Currently, it is recommended that lung sealants are only used if there is intraoperative pulmonary air leakage (IAL), that the severity of the intraoperative air leakage should be graded, and that patients with increased risk for pPAL have a stronger indication for lung sealant use (summarized in **Table 3**). (4, 6, 28, 49, 57-59) These recommendations can be considered as a reflection of the "number needed"

to treat (NNT)"-problem with pPAL. (44) Despite the high incidence of IAL (up to 70%), only 7-12% of patients actually develop pPAL. (44, 57, 60) If lung sealants would prevent pPAL completely, this would still indicate a NNT of 8-14, which may be acceptable for low-risk and cheap medications to prevent disease, but not for expensive surgical interventions. (44)

Table 3: current clinical practice recommendations based on recent publications.

Author, year	Туре	Recommendation	
Aprile 2023	Systematic review	Only recommended for intra-operative treatment of air leak, not for pPAL prevention. (57)	
McGuire, 2018	Sealants may be useful in case of intra-operative leak, or with increased risk of pPAL. (58)		
Belda-Sanchis, 2010		Sealant use aiming to reduce length of hospital stay is not recommended. $^{(49)}$	
Cardillo, 2022	Delphi Consensus	Use of sealants when: intraoperative AL 150-300cc, VATS, other methods difficult, modest lymphatic losses. Indication increased with risk factors. (28)	
Zaraca, 2022		Treat moderate (100-400mL/min) AL in high- risk cases and severe (>400mL/min) air leak. No consensus regarding sealant use. (4)	
Brunelli, 2020		Determine use based on patient factors, including whether there is an air leak and the volume of the air leak. $^{(6)}$	
Singhal, 2010	Expert review	No use on a routine basis, but incomplete evaluation in high-risk subgroups. (59)	

Several studies have attempted to predict pPAL to improve patient selection (outlined in Table 4). Zaraca et. al. investigated pre-operative prediction of pPAL, validating four previous models on their dataset of VATS anatomical lung resections (n=3965), finding that at best pPAL can be predicted with high false positives. (44) Considering the numbers of the best-predicting model (Bordeaux model), the a-priori probability for pPAL in a pre-selected sample of highrisk patients may be increased up to 16.1% (64/397) from the 11% prevalence baseline, but also missing 7.6% pPAL cases (46/603) in the identified lowrisk group. (44, 61) Smaller studies have assessed other variables (radiological emphysema index and intra-operative air leak size) that might further be able to improve the current prediction models, but this has not been integrally validated in a comprehensive prediction model in a large dataset. (22, 62) Of note, Brunelli et. al. describes that pPAL may be present in 55% of patients with an intra-operative air leak of >500mL/min (vs 9% when <500mL/min), but this was only assessed in a small cohort (n=111). (21)

Table 4: identification of high-risk patients for developing pPAL

Author, year	Туре	N	Predictors	Relevant findings
Zaraca, 2021 ⁽⁴⁴⁾	Validation of four previously published pre-operative prediction models	3965	Best model (Bordeau model, Rivera et. al. ⁽⁶¹⁾) used male gender, linear BMI, dyspnea score, pleural adhesions, type of resection and location of resection (originally validated on n=24,113)	Net benefit: 23/1000 patients High false positives: 333 cases C-statistic = 0.65 (0.62- 0.68)
Moon, 2019 ⁽⁶³⁾	Radiological prediction score	41	Emphysema index (EI) Lobe-specific emphysema index (LEI)	EI AUC 0.810 LEI AUC 0.931
Murakami, 2018 ⁽⁶²⁾	Radiological prediction score	284	Emphysema index (EI)	EI AUC 0.85 (0.73-0.98)
Brunelli, 2017 ⁽²¹⁾	Intra-operative air leak prediction	111	Intraoperative air leak (IAL)	pPAL in 55% if IAL >500mL/min, in 6% if IAL <500mL/min
Kim, 2017 ⁽²²⁾	Intra-operative air leak prediction	1060	Ventilatory leak >9.5% of tidal volume	Predictor of pPAL (adjusted OR 1.59 [1.37-1.85)

Perspectives from previous clinical trials

A clinical trial should be designed to mirror clinical practice and use relevant outcome measures, to maximize external validity. (38) In the systematic review by McGuire et. al., several methodological issues are observed, including lack of clinically realistic selection of patients and procedures, control groups and outcome measures. (58) Outcome measures other than pPAL or length of hospital stay are often used, indicated by the data that 12/21 trials contributed to meta-analysis of effects on pPAL, and 9/21 to effects on length of stay. (58) Head-to-head comparisons between lung sealants are rare, and only performed by 2/21 trials. (15, 33, 58, 64) Standardized air leak quantification measurements (such as the one validated in **Chapter 2**) are rarely used (most use the visual bubble scale). (60, 65, 66) With respect to internal validity, lack of outcome assessor blinding, standardization of air leak assessment and chest-tube protocols was observed. (58)

Taking this into account, there are some noteworthy trial designs to be considered in the context of the NNT-problem. Intraoperative air leak measurement to guide lung sealant indication was used by Zaraca et. al. (air leak 150-400mL/min), overcoming the problem of inter-observer variability with visual bubbling scores. (20) Rena et. al. tested TachoSil® in high-risk

patients, with chronic-obstructive pulmonary disease undergoing upper lobectomies, which led to prolonged PAL (>7 days) in 8/30 (26.7%) in the control group and only 1/30 in the treatment group (3.3%) (NNT = 4.3). (65) Moser et. al. studied sealant effectiveness in bilateral lung volume reduction surgery, using one side as intervention and one side as control, demonstrating pPAL (>7 days) in 7/22 (31.8%) control and 1/22 (4.5%) treated sides (NNT = 3.7). (34) DeLeyn and Wain propose a risk-stratification score for their randomization scheme to increase the comparability between groups. (60,67)

Recommendations for a randomized clinical trial

With many lung sealants tested and the problem of pPAL still unresolved, a modern randomized clinical trial with a new device should attempt to incorporate all the best principles and practices based on previous knowledge. An example of such a design is provided in **Figure 3.** The following aspects may be considered:

- Selection of high-risk patients for inclusion to heighten the a-priori odds of pPAL. (44, 65)
- Inclusion of both open surgery and VATS to reflect the reality of clinical practice. (58, 68)
- Test new sealants in head-to-head comparative trials. (15, 58)
- Use of quantifiable measures of air leakage together with standardized ventilator settings intra-operatively for selection of patients. (20)
- Use of quantifiable measures of air leakage post-operatively (digital chest drainage), to improve standardization of assessment and drain removal protocols.⁽⁶⁹⁾
- Apply principles of blinding for outcome assessment and data-analysis. (58)
- Power trials on pPAL as primary outcome measure, since this is the clinical problem that is associated with increased complications. (70)
- Length of hospital stay and length of chest drainage should only be considered reliable if the outcome assessors were blinded and the protocols adequately standardized. These measures may be used for costeffectiveness calculations of the new treatment. (20, 58)
- Ensure adequate long-term follow-up to investigate any possible unknown adverse long-term consequences (e.g. imaging for adhesions, lung function tests, blood tests).(71-73)

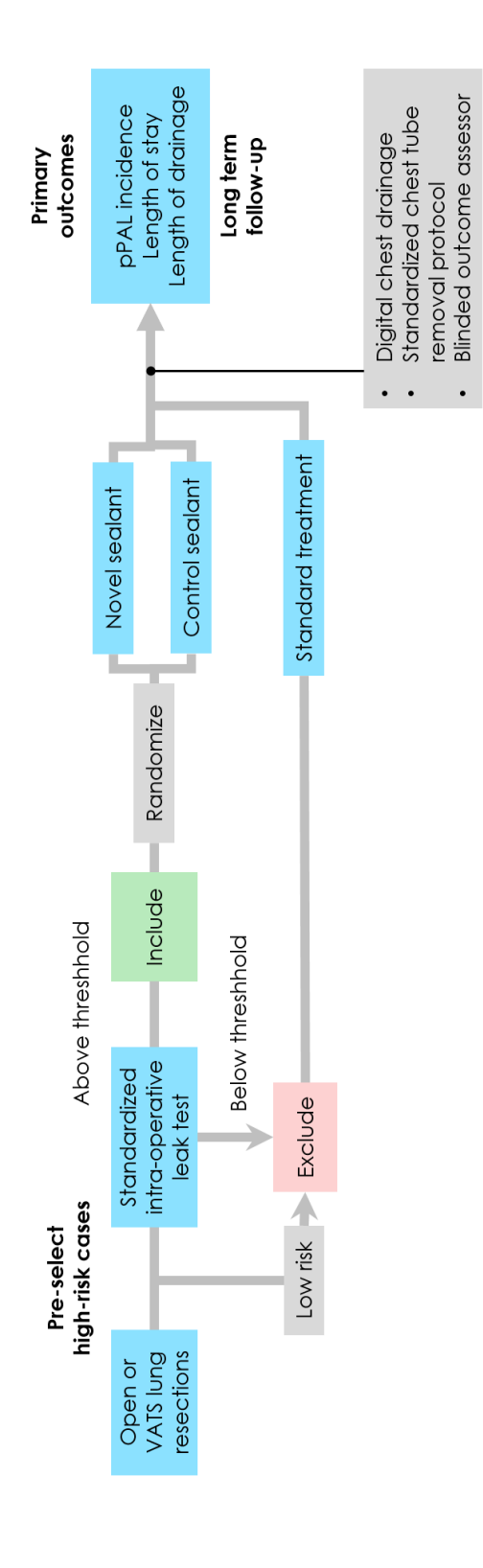


Figure 3: Example of aspects to consider in a possible clinical trial design to test the efficacy of a novel lung sealant, based on modern insights from literature.

General conclusions

The preclinical findings with the NHS-POx patch as a lung sealant are promising, but there still are several research questions that remain unanswered. The NHS-POx double layer application methods does not seem clinically feasible, so the NHS-POx single layer application method should be further improved and comparatively tested in clinically realistic scenario's and VATS. Face validity was found to be an important characteristic in preclinical model design, and as a consequence there still are open questions regarding efficacy on lung emphysema, reduced intrinsic healing capacity, temporal aerostatic efficacy and safety parameters. There are various future study designs possible to answer these research questions. As a next step, I would propose testing the NHS-POx patch in a preclinical model of more clinically realistic lesions, preferably in an emphysema model. Ultimately, novel therapies need to be tested in well-designed randomized clinical trials that reflect the target patient population, to ensure translation from bench to bedside.

Referenties

- 1. Tsuchiya T, Doi R, Obata T, Hatachi G, Nagayasu T. Lung Microvascular Niche, Repair, and Engineering. Front Bioeng Biotechnol. 2020;8:105.
- Rogers CS, Abraham WM, Brogden KA, Engelhardt JF, Fisher JT, McCray PB, Jr., et al. The porcine lung as a potential model for cystic fibrosis. Am J Physiol Lung Cell Mol Physiol. 2008;295(2):L240-63.
- Allen MS, Wood DE, Hawkinson RW, Harpole DH, McKenna RJ, Walsh GL, et al. Prospective randomized study evaluating a biodegradable polymeric sealant for sealing intraoperative air leaks that occur during pulmonary resection. Ann Thorac Surg. 2004;77(5):1792-801.
- Zaraca F, Brunelli A, Pipitone MD, Abdellateef A, Abu Akar F, Augustin F, et al. A Delphi Consensus report from the "Prolonged Air Leak: A Survey" study group on prevention and management of postoperative air leaks after minimally invasive anatomical resections. Eur J Cardiothorac Surg. 2022.
- van der Worp HB, Howells DW, Sena ES, Porritt MJ, Rewell S, O'Collins V, Macleod MR. Can Animal Models of Disease Reliably Inform Human Studies? PLOS Medicine. 2010;7(3):e1000245.
- Brunelli A, Bölükbas S, Falcoz PE, Hansen H, Jimenez MF, Lardinois D, et al. Exploring consensus for the optimal sealant use to prevent air leak following lung surgery: a modified Delphi survey from The European Society of Thoracic Surgeons. Eur J Cardiothorac Surg. 2020.
- Kausel HW, Lindskog GE. The healing of raw lung surfaces after experimental segmental resection. J Thorac Surg. 1955;29(2):197-211.
- 8. Ranger WR, Halpin D, Sawhney AS, Lyman M, Locicero J. Pneumostasis of experimental air leaks with a new photopolymerized synthetic tissue sealant. Am Surg. 1997;63(9):788-95.
- 9. Hermans BP, Poos SEM, van Dort DIM, Evers J, Li WWL, van der Heijden E, et al. Evaluating and developing sealants for the prevention of pulmonary air leakage: A systematic review of animal models. Lab Anim. 2023:236772231164873.
- 10. Hermans BP, Li WWL, Roozen EA, van Dort DIM, Vos S, van der Heide SM, et al. Intrinsic pulmonary sealing, its mechanisms and impact on validity and translational value of lung sealant studies: a pooled analysis of animal studies. Journal of Thoracic Disease. 2023.
- 11. Pommergaard HC, Rosenberg J, Schumacher-Petersen C, Achiam MP. Choosing the Best Animal Species to Mimic Clinical Colon Anastomotic Leakage in Humans: A Qualitative Systematic Review. European Surgical Research. 2011;47(3):173-81.
- 12. Gika M, Kawamura M, Izumi Y, Kobayashi K. The short-term efficacy of fibrin glue combined with absorptive sheet material in visceral pleural defect repair. Interact Cardiovasc Thorac Surg. 2007;6(1):12-5.
- 13. DeCamp MM, Blackstone EH, Naunheim KS, Krasna MJ, Wood DE, Meli YM, McKenna RJ, Jr. Patient and surgical factors influencing air leak after lung volume reduction surgery: lessons learned from the National Emphysema Treatment Trial. Ann Thorac Surg. 2006;82(1):197-206; discussion -7.
- 14. Nam S, Mooney D. Polymeric Tissue Adhesives. Chem Rev. 2021;121(18):11336-84.
- 15. Hermans BP, Li WWL, Roozen EA, van Dort DIM, Evers J, van der Heijden EHFM, et al. Sealing effectiveness of a novel NHS-POx based patch: experiments in a dynamic ex vivo porcine lung. Journal of Thoracic Disease. 2023;15(7):3580-92.

- 16. Hermanson GT. Chapter 3 The Reactions of Bioconjugation. In: Hermanson GT, editor. Bioconjugate Techniques (Third Edition). Boston: Academic Press; 2013. p. 229-58.
- 17. D'Armini AM, Roberts CS, Griffith PK, Lemasters JJ, Egan TM. When does the lung die? I. Histochemical evidence of pulmonary viability after "death". J Heart Lung Transplant. 1994;13(5):741-7.
- 18. Klassen C, Eckert CE, Wong J, Guyette JP, Harris JL, Thompson S, et al. Ex Vivo Modeling of Perioperative Air Leaks in Porcine Lungs. IEEE Trans Biomed Eng. 2018;65(12):2827-36.
- 19. Elvin CM, Vuocolo T, Brownlee AG, Sando L, Huson MG, Liyou NE, et al. A highly elastic tissue sealant based on photopolymerised gelatin. Biomaterials. 2010;31(32):8323-31.
- 20. Zaraca F, Vaccarili M, Zaccagna G, Maniscalco P, Dolci G, Feil B, et al. Cost-effectiveness analysis of sealant impact in management of moderate intraoperative alveolar air leaks during video-assisted thoracoscopic surgery lobectomy: a multicentre randomised controlled trial. J Thorac Dis. 2017;9(12):5230-8.
- 21. Brunelli A, Salati M, Pompili C, Gentili P, Sabbatini A. Intraoperative air leak measured after lobectomy is associated with postoperative duration of air leak. Eur J Cardiothorac Surg. 2017;52(5):963-8.
- Kim WH, Lee HC, Ryu HG, Yoon HK, Jung CW. Intraoperative ventilatory leak predicts prolonged air leak after lung resection: A retrospective observational study. PLoS One. 2017;12(11):e0187598.
- 23. Cárdenes N, Sembrat J, Noda K, Lovelace T, Álvarez D, Bittar HET, et al. Human ex vivo lung perfusion: a novel model to study human lung diseases. Sci Rep. 2021;11(1):490.
- 24. Mazur P. Freezing of living cells: mechanisms and implications. Am J Physiol. 1984;247(3 Pt 1):C125-42.
- 25. Okaniwa G, Nakada T, Kawakami M, Fujimura S, Arakaki Y. Studies on the preservation of canine lung at subzero temperatures. J Thorac Cardiovasc Surg. 1973;65(2):180-6.
- 26. Murray KD, Ho CH, Hsia JY, Little AG. The influence of pulmonary staple line reinforcement on air leaks. Chest. 2002;122(6):2146-9.
- 27. Liang GB, He ZH. Animal models of emphysema. Chin Med J (Engl). 2019;132(20):2465-75.
- 28. Cardillo G, Nosotti M, Scarci M, Torre M, Alloisio M, Benvenuti MR, et al. Air leak and intraoperative bleeding in thoracic surgery: a Delphi consensus among the members of Italian society of thoracic surgery. J Thorac Dis. 2022;14(10):3842-53.
- 29. Homma T. A series of experiences with TissuePatch™ for alveolar air leak after pulmonary resection. Gen Thorac Cardiovasc Surg. 2023;71(10):570-6.
- 30. Gondé H, Le Gac C, Gillibert A, Bottet B, Laurent M, Sarsam M, et al. Feedback on the use of three surgical sealants for preventing prolonged air leak after robot-assisted anatomical lung resection. J Thorac Dis. 2019;11(7):2705-14.
- 31. Paul S, Altorki NK, Sheng S, Lee PC, Harpole DH, Onaitis MW, et al. Thoracoscopic lobectomy is associated with lower morbidity than open lobectomy: a propensity-matched analysis from the STS database. J Thorac Cardiovasc Surg. 2010;139 (2):366-78.
- 32. D'Hondt M, Roozen EA, Nuytens F, Bender J, Mottrie A, Bauwens K, Head SJ. NHS-POx-loaded patch versus fibrin sealant patch in a porcine robotic liver bleeding model. BMC Surg. 2023;23(1):257.

- 33. Kılıç B, Erşen E, Demirkaya A, Kara HV, Alizade N, İşcan M, et al. A prospective randomized trial comparing homologous and autologous fibrin sealants for the control of alveolar air leak. J Thorac Dis. 2017;9(9):2915-22.
- 34. Moser C, Opitz I, Zhai W, Rousson V, Russi EW, Weder W, Lardinois D. Autologous fibrin sealant reduces the incidence of prolonged air leak and duration of chest tube drainage after lung volume reduction surgery: a prospective randomized blinded study. J Thorac Cardiovasc Surg. 2008;136(4):843-9.
- Grossi W, Masullo G, Londero F, Morelli A. Small incisions, major complications: videoassisted thoracoscopic surgery management of intraoperative complications. J Vis Surg. 2018;4:12.
- Nakazawa S, Shimizu K, Kosaka T, Ohtaki Y, Mogi A, Shirabe K. Management of intraoperative bleeding during video-assisted thoracoscopic surgery. Journal of Visualized Surgery. 2018;4.
- 37. Kajiwara M, Naito S, Sasaki T, Nakashima R, Hasegawa S. Quick and Easy Application Method of TachoSil® During Laparoscopic and Robotic Liver Resections. Cureus. 2023;15(4):e37252.
- 38. Rothwell PM. Factors that can affect the external validity of randomised controlled trials. PLoS Clin Trials. 2006;1(1):e9.
- 39. Roozen E, Lomme R, Calon N, Broek R, Goor H. Efficacy of a novel polyoxazoline based hemostatic patch in liver and spleen surgery2023.
- 40. Lombardo C, Lopez-Ben S, Boggi U, Gutowski P, Hrbac T, Krska L, et al. Hemopatch(®) is effective and safe to use: real-world data from a prospective European registry study. Updates Surg. 2022;74(5):1521-31.
- 41. Toro A, Mannino M, Reale G, Di Carlo I. TachoSil use in abdominal surgery: a review. J Blood Med. 2011;2:31-6.
- 42. Ennker IC, Ennker J, Schoon D, Schoon HA, Rimpler M, Hetzer R. Formaldehyde-free collagen glue in experimental lung gluing. Ann Thorac Surg. 1994;57(6):1622-7.
- 43. Attaar A, Tam V, Nason KS. Risk Factors for Prolonged Air Leak After Pulmonary Resection: A Systematic Review and Meta-analysis. Ann Surg. 2020;271(5):834-44.
- 44. Zaraca F, Pipitone M, Feil B, Perkmann R, Bertolaccini L, Curcio C, Crisci R. Predicting a Prolonged Air Leak After Video-Assisted Thoracic Surgery, Is It Really Possible? Semin Thorac Cardiovasc Surg. 2021;33(2):581-92.
- 45. Hutmacher DW. Scaffolds in tissue engineering bone and cartilage. Biomaterials. 2000;21(24):2529-43.
- 46. Kanai E, Matsutani N, Aso T, Yamamoto Y, Sakai T. Long-term effects of pleural defect repair using sheet materials in a canine model. Gen Thorac Cardiovasc Surg. 2020;68(6):615-22.
- 47. Li S-J, Zhou K, Wu Y-M, Wang M-M, Shen C, Wang Z-Q, et al. Presence of pleural adhesions can predict conversion to thoracotomy and postoperative surgical complications in patients undergoing video-assisted thoracoscopic lung cancer lobectomy. Journal of Thoracic Disease. 2018;10(1):416-31.
- 48. Doelken P, Sahn SA. Trapped lung. Semin Respir Crit Care Med. 2001;22(6):631-6.
- 49. Belda-Sanchis J, Serra-Mitjans M, Iglesias Sentis M, Rami R. Surgical sealant for preventing air leaks after pulmonary resections in patients with lung cancer. Cochrane Database Syst Rev. 2010(1):Cd003051.
- 50. Boerman MA, Roozen EA, Franssen GM, Bender JCME, Hoogenboom R, Leeuwenburgh SCG, et al. Degradation and excretion of poly(2-oxazoline) based hemostatic materials. Materialia. 2020;12:100763.

- 51. Balakrishnan B, Payanam U, Laurent A, Wassef M, Jayakrishnan A. Efficacy evaluation of anin situforming tissue adhesive hydrogel as sealant for lung and vascular injury. Biomed Mater. 2021;16(4).
- 52. Flynn K, Mahmoud NN, Sharifi S, Gould LJ, Mahmoudi M. Chronic Wound Healing Models. ACS Pharmacology & Translational Science. 2023;6(5):783-801.
- 53. van der Ham AC, Kort WJ, Weijma IM, van den Ingh HF, Jeekel H. Healing of ischemic colonic anastomosis: fibrin sealant does not improve wound healing. Dis Colon Rectum. 1992;35(9):884-91.
- 54. Kojima C, Niki Y, Ogawa M, Magata Y. Prolonged local retention of subcutaneously injected polymers monitored by noninvasive SPECT imaging. International Journal of Pharmaceutics. 2014;476(1):164-8.
- 55. Polyak A, Képes Z, Trencsényi G. Implant Imaging: Perspectives of Nuclear Imaging in Implant, Biomaterial, and Stem Cell Research. Bioengineering. 2023;10(5):521.
- 56. Mels F, van Dort D. V+ model-a Medical Perspective for Device Development. Research in Medical & Engineering Sciences. 2020;8(5).
- 57. Aprile V, Bacchin D, Calabrò F, Korasidis S, Mastromarino MG, Ambrogi MC, Lucchi M. Intraoperative prevention and conservative management of postoperative prolonged air leak after lung resection: a systematic review. Journal of Thoracic Disease. 2023;15(2):878-92.
- 58. McGuire AL. Yee J. Clinical outcomes of polymeric sealant use in pulmonary resection: a systematic review and meta-analysis of randomized controlled trials. J Thorac Dis. 2018;10(Suppl 32):S3728-s39.
- 59. Singhal S, Shrager JB. Should buttresses and sealants be used to manage pulmonary parenchymal air leaks? J Thorac Cardiovasc Surg. 2010;140(6):1220-5.
- 60. Wain JC, Kaiser LR, Johnstone DW, Yang SC, Wright CD, Friedberg JS, et al. Trial of a novel synthetic sealant in preventing air leaks after lung resection. Ann Thorac Surg. 2001;71(5):1623-8; discussion 8-9.
- 61. Rivera C, Bernard A, Falcoz PE, Thomas P, Schmidt A, Bénard S, et al. Characterization and prediction of prolonged air leak after pulmonary resection: a nationwide study setting up the index of prolonged air leak. Ann Thorac Surg. 2011;92(3):1062-8; discussion 8.
- 62. Murakami J, Ueda K, Tanaka T, Kobayashi T, Hamano K. Grading of Emphysema Is Indispensable for Predicting Prolonged Air Leak After Lung Lobectomy. Ann Thorac Surg. 2018;105(4):1031-7.
- 63. Moon DH, Park CH, Kang DY, Lee HS, Lee S. Significance of the lobe-specific emphysema index to predict prolonged air leak after anatomical segmentectomy. PLoS One. 2019;14(11):e0224519.
- 64. Belcher E, Dusmet M, Jordan S, Ladas G, Lim E, Goldstraw P. A prospective, randomized trial comparing BioGlue and Vivostat for the control of alveolar air leak. J Thorac Cardiovasc Surg. 2010;140(1):32-8.
- 65. Rena O, Papalia E, Mineo TC, Massera F, Pirondini E, Turello D, Casadio C. Air-leak management after upper lobectomy in patients with fused fissure and chronic obstructive pulmonary disease: a pilot trial comparing sealant and standard treatment. Interact Cardiovasc Thorac Surg. 2009;9(6):973-7.
- 66. Macchiarini P, Wain J, Almy S, Dartevelle P. Experimental and clinical evaluation of a new synthetic, absorbable sealant to reduce air leaks in thoracic operations. J Thorac Cardiovasc Surg. 1999;117(4):751-8.

- 67. De Leyn P, Muller MR, Oosterhuis JW, Schmid T, Choong CK, Weder W, Sokolow Y. Prospective European multicenter randomized trial of PleuraSeal for control of air leaks after elective pulmonary resection. J Thorac Cardiovasc Surg. 2011;141(4):881-7.
- 68. Sihoe ADL. Video-assisted thoracoscopic surgery as the gold standard for lung cancer surgery. Respirology. 2020;25(S2):49-60.
- 69. Varela G, Jiménez MF, Novoa NM, Aranda JL. Postoperative chest tube management: measuring air leak using an electronic device decreases variability in the clinical practice. Eur J Cardiothorac Surg. 2009;35(1):28-31.
- 70. Lequaglie C, Giudice G, Marasco R, Morte AD, Gallo M. Use of a sealant to prevent prolonged air leaks after lung resection: a prospective randomized study. J Cardiothorac Surg. 2012;7:106.
- 71. Cuzick J. The importance of long-term follow up of participants in clinical trials. British Journal of Cancer. 2023;128(3):432-8.
- 72. Shiroshita A, Nakashima K, Takeshita M, Kataoka Y. Preoperative Lung Ultrasound to Detect Pleural Adhesions: A Systematic Review and Meta-Analysis. Cureus. 2021;13(5):e14866.
- 73. Nagatani Y, Hashimoto M, Oshio Y, Sato S, Hanaoka J, Fukunaga K, et al. Preoperative assessment of localized pleural adhesion: Utility of software-assisted analysis on dynamic-ventilation computed tomography. Eur J Radiol. 2020;133:109347.



Chapter 9

English summary
Dutch summary
(Nederlandse samenvatting)

English Summary

Worldwide, more than two million people are diagnosed with lung cancer each year, and many of them have to undergo surgery. Often, air leakage occurs afterward, and in about one in ten cases, this persists for a longer duration. This is known as prolonged air leakage, leading to more complications and higher mortality. Additionally, patients must stay in the hospital longer, require a chest tube to continuously suction air from the chest cavity, and this results in higher costs for society.

The lung consists of airways branching into small air sacs (alveoli), allowing the lung to hold a lot of air (five to six liters). The structure of the lung, therefore, resembles a sponge. In healthy lungs, air leakage often heals on its own, but certain factors increase the risk of prolonged air leakage. For instance, in people with chronic obstructive pulmonary disease (COPD), the walls between the alveoli break down, making their lungs consist of an even larger portion of air.

Surgeons typically use medical staplers or sutures to stop air leakage. If these are insufficient, medical glues, sprays, or patches (lung sealants) can be used. Unfortunately, current lung sealants are still inadequate. Recently, a new synthetic sealant based on the polymer polyoxazoline has been developed, which has strong adhesive properties and is biodegradable. This polymer has been incorporated into a gelatin patch, allowing it to be applied to tissues during surgery (NHS-POx patch). This patch has already been investigated for stopping bleeding. This thesis will investigate whether the NHS-POx patch is also suitable for air leaks of the lung.

It is important to treat only those patients with a lung sealant who will truly benefit from it. It has been shown that larger air leaks in particular, are more likely to persist. The test most commonly used now (the 'water submersion test') is subjective, and more research is needed to standardize treatment. In **Chapter 2**, the reliability of existing measurements using a ventilator was further investigated in a laboratory setting. It was found that relevant air leaks can be reliably measured. This measurement technique is further used in this thesis.

Before the NHS-POx patch can be tested in humans, it must first be tested in animals. A literature review was conducted on the animal models previously

used (**Chapter 3**). It was found that there is no standard model available for this research. Most research is conducted on healthy young animals, and only a minority describe the use of control groups to demonstrate the reliability of the model. The animals are therefore difficult to compare with patients who develop prolonged air leaks. The knowledge gained from this literature review was used in the development of the animal models in **Chapters 5**, **6**, and **7**.

Before research was conducted with live animals, pig lungs obtained from the slaughterhouse were used (**Chapter 4**). These lungs were cooled, transported to the laboratory and re-ventilated. Superficial lesions were created, mimicking a realistic air leak. The NHS-POx patch was then tested as a single layer and double layer, and compared to four other lung sealants. The pressure was gradually increased until leakage occurred, and these pressures and leaks were compared. It was found that the new patch performed better when compared to existing treatments. Based on these results, further research in live animals was conducted.

Since there is no standardized animal model available for lung sealant research, **Chapter 5** describes how different types of lung injuries in healthy sheep can lead to air leakage. The experiments are conducted under general anesthesia, and the sheep are euthanized at the end of the experiment. This study showed that superficial injuries, like those in **Chapter 4**, do not lead to realistic leakage in live animals due to rapidly occurring healing mechanisms in healthy lungs. A model based on larger injuries that lead to air leakage over several hours was developed afterward.

In **Chapter 6**, the NHS-POx patch was tested as a single and double layer on these injuries and compared to untreated injuries. It was found that the patch can be applied to the lung through a cut between the ribs and is flexible enough to cover the edges of the lung. Under general anesthesia, the sheep continued to breathe for several hours to simulate the situation after lung surgery. Compared to untreated injuries, air leakage was reduced, confirming that the NHS-POx patch can also be effective in realistic scenarios.

Hereafter, the safety of the NHS-POx patch on the lung is also investigated in a sheep model (**Chapter 7**). In this study, the animals need to recover from the surgery. The procedure is performed through a smaller incision, and pain relief is provided postoperatively, as is done in humans. The patch is tested on superficial injuries that do not cause air leaks, allowing for the

assessment of biodegradability and wound healing compared to another patch and an untreated injury. All the sheep recover well from the surgery and are euthanized for microscopic examination at five days, two weeks, or six weeks post-operation. The results showed that the NHS-POx patch caused more inflammation than the untreated injury before it was degraded, but after six weeks, it was likely completely biologically degraded without causing significant inflammation. Local healing with scar formation was observed, similar to the other patch and the untreated control group.

Overall, the NHS-POx patch appears to be a promising material for preventing long-term air leaks. However, further research is needed. The long-term effectiveness and safety need to be investigated in diseased lungs (such as COPD) compared to existing lung sealants. The double layer of the patch could be developed into a thicker single layer, and its applicability via thoracoscopic surgery needs further investigation. Ultimately, studies in patients are necessary before the NHS-POx patch can be used in clinical practice.

Nederlandse samenvatting

Wereldwijd krijgen er jaarlijks meer dan twee miljoen mensen longkanker, en veel van hen moeten een operatie ondergaan. Vaak ontstaat er hierna luchtlekkage, en in ongeveer één op de tien gevallen houdt dit langdurig aan. Dit wordt langdurige luchtlekkage genoemd, wat leidt tot meer complicaties en sterfte. Daarnaast moeten patiënten langer in het ziekenhuis blijven, is er langdurig een slangetje nodig om de lucht uit de borstholte af te zuigen en leidt dit tot hogere kosten voor de maatschappij.

De long bestaat uit luchtwegen die vertakken tot kleine longblaasjes (alveoli), waardoor de long veel lucht kan vasthouden (vijf tot zes liter). De structuur van de long heeft hierdoor iets weg van een spons. Bij gezonde longen geneest de luchtlekkage vaak weer vanzelf, maar bepaalde factoren verhogen de kans op het krijgen van langdurige luchtlekkage. Zo gaan bij mensen met chronische obstructieve long ziekte (COPD) de wandjes tussen de alveoli kapot, waardoor de long bij deze mensen voor een nog groter deel uit lucht bestaat.

Chirurgen gebruiken meestal medische nietapparaten of hechtingen om luchtlekkage te stoppen. Als dit onvoldoende helpt, kunnen medische lijmen, sprays of pleisters gebruikt worden (long sealants). De huidige long sealants werken helaas nog onvoldoende. Recent is een nieuwe kunststof ontwikkeld op basis van het polymeer polyoxazline, dat een sterke plakkracht heeft en biologisch afbreekbaar is. Deze kunststof is in een gelatine pleister verwerkt, waardoor deze tijdens operaties aangebracht kan worden op weefsels (NHS-POx patch). Deze pleister is al onderzocht om bloedingen te stelpen. In dit proefschrift zal worden onderzocht of de NHS-POx patch ook geschikt is voor luchtlekkages van de long.

Het is van belang om alleen patiënten te behandelen met een lung sealant, die hier ook echt baat bij hebben. Het is gebleken dat vooral grotere luchtlekkages een grotere kans hebben langer aan te houden. De test die nu meestal gebruikt wordt (de 'fietsbandproef') is subjectief, en er is meer onderzoek nodig om behandeling te standaardiseren. In Hoofdstuk 2 is de betrouwbaarheid van bestaande metingen met behulp van een beademingsapparaat verder onderzocht in een laboratorium opstelling. Hier is gebleken dat relevante luchtlekkages betrouwbaar gemeten kunnen worden. Deze meettechniek wordt verder gebruikt in het proefschrift.

Voordat de NHS-POx patch in mensen getest kan worden, zal deze eerst in dieren getest moeten worden. Er is een literatuuronderzoek gedaan naar de diermodellen die eerder zijn toegepast (Hoofdstuk 3). Hieruit is gebleken dat er geen standaard model is dat voor dit onderzoek gebruikt kan worden. Veel onderzoek wordt gedaan in gezonde jonge dieren, en slechts een minderheid beschrijft het gebruik van controlegroepen om de betrouwbaarheid van het model aan te tonen. De dieren zijn dus lastig te vergelijken met patiënten die langdurige luchtlekkage krijgen. De kennis die is verkregen met dit literatuuronderzoek werd gebruikt bij de ontwikkeling van de diermodellen in Hoofdstuk 5, 6 en 7.

Voordat er onderzoek met levende dieren gedaan werd, zijn er longen gebruikt van varkens uit het slachthuis (**Hoofdstuk 4**). Deze longen werden gekoeld getransporteerd naar het laboratorium en opnieuw beademd. Er werden oppervlakkige letsels gemaakt, welke een realistisch luchtlek nabootste. Hierop werd de NHS-POx patch als enkele laag en dubbele laag getest, in vergelijking met vier andere lung sealants. De druk werd geleidelijk aan verhoogd tot er lekkage op trad, en deze drukken en lekkages werden vergeleken. Het bleek dat de nieuwe patch het beter deed dan de bestaande behandelingen. Op basis van de resultaten werd verder onderzoek in levende dieren verricht.

Omdat er nog geen gestandaardiseerd diermodel beschikbaar is voor het onderzoek naar long sealants, wordt in **Hoofdstuk 5** beschreven hoe verschillende types letsel aan de long in gezonde schapen kunnen leiden tot luchtlekkage. De experimenten worden onder algehele narcose verricht, en de schapen worden aan het eind van het experiment geëuthanaseerd. Uit dit onderzoek blijkt dat oppervlakkige letsels zoals in **Hoofdstuk 4** niet leiden tot realistische lekkage in levende dieren, door snel optredende genezingsmechanismen in gezonde longen. Er wordt hierna een model ontwikkeld op basis van grotere letsels, die over enkele uren leiden tot luchtlekkage.

In **Hoofdstuk 6** de NHS-POx patch als enkele en dubbele laag op deze letsels getest en vergeleken met onbehandelde letsels. Het bleek dat de patch via een snee tussen de ribben kan worden aangebracht op de long en flexibel genoeg is om randen van de long te bedekken. Onder algehele narcose blijven de schapen enkele uren ademen om de situatie na een longoperatie na te bootsen. In vergelijking met de onbehandelde letsels is de luchtlekkage

verminderd, wat bevestigt dat de NHS-POx patch ook werkzaam kan zijn in realistische scenario's.

Hierna wordt ook de veiligheid van de NHS-POx patch op de long onderzocht in een schapenmodel (Hoofdstuk 7). Hier moeten de dieren ook weer bijkomen van de operatie. Er wordt via een kleinere snee gewerkt, en pijnstilling gegeven na de operatie zoals dit ook bij mensen gedaan wordt. De patch wordt getest op oppervlakkige letsels die geen luchtlek veroorzaken, zodat alleen naar de biologische afbreekbaarheid en wondgenezing gekeken kan worden, in vergelijking met een andere patch en een onbehandeld letsel. Al de schapen herstellen voorspoedig van de operatie, en worden voor microscopisch onderzoek op vijf dagen, twee of zes weken geëuthanaseerd. Hieruit bleek dat de NHS-POx patch voordat deze afgebroken was meer ontsteking had dan de onbehandelde letsel, maar na zes weken waarschijnlijk helemaal biologisch afgebroken was zonder relevante ontstekingsreactie. Er werd lokaal genezing gezien met littekenvorming, vergelijkbaar met de andere patch en onbehandelde controlegroep.

Alles tezamen, lijkt de NHS-POx patch een veelbelovend materiaal om langdurige luchtlekkage te voorkomen. Wel is er nog verder onderzoek nodig. De lange termijn effectiviteit en veiligheid moet onderzocht worden op zieke longen (COPD) in vergelijking met bestaande long sealants. De dubbele laag van de patch zou doorontwikkeld kunnen worden tot dikkere enkele laag, en toepasbaarheid via kijkoperaties moet verder onderzocht worden. Uiteindelijk zijn onderzoeken in patiënten nodig voordat de NHS-POx patch gebruikt kan worden in de gezondheidszorg.



Attachments

Research data management
Portfolio
Dankwoord
<u>Curricilum</u> vitae

Publication list

Research Data Management

Data collection, analysis and storage

Animal experiments were performed after ethical review by an independent ethical committee and a project license was provided by the 'Centrale Comissie Dierproeven'. All experiments were performed in accordance with national and international legislation. Protocols were always prepared prior to experiments, and in case of studies involving live animals these were additionally registered with the institutional animal welfare body. The systematic review protocol was published in the International Platform of Registered Systematic Review and Meta-analysis Protocols (INPLASY). Data was collected during the period of this thesis (April 2020 - July 2023) in the form of spreadsheets, notes (PDF). photos, videos, Matlab files and histological samples. Data was processed and analyzed as described in the individual chapters. Processed data is saved in SPSS Databases for statistical analysis. All study data is digitized and stored on the Radboud Bulk Storage environment '\umcsanfsclp01\CTC Sealants', and will be stored for at least 15 years after termination of the study. This data is backed-up by the Information and Communication Technology (ICT) department. Storage is structured per research study, where raw data is kept separate from processed data. Access is managed through the department of cardiothoracic surgery and only granted to persons directly working with the study data. Paper files and notes are also stored in locked cabinets in the central animal laboratory, as well as histological samples.

Data sharing

Relevant data on which the conclusions are based are generally published in the article in tables and figures, or as an additional supplement. Additional data (e.g. raw data files) can be shared upon reasonable request, considering the goal of the request (e.g. academic or commercial) and intellectual property rights. To allow for reuse, relevant documentation (e.g. protocols, experiments notes) can be shared alongside this data.

Data management was performed as much as possible in accordance with the FAIR principles (Findable, Accessible, Interoperable, Reusable).

Portfolio

Department: Department of Cardio-thoracic surgery

PhD period: 17/04/2020 - 17/04/2024

PhD Supervisor(s): prof. dr. A.F.T.M. Verhagen, prof. dr. H. van Goor,

prof. dr. H.F.M. van der Heijden

PhD Co-supervisor(s): dr. R.P.G. ten Broek

Training activities	Hours	
Courses		
- Radboudumc - Laboratory animal science (2021)		
- RIHS - Introduction course for PhD candidates (2022)		
- Radboudumc - Scientific integrity (2022)		
- Matlab self-paced online courses (2021)	12,5	
- Technical University Eindhoven Systems in time and space (2022)	140	
Seminars		
- 2nd Postoperative Complications Summit Virtual Edition (2021)	4	
- Research Integrity Round: The dark side of science (2021)		
 Research Integrity Round: Collaboration with profit and non-profit organisations (2021) 		
- Research Integrity in times of crisis: Juggling slow and fast science	1,5	
Conferences		
 Nederlandse Vereniging voor Thoraxchirurgie (NVT) Wetenschappelijke voorjaarsvergadering, oral presentation (2021) 		
 Symposium Experimenteel Onderzoek Heelkundige Specialismen (SEOHS), oral presentation (2021) 		
- Society of Thoracic Surgery (STS) Annual Meeting, pre-recorded presentation (2022)		
- Symposium Experimenteel Onderzoek Heelkundige Specialismen (SEOHS), oral presentation (2022)		
- European Association for Cardio-Thoracic Surgery (EACTS) Annual Meeting, oral presentation (2023)	24	
Other		
- Species specific training in laboratory animals: sheep (2021)	40	
- Presentation coaching (2021)	3	
Teaching activities		
Supervision of internships / other		
- Guiding Bachelor Biomedical Science internship (2023)	20	
Total	390,5	



Dankwoord

"If I have seen further, it is by standing on the shoulders of giants", luidde de woorden van Sir Isaac Newton. En zo ook was dit academische werk nooit mogelijk geweest zonder het team om me heen en iedereen die me de afgelopen jaren gesteund heeft.

Prof. dr. Ad Verhagen, vanaf het moment dat ik als vierdejaars student geneeskunde bij u kwam, voelde ik mij gesteund in mijn promotieonderzoek. Naast al de wetenschappelijke discussies die dit proefschrift inhoudelijk mede hebben gevormd, wil ik u bedanken voor het vertrouwen wat ik heb gekregen en de vrijheid om me te ontwikkelen tot een zelfstandig onderzoeker. Daarnaast bent u op klinisch vlak een rolmodel: empathisch, betrokken, respectvol en kundig; als arts en chirurg plaatst u de patiënt centraal.

Prof. dr. Harry van Goor, uw oprechte betrokkenheid om mij te laten groeien tot een kritische denker is onmiskenbaar. Zonder onze discussies en uw visie, soms anders dan die van mij, was dit proefschrift nooit geworden wat het is. Zoals de woorden die u aanhaalde bij uw afscheidsrede "Off Balance, On Purpose", heeft u mij tijdens dit traject ook geïnspireerd om buiten mijn comfort zone te gaan en te groeien, ook al is dit niet altijd eenvoudig.

Prof. dr. Erik van der Heijden, uw doortastendheid als wetenschapper om zaken tot op de bodem uit te zoeken waren belangrijk voor het wetenschappelijke proces. Ik wil u bedanken voor uw aanmoediging, geduld en vertrouwen in mij en dit proefschrift.

Dr. Richard ten Broek, hoewel je pas wat later bij het promotieteam kwam, heb je een grote rol gespeeld in mijn academische ontwikkeling. Je intelligentie, werk ethiek, perfectionisme en integriteit zijn terug te vinden in dit proefschrift. En naast de vele uren dat we hebben besteed aan inhoudelijke discussie en het schrijven van wetenschappelijke artikelen, waren onze dialogen over uiteenlopende onderwerpen een verrijkende toevoeging.

De leden van de manuscriptcommissie, **Prof. dr. Otto Boerman, Prof. dr. Michel van den Heuvel** en **Prof. dr. Jerry Braun,** wil ik graag bedanken voor het lezen en beoordelen van dit proefschrift.

Wilson Li, ik kwam al als tweedejaars student bij je voor het wetenschapsproject, en je hebt me al die tijd gesteund in mijn ontwikkeling en deze promotie. Je geduld, visie en perfectionisme bij het schrijven van mijn eerste wetenschappelijke artikel waren ontzettend waardevol. Jouw lessen in academisch schrijven, zijn terug te lezen in de wetenschappelijke stukken in dit proefschrift. Daarnaast ben je een uitstekend onderwijzer, en je enthousiasme hierin is aanstekelijk.

Daniël van Dort, zonder jou was dit proefschrift er nooit geweest. Van het eerste idee en proefopstelling tot de geavanceerde experimenten. Je buitengewoon creatieve visie, oplossingsvermogen en jou vermogen om mensen met elkaar te verbinden zijn slechts een aantal eigenschappen die dit mogelijk hebben gemaakt. Je hebt me de afgelopen jaren helpen groeien door te vertrouwen, als mentor en als vriend.

Edwin Roozen, je passie voor wetenschappelijk onderzoek en de nieuwsgierigheid naar de wereld om ons heen zijn aanstekelijk. We hebben vele uren samen doorgebracht in het lab in de ontwikkeling van de proefopstellingen, waarbij je altijd problemen vanuit een andere creatieve hoek wist te bekijken. Bovenal heb je me ook laten zien dat ik soms stil moet staan, en genieten van de wereld om ons heen.

Shoko Vos, toen ik begon met dit promotieonderzoek had ik niet gedacht dat ik zo veel tijd zou spenderen aan het bestuderen van microscopische coupes. Hoewel het urenlang zelfstandig bestuderen van immuunreacties op weefsels soms lastig was, maakte jou enthousiasme en geduld voor het vak dit een ontzettend leerzaam en waardevol deel van dit proefschrift.

Ik wil iedereen van GATT-Technologies bedanken voor de steun en het vertrouwen, om mij als onafhankelijke onderzoeker de door hen ontwikkelde NHS-POx patch te laten onderzoeken als lung sealant, in het bijzonder **Johan Bender** en **Stuart Head**. Zonder hen was dit project niet mogelijk geweest.

Het werk dat achter de schermen is verricht door het team van het centrale dierenlaboratorium is van onschatbare waarde. Ik wil al het betrokken personeel bedanken voor hun toewijding aan zorg voor de dieren en deskundigheid op wetenschappelijk gebied. Alex, Maikel, Stefanie, jullie jarenlange expertise en flexibiliteit als biotechnici hebben deze chirurgische experimenten mogelijk gemaakt. Pieter, Jeanette, Manon, Anke, jullie input



heeft gezorgd voor experimenten van hoge wetenschappelijke waarde en een optimaal dierenwelzijn. **Tom, Conrad,** ik wil jullie bedanken voor de goede zorg voor de schapen op de boerderij.

Wetenschappelijk onderzoek is niet mogelijk zonder toewijding, aandacht voor details en perfectionisme van het hele team. **Roger,** naast deze eigenschappen stelde je altijd de juiste kritische vragen en hebben deze experimenten naar een hoger niveau gebracht. **Nicole,** dit geld ook voor jou, en ik wil je daarnaast bedanken voor je enthousiasme en toewijding voor het onderzoek tijdens onze lange dagen in het lab.

Juul, je hebt als ambitieuze student grote wetenschappelijke interesse getoond in verschillende onderwerpen en met veel enthousiasme dit proefschrift ondersteund. Het was een genoegen om met je samen te werken en ik wil je hiervoor bedanken. Daarnaast wil ik **Merve, Pim** en **Jort** bedanken, die als student dit proefschrift op verschillende vlakken ondersteund hebben.

Data-acquisitie en analyse met Matlab zit niet in het standaard pakket van de medische opleiding. **Jeroen, René, Timo, Jasper,** ik wil jullie bedanken voor jullie hulp en begeleiding hierin, ik heb ontzettend veel van jullie geleerd. **Jan Hofland** en **Lisanne Roesthuis,** ik wil jullie bedanken voor jullie hulp op het vlak van beademing- en luchtlekmetingen. Voor de technische expertise betreffende de luchtlek-metingen en experimentele opstellingen wil ik **Joris, Tonny, Ben, Raymond, Marco** en **Erik** bedanken.

Mijn eerste ervaring met wetenschappelijk onderzoek begon bij **Joris** en **Jos** op de afdeling cardiologie, ik wil jullie bedanken voor de begeleiding om aandacht voor details te ontwikkelen tijdens data-verzameling.

Naast het onderzoek voor dit proefschrift heb ik ook mijn coschappen gelopen voor mijn geneeskunde studie. Ik wil de **A(N)IOs** en **PA(io)s** bedanken voor het geduld om mij als senior-coassistent te laten ontwikkelen tot een zelfstandig arts-assistent. Ik ben dankbaar om hierna als collega deel uit te mogen maken van het team, waarbij humor en gezelligheid essentiële luchtigheid brengen in de soms stressvolle en droevige klinische praktijk.

Het is een eer om de operaties aan hart en long bij te mogen wonen en hierbij te assisteren, en de vaardigheid, stressbestendigheid en discipline van de cardio-thoracaal chirurgen van het Radboudumc **Dr. Verkroost,**

Dr. Van Garsse, Prof. Heijmen, Dr. Geuzenbroek, Dr. Van Wetten, Dr. Saouti en **Dr. Nauta,** is ontzagwekkend en inspirerend. In het bijzonder wil ik **Dr. van der Heide** bedanken voor het ontwikkelen van de chirurgische technieken voor experimenten in dit proefschrift. Als laatste wil ik iedereen van het stafsecretariaat bedanken voor de ondersteuning tijdens dit promotietraject, in het bijzonder **Harold Kerstens** voor de projectmatige ondersteuning.

Tijdens mijn studie geneeskunde heb ik meerdere mentoren gehad, en ik wil Hanneke Nabuurs, Hans Timmermans, Dirk Geurts en Anne van Altena voor hun steun in verschillende fasen van mijn opleiding en ontwikkeling tot een zelfstandig arts, en Prof. Kramers voor het mentorschap tijdens dit promotieonderzoek. Het uitvoeren van promotieonderzoek tijdens de studie geneeskunde is geen standaard pad, en dit was nooit mogelijk geweest zonder de steun van de studieadviseur Nikkie Meijers, die zich hard heeft gemaakt voor mijn project en mij heeft geholpen met een tijdelijke onderbreking van de coschappen om me fulltime te focussen op wetenschap, met de visie om de hoogste kwaliteit in zowel mijn opleiding tot arts als wetenschapper te garanderen. Ik wil mijn dankbaarheid naar Nikkie en hierna haar opvolger Gaby van Welsem hiervoor uitspreken. Daarnaast wil ik het Radboud Institute for Health Sciences bedanken voor hun steun van dit promotietraject.

Zonder vrienden zou het een eenzaam pad zijn, en ik ben dankbaar voor al de mooie vriendschappen die ik onderweg heb gemaakt. Natuurlijk de mannen uit Brabant, Lars, Bram, Thijs, Emiel, Dirk, Luc, Sander, Koen, Timo, Cor, Tom, humor en gezelligheid staan altijd voorop. En hoewel we elkaar de afgelopen jaren minder vaak zien, voelt het altijd als thuiskomen. Steven, naast onze wetenschappelijke samenwerkingen, hebben we onze fysieke en mentale grenzen verlegd met intervaltrainingen voor dag en douw op de atletiekbaan, zwemtochten door Nijmeegse wateren en natuurlijk de Ironman in Duisburg. Sven, we kennen elkaar vanaf dag één van de geneeskundestudie en hebben veel mooie avonturen mogen beleven, op fietstochten, wildkampeertochten en triatlons. Kenney, jouw promotieonderzoek was voor mij mede een inspiratie. We kunnen goed over gedeelde interesses praten of over uiteenlopende onderwerpen discussiëren, maar gezelligheid staat altijd voorop. Michelle en Sophie, jullie ambitie en sportiviteit is aanstekelijk.

Ik ben bevoorrecht om uit een bijzonder hechte en warme familie te komen. **Pap,** je hebt me geleerd om te vallen en weer op te staan, door de zure appel heen te bijten en hoe je door hard werk en discipline de stip op de horizon kunt

nastreven. **Mam,** je hebt mijn nieuwsgierigheid in de wereld al vanaf jonge leeftijd aangemoedigd, en bent er altijd, onvoorwaardelijk voor ons geweest, ook als het moeilijk was. Jullie hebben mij mijn eigen keuzes (en fouten) laten maken, waar ik jullie ontzettend dankbaar voor ben. **Rik** en **Jasmijn,** gelukkig is het altijd gezellig met zijn drieën, en het is geweldig om jullie ambitie, passie en ondernemerschap te mogen aanschouwen.

Mijn echtgenote **Jill,** met jou humor, gezelligheid en lach laat je me altijd genieten van het moment. We hebben veel mooie avonturen beleefd samen en kunnen voor alles op elkaar vertrouwen. Je hebt mij vanaf het begin gesteund in mijn ambities, en zonder jouw steun, ook op de momenten dat ik het moeilijk had, was dit nooit gelukt. Mijn dank gaat uit naar jouw onvoorwaardelijke liefde, warmte en steun in voor en tegenspoed.

Zoals ijzer met ijzer wordt geslepen, Zo scherpt de ene mens de ander Spreuken 27:17

Curriculum vitae



Bob P. Hermans was born on the 18th of August 1998 in Veldhoven, the Netherlands. In 2016 he obtained his pre-university education. He studied medicine at the Radboud University Medical Center in Nijmegen, obtaining his bachelor's degree *Cum Laude* in 2019

His affinity with research began as a first year medical student, starting out as a research assistant at the department of cardiology. Later, he started working with at CardiacBooster B.V., a

company developing a new cardiac assist device, where he acquired skills in (animal) experimentation, innovation, and research. Concurrently, he also ran a small company called SurgicalTraining, with the aim of providing low-cost training materials for acquisition of basic surgical skills to medical students.

He started his master's degree in 2019, but during the COVID-pandemic, clinical rotations were temporarily put on hold. Bob used this time to start his PhD research, after having heard of the new polyoxazoline patch as a hemostatic agent. Under supervision of Prof. Verhagen, he completed a survey amongst Dutch thoracic surgeons into the use of lung sealants, and developed the ex-vivo model for testing of lung sealants. With these studies, the foundation was laid for the PhD-trajectory.

He combined his PhD research and his clinical internships for some time, until taking a one-year break to focus on the experimental research phase in 2022. During this time, he also completed a course at the Technical University Eindhoven into mathematical subjects including vector calculus. In 2023, he completed his final internships at cardiology and cardio-thoracic surgery departments, graduating as a medical doctor in November 2023.

He has presented research at multiple national and international conferences, and has been awarded several awards, winning the 'best presentation' award at the symposium for experimental research in surgical specialties in 2021 and 2022 and the award for 'best abstract' in the Dutch society of cardiothoracic surgery annual meeting. He was recognized as an Outstanding Author by the Journal of Thoracic Disease in 2023.

List of publication

Peer-reviewed publications

Hermans BP, Li WWL, Roozen EA et al. Sealing effectiveness of a novel NHS-P0x based patch: experiments in a dynamic ex vivo porcine lung. J Thorac Dis. 2023. DOI: 10.21037/jtd-22-1821.

Hermans BP, Li WWL, Roozen EA et al. Intrinsic pulmonary sealing, its mechanisms and impact on validity and translational value of lung sealant studies: a pooled analysis of animal studies. J Thorac Dis. 2023. DOI: 10.21037/jtd-23-180

Hermans BP, Poos SEM, van Dort DIM et al. Evaluating and developing sealants for the prevention of pulmonary air leakage: A systematic review of animal models. Lab Anim. 2023. DOI: 10.1177/00236772231164873

Hermans BP, Ten Broek RPG, Li WWL et al. Proof-of-principle of a lung sealant based on functionalized polyoxazolines: experiments in an ovine acute aerostasis model, Interdisciplinary CardioVascular and Thoracic Surgery, 2024. DOI: 10.1093/icvts/ivae113

Hermans BP, van Doorn JLM, Roesthuis LH et al. Characterisation of pulmonary air leak measurements using a mechanical ventilator in a bench setup. Journal of Medical Engineering & Technology. 2024. DOI: 10.1080/03091902.2024.2381540

Poos SEM, **Hermans BP**, van Goor H et al. Animal models for preventing seroma after surgery: a systematic review and meta-analysis. Lab Anim. 2024. doi: 10.1177/00236772241273010.

Patents

Daniël van Dort, Florian Ludwig, **Bob Hermans**, Koen Peij, Jos Thanhauser. Collapsible device for circulatory assistance. 2020. Publication number: WO/2020/180177



